

Genetic and Epigenetic Interplay in Congenital Diaphragmatic Hernia

Daniëlle Veenma

The research presented in this dissertation was performed at the Departments of Paediatric Surgery and Clinical Genetics, Erasmus University Medical Centre, Rotterdam, the Netherlands. The study was financially supported by the “Sophia Stichting Wetenschappelijk Onderzoek” (project 551), Rotterdam, the Netherlands



ISBN/EAN: 978-94-6191-305-0

Cover illustration by: Tom de Vries Lentsch

Lay-out: Legatron Electronic Publishing, Rotterdam

Printing: Ipskamp Drukkers BV, Enschede

© Danielle Cornelia Marina Veenma

All rights reserved. No part of this thesis may be reproduced or transmitted in any form, by any means, without prior written permission of the author, or where appropriate, of the publisher of the articles and figures

Genetic and Epigenetic Interplay in Congenital Diaphragmatic Hernia

Genetische en epigenetische interacties in
congenitale hernia diafragmatica

Proefschrift

ter verkrijging van de graad van doctor aan de
Erasmus Universiteit Rotterdam
op gezag van de rector magnificus
Prof.dr. H.G. Schmidt
en volgens besluit van het College voor Promoties

De openbare verdediging zal plaatsvinden op
woensdag 6 juni 2012 om 15.30 uur

door

Daniëlle Cornelia Marina Veenma

geboren te Geleen



Promotiecommissie

Promotor: Prof.dr. D. Tibboel

Overige leden: Prof.dr. B.A. Oostra
Prof.dr. I. Reiss
Prof.dr. E. Dzierzak

Co-promotor: Dr. J.E.M.M. de Klein

**Intense life is not complete
without a touch of madness**

Paul Coelho

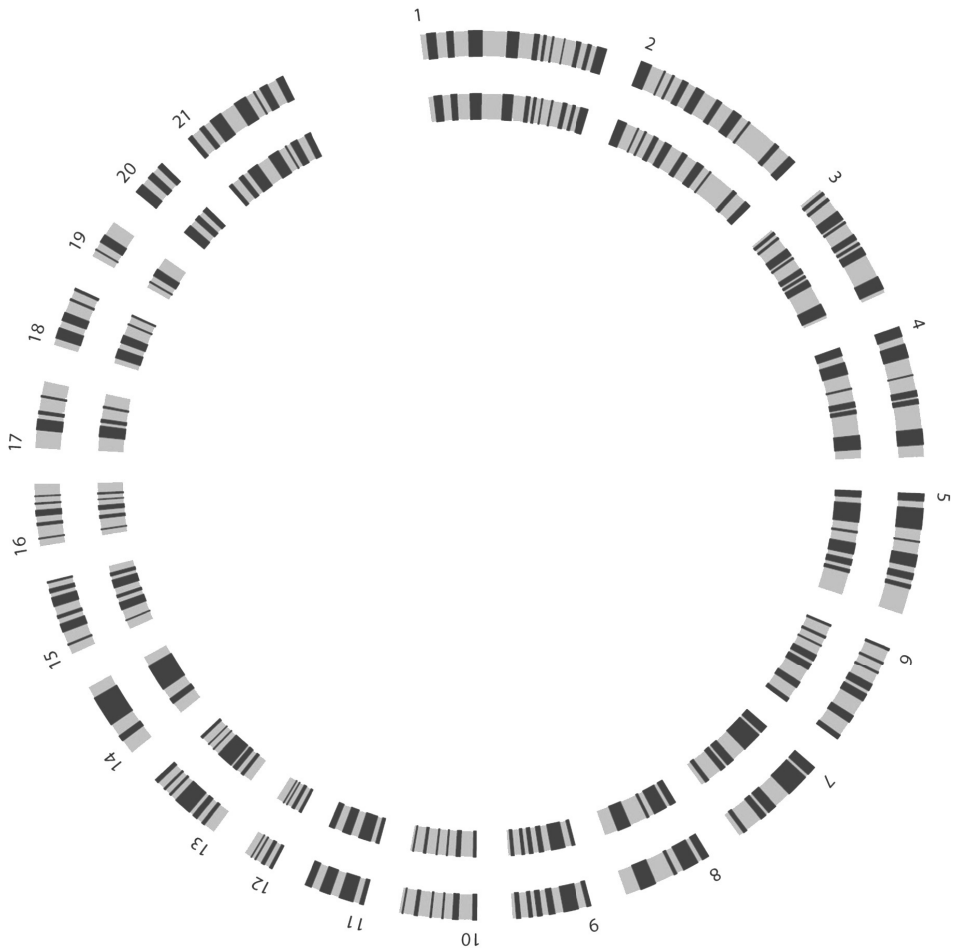
Table of Contents

| | | |
|------------------|--|-----------|
| Chapter 1 | Introduction | 9 |
| | 1.1 Congenital diaphragmatic hernia: A brief introduction to its versatile clinical aspects, embryology and challenges in care | 10 |
| | 1.2 CDH Aetiology; complexity as a central theme | 14 |
| | 1.3 The Rotterdam cohort of CDH patients | 19 |
| | 1.4 Epigenetic analysis in CDH | 21 |
| | 1.5 Aim and Outline of this thesis | 26 |
| Chapter 2 | Copy Number Variations and Chtop Mutations in the CDH Cohort | 37 |
| | 2.1 Germline and Somatic SNP-array analysis of 117 isolated and complex Congenital Diaphragmatic Hernia patients – the Rotterdam cohort – | 39 |
| | 2.2 Complex Congenital Diaphragmatic Hernia in Mice Lacking Chromatin Target of PRMT1 <i>Submitted</i> | 59 |
| | 2.3 Genomic Alterations that Contribute to the Development of Isolated and Non-Isolated Congenital Diaphragmatic Hernia <i>J Med Genet (2011 May;48(5):299-307)</i> | 79 |
| | 2.4 Copy Number Detection in Discordant Monozygotic Twins of Congenital Diaphragmatic Hernia (CDH) and Esophageal Atresia (EA) Cohorts <i>Eur J Hum Genet. 2012 Mar;20(3):298-304</i> | 101 |
| | 2.5 Comparable Low-Level Mosaicism in Affected and Non-affected Tissue of a Complex CDH Patient <i>PLOS One (2010 Dec 21; 5(12): e15348)</i> | 117 |

| | | |
|------------------|---|------------|
| Chapter 3 | Disrupted RA Signalling in CDH: Gene-Expression & Patho-Epigenetic Mechanisms in 15q26 Monosomy Patients and a Nitrofen Rodent Model | 133 |
| | 3.1 Spatial Positioning of CDH Candidate Genes in a 15q26 Deleted Fibroblast Patient Model | 135 |
| | 3.2 Expression Profiling with and without Retinoic Acid (RA) in 15q26-Deleted Congenital Diaphragmatic Hernia Fibroblasts: Relative Cellular RA Deficiency | 151 |
| | 3.3 <i>NR2F2</i> Promoter Interactions in Diaphragm Development: Chromosome Conformation Capture-Sequencing (4C-Seq) in a Rodent Model of Congenital Diaphragmatic Hernia (CDH) | 173 |
| Chapter 4 | General Discussion | 195 |
| | <i>Adapted from: "Developmental and Genetic aspects of Congenital Diaphragmatic Hernia" Paediatric Pulmonology 2012, in press</i> | |
| | 4.1 The clinical context of Copy Number Variations (CNV) in general and for CDH specifically: Methodological considerations | 196 |
| | 4.2 Current perspectives on the role of spatial organization on gene expression regulation: Methodological considerations of 3D multicolor FISH and 4C technology data | 201 |
| | 4.3 Embryology of the Diaphragm, its remaining issues and Molecular-Genetic Pathways in CDH pathophysiology | 203 |
| | 4.4 Future perspectives | 211 |
| Chapter 5 | Appendices | 221 |
| | 5.1 Summary | 223 |
| | 5.2 Samenvatting | 227 |
| | 5.2 Dankwoord | 231 |
| | 5.3 Curriculum Vitae | 237 |
| | 5.4 PhD Portfolio | 239 |
| | 5.5 List of publications | 241 |
| | Color figures | 243 |

Chapter 1

Introduction



Introduction

1.1 Congenital diaphragmatic hernia: A brief introduction to its versatile clinical aspects, embryology and challenges in care

Congenital diaphragmatic hernia (CDH) is a common and life-threatening developmental anomaly, which arises early during human development. Its birth incidence fluctuates worldwide around 1 in 2000-3000 live births and it is an important cause of stillbirths and abortions [1-3]. Despite advances in treatment, mortality from CDH continues to be high. The CDH registry shows a current overall survival rate of 67%, but rates vary widely based on patient selection [4].

Children born with CDH suffer from severe respiratory distress caused by a classical “trio” of features: a defect in the muscular or tendinous portion of the diaphragm, pulmonary hypoplasia, and pulmonary hypertension. The diaphragm muscle is a critical organ for proper respiration and physically prevents the abdominal content from moving up into the thorax during respiration. In CDH this function is disturbed [5]. As a result, during the prenatal period the abdominal contents may herniate into the thorax and compete with the lungs for space, thereby disturbing lung development. Aside from this secondary effect on lung development, some authors argue for a primary pulmonary defect in CDH [6, 7]. More importantly, since it has become relatively easy to repair the diaphragm defect, lung aberrations are now considered the main determinant for postnatal outcome. Therefore many CDH research initiatives focus on finding good treatment options for both the underdevelopment of the lungs and the persistent high resistance of the pulmonary vasculature.

Diaphragm development

Studies on the embryological origin of the diaphragm are sparse despite its presence in all mammalian species and its importance in respiratory system functioning. Conventional understanding of diaphragm embryology and pathophysiology – the so-called classical four-structure view – was based on analysis of the Carnegie collection of human embryos [8-10].

In this traditional view, it was suggested that the diaphragm (including its musculature component) arises from four different structures between the fourth and twelfth week of human gestation: the septum transversum would give rise to the anterior portion of the diaphragm, the pleuro-peritoneal folds (PPFs) to its postero-lateral part, the esophageal mesentery to its central portion and finally the thoracic body wall to the rim of musculature around the diaphragm’s periphery. However, more recent insights suggested that the neuromuscular component arises from myogenic cells that coalesce within the mesenchymal pleuro-peritoneal folds instead and then migrate to the other diaphragm parts. So, in this revised model it is hypothesized that a four-structure derived *mesenchymal* substrate provides a migration platform for the “true” diaphragm muscle cells. These new insights were founded on experiments both in normal Retinoic Acid rodent animal models and rodent models of chemically induced diaphragm defects

that target the RA-signalling pathway at various levels (i.e. the Nitrofen-, BMS493- models) [11-17]. Advantages of the use of rat over human material were: 1) the presence of the diaphragm as a thin and essentially two-dimensional structure; and 2) the opportunity to visualize the migratory path of the nervus phrenicus and primordial diaphragm tissue with immuno-labelling [11, 12].

Diaphragm development is intrinsically related to the separation of the intra-embryonic coelom into pleural, pericardial, and peritoneal cavities. In the second month of gestation, these cavities interconnect via two large openings: the pleuro-pericardio-peritoneal canals. Next, at the level of the pericardial cavity (Figure 1A [18]), the lungs begin to expand into the pleuro-peritoneal cavity and the heart into its pericardial cavity raising two ridges of tissue termed the pleuro-pericardial folds [19]. More distal at the level of the septum transversum, two paired pleuro-peritoneal folds arise as well, separating the pleural and peritoneal cavities (Figure 1B). A breakthrough into CDH research was the realization that the primordial posterolateral part of the diaphragm – and its defects in chemically exposed rats – could be traced back to an (abnormality of) these PPFs [11]. In retrospect, this tissue was labelled Post-Hepatic Mesenchymal Plate (PHMP) by Iritani et al. and most probably arises from lateral plate mesoderm that is associated with the lateral body wall [8, 20, 21]. The PPF structure was identified as the most likely candidate for the primordial diaphragm, because it is targeted by migrating diaphragmatic muscle precursor cells extending from the phrenic population. In transverse sections of 10 to 14-day-old rat embryos the mesenchymal-derived PPFs can be transiently visualized as paired, pyramid-shaped fusion structures. In humans this can be demonstrated between the 4th and 5th week of gestation [15]. As explained above, the PPFs shape the dorsolateral part of the future diaphragm and in turn protrude ventrally and medially to merge with the esophageal mesentery and with the septum transversum. Note that in contrast to earlier hypotheses, defects in the PPFs are not merely restricted to the mesoderm tissue that expands to close the pleuro-peritoneal canals.

Summarised, the current hypothesis on CDH pathophysiology posits that genetic and/or environmental triggers disrupt formation of mesenchymal cells encompassing the future posterolateral part of the diaphragm (the mesenchymal-hit hypothesis). In the discussion section of this thesis we will provide a more extended summary on the current issues of lung- and diaphragm development in relation to CDH, focusing specifically on the underlying molecular and cellular signalling pathways.

Clinical presentation and management

CDH can broadly be classified into two types based on its anatomical position: posterolateral and non-posterolateral. The defect is most often located on the left side (85%); less frequently on the right side (13%) or bilateral (2%). The posterolateral defect commonly referred to as Bochdalek hernia accounts for 70-75% of cases [22-25]. Non-posterolateral defects can be further distinguished into anterior- and central types. The anterior type occurs in approximately 23-28% of cases and is labelled the Morgagni-Larrey type if the defect is positioned para- or retrosternal and a so-called “hernia sac” is seen. Central hernias account for the remaining 2-7% of cases

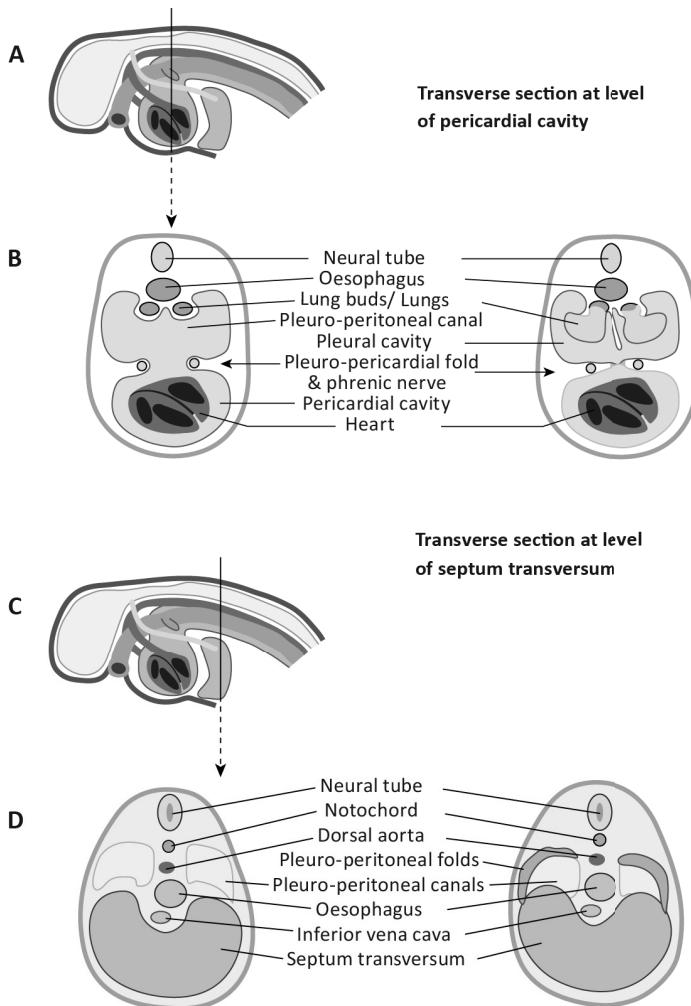


Figure 1 | Embryological overview of the development of the Pleuro-Pericardio-Peritoneal Folds (PPFs)

A: depicts the level of cross-sections in the embryo: PPFs at the level of the pericardial cavity. **B (left):** shows the development of the mesodermal pleuro-*pericardial* folds (PPFs) from the dorsolateral body wall. As these PPFs grow toward the midline (**B (right)**), they separate the heart from the expanding lungs resulting in a division of the thoracic cavity into one pericardial cavity and two pleural cavities. The phrenic nerves are positioned within these PPFs as they descend to innervate the diaphragm. **C:** PPFs at the level of the septum transversum. **D (left):** the pleuro-*peritoneal* folds arise from the posterior body wall as well and lie in a plane that is parallel to the septum transversum and perpendicular to the pleuro-*pericardial* folds. As they grow (**D (right)**) these folds will separate the pleural from the peritoneal cavities and attach to the other three diaphragm-building structures: the lateral body wall mesoderm, the septum transversum, and the dorsal mesentery of the esophagus (see page 244 for color figure).

and may occur together with a distinct constellation of birth defects referred to as Pentalogy of Cantrell (OMIM 313850). Although these different manifestations of CDH have been well-described [26], identifying them in daily practice can be problematic because there is considerable overlap in locations. Furthermore, subtle details – such as the presence or absence of a rim of musculature might be of importance – and these are usually not recorded in medical records. The classification process is further complicated by the occurrence of another type of CDH called an eventration. This subtype is characterized by a lack of muscularization of the diaphragm leading to a thin membranous sheet of diaphragm tissue. Because eventrations can coexist with and/or be misdiagnosed as Bochdalek hernias, it is difficult to estimate its true occurrence frequency. Yet, accurate identification of the basic anatomical defect in each patient is highly important for our understanding of the molecular genetic pathways that underlie this heterogeneous disease and is considered a good risk assessment tool [27].

Further clinical classification is based on the presence or absence of other non-hernia related anomalies. If present, the case is referred to as non-isolated or complex. This is seen in 37 to 48% of infants diagnosed with CDH and display mostly cardiac, limb, orofacial, or body wall defects [23-26, 28-31]. The remaining 52-63% of the patients have isolated CDH. Malformations that are considered secondary to CDH are patent ductus arteriosus, persistent foramen ovale, intestinal malrotation and cardiac shift away from the defect.

An increasing number of CDH cases are diagnosed in the prenatal period by means of structural ultrasound in the second trimester of pregnancy. Therefore, parental counselling and treatment planning (including abstinence of care or termination of pregnancy) have evolved into detailed assessment of the fetus by a multidisciplinary team of clinicians both in terms of prognosis and presence of genetic defects. Early assessment also allows to consider fetal endoscopic interventions such as tracheal occlusion to improve lung prognostics in severe cases [32, 33]. Indeed, a recent multicentre trial showed that this procedure improved survival rates in fetuses with severe CDH, both left- and right-sided, despite more preterm deliveries [34]. However, international debate on the safety of this procedure continues and additional studies are warranted to analyse its long-term effects and its use in less severe cases.

The current postnatal treatment approach focuses in the acute phase on stabilisation of the cardio-pulmonary status and a gentle ventilation strategy, followed by surgical repair of the defect usually within 2-5 days after birth. Some 20 to 30% of the patients fail to respond to this “conventional” approach and require Extra-Corporeal Membrane Oxygenation (ECMO). Survivors of the acute phase may encounter a wide variety of short-term and long-term complications, which determine morbidity and quality of life and need to be monitored by a multidisciplinary team. It can be difficult to decide whether a chronic complication is intrinsic to CDH or secondary to its treatment. However, two international initiatives (the CDH registry and the CDH-Euro consortium) have been launched to register (acute and) chronic aspects prospectively [35-37]. It is expected that the data will allow for an evidence-based standardisation of (postnatal) care of CDH patients worldwide.

Future challenges in CDH treatment

Effectiveness of CDH-treatment protocols is hard to assess because management is not standardised internationally and population-based reports yielding enough statistical power are lacking [1, 3, 35, 37-42]. Researchers encounter differences in, for example, timing and operative approach, ventilator technique, and preference of diagnostic tests to accurately predict mortality and morbidity. Furthermore, outcome figures are greatly influenced by time of diagnosis (prenatal or at birth) and heterogeneity of the patient cohort with regard to additional malformations, size of the defect, severity of the pulmonary manifestations, CDH laterality, and presence of liver herniation [36, 40, 43]. Finally, as more patients survive, the prevalence of (long-term) morbidity will increase [44]. Notably respiratory, nutritional, musculoskeletal, neurological and gastrointestinal complications are frequent and require coordinated long-term clinical follow up [44-49].

Improved insights into the pathogenesis of CDH and its co-occurring pulmonary problems will aid the development of new treatment modalities and will enable more evidence-based counselling of parents on expected outcomes.

1.2 CDH Aetiology; complexity as a central theme

Identifying the exact cause of the congenital diaphragm anomaly has proven to be very difficult for several reasons. First of all, due to its heterogeneous and multifactorial character. The heterogeneity is reflected in the contiguous spectrum of diaphragm-defect sizes and variability in pulmonary hypoplasia severity presented in CDH children worldwide. Moreover, the diversity in associated anomalies in the complex CDH cases suggests a multifactorial base. Secondly, although strong evidence points to a genetic predisposition [26, 50-57], a significant percentage of isolated CDH cases might be the result of exposure to environmental factors at a critical embryologic time window.

The environmental base of CDH

Epidemiological studies presented evidence for an increased risk for the development of CDH by prenatal exposure to various nutritious and medicinal maternal factors such as: alcohol, smoking, periconceptional low intake of retinol, maternal body mass index above 30, antimicrobial drugs and antiepileptic drugs [24, 58-67]. Large patient cohorts would be needed to identify additional contributing environmental components, each presumably with a small effect size. However, this is hardly feasible because the disease is so rare. In addition, the maternal factors associated with an increased CDH risk identified to date are correlated to an increased risk for congenital anomalies in general and therefore not specifically linked to diaphragm defects [24, 58-63]. Recently, a potential association with the immunosuppressive drug mycophenylate mofetil (MMF) was suggested for one syndromic case of CDH with a Fryns-like phenotype [68]. The mechanism by which MMF could cause this defect is unknown. Another study reported on a low plasma free vitamin A level (consistent with moderate to severe vitamin A deficiency) in a CDH case diagnosed with PAGOD syndrome, while maternal plasma vitamin A levels were normal [69].

This report thereby refers to the “retinoid-hypothesis”, stating that disruption of the retinoid signalling pathway is involved in the pathogenesis of CDH. On a population level, association with low levels of retinol and retinol binding protein (RBP) in newborns, again independent of maternal retinol status, was recently confirmed in a case-control study [70, 71]. However, the question remains whether these changes are a primary cause of CDH or merely reflect the diseased state. Up till now, no cases of CDH in humans have been unequivocally attributed to teratogenic or environmental factors [72].

Evidence for the retinoid-hypothesis will only be briefly summarized below, since others have reviewed it extensively [54, 73-76]. Figure 2 presents a schematic overview of all the key players in the canonical retinoic acid (RA) pathway.

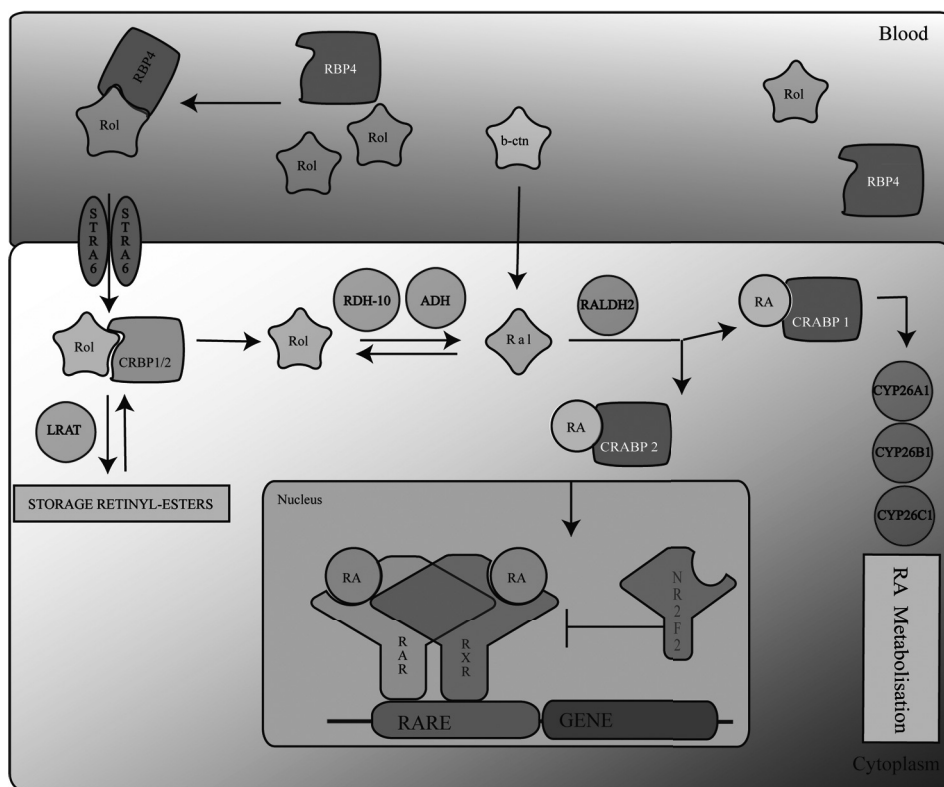


Figure 2 | Overview of ATRA metabolism and nuclear canonical RA-signalling

Circulating retinol is taken up by RBP4 and transferred intracellularly by STRA6. Transformation into retinaldehyde occurs mainly by RDH10, after which RALDH2 can generate RA. RA in turn can either bind to CRABP1 and be transported to CYP26 enzymes and metabolized into polar metabolites or bind to CRABP2 and be transported to the nucleus. In the nucleus RA will bind to a RAR/RXR heterodimer, which in turn can bind to RAREs located in the promoter area of specific genes and activate/inhibit transcription.

Rol, retinol; RBP, retinol binding protein; STRA6, stimulated by retinoic acid 6; CRBP, cellular retinol binding protein; Ra1, retinaldehyde; ADH, alcohol dehydrogenase; RALDH, retinaldehyde dehydrogenase; CYP26, cytochrome P450 26 enzymes; RAR, retinoic acid receptor; RXR, retinoid X receptor; RARE retinoic acid response element; B-ctn, beta-carotene; LRAT, Lecithin retinol acyltransferase; NR2F2; Nuclear receptor 2, subfamily F2 (see page 244 for color figure).

In the early fifties, abnormalities – among which diaphragmatic defects – observed in animal models fed on a vitamin A deficient diet (VAD) formed the first clue for the importance of vitamin A in the development of the diaphragm. Since then several studies have backed up this theory showing: 1) reduced CDH incidence after reintroduction of vitamin A in the VAD models in addition to a similar effect in teratogenic RA models [13, 15, 77-82]; 2) occurrence of CDH, albeit with markedly reduced penetrance, in (partial) knock-out models of RA-pathway genes [83-87]; 3) expression of RA pathway genes in the primordial diaphragm of in-vitro RARE perturbation studies with and without RA [14]; 4) recurrent identification in human CDH patients of affected genomic areas that harbour crucial RA-pathway genes [52]; 5) identification of mutations of the cellular retinol-binding protein-receptor (STRA6) in complex human phenotypes featuring diaphragmatic defects [88, 89]; and 6, our recent paper confirming the association between CDH and low retinol or low retinol-binding protein levels in human cases, independent of maternal status [70, 71].

Genetic strategies in the unravelling of CDH causes

When we focus on the genetic factor contributing to CDH, complexity seems to be the general theme as well. Aside from a small percentage of complex CDH cases caused by a single rare genetic mutation i.e. the monogenic disorders [72], the genetic basis in most isolated cases is expected to be complex. Large patient numbers would be needed to identify individual CDH causing genes and modifiers. This complex nature implies that most of the classic genetic approaches, based on the Mendelian laws, are difficult to apply in CDH research. A brief summary of their limitations is given below, followed by a more detailed overview of genetic data generated in human CDH cohorts by genome-wide array approaches.

Classic genetic analysis in CDH

In the ***linkage-approach*** a common haplotype among relatives with the same condition can point to a specific chromosomal region or gene causing that disease. This method requires the availability of phenotypically homogenous CDH families in which more than one child is affected. However, the majority of CDH cases are sporadic with a recurrence risk for isolated defects typically quoted as <2% [90]. In our CDH registry 12 small families have been identified, of which 9 of Dutch origin. Increasing survival rates and second-trimester ultrasound screening are expected to increase the number of reported CDH-families worldwide. Although each of these multiple kindreds deserves detailed genetic investigation, the phenotypic heterogeneity of these family cohorts itself will limit successful contribution to general CDH aetiology insights.

The ***homozygosity mapping-approach*** (which is a linkage-analysis derivative) was introduced to identify genes underlying recessive diseases [91]. It is based on the premise that there will be evidence of an enrichment of homozygosity in the genomic region harbouring the affected genes in the affected subjects. Subsequently, this method identified autosomal recessive CDH-associated syndromes such as Donnai-Barrow syndrome (OMIM 222448)[92-95] and more recently Matthew-Wood syndrome (OMIM 661086)[69, 88, 89, 96-100]. The limitation

of this method is that it can only contribute to the general knowledge of CDH if autosomal recessive syndromes have a high penetrance rate for the diaphragm defect. Yet, CDH associated syndromes usually show occurrence rates for diaphragm defects in the order <5% [72]. [Table 1]. A central registration point for detailed CDH syndrome data is available in the London Dysmorphology Medical Database; over 130 different CDH-syndromes have been reported to date [www.lmdatabases.com]. This database was recently complemented by three other genetic databases which focus on the phenotypic effects of submicroscopic chromosomal imbalances in humans including CDH: ECARUCA [http://www.ecaruca.net/], DECIPHER [http://decipher.sanger.ac.uk/] and the database of the ISCA consortium [International Standards for Cytogenomic Arrays, https://www.iscaconsortium.org/]. These find their basis in the application of molecular cytogenetic techniques such as SNP- and oligo-based arrays, which allow for the smallest-region of overlap approach at a whole new resolution level [101]. Furthermore, a database of naturally occurring and transgenic mice mutants has been set up [http://www.informatics.jax.org/]. Because the human and mice databases are linked through phenotype, gene location and synteny, they will allow for a quicker application of the **candidate-gene approach**. This method is based on phenotypic data in (knock-out) animal models and provides a platform for targeted mutation screening of human gene homologues in selected cases.

Currently, 102 CDH associated mice models are registered in the MGI database. The most informative ones have been extensively reviewed by others [28, 63, 102]. Summarized, mice that lack *c-Met*, *MyoD* or *Pax3* displayed muscularisation defects of the diaphragm, while incomplete closure of the diaphragm was observed in null mutants for *Wt1*, *RaRa/RaRβ2*, *Gata4* and *CoupTF-II*. The most recently published null mutant suggested the *Fgfr1* gene as the candidate for diaphragm defects associated with the phenotype of Wolf-Hirschhorn [57, 103, 104]. In chapter 2.2, we will show that the *Chtop* gene can be added to this list of genes causing CDH as part of a complex phenotype. However, similar to human CDH associated syndromes, diaphragmatic defects in these mice models might merely be incidental to the other observed “core” malformations since mice often do not display the diseased phenotype in a heterozygous state [104]. These dissimilarities may arise from differences between mice and humans in the genomic region surrounding the candidate gene.

The **smallest-region of overlap approach** is based on the identification of overlapping (submicroscopic) structural chromosomal anomalies in unrelated patients with a similar phenotype. These small overlapping structural aberrations (also called hot-spots) are then presumed to contain a gene or genes responsible for the development of the investigated disorder, in our case CDH. The detection-resolution of these overlapping anomalies was greatly enhanced in recent years by the development of the array technique. Subsequently, arrays were applied incidentally to a few CDH cohorts worldwide [50, 56, 105-107] and have led to the identification of the most common chromosomal CDH hot spot to date; the 15q26 monosomy [108]. Other apparent chromosome “hotspots” for CDH include: 1(q41-q42), 8p23.1 (the *GATA4* locus), 8q22.3 (the *ZFPM2* locus), and possibly (11)(q23-qter) [54], which all have been

Table 1 | CDH associated syndromes with high penetrance for diaphragm defects

| Syndrome | Locus/Gene | Associated anomalies | Proportion of patients with diaphragm defect \$ |
|----------------------------------|--|--|---|
| 15q26 microdeletion "Fryns like" | Unknown | Facial anomalies, cardiac-and urogenital anomalies, growth/mental retardation | >80% |
| Fryns | Unknown | Facial anomalies, cardiac-and renal anomalies, growth/mental retardation | >80% |
| Donnai Barrow | LRP2 | Hypertelorism, agenesi corpus callosum, omphalocele seizures | ~70% |
| Matthew Wood | STRA6 | Microphthalmia, cardiac malformation, intrauterine growth retardation | ~50% |
| Pallister Killian | Tetrasomy 12p Isochromosome 12p | Facial anomalies, CNS anomalies: mental retardation, seizures, itemporal sparseness of hair, short neck, linear streaks of skin hyperpigmentation, short broad hands | ~30% |
| 8p23.1 microdeletion | (interstitial) deletion 8p23.1 | Cardiovascular anomalies, facial dysmorphology, renal anomalies, intellectual disability | ~30% |
| Trisomy 22 or 11 | +der (22)t(11;22)(q23;q11) Trisomy 22 | Growth retardation, intellectual disability, cardiovascular malformations, facial anomalies | 5-10% |
| Cornelia de Lange | Monosomy 5pter NIPBL gene mutation | Facial anomalies, cardiac anomaly, microbrachycephaly, mental-and growth retardation | ~5% |
| Edwards | Trisomy 18 | Intrauterine growth retardation, cardiovascular anomaly, facial anomalies, clenched hands | ~1-2% |
| Wolf-Hirschhorn | Monosomy 4p16pter | Facial anomalies, midline defects, cardiac anomaly, growth-mental retardation | rare (14 cases) |
| 8q22.3-23.1 microdeletion | Monosomy 8q22.3-23.1 | Isolated congenital diaphragmatic hernia or eventration | rare ? (6? cases) |
| 1q41-42 microdeletion | Monosomy 1q41-42 | "Fryns like"-phenotype | rare ? (5? cases) |

\$ Pober et al. (2010), Goumy et al. (2010), Brady et al (2010), Wat et al. (2011)

extensively reviewed by others [52, 54, 75, 76, 109]. Because arrays are much more sensitive and cost-effective than G-banded karyotyping, the ISCA consortium recently advised this approach as an initial cytogenetic diagnostic step in congenital anomaly cohorts [110]. Application of this advise to the international CDH cohort will therefore yield more small chromosomal areas that could harbour genes involved in lung- and diaphragm development. Yet, this approach also has some limitations and flaws in general and specifically for CDH [56]. These limitations will be discussed separately in Chapters 2 and 4 of this thesis.

1.3 The Rotterdam cohort of CDH patients

The Erasmus MC – Sophia Children’s Hospital in Rotterdam, the Netherlands, is a tertiary referral centre for the multidisciplinary treatment of various congenital anomalies, including CDH. It is one of the two hospitals in the Netherlands offering ECMO treatment to CDH patients. A long-standing clinical and molecular oriented CDH research program at the department of paediatric surgery has resulted in a clinical database with detailed phenotypic data of over 600 CDH patients and a rich tissue bank of genetic material (i.e. DNA, RNA, cell lines) of these patients and their parents.

The Rotterdam CDH database currently (reference date 01-06-2011) consists of 639 CDH patients treated at the Erasmus MC – Sophia Children’s Hospital since 1988. These numbers also include 110 patients from VUmc and AMC in Amsterdam, the university medical centres in Nijmegen and Groningen and University Hospital of Mannheim, Germany; University Hospital in Leuven, Belgium, and Baylor College of Medicine, Houston, USA. Table 2 gives an overview of this cohort. Table 3 and figure 3 show the phenotype characteristics.

CDH occurs in isolated form in 339 of the 639 patients (53%), with all 53% having no identified cause. The other 300 patients (47%) exhibited at least one other congenital anomaly apart from malformations that are considered secondary to CDH. These patients are designated Complex in Table 3 and are further subdivided into Complex-Multiple major (93/300) and Complex-simple (203/300). Complex-Multiple major indicates the co-occurrence of at least two other *major* congenital anomalies. These patients are more likely to have a genetic cause or to be diagnosed with a well-defined syndrome, which indeed was demonstrated in 37 out of 93 cases. In the remaining subcohort of 203 Complex CDH patients, the additional phenotype could be classified based on the co-affected organ system (=Table 3 Complex-Simple), although this meant that some patients were assigned to multiple groups. The most frequently affected organ systems included the cardiac, urogenital and gastro-intestinal system, which is in line with literature [23, 31].

Table 4 shows an overview of the large structural chromosomal aberrations identified in the Rotterdam database in total, several of which were published before. Further detailed information on the genetic features of this cohort will be presented in Chapter 2, which deals with the clinical utility of screening for genomic alterations – using the SNP array technique – in individuals with both isolated and non-isolated diaphragmatic defects.

Table 2 | General characteristics CDH cohort Rotterdam

| Characteristic | Number of Patients | Proportion (%) | Median (range) |
|-------------------------------------|--------------------|----------------|------------------|
| Maternal obstetric | | | |
| Maternal age at delivery (years) | 288 | | 21.9 [12.6-29.4] |
| Complication during pregnancy § | 146 (355)* | 41.1 | |
| Number of Pregnancies | 277 | | |
| G1 | 113 | 40.8 | |
| G2 | 84 | 30.3 | |
| G3 | 41 | 14.8 | |
| >G3 | 39 | 14.1 | |
| Parity | 277 | | |
| P0 | 130 | 46.9 | |
| P1 | 85 | 30.7 | |
| P2 | 23 | 8.3 | |
| >P2 | 39 | 14.1 | |
| Consanguinity | 17 (557)* | 3.1 | |
| Neonatal | | | |
| Birth features | | | |
| Gestational age at delivery (weeks) | 485 | | 37.3 [27-42.5] |
| Preterm births (<37 weeks) | 117 | 24.1 | |
| Birthweight (gram) | 485 | | 2793 [726-5630] |
| Gender | 639 | | |
| Male | 366 | 57.2 | |
| Female | 273 | 42.8 | |
| Outcome variables | | | |
| Side of herniation | 639 | | |
| (Bochdalek) Left | 460 | 72.0 | |
| Right | 107 | 16.7 | |
| Bilateral | 17 | 2.7 | |
| Unknown | 55 | 8.6 | |
| Liver herniation | 145 (348)* | 41.7 | |
| L/H ratio less than 1.0 | incomplete data | | |
| Size of the defect | incomplete data | | |
| Time of diagnosis | 470 | | |
| Prenatal | 252 | 53.6 | |
| Within 1 day | 171 | 36.4 | |
| Within 1 week | 15 | 3.2 | |
| Within 4 weeks | 32 | 6.8 | |
| Outcome | 563 | | |
| Livebirths | 537 | 95.4 | |
| Stillbirths | 0 | 0.0 | |
| Termination of pregnancy | 26 (366)* | 7.1 | |
| Postnatal death | 254 | 45.1 | |
| Surgical treatment | 329 | | |
| Primary closure | 131 | 39.8 | |
| ECMO | 88 | 26.7 | |

§ including maternal drug-(ab)use, medication and maternal disease. *Number of cases with with available; info on item: It was not possible to obtain complete information on all 639 CDH cases due to incomplete medical records or medical care in other hospitals.

Table 3 | Distribution of associated malformations in Rotterdam CDH cohort

| System | Number of patients | Proportion |
|---|--------------------|------------|
| Complex-"Multiple major" § | 93 | 14.6 |
| Known structural chromosomal anomaly | 6 | 6.5 |
| Known mutation or well-defined syndrome | 37 | 39.8 |
| Unknown Cause | 56 | 60.2 |
| Complex-"simple" | 207 | 32.4 |
| Cardiovascular | 60 | 29.0 |
| Gastro-intestinal | 38 | 18.4 |
| Urogenital | 50 | 24.2 |
| Musculoskeletal | 30 | 14.5 |
| Central Nervous (Neuro-general and Cranium-Brain) | 20 | 35.7 |
| Limb abnormalities | 39 | 18.8 |
| Syndromic (including facial dysmorphisms) & | 72 | 34.8 |
| Isolated | 339 | 53.1 |
| Totaal | 639 | |

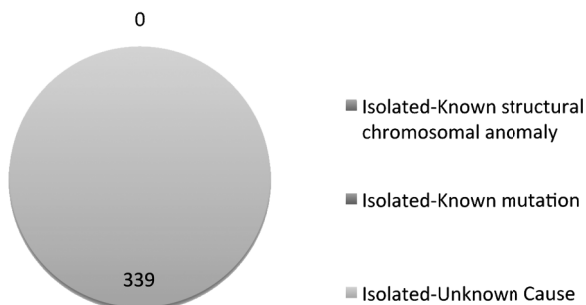
§ Multiple Major defined as more than 2 additional major anomalies. An anomaly is considered major if it implicates loss of function or requires operative care.

& Defined as abnormalities that go along with an increased risk of malformations or genetic abnormalities but do not define a disease themselves.

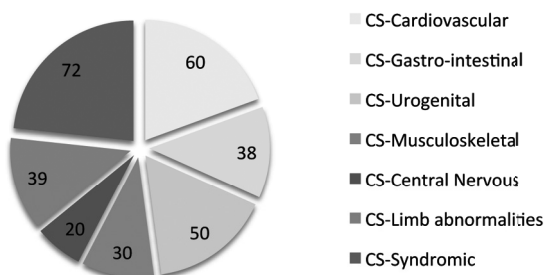
1.4 Epigenetic analysis in CDH

The primary focus of congenital anomaly studies in the past has been solely on the identification of genetic mutations – in other words, errors that changed the linear order of the DNA sequence. Indeed, increasing insights into the frequency of DNA-variation and errors -both in normal as well as in diseased cohorts- has provided valuable insight into the genetic mechanisms behind physiologic and pathophysiologic human phenotypes. However, epigenetic features of the genome might be of equal and crucial importance to genomic functions. The hypothesis of multiple environmental factors disrupting normal diaphragm development by means of alterations in the epigenome therefore reflects on a more general paradigm shift in developmental biology [111]. Both epigenetic factors and genetic factors are now thought to regulate embryonic development. Since numerous epigenetic factors – each with a distinct role – have been identified since the 1970s (DNA methylation, histone modification, chromatin structure, small non-coding RNAs) another complex layer in the process of developmental regulation is added. New high-resolution, genome-wide, molecular techniques enable rapid identification of these epigenetic marks nowadays. Yet, the lack of human early-embryonic diaphragm- and lung-tissue remains an impediment to this process. Interestingly, the epigenome now provides us with a mechanism in which paternal exposure to environmental factors may induce developmental defects [112], including those of the diaphragm.

Isolated



Complex-Simple



Complex-Multiple Major

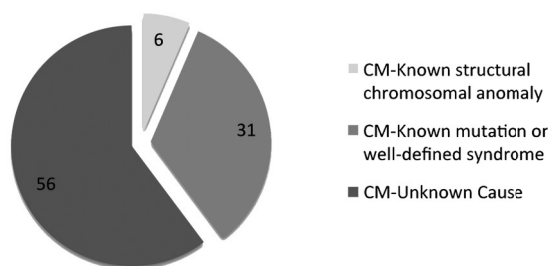


Figure 3 | Classification of patients Rotterdam CDH cohort

CDH patients can either present with an isolated defect only (Isolated) or as part of a complex phenotype (Complex), meaning that in the latter group the defect is accompanied by other congenital anomalies. Usually these additional birth defects only affect 1 other organ system or consist of minor abnormalities (Complex-Simple). The term Complex-Major describes those CDH subjects that are more severely affected, defined by the co-occurrence of *at least two other major* congenital anomalies. In turn, these three subgroups can be further subdivided based on the type of causative genetic aberration present (Isolated and Complex-Major) or based on the type of additional affected organ system (complex-Simple). CM, Complex-Major; CS, Complex-Simple (see page 245 for color figure).

Table 4 | Structural Chromosomal anomalies/Syndromes identified in Rotterdam CDH cohort

| Type of (large) Structural Chromosomal anomaly | Number of patients | Reference |
|--|--------------------|----------------------------------|
| 46,XX,del(1)(p36.23),dup(1)(p36.23p36.22) | 1 | |
| 46,XX,inv(1)(p36.1q42)pat | 1 | Thesis Klaassens et al. |
| 46,XY,der(3)t(3;8)(p23.1;p23.1)pat | 1 | Thesis Klaassens et al. |
| 46,XY,der(3)t(3;11)(p25.1;q23.1)mat | 1 | |
| 46,XY,ish del(4)(p16.1) | 2 | van Dooren et al., Veenma et al. |
| 46,XY.arr 4p15.2p14(22,819,570-36,306,519)x1 | 1 | |
| 46,XX,der(5)t(5;12)(p13.2;p12.3) | 1 | Veenma et al. |
| 46,XY,inv(6),t(1:14), del(15)(q26) | 1 | Klaassens et al. |
| 46,XX,del(8)(q23.1q23.1)(mat) | 1 | Wat et al. |
| 46,XX.arr 9p11(0- 46.310.390)x4 | 1 | |
| 47,XX,+i(12)p | 2 | Thesis Klaassens et al. |
| 46,XY,der(12)t(11;12)(q23.3;q24.3)mat | 1 | Klaassens et al. |
| 47,XX,+13 or 47,XY, +13 | 2 | Thesis Klaassens et al. |
| 46,XX,r(15)(p11q26.1) | 1 | Klaassens et al. |
| 46,XY,r(15)(p11q26) | 1 | Klaassens et al. |
| 46,XX,der(15)t(2:15)(q37.2;q26.2) | 1 | Klaassens et al. |
| 46,XX,der(15)t(4;15)(q35;q26.1) | 1 | |
| 46,XY.arr 15q11.2q13.1(18.421.386-27.018.622)x3 | 1 | |
| 46,XX.arr 15q25.2q25.2(80,689,404-82,938,351)x1, 17p12 (14.049.619-15.497.020)x3 | 1 | |
| 46,XY.arr 17q21q21(39,182,612-39,660,170)x1 | 1 | |
| 47,XX,+18 or 47, XY, +18 | 9 | Thesis Klaassens et al. |
| 47,XX,+21 or 47, XY, +21 | 4 | Thesis Klaassens et al. |
| 47,XY,t(5:21),+21 | 1 | Thesis Klaassens et al. |
| 46,XX,der(22)t(9;22)(q13;q13) | 1 | |
| 47,XY,der(22)t(11;22)q23.3;q11.2)mat | 1 | Klaassens et al. |
| 46,XX.arr 22q11.21(17,249,767-17,392,385)x1 pat | 1 | |
| 46,XX.arr Xp22.31(0-8681596)x1, Xp22.31p22.11(8681596-24776649)x3 pat | 1 | |
| 46,XY.arr Xq21.1q21.32(79,399,169-92,250,507)x3 | 1 | |
| | 42 | |

| Type of Syndrome | Number of patients |
|---|-----------------------------|
| Babuki | 1 |
| Beckwith-wiedemann | 1 |
| Cohen | 1 |
| Cornelia de Lange | 4 (1 proven NIPBL mutation) |
| OAIS complex | 1 |
| Opitz | 1 |
| Pentology of Cantrell | 1 |
| Sex-reversal | 3 |
| Simpson-Golabi | 1 (proven GPC3 mutation) |
| Steinert's | 3 |
| VACTERL | 2 |
| | 19 |
| New genetic Mutations of undefined significance | Number of patients |
| HCCS mutation (paternal) | 1 |
| FOP mutation (maternal) | 1 |
| SHOX duplication (maternal) | 1 |
| | 3 |
| Total | 64 |

Grey color; recently identified and/or Discussed in this thesis.

The role of three-dimensional nuclear genome organisation on gene transcription

Numerous factors are known to be key in gene expression regulation. For instance, the binding of a specific transcription factor (TF) complex (consisting of several tissue-specific units) to the promoter of a gene has been recognized for a long time. Yet, this TF-complex binding requires accessibility of the chromatin fiber by means of recruitment of remodeling factors and DNA/Histone modifying enzymes in a so called "chromatin hub". The human genome consists of 3×10^9 base pairs divided over 23 chromosomes and is packaged and folded to allow for storage in a cell nucleus with a diameter of around 5 micrometres. Therefore, modification of the chromatin fiber – leading to dynamic changes in DNA strand accessibility- is considered equally important to the process of gene transcription. Besides these primary and secondary characteristics of chromatin structure, researchers gained interest in a possible role of the genome's three-dimensional positioning in the nuclear space on its expression regulation. It was found that chromosome territories (CT) occupy an evolutionary well-conserved specific radial location within the nucleus [113], yet cell-type specific [114-116]. Moreover, spatial positioning on an individual gene level was shown to impact gene expression regulation. In this respect, several groups studied the positioning of genes/chromosome segments relative to their CT and relative to the lamina [117-123]. Interestingly, some of these lamina-related processes have already been linked to

the pathophysiology of certain neurodegenerative and muscular diseases [124-126], which emphasizes the functional relevance of spatial positioning. Preferential long-range interactions between gene-loci have been identified as well, mainly in-cis and on the same chromosome [127, 128] but also in-trans and between different chromosomes [129-133]. These physical associations may serve different processes, such as 1) the sharing of common regulatory resources for gene activation/silencing during specific differentiation- and developmental programs; 2) the association and notification of homologous alleles prior to silencing during imprinting or X-inactivation; and 3) the induction of physiologic rearrangements (in case of olfactory and cytokine receptor choice) or even pathologic translocation events [134, 135].

Although debate continues on several aspects of chromosomal interactions, changes in these interaction patterns during development and/or as a consequence of cell differentiation are thought to represent a specific blueprint of the functional output of the genome. Interestingly, these blueprints might in turn serve as markers to identify diseased states [125, 136, 137]. Therefore, many research initiatives have focused on adequate research techniques to investigate the spatial ordering of the genome. Below, we will briefly elaborate on Multicolour three-dimensional FISH (M-FISH) and Chromosome Conformation Capture-sequence (3C-seq): complementary epigenetic research tools that enable identification of interacting elements of the genome. Both techniques were applied to analyse the possibility of a changing nuclear architecture as one of the elements in CDH-pathophysiology (Chapter 3).

Conventional fluorescence in situ hybridization (FISH) is a widely used molecular cytogenetic technique in which fluorescently labelled DNA probes are hybridised to metaphase spreads or interphase nuclei for chromosome analysis or for studies of the chromosomal location of specific DNA segments [138]. Cremer et al. [139] developed an adaptation to the standard FISH protocol, which allowed for both preservation of the nuclear structure and for an efficient probe accessibility. In turn, FISH on 3D-preserved nuclei (3D-FISH) in combination with 3D-(confocal) microscopy and image reconstruction emerged as an efficient tool to analyse the spatial arrangement of targeted genomic sequences in the nucleus [139]. Subsequently, developments in next-generation confocal microscopes made possible distinct visualization of at least five different fluorochromes within one experiment and opened up the way for multicolour 3D-FISH experiments. Thus, numerous differently labelled nuclear targets could now be delineated simultaneously and their spatial interrelationships could be analysed on the level of individual nuclei [139]. However, multicolour 3D-FISH has several limitations. It is a relatively low-throughput technique that allows the analysis of only a few hundred nuclei in a single experiment. Perhaps this limitation will be overcome as more high-throughput and automated FISH scanning techniques are being developed [140]. Sensitive detection and discrimination of separate DNA loci is limited by the size of the used probes (commonly 100-150 kb) and the size of the recorded image stacks by confocal microscopy. Also, multicolour 3D-FISH cannot distinguish between loci that are very close to each other or come into contact and it is also biased towards the loci or nuclear structures selected for analysis. Finally, when fixed cells are used, this technique only enables analysis of spatial arrangements in a non-dynamic/static way.

In order to get a less biased look on the general concepts of nuclear spatial organisation, several high-throughput approaches were recently developed, among which the Chromosome Conformation Capture (3C) technique – first described by Dekker et al. [141] and adjusted (4C) by de Laat and co-workers [128, 142]. The 4C-technique identifies all the DNA fragments in the genome that are frequently in spatial vicinity to a selected locus. 4C protocols (Figure 4, adapted from E. Splinter [143]) begin with “cross-linking” using formaldehyde to fix the DNA to its associated proteins. Next, the DNA is cut up with restriction enzymes giving rise to “hairballs” of tangled DNA and protein. Then, ligation products of DNA strands that had been close together on the same “hairball” are generated to create hybrid molecules. The ligation junctions are then trimmed and circularised after de-crosslinking. Next, DNA fragments captured by a locus of interest are simultaneously amplified via inverse PCR using bait-specific primers that amplify circularised ligation products. Finally, PCR products are analysed by large-scale sequencing.

In parallel to 3D-FISH, the 4C-technique has disadvantages as well. Separation of relevant hybrid molecules from the background signal requires replication of experiments and specialised bio-informatics approaches. Most of the hybrid DNA molecules produced by 4C are the result of random interactions, particularly between loci that are just a few kilobases apart on the same chromosome. In addition, chromosome conformation capture represents a stochastic “averaged” view of genomic interactions in millions of cells at the same time. The resulting high number of interacting regions makes it unlikely that all these contacts are made simultaneously in the same nucleus. Instead, many different combinations of preferential contacts exist in a population of cells at any point in time, and 4C-confirmatory FISH experiments showed that co-associations are usually of low frequency (less than 10% of cells at a given point in time)[144, 145]. In conclusion, Multicolour 3D-FISH and 4C are complementary epigenetic research tools, which enable to identify interacting elements of the genome.

1.5 Aim and Outline of this thesis

Chapter 2: Copy Number Variations and mutations in the CDH cohort

In line with the paragraph on “genetic strategies in the unravelling of CDH causes”, the second chapter of this thesis will mainly focus on all different aspects of Copy Number Variation (CNV) research in article 1 describing CDH cases.

It starts with the search for germ-line and somatic CNV events in 117 CDH patients registered in Rotterdam that yielded both known CDH-associated chromosomal hot spots and new ones. The possibility of somatic mutations restricted to the affected diaphragm tissue was excluded by screening for CNVs in affected tissue of 13 isolated CDH patients. Finally, targeted screening of a new CDH-candidate gene in a selected subgroup of complex patients identified an inherited Chromatin target of Prmt1 (*Chtop*) mutation (Article 2). Since *Chtop* is a main target of the protein arginine methyltransferase Prmt1 [146], this mutation stresses the possibility that DNA errors in chromatin associated protein genes might confer epigenetic susceptibility to CDH.

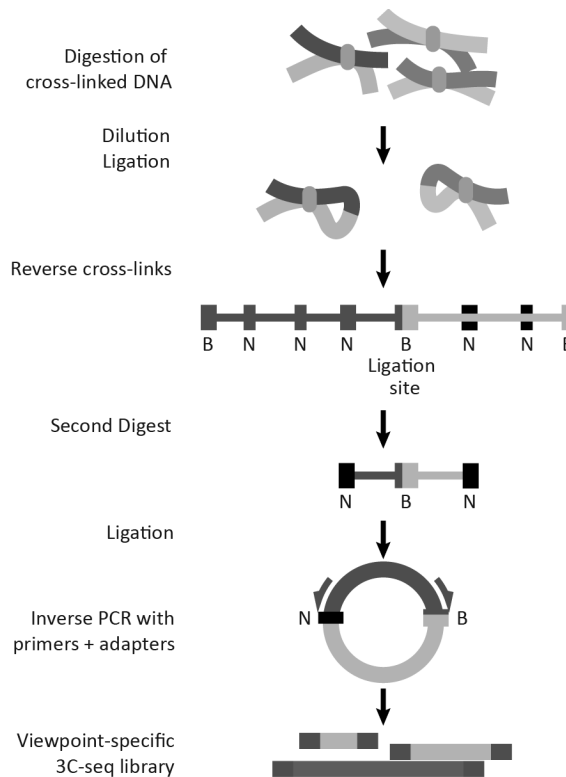


Figure 4 | Schematic overview of the 4C-sequencing (4C-seq) method

Sample preparation in *4C-sequencing (4C-seq)* is similar to the earlier published *4C-array* protocols [127] apart from some small adjustments (adding adapter-sequences) in the primer design stage. The *4C-seq* method has the advantage of improved signal to noise ratios over the *4C-array* approach. Briefly, nuclei are fixed with formaldehyde to cross-link co-localising chromatin (red and blue lines, light-and dark-green lines). DNA is digested with a restriction enzyme, for example Bgl-II. After dilution of the sample, cross-linked fragments are ligated (ideally only at one end), and subsequently cross-links are reversed. This way, the Bgl-II fragment of interest (red line) is ligated to fragments co-localised (blue line) within the studied cell-population. Next, ligation products are trimmed by digestion with a frequent cutting enzyme (NLA-III), because Bgl-II fragments are too big to be amplified by PCR. The trimmed products are circularised, such that an inverse PCR on the red fragment will amplify its interacting (blue) partners. Of note, the “contents” of the circles formed between cross-linked DNA fragments vary depending on the three-dimensional structure at the start of the protocol and whether ligation occurs to one or both ends of the cross-linked material (grey and black lines [127]). All these sequences can be analysed by next-generation sequencing (see page 245 for color figure).

Chapter 2 then continues with article 3, describing germ-line CNV events in another international cohort of CDH patients. In addition, in this article we searched for *Zfpm2* (alias *fog2*) mutations in a specific cohort of 52 CDH/Eventration patients. The discussion highlights the identification of *Zfpm2* aberrations in isolated patients with reduced penetrance, the further delineation of the well-known 1q41-42 CDH hot spot, and the identification of a new CDH candidate gene called frizzled-2 (*Fzd2*). All these elements strongly endorse the recent initiative of the ISCA consortium

for screening CDH patients with array-based techniques. It also shows the importance of availability of parental material, since most rare CNVs in the isolated CDH subgroup are inherited.

The fourth article in this chapter elaborates on the possibility of CNV (mutations) occurring in somatic cells only, by looking into the CNV status of a unique cohort of discordant monozygotic twins. The occurrence of phenotypic differences between MZ twins is commonly attributed to environmental factors. Yet, recently several lines of evidence showed that both genetic and epigenetic factors could play a role in phenotypic discordance after all.

In the fifth article of Chapter 2, we present the detailed clinical and cytogenetic analysis of a prenatally detected complex CDH in a patient with a mosaic unbalanced translocation t(5;12). Identification of this specific case underscores the possibility of association of low-level mosaicism with severe birth defects. It also stresses the importance of collecting and analysing tissues of both spontaneous and induced CDH-abortions. Because these fetuses are more likely genetically affected, tissue analysis might provide valuable insight into CDH pathophysiology. To put similar (mosaic) results into a better clinical perspective, material from terminated pregnancies of phenotypically normal fetuses should be checked for the occurrence of this type of somatic aberrations as well.

Chapter 3: Disrupted RA signalling in CDH: gene-expression & patho-epigenetic mechanisms in 15q26 monosomy patients and the nitrofen rodent model

The first article in this chapter describes the spatial positioning of CDH candidate genes in a 15q26 deleted fibroblast patient model. Disruption of the multi-gene locus on chromosome 15q leads to a distinct constellation of birth defects with 100% mortality. The cardinal clinical finding of this microdeletion syndrome is a defect of the diaphragm, which suggests a causative role of haploinsufficiency of 15q26 genes in diaphragm development. In addition, candidate genes in this region are involved in retinoic acid signalling, one of the most important pathways thought to be disrupted in CDH. Subsequently, gene-ontology analysis pointed to the *NR2F2* gene (OMIM 107773) as one of the most promising 15q candidates. Nevertheless, a concomitant search for pathologic *NR2F2* mutations in >450 isolated CDH samples worldwide failed to identify any. These data implied that additional – possibly epigenetic – mechanisms affecting the normal expression of 15q26 genes could account for the diaphragm defect. Therefore, in this article we hypothesise and investigate the possible role of three-dimensional co-association of CDH candidate genes in the nuclear space as a requirement for their coordinated expression during diaphragm development.

Article 2 continues with work on the 15q26 monosomy model. In this manuscript we compared the genome-wide expression patterns of two 15q deleted fibroblast cell lines to those of healthy controls with and without RA induction. Extensive patient-oriented and animal based research suggests that disruption of RA- signalling plays a small but crucial role in the pathophysiology of CDH. In this manuscript, we assumed that deleted genes in the 15q area could be crucial for both CDH and RA-signalling. Secondly, we hypothesized that overstimulation of 15q26 deleted fibroblast cell cultures with vitamin A could mimic a normal “healthy” genome

wide expression status or at least elicit different effects as compared to controls. Goumy et al. [147] proposed that skin fibroblasts form an excellent model system to study the different components of the RA pathway in CDH, since they have the same mesodermal origin as diaphragm tissue and express all the necessary metabolic components of this pathway. The main output measures in this study concerned the expression array profiles of RNA isolated from the two 15q26 monosomy CDH patients versus two sex-matched controls after a 48-hour period of four different RA-concentration stimulations. Results showed that this “complex-phenotype approach” is indeed able to shed new light on the existent knowledge of 15q26- and RA- candidate CDH-genes and point to several new early mesenchymal and lung vascular candidate factors.

In the third article of Chapter 3 we show the results of our search for new association partners of the *NR2F2* gene in a rodent CDH model using Chromosome Conformation Capture-sequencing (4C-seq). This technique, which was recently developed in Erasmus MC, identifies all the genomic regions in contact with a locus of interest. It is based on formaldehyde cross-linking and locus-specific PCR to detect the physical contacts between genomic loci. We hypothesized that we would find differences in global DNA interactions patterns by comparing 4C contacts between normal and CDH-induced (Nitrofen) rats. Since such contacts are known to be tissue-specific, we analysed material of both CDH-affected (lung, diaphragm) and unaffected-tissues (liver, heart).

Chapter 4: General Discussion

In this chapter we place all findings in a broader perspective.

We start off with the current views and pitfalls of application of array techniques to congenital anomaly cohorts such as CDH. Next, we briefly comment on the usefulness of the 4C technique in general and summarise the current views on how genome-wide DNA-DNA interactions can contribute to gene-expression regulation. Our expression array results of chapter 3 stressed the putative importance of disruption of early developmental factors/master regulators in CDH, which in turn may cause or confer susceptibility to both the lung- and diaphragm defects in patients. We speculate that it is likely that the same genetic disturbances target both similar cell types and cell-processes in lung- and diaphragm development. An overall summary of the current knowledge of diaphragm development is provided, thereby specifically focusing on the underlying molecular signalling pathways. In this respect, an alternative RA-signalling disruption pathway is hypothesized to be important for diaphragm maldevelopment as well. Finally, we close off with some ideas on future CDH research; proposing the induced Pluripotent Stem Cell (iPSC) technique as a sophisticated way to circumvent the lack of human early-embryonic diaphragm and lung-tissue.

References

1. Brownlee, E.M., et al., *The hidden mortality of congenital diaphragmatic hernia: a 20-year review*. Journal of pediatric surgery, 2009. **44**(2): p. 317-20.
2. Gallot, D., et al., *Prenatal detection and outcome of congenital diaphragmatic hernia: a French registry-based study*. Ultrasound in obstetrics & gynecology : the official journal of the International Society of Ultrasound in Obstetrics and Gynecology, 2007. **29**(3): p. 276-83.
3. Mah, V.K., P. Chiu, and P.C. Kim, *Are we making a real difference? Update on 'hidden mortality' in the management of congenital diaphragmatic hernia*. Fetal diagnosis and therapy, 2011. **29**(1): p. 40-5.
4. Sluiter, I., et al., *Congenital diaphragmatic hernia: Still a moving target*. Seminars in fetal & neonatal medicine, 2011.
5. Keijzer, R. and P. Puri, *Congenital diaphragmatic hernia*. Seminars in pediatric surgery, 2010. **19**(3): p. 180-5.
6. Keijzer, R., et al., *Dual-hit hypothesis explains pulmonary hypoplasia in the nitrofen model of congenital diaphragmatic hernia*. The American journal of pathology, 2000. **156**(4): p. 1299-306.
7. Jesudason, E.C., et al., *Early lung malformations in congenital diaphragmatic hernia*. Journal of pediatric surgery, 2000. **35**(1): p. 124-7; discussion 128.
8. Iritani, I., *Experimental study on embryogenesis of congenital diaphragmatic hernia*. Anatomy and embryology, 1984. **169**(2): p. 133-9.
9. Kluth, D., et al., *Nitrofen-induced diaphragmatic hernias in rats: an animal model*. Journal of pediatric surgery, 1990. **25**(8): p. 850-4.
10. Wells, L., *Development of the human diaphragm and pleural sacs*, C.E.C. Inst, Editor 1954.
11. Allan, D.W. and J.J. Greer, *Embryogenesis of the phrenic nerve and diaphragm in the fetal rat*. The Journal of comparative neurology, 1997. **382**(4): p. 459-68.
12. Allan, D.W. and J.J. Greer, *Pathogenesis of nitrofen-induced congenital diaphragmatic hernia in fetal rats*. Journal of applied physiology, 1997. **83**(2): p. 338-47.
13. Clugston, R.D., et al., *Understanding abnormal retinoid signalling as a causative mechanism in congenital diaphragmatic hernia*. Am J Respir Cell Mol Biol, 2010. **42**(3): p. 276-85.
14. Clugston, R.D., W. Zhang, and J.J. Greer, *Gene expression in the developing diaphragm: significance for congenital diaphragmatic hernia*. American journal of physiology. Lung cellular and molecular physiology, 2008. **294**(4): p. L665-75.
15. Clugston, R.D., W. Zhang, and J.J. Greer, *Early development of the primordial mammalian diaphragm and cellular mechanisms of nitrofen-induced congenital diaphragmatic hernia*. Birth defects research. Part A, Clinical and molecular teratology, 2010. **88**(1): p. 15-24.
16. Greer, J.J., et al., *Recent advances in understanding the pathogenesis of nitrofen-induced congenital diaphragmatic hernia*. Pediatric pulmonology, 2000. **29**(5): p. 394-9.
17. Greer, J.J., et al., *An overview of phrenic nerve and diaphragm muscle development in the perinatal rat*. Journal of applied physiology, 1999. **86**(3): p. 779-86.
18. Cuschieri, A., *Development of the Respiratory System and Diaphragm*, University of Malta: Malta.
19. Smith, N.P., et al., *Recent advances in congenital diaphragmatic hernia*. Archives of disease in childhood, 2005. **90**(4): p. 426-8.
20. Mayer, S., R. Metzger, and D. Kluth, *The embryology of the diaphragm*. Seminars in pediatric surgery, 2011. **20**(3): p. 161-9.
21. Kluth, D., et al., *Embryology of congenital diaphragmatic hernia*. Seminars in pediatric surgery, 1996. **5**(4): p. 224-33.
22. Torfs, C.P., et al., *A population-based study of congenital diaphragmatic hernia*. Teratology, 1992. **46**(6): p. 555-65.
23. Zaiss, I., et al., *Associated malformations in congenital diaphragmatic hernia*. American journal of perinatology, 2011. **28**(3): p. 211-8.
24. Caspers, K.M., et al., *Maternal periconceptional exposure to cigarette smoking and alcohol consumption and congenital diaphragmatic hernia*. Birth Defects Res A Clin Mol Teratol, 2010.

25. Robert, E., B. Kallen, and J. Harris, *The epidemiology of diaphragmatic hernia*. European journal of epidemiology, 1997. **13**(6): p. 665-73.
26. Pober, B.R., *Overview of epidemiology, genetics, birth defects, and chromosome abnormalities associated with CDH*. Am J Med Genet C Semin Med Genet, 2007. **145C**(2): p. 158-71.
27. Congenital Diaphragmatic Hernia Study, G., et al., *Defect size determines survival in infants with congenital diaphragmatic hernia*. Pediatrics, 2007. **120**(3): p. e651-7.
28. Ackerman, K.G. and J.J. Greer, *Development of the diaphragm and genetic mouse models of diaphragmatic defects*. Am J Med Genet C Semin Med Genet, 2007. **145**(2): p. 109-16.
29. Wung, J.T., et al., *Congenital diaphragmatic hernia: survival treated with very delayed surgery, spontaneous respiration, and no chest tube*. Journal of pediatric surgery, 1995. **30**(3): p. 406-9.
30. Tennant, P.W., et al., *20-year survival of children born with congenital anomalies: a population-based study*. Lancet, 2010. **375**(9715): p. 649-56.
31. Witters, I., et al., *Associated malformations and chromosomal anomalies in 42 cases of prenatally diagnosed diaphragmatic hernia*. Am J Med Genet A, 2001. **103**(4): p. 278-82.
32. Deprest, J.A., K. Nicolaidis, and E. Gratacos, *Fetal surgery for congenital diaphragmatic hernia is back from never gone*. Fetal diagnosis and therapy, 2011. **29**(1): p. 6-17.
33. Deprest, J.A., et al., *Changing perspectives on the perinatal management of isolated congenital diaphragmatic hernia in Europe*. Clin Perinatol, 2009. **36**(2): p. 329-47, ix.
34. Jani, J.C., et al., *Severe diaphragmatic hernia treated by fetal endoscopic tracheal occlusion*. Ultrasound in obstetrics & gynecology : the official journal of the International Society of Ultrasound in Obstetrics and Gynecology, 2009. **34**(3): p. 304-10.
35. Reiss, I., et al., *Standardized postnatal management of infants with congenital diaphragmatic hernia in Europe: the CDH EURO Consortium consensus*. Neonatology, 2010. **98**(4): p. 354-64.
36. Tsao, K. and K.P. Lally, *The Congenital Diaphragmatic Hernia Study Group: a voluntary international registry*. Seminars in pediatric surgery, 2008. **17**(2): p. 90-7.
37. van den Hout, L., et al., *Can we improve outcome of congenital diaphragmatic hernia?* Pediatric surgery international, 2009. **25**(9): p. 733-43.
38. Colvin, J., et al., *Outcomes of congenital diaphragmatic hernia: a population-based study in Western Australia*. Pediatrics, 2005. **116**(3): p. e356-63.
39. Dott, M.M., L.Y. Wong, and S.A. Rasmussen, *Population-based study of congenital diaphragmatic hernia: risk factors and survival in Metropolitan Atlanta, 1968-1999*. Birth defects research. Part A, Clinical and molecular teratology, 2003. **67**(4): p. 261-7.
40. Stege, G., A. Fenton, and B. Jaffray, *Nihilism in the 1990s: the true mortality of congenital diaphragmatic hernia*. Pediatrics, 2003. **112**(3 Pt 1): p. 532-5.
41. van den Hout, L., et al., *Actual outcome in infants with congenital diaphragmatic hernia: the role of a standardized postnatal treatment protocol*. Fetal diagnosis and therapy, 2011. **29**(1): p. 55-63.
42. Mah, V.K., et al., *Absolute vs relative improvements in congenital diaphragmatic hernia survival: what happened to "hidden mortality"*. Journal of pediatric surgery, 2009. **44**(5): p. 877-82.
43. Skari, H., et al., *Congenital diaphragmatic hernia: a meta-analysis of mortality factors*. J Pediatr Surg, 2000. **35**(8): p. 1187-97.
44. Peetsold, M.G., et al., *The long-term follow-up of patients with a congenital diaphragmatic hernia: a broad spectrum of morbidity*. Pediatric surgery international, 2009. **25**(1): p. 1-17.
45. Peetsold, M.G., et al., *Pulmonary function and exercise capacity in survivors of congenital diaphragmatic hernia*. The European respiratory journal : official journal of the European Society for Clinical Respiratory Physiology, 2009. **34**(5): p. 1140-7.
46. Peetsold, M.G., et al., *Psychological outcome and quality of life in children born with congenital diaphragmatic hernia*. Archives of disease in childhood, 2009. **94**(11): p. 834-40.
47. Peetsold, M.G., et al., *Congenital diaphragmatic hernia: long-term risk of gastresophageal reflux disease*. Journal of pediatric gastroenterology and nutrition, 2010. **51**(4): p. 448-53.
48. Valfre, L., et al., *Long term follow-up in high-risk congenital diaphragmatic hernia survivors: patching the diaphragm affects the outcome*. Journal of pediatric surgery, 2011. **46**(1): p. 52-6.

49. van der Cammen-van Zijp, M.H., et al., *Motor-function and exercise capacity in children with major anatomical congenital anomalies: an evaluation at 5 years of age*. Early Hum Dev, 2010. **86**(8): p. 523-8.
50. Holder, A.M., et al., *Genetic factors in congenital diaphragmatic hernia*. Am J Hum Genet, 2007. **80**(5): p. 825-45.
51. Kantarci, S. and P.K. Donahoe, *Congenital diaphragmatic hernia (CDH) etiology as revealed by pathway genetics*. Am J Med Genet C Semin Med Genet, 2007. **145C**(2): p. 217-26.
52. Scott, D.A., *Genetics of congenital diaphragmatic hernia*. Semin Pediatr Surg, 2007. **16**(2): p. 88-93.
53. Pober, B.R., *Genetic aspects of human congenital diaphragmatic hernia*. Clin Genet, 2008. **74**(1): p. 1-15.
54. Klaassens, M., A. de Klein, and D. Tibboel, *The etiology of congenital diaphragmatic hernia: still largely unknown?* Eur J Med Genet, 2009. **52**(5): p. 281-6.
55. Slavotinek, A.M., et al., *Sequence variants in the HLX gene at chromosome 1q41-1q42 in patients with diaphragmatic hernia*. Clin Genet, 2009. **75**(5): p. 429-39.
56. Wat, M.J., Veenma, D.C.M, *Genomic alterations that contribute to the development of isolated and non-isolated congenital diaphragmatic hernia*. J med Genet, 2011. **48**(5): p. 299-307.
57. LopezJimenez, N., et al., *Examination of FGFR1 as a candidate gene for diaphragmatic defects at chromosome 4p16.3 shows that Fgfr1 null mice have reduced expression of Tpm3, sarcomere genes and Lrtm1 in the diaphragm*. Hum Genet, 2010. **127**(3): p. 325-36.
58. Yang, W., et al., *Nutrient intakes in women and congenital diaphragmatic hernia in their offspring*. Birth Defects Res A Clin Mol Teratol, 2008. **82**(3): p. 131-8.
59. Yang, W., et al., *Epidemiologic characteristics of congenital diaphragmatic hernia among 2.5 million California births, 1989-1997*. Birth Defects Res A Clin Mol Teratol, 2006. **76**(3): p. 170-4.
60. Waller, D.K., et al., *Prepregnancy obesity as a risk factor for structural birth defects*. Arch Pediatr Adolesc Med, 2007. **161**(8): p. 745-50.
61. Felix, J.F., et al., *Environmental factors in the etiology of esophageal atresia and congenital diaphragmatic hernia: results of a case-control study*. Birth Defects Res A Clin Mol Teratol, 2008. **82**(2): p. 98-105.
62. Bos, A.P., et al., *Etiological aspects of congenital diaphragmatic hernia: results of a case comparison study*. Hum Genet, 1994. **94**(4): p. 445-6.
63. Beurskens, L.W., D. Tibboel, and R.P. Steegers-Theunissen, *Role of nutrition, lifestyle factors, and genes in the pathogenesis of congenital diaphragmatic hernia: human and animal studies*. Nutr Rev, 2009. **67**(12): p. 719-30.
64. Silvani, P. and A. Camporesi, *Drug-induced pulmonary hypertension in newborns: a review*. Curr Vasc Pharmacol, 2007. **5**(2): p. 129-33.
65. Crider, K.S., et al., *Antibacterial medication use during pregnancy and risk of birth defects: National Birth Defects Prevention Study*. Arch Pediatr Adolesc Med, 2009. **163**(11): p. 978-85.
66. Cook, J.C., et al., *Analysis of the nonsteroidal anti-inflammatory drug literature for potential developmental toxicity in rats and rabbits*. Birth Defects Res B Dev Reprod Toxicol, 2003. **68**(1): p. 5-26.
67. Carter, T.C., et al., *Antifungal drugs and the risk of selected birth defects*. Am J Obstet Gynecol, 2008. **198**(2): p. 191 e1-7.
68. Parisi, M.A., et al., *Congenital diaphragmatic hernia and microtia in a newborn with mycophenolate mofetil (MMF) exposure: phenocopy for Fryns syndrome or broad spectrum of teratogenic effects?* Am J Med Genet A, 2009. **149A**(6): p. 1237-40.
69. Gavrilova, R., et al., *Vitamin A deficiency in an infant with PAGOD syndrome*. American journal of medical genetics. Part A, 2009. **149A**(10): p. 2241-7.
70. Beurskens, L.W., et al., *Retinol status of newborn infants is associated with congenital diaphragmatic hernia*. Pediatrics, 2010. **126**(4): p. 712-20.
71. Major, D., et al., *Retinol status of newborn infants with congenital diaphragmatic hernia*. Pediatr Surg Int, 1998. **13**(8): p. 547-9.

72. Pober, B.R., M.K. Russell, and K.G. Ackerman, *Congenital Diaphragmatic Hernia Overview*, in *GeneReviews*, R.A. Pagon, et al., Editors. 2006: Seattle (WA).
73. Montedonico, S., N. Nakazawa, and P. Puri, *Congenital diaphragmatic hernia and retinoids: searching for an etiology*. *Pediatr Surg Int*, 2008. **24**(7): p. 755-61.
74. Greer, J.J., R.P. Babiuk, and B. Thebaud, *Etiology of congenital diaphragmatic hernia: the retinoid hypothesis*. *Pediatr Res*, 2003. **53**(5): p. 726-30.
75. Goumy, C., et al., *Retinoid Pathway and Congenital Diaphragmatic Hernia: Hypothesis from the Analysis of Chromosomal Abnormalities*. *Fetal Diagn Ther*, 2010. **28**(3): p. 29-39.
76. Brady, P.D., et al., *Recent developments in the genetic factors underlying congenital diaphragmatic hernia*. *Fetal diagnosis and therapy*, 2011. **29**(1): p. 25-39.
77. Babiuk, R.P., B. Thebaud, and J.J. Greer, *Reductions in the incidence of nitrofen-induced diaphragmatic hernia by vitamin A and retinoic acid*. *Am J Physiol Lung Cell Mol Physiol*, 2004. **286**(5): p. L970-3.
78. Nakazawa, N., et al., *Disturbance of retinol transportation causes nitrofen-induced hypoplastic lung*. *J Pediatr Surg*, 2007. **42**(2): p. 345-9.
79. Nakazawa, N., et al., *Altered regulation of retinoic acid synthesis in nitrofen-induced hypoplastic lung*. *Pediatr Surg Int*, 2007. **23**(5): p. 391-6.
80. Noble, B.R., et al., *Mechanisms of action of the congenital diaphragmatic hernia-inducing teratogen nitrofen*. *American journal of physiology. Lung cellular and molecular physiology*, 2007. **293**(4): p. L1079-87.
81. Thebaud, B., et al., *Vitamin A decreases the incidence and severity of nitrofen-induced congenital diaphragmatic hernia in rats*. *Am J Physiol*, 1999. **277**(2 Pt 1): p. L423-9.
82. Wilson, J.G., C.B. Roth, and J. Warkany, *An analysis of the syndrome of malformations induced by maternal vitamin A deficiency. Effects of restoration of vitamin A at various times during gestation*. *Am J Anat*, 1953. **92**(2): p. 189-217.
83. Ackerman, K.G., et al., *Fog2 is required for normal diaphragm and lung development in mice and humans*. *PLoS Genet*, 2005. **1**(1): p. 58-65.
84. Jay, P.Y., et al., *Impaired mesenchymal cell function in Gata4 mutant mice leads to diaphragmatic hernias and primary lung defects*. *Developmental biology*, 2007. **301**(2): p. 602-14.
85. Mark, M., N.B. Ghyselinck, and P. Chambon, *Function of retinoic acid receptors during embryonic development*. *Nucl Recept Signal*, 2009. **7**: p. e002.
86. Norden, J., et al., *Wt1 and retinoic acid signalling in the subcoelomic mesenchyme control the development of the pleuropericardial membranes and the sinus horns*. *Circulation research*, 2010. **106**(7): p. 1212-20.
87. You, L.R., et al., *Mouse lacking COUP-TFII as an animal model of Bochdalek-type congenital diaphragmatic hernia*. *Proc Natl Acad Sci U S A*, 2005. **102**(45): p. 16351-6.
88. Chassaing, N., et al., *Phenotypic spectrum of STRA6 mutations: from Matthew-Wood syndrome to non-lethal anophthalmia*. *Human mutation*, 2009. **30**(5): p. E673-81.
89. Pasutto, F., et al., *Mutations in STRA6 cause a broad spectrum of malformations including anophthalmia, congenital heart defects, diaphragmatic hernia, alveolar capillary dysplasia, lung hypoplasia, and mental retardation*. *American journal of human genetics*, 2007. **80**(3): p. 550-60.
90. Edwards, J.H., *The simulation of mendelism*. *Acta genetica et statistica medica*, 1960. **10**: p. 63-70.
91. Lander, E.S. and D. Botstein, *Homozygosity mapping: a way to map human recessive traits with the DNA of inbred children*. *Science*, 1987. **236**(4808): p. 1567-70.
92. Kantarci, S., et al., *Donnai-Barrow Syndrome*, in *GeneReviews*, R.A. Pagon, et al., Editors. 1993: Seattle (WA).
93. Gripp, K.W., et al., *Diaphragmatic hernia-exomphalos-hypertelorism syndrome: a new case and further evidence of autosomal recessive inheritance*. *Am J Med Genet A*, 1997. **68**(4): p. 441-4.
94. Kantarci, S., et al., *Mutations in LRP2, which encodes the multiligand receptor megalin, cause Donnai-Barrow and facio-oculo-acoustico-renal syndromes*. *Nat Genet*, 2007. **39**(8): p. 957-9.

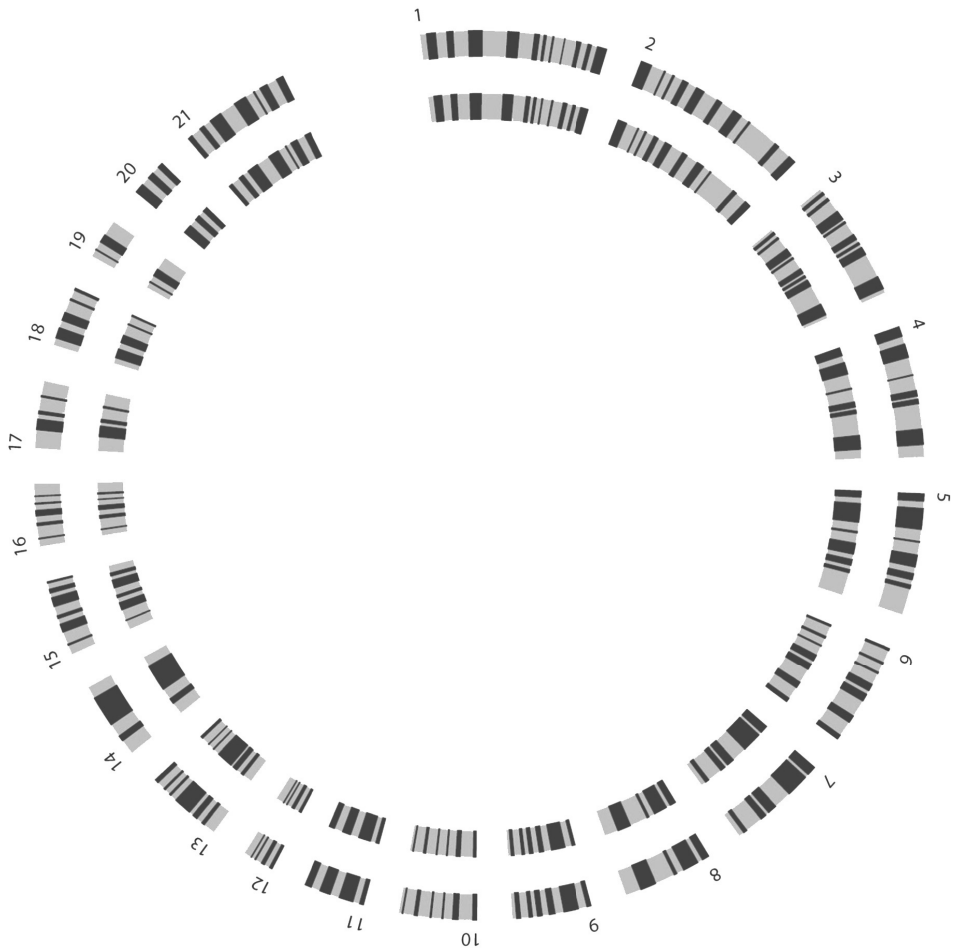
95. Pober, B.R., M. Longoni, and K.M. Noonan, *A review of Donnai-Barrow and facio-oculo-acoustico-renal (DB/FOAR) syndrome: clinical features and differential diagnosis*. Birth defects research. Part A, Clinical and molecular teratology, 2009. **85**(1): p. 76-81.
96. Seller, M.J., et al., *Two sibs with anophthalmia and pulmonary hypoplasia (the Matthew-Wood syndrome)*. Am J Med Genet A, 1996. **62**(3): p. 227-29.
97. Li, L. and J. Wei, *A newborn with anophthalmia and pulmonary hypoplasia (the Matthew-Wood syndrome)*. American journal of medical genetics. Part A, 2006. **140**(14): p. 1564-6.
98. Chitayat, D., et al., *The PDAC syndrome (pulmonary hypoplasia/agenesis, diaphragmatic hernia/eventration, anophthalmia/microphthalmia, and cardiac defect) (Spear syndrome, Matthew-Wood syndrome): report of eight cases including a living child and further evidence for autosomal recessive inheritance*. American journal of medical genetics. Part A, 2007. **143A**(12): p. 1268-81.
99. Golzio, C., et al., *Matthew-Wood syndrome is caused by truncating mutations in the retinol-binding protein receptor gene STRA6*. American journal of human genetics, 2007. **80**(6): p. 1179-87.
100. Martinovic-Bouriel, J., et al., *Matthew-Wood syndrome: report of two new cases supporting autosomal recessive inheritance and exclusion of FGF10 and FGFR2*. American journal of medical genetics. Part A, 2007. **143**(3): p. 219-28.
101. Manning, M. and L. Hudgins, *Array-based technology and recommendations for utilization in medical genetics practice for detection of chromosomal abnormalities*. Genetics in medicine : official journal of the American College of Medical Genetics, 2010. **12**(11): p. 742-5.
102. Bielinska, M., et al., *Molecular genetics of congenital diaphragmatic defects*. Ann Med, 2007. **39**(4): p. 261-74.
103. Catela, C., et al., *Multiple congenital malformations of Wolf-Hirschhorn syndrome are recapitulated in Fgfr1 null mice*. Disease models & mechanisms, 2009. **2**(5-6): p. 283-94.
104. Tautz, J., et al., *Congenital diaphragmatic hernia and a complex heart defect in association with Wolf-Hirschhorn syndrome*. American journal of medical genetics. Part A, 2010. **152A**(11): p. 2891-4.
105. Machado, I.N., et al., *Copy number imbalances detected with a BAC-based array comparative genomic hybridization platform in congenital diaphragmatic hernia fetuses*. Genetics and molecular research : GMR, 2011. **10**(1): p. 261-7.
106. Teshiba, R., et al., *Identification of TCTE3 as a gene responsible for congenital diaphragmatic hernia using a high-resolution single-nucleotide polymorphism array*. Pediatric surgery international, 2011. **27**(2): p. 193-8.
107. Srisupundit, K., et al., *Targeted array comparative genomic hybridisation (array CGH) identifies genomic imbalances associated with isolated congenital diaphragmatic hernia (CDH)*. Prenat Diagn, 2010. **30**(12-13): p. 1198-206.
108. Klaassens, M., et al., *Congenital diaphragmatic hernia and chromosome 15q26: determination of a candidate region by use of fluorescent in situ hybridization and array-based comparative genomic hybridization*. Am J Hum Genet, 2005. **76**(5): p. 877-82.
109. Scott, D.A., et al., *Genome-wide oligonucleotide-based array comparative genome hybridization analysis of non-isolated congenital diaphragmatic hernia*. Human molecular genetics, 2007. **16**(4): p. 424-30.
110. Miller, D.T., et al., *Consensus statement: chromosomal microarray is a first-tier clinical diagnostic test for individuals with developmental disabilities or congenital anomalies*. American journal of human genetics, 2010. **86**(5): p. 749-64.
111. Skinner, M.K., *Role of epigenetics in developmental biology and transgenerational inheritance*. Birth defects research. Part C, Embryo today : reviews, 2011. **93**(1): p. 51-5.
112. Cordier, S., *Evidence for a role of paternal exposures in developmental toxicity*. Basic & clinical pharmacology & toxicology, 2008. **102**(2): p. 176-81.
113. Ktistaki, E., et al., *CD8 locus nuclear dynamics during thymocyte development*. J Immunol, 2010. **184**(10): p. 5686-95.

114. Cremer, T., et al., *Chromosome territories--a functional nuclear landscape*. *Curr Opin Cell Biol*, 2006. **18**(3): p. 307-16.
115. Foster, H.A. and J.M. Bridger, *The genome and the nucleus: a marriage made by evolution. Genome organisation and nuclear architecture*. *Chromosoma*, 2005. **114**(4): p. 212-29.
116. Meaburn, K.J. and T. Misteli, *Cell biology: chromosome territories*. *Nature*, 2007. **445**(7126): p. 379-781.
117. Finlan, L.E., et al., *Recruitment to the nuclear periphery can alter expression of genes in human cells*. *PLoS Genet*, 2008. **4**(3): p. e1000039.
118. Kosak, S.T., et al., *Subnuclear compartmentalization of immunoglobulin loci during lymphocyte development*. *Science*, 2002. **296**(5565): p. 158-62.
119. Williams, R.R., et al., *Neural induction promotes large-scale chromatin reorganization of the Mash1 locus*. *J Cell Sci*, 2006. **119**(Pt 1): p. 132-40.
120. Chambeyron, S. and W.A. Bickmore, *Chromatin decondensation and nuclear reorganization of the HoxB locus upon induction of transcription*. *Genes Dev*, 2004. **18**(10): p. 1119-30.
121. Christova, R., et al., *P-STAT1 mediates higher-order chromatin remodelling of the human MHC in response to IFNgamma*. *J Cell Sci*, 2007. **120**(Pt 18): p. 3262-70.
122. Volpi, E.V., et al., *Large-scale chromatin organization of the major histocompatibility complex and other regions of human chromosome 6 and its response to interferon in interphase nuclei*. *J Cell Sci*, 2000. **113 (Pt 9)**: p. 1565-76.
123. Chuang, C.H. and A.S. Belmont, *Moving chromatin within the interphase nucleus-controlled transitions?* *Semin Cell Dev Biol*, 2007. **18**(5): p. 698-706.
124. Masny, P.S., et al., *Localization of 4q35.2 to the nuclear periphery: is FSHD a nuclear envelope disease?* *Hum Mol Genet*, 2004. **13**(17): p. 1857-71.
125. Meaburn, K.J., et al., *Primary laminopathy fibroblasts display altered genome organization and apoptosis*. *Aging Cell*, 2007. **6**(2): p. 139-53.
126. Malhas, A., et al., *Defects in lamin B1 expression or processing affect interphase chromosome position and gene expression*. *J Cell Biol*, 2007. **176**(5): p. 593-603.
127. Fullwood, M.J. and Y. Ruan, *ChIP-based methods for the identification of long-range chromatin interactions*. *J Cell Biochem*, 2009. **107**(1): p. 30-9.
128. Simonis, M., et al., *Nuclear organization of active and inactive chromatin domains uncovered by chromosome conformation capture-on-chip (4C)*. *Nat Genet*, 2006. **38**(11): p. 1348-54.
129. Bacher, C.P., et al., *Transient colocalization of X-inactivation centres accompanies the initiation of X inactivation*. *Nat Cell Biol*, 2006. **8**(3): p. 293-9.
130. Lomvardas, S., et al., *Interchromosomal interactions and olfactory receptor choice*. *Cell*, 2006. **126**(2): p. 403-13.
131. Osborne, C.S., et al., *Active genes dynamically colocalize to shared sites of ongoing transcription*. *Nat Genet*, 2004. **36**(10): p. 1065-71.
132. Osborne, C.S., et al., *Myc dynamically and preferentially relocates to a transcription factory occupied by Igh*. *PLoS Biol*, 2007. **5**(8): p. e192.
133. Spilianakis, C.G. and R.A. Flavell, *Long-range intrachromosomal interactions in the T helper type 2 cytokine locus*. *Nat Immunol*, 2004. **5**(10): p. 1017-27.
134. de Laat, W. and F. Grosveld, *Inter-chromosomal gene regulation in the mammalian cell nucleus*. *Curr Opin Genet Dev*, 2007. **17**(5): p. 456-64.
135. Misteli, T., *Beyond the sequence: cellular organization of genome function*. *Cell*, 2007. **128**(4): p. 787-800.
136. Meaburn, K.J., et al., *Disease-specific gene repositioning in breast cancer*. *J Cell Biol*, 2009. **187**(6): p. 801-12.
137. Meaburn, K.J. and T. Misteli, *Locus-specific and activity-independent gene repositioning during early tumorigenesis*. *J Cell Biol*, 2008. **180**(1): p. 39-50.

138. Van Prooijen-Knegt, A.C., et al., *In situ hybridization of DNA sequences in human metaphase chromosomes visualized by an indirect fluorescent immunocytochemical procedure*. *Exp Cell Res*, 1982. **141**(2): p. 397-407.
139. Cremer, M., et al., *Multicolor 3D fluorescence in situ hybridization for imaging interphase chromosomes*. *Methods Mol Biol*, 2008. **463**: p. 205-39.
140. Baker, M., *Genomics: Genomes in three dimensions*. *Nature*, 2011. **470**(7333): p. 289-94.
141. Dekker, J., et al., *Capturing chromosome conformation*. *Science*, 2002. **295**(5558): p. 1306-11.
142. Simonis, M., J. Kooren, and W. de Laat, *An evaluation of 3C-based methods to capture DNA interactions*. *Nature methods*, 2007. **4**(11): p. 895-901.
143. Splinter, E., et al., *The inactive X chromosome adopts a unique three-dimensional conformation that is dependent on Xist RNA*. *Genes Dev*, 2011. **25**(13): p. 1371-83.
144. Schoenfelder, S., et al., *Preferential associations between co-regulated genes reveal a transcriptional interactome in erythroid cells*. *Nat Genet*, 2010. **42**(1): p. 53-61.
145. Noordermeer, D., et al., *Variegated gene expression caused by cell-specific long-range DNA interactions*. *Nat Cell Biol*, 2011.
146. van Dijk, T.B., et al., *Friend of Prmt1, a novel chromatin target of protein arginine methyltransferases*. *Mol Cell Biol*, 2010. **30**(1): p. 260-72.
147. Goumy, C., et al., *Fetal skin fibroblasts: a cell model for studying the retinoid pathway in congenital diaphragmatic hernia*. *Birth Defects Res A Clin Mol Teratol*, 2010. **88**(3): p. 195-200.

Chapter 2

Copy Number Variations and Chtop Mutations in the CDH Cohort



Chapter 2.1

Germline and Somatic SNP-array analysis of 117 isolated and complex Congenital Diaphragmatic Hernia patients – the Rotterdam cohort –

D.Veenma, E.Brosens, D.Huigh, A.van Bodegom, H.Douben, B.Eussen,
M.Jhamai, A.Brooks, Y.van Bever, R.Galjaard, C.Wouters, A.Uitterlinden,
A.Flake, K.Kutsche, T.Schaible, R.Wijnen, D.Tibboel and A.de Klein

Manuscript in preparation

Supplementary files available on request

Abstract

Copy number analysis has proven to be a powerful tool for identifying individual genes and genomic regions that contribute to the development of congenital diaphragmatic hernia (CDH) and associated structural birth defects. In this study, we screened a cohort of 117 subjects with isolated or complex CDH of varying severity for genome-wide copy number imbalances using high-resolution SNP-array. This approach yielded 25 inherited and 16 *de novo* CNVs of which several new genetic aberrations that involved interesting disease related genes. These variations were absent or rarely occurring in published cohorts of normal individuals and an in-house control cohort. In addition, we performed paired analysis of the copy number pattern of diaphragm tissue to blood of 13 isolated CDH cases. Results showed no evidence for somatic CNVs neither for discrepancies in Loss Of Heterozygosity (LOH) between the two tissues.

Data from this large cohort study gave us a valuable insight into the incidence of *de novo* and inherited copy number events in both complex as well as isolated patients. We showed overlap with various previously identified CDH associated hot spots such as on chromosome 11q23 and 8p23.1 and added cardiac features to the recently described microdeletion syndrome of 15q25. Finally, we propose various new CDH-candidate genes (i.e. on chromosome 5p15.31, 9p22.3 and 12q24.13-q24.21) with the latter two associated with mild complex CDH.

In conclusion, high-resolution SNP-arrays allow for implementation of the smallest-region of overlap approach at a whole new resolution level and will increase the identified number of small chromosomal areas which harbour genes involved in diaphragm development in both isolated and complex CDH cases.

Introduction

Congenital Diaphragmatic Hernia (CDH)[OMIM 142340] is a life-threatening birth defect with an estimated incidence of 1 in 2000-3000 live birth and accounts for 8% of all major congenital anomalies [1, 2]. Despite medical advances, mortality from CDH continues to be high with an overall survival rate of 67% [3]. CDH is viewed as a phenotypically heterogeneous disorder with a complex inheritance pattern [4]. Patients either present with an isolated defect (isolated CDH) or with a diaphragm defect in addition to other non-hernia related anomalies. These cases are classified as complex CDH patients and encompass 40-50% of the CDH cohort. Further subdivision into complex-major and complex-simple might be instrumental, since the complex-major subgroup is more likely to have a genetic cause or to be diagnosed with a well-defined syndrome. The term complex-major describes those CDH patients that are severely affected, defined by the co-occurrence of at least two other *major* congenital anomalies. Aside from the small percentage of complex cases caused by one rare genetic mutation [5], the majority of CDH patients is expected to have a complex genetic basis with multiple CDH causing- and modifier genes.

An international consortium recently advised for the implementation of arrays as an initial cytogenetic diagnostic step in congenital anomaly cohorts, as they were shown to be much more sensitive and cost-effective in the identification of genetic aberrations than G-banded karyotyping [6]. Subsequently, application of this technique to complex and syndromic forms of CDH already lead to the discovery of the most common chromosomal CDH hot spot to date; the 15q26 monosomy [7]. Whether screening for genome wide (copy number) alterations is of clinical-diagnostic value for isolated CDH as well will become clear in the next few years. Other apparent chromosome hotspots for complex CDH include: 1(q41-q42) [8, 9], 8p23.1 (the *GATA4* locus) [10-13], 8q23.1-22.3 (the *ZFPM2* locus) [14], and possibly (11)(q23-qter) [15], which have been extensively reviewed by others [4, 16-18].

These genetic overviews are recently complemented by array data from four additional international CDH research groups [19-22]. Patient numbers, ethnic background, phenotype and timing of array analysis varied widely between the studies. The smallest one concerned 12 prenatal cases and the largest one demonstrated data of 79 isolated subjects. Some of the structural events identified in these studies overlapped with recurrently deleted or duplicated regions in CDH-individuals, but no new hot spots were discovered. However, applied array techniques differed from high-resolution genome-wide, to high-resolution targeted and low-resolution approaches and therefore don't allow for a proper meta-analysis on screening effectiveness. In contrast, the recent study of Wat et al. [19] did demonstrate the value of oligo-array techniques in the identification of new genomic changes and in the discovery of inheritance patterns, also for isolated cases. This type of evidence will lead to better parental counselling opportunities for CDH. In addition, it stresses on the importance of screening larger isolated patient groups using high-resolution techniques in order to identify the possibly overlapping (rare) genetic aberrations in non-related CDH subjects.

In this study, we screened a previously unpublished cohort of 117 subjects with diaphragmatic hernias- or eventrations of varying severity for genome-wide copy number imbalances using SNP-based array. We identified 208 structural events in total of which 167 concerned polymorphisms. Sixteen were de novo causative aberrations, some of which allowed us to make new phenotype-genotype associations. Twenty-five CNVs were inherited. Thirteen out of these 25 inherited events were absent or rarely occurring in normal cohorts and might therefore confer susceptibility to CDH as well. The remainder 12 inherited cases did not show an obvious link to the diaphragm phenotype. To analyse the possibility of CNVs restricted to the affected diaphragm tissue, we screened DNA derived from a subcohort of isolated CDH subjects and found no evidence for somatic CNVs.

Materials & methods

Subject accrual

Since February 2008, high-resolution SNP-array screening of specific sub-cohorts of complex CDH was performed in a research setting at the Erasmus MC-Sophia Children's hospital in Rotterdam. Erasmus MC's review board approved for blood withdrawal of the proband and his/her parents in addition to diaphragm biopsy during corrective surgery. Diaphragm sampling was executed only after obtaining separate informed consent of the parents. Patient material was selected based on the existence of specific co-occurring anomalies and availability of good quality DNA, which is recorded in an in-house CDH registry. Currently this database consists of 639 CDH patients treated at Erasmus MC since 1988 and also includes patients from various national and international collaborating centres (University Hospital of Mannheim, Germany; University Hospital in Leuven, Belgium). The screened cohort constituted of 50 non-isolated CDH patients in total. In the past 2 years, isolated CDH cases (n=67) were added to this array-routine and in 13 out of 67 isolated subjects the blood-derived copy number profile was compared to diaphragm-tissue derived DNA of the corresponding patient. Finally, as a consequence of changing international protocols, the screening of CDH subjects recently switched from a research setting to a diagnostic one [6].

DNA isolation and pre-array genetic screening

Karyotyping was performed according to standard analysis methods. DNA for genomic analysis was extracted from peripheral blood or fibroblast cells by the puregene DNA purification kit (Gentra Systems, USA).

Diaphragm biopsies were excised from the (remaining) left posterolateral- or anteriolateral part of the diaphragm and snap frozen immediately in liquid isopentane containing canisters in conjunction with liquid nitrogen. Ten out of 13 patients required a patch repair due to a considerable diaphragm defect size. Samples were stored at -80°C. From each frozen sample 20 slices of five µm were used to isolate DNA via the Qiagen DNeasy Blood & Tissue Kit method (Qiagen Benelux BV, Venlo, the Netherlands).

All DNA was tested for subtelomeric aberrations, using the P0361 and P070A2 Salsa telomere kits (MRC Holland, Amsterdam, the Netherlands) as published previously [23]. In some cases, prenatal targeted FISH analysis according to local standard protocols was performed as well.

Microarrays

DNA of 117 patients was hybridized to high-resolution Illumina cyto-SNP bead chips version 12.2 (Illumina, San Diego, CA, USA). Ten respectively eleven DNA samples were hybridized to earlier chip versions Quad 610 and Affymetrix NSP 250K arrays (Affymetrix, Santa Clara, USA) instead. Filtering, normalization and data analysis of each array was done using the Nexus[®] software program (version five, Biodiscovery, El Segundo, CA, USA) as previously described [24]. To review functionality of each putative CNV, occurrence frequencies in qualified normal cohorts of CHOP [<http://www.chop.edu>], DGV [projects.tcag.ca/variation/] and Decipher databases [<https://decipher.sanger.ac.uk>] were checked. Since these populations display various ethnic backgrounds, comparison to an in-house local reference set of 470 normal individuals was executed also.

Validation of microarray results

Confirmation of each putative candidate with q-PCR and/or FISH was executed in the proband and his/her parents according to local standard protocols as recently described [24, 25]. Briefly, for FISH, BAC clones were selected from the UCSC genome browser [<http://genome.ucsc.edu/>], purchased at BACPAC resources centre (Oakland, California, USA) and labelled (Random Prime labelling system Invitrogen Corporation, Carlsbad, California, USA) with Bio-16-dUTP or Dig-11-dUTP (Roche applied science, Indianapolis, USA). After validation on control metaphases, BAC clones were used on chromosome preparations from specific patients for confirmation. Primer pairs for quantitative real-time PCR were designed from unique sequences within the minimal deleted or duplicated regions of each copy number change using Primer Express software v2.0 (Applied Biosystems, Carlsbad, California, USA). The nucleotide-nucleotide BLAST algorithm at NCBI [<http://www.ncbi.nlm.nih.gov/BLAST/>] was used to confirm that each PCR amplification product was unique. Quantitative PCR analyses were performed using an ABI7300 Real-time PCR system in combination with KAPA-SYBR fast master mix (KapaBiosystems, Woburn, MA, USA). Experiments were designed with a region of the C14ORF145 gene serving as a control locus. Recently, MAC assays (Multiplicon N.V., Gent, Belgium) were used as a substitute for q-PCR as well and performed according to the manufactures protocol.

Results

The study cohort consisted of 117 patients. Patients with defined syndromes, such as trisomies or proven mutations in disease causing genes such as Simpson-Golabi or Cornelia de Lange syndrome had been excluded (n=5). Over 40% of patients showed an isolated diaphragmatic defect (n=64) or eventration (n=3) with varying degrees of lung hypoplasia and lung hypertension.

The remainder complex-CDH group was sub classified into: CDH and heart anomalies (n=10 including VSD (n=3), hypoplastic left heart n=2, coarctatio aortae n=1, other n=4), CDH and craniosynostosis (n=3), CDH and esophageal atresia (n=4), CDH and various dysmorphologies (n=15, including patients with facial dysmorphisms without a recognisable pattern n=3, complex dysmorphisms n=7, other n=5), CDH in discordant monozygotic twin subjects (n=5, except 1 concordant pair). Large(r) structural anomalies were identified (n=4) or confirmed (n=8) by array screening in 12 additional cases (CDH and structural anomalies (n=12)).

Table 1 depicts the detailed genetic results of the twelve large de novo anomalies, all of which are most likely phenotype affecting. Further results from this array cohort are summarised in Supplemental Table 1 showing only those CNVs that were considered de novo- or registered as a rare variant. Included were also those CNVs that had a -minor- partial overlap with events in normal individuals. A Copy Number Polymorphism (CNP) was defined by the occurrence in more than 5 individuals of appropriate online or in-house CNV databases of unaffected controls [<http://cnv.chop.edu> and (depending on the technique used in the original source), <http://projects.tcag.ca/variation>]. In total, 167 benign Copy Number Polymorphisms were established. All rare variants were confirmed in both the proband and his/her parents.

The significance of the majority of the changes presented in Supplemental Table I is currently unknown, yet future research in both humans and animals will help clarify whether they oppose an increased risk for CDH or not. Below, we will briefly discuss the six most remarkable events (Table 2A and 2B), which might provide us with a few new CDH-candidacy regions and/or provide us with valuable insight into the genetic mechanisms causing the variable CDH phenotypes.

Table 1 | Large, putatively phenotype affecting, de novo Copy Number changes in Rotterdam CDH cohort

| Subject | Event | Patient Phenotype |
|---------|---|-------------------|
| RD 1 | 46,XX,arr 1p36.23(0-8,049,376)x1,1p36.23p36.22(8,049,376-10,206,849)x3 | Complex |
| RD 2 | 46,XY,der(3)t(3;11)(p25.1;q23.1) | Complex |
| RD 3 | 46,XX,arr 4p16.1(0-9,945,373)x1 | Complex |
| RD 4 | 46,XY,arr 4p15.2p14(22,819,570-36,306,519)x1 | Isolated-right |
| RD 5 | 46,XX,der(5)t(5;12)(p13.2;p12.3)[27]/46,XX[4] | Complex |
| RD 6 | 46,XX,arr 8p23.1(8,139,051-11,916,439)x1 | Complex |
| RD 7 | arr 9ptelp11.2(0-46,310,390)x4 | Isolated-left |
| RD 8 | 46,XY,arr 15q11.2q13.1(18,421,386-27,018,622)x3 | Isolated-left |
| RD 9 | 46,XX,der(15)t(4;15)(q35;q26.1). | Complex |
| RD 10 | 46,XX,arr 15q25.2(80,689,404-82,938,351)x1,17p12(14,049,619-15,497,020)x3 | Complex |
| RD 11 | 46,XY,arr 17q21q31(39,182,612-39,660,170)x1 | Complex |
| RD 12 | 46,XX,arr Xp22.31(0-8,681,596)x1,Xp22.31p22.11(8,681,596-24,776,649)x3 | Complex |

RD: Rotterdam CDH subjects

Causative Genomic changes in complex-major CDH patients of the Rotterdam cohort

Event 1 is a de novo 2.5 Mb deletion on chromosome 15q25 identified in a female patient (RD 10, Table 1 + 2) that was prenatally diagnosed with left-sided CDH. Prenatal tracheal occlusion was executed to improve her prognostic poor lung-hypoplasia (L/H ratio of 0.7 and liver-up). At 38 weeks gestation she was born in a tertiary centre with ECMO facilities. Postnatal cardiac evaluation showed an additional major anomaly of the heart (coarctatio aortae) for which she was transferred to our hospital for surgical treatment. Unfortunately, despite ECMO treatment, her cardiac-and pulmonary condition did not stabilise to permit surgical intervention. She died at 15 days of age from respiratory insufficiency and pulmonary hypertension.

Event 2 is a maternally inherited 759 Kb deletion on chromosome 5p15.3-p15.2 which includes the methionine synthase reductase (*MTRR*) gene. The affected patient (RD 21, Table 2 & Supplemental Table 1) was a Caucasian female born at 36 weeks of gestation and diagnosed prenatally with left-sided CDH. Postnatal screening revealed a VACTERL association with bilateral dilatation of the ventral basis of the kidneys, abnormalities of the vertebral bodies and an esophageal atresia type IIIb. Surgical ligation of the fistula was performed within 24 hours of birth, yet she died shortly after because of respiratory insufficiency.

In a Caucasian German family, we identified event 3 in a complex female CDH patient (RD12, Table 1 and 2) with a combined deletion/duplication event on chromosome Xp that was 8.72 Mb and 16.1 Mb in size respectively. Classical cytogenetic analysis of parental blood showed no signs of a predisposing Xp inversion. Familial history suggested a genetic predisposition to congenital anomalies with multiple spontaneous abortions and a brother who exhibited a heart defect (VSD). Yet, SNP array analysis of both parents and the sibling were normal showing no evidence for pathologic CNVs. The patient died 1 day after birth apart from CDH because of oxygenation difficulties. Post-mortem exam demonstrated the following anomalies: Facial dysmorphisms including micrognathia and abnormal position and shape of external ears, pulmonary atresia, ventricular septum defect, microstomy, syndactyly of toes 2-3, overlapping toes 4-5, hydronephrosis and intra-uterine growth retardation.

Causative Genomic changes in Complex-simple CDH patients of the Rotterdam cohort

Event 4 is a very small maternally inherited 86 Kb deletion which involves only the *FRAS1*-related extracellular matrix protein 1 (*FREM1*) gene on chromosome 9p22.3. Primarily, this patient (RD 23 in Supplemental Table 1 and Table 2) was diagnosed with isolated CDH identifying only mild dysmorphisms of the toes (soft-tissue syndactyly of toe 2-3). However, at clinical follow-up dysmorphisms of the nose (bifid nose) and growth-retardation were recognised as well. These additional features overlapped with the clinical phenotype described in affected members of 3 consanguineous families with *homozygous* *FREM1* mutations (BNAR syndrome (OMIM 608980): Bifid Nose with or without Anorectal and Renal anomalies [26, 27] but were absent in the mother.

Table 2A | Genetic results Rotterdam subjects with chromosomal changes that likely have contributed to their diaphragm defects

| | Event 1 | Event 2 | Event 3 | Event 4 | Event 5 | Event 6 |
|---------------------------------------|--|--|--|--|--|--|
| RD # Supp.Table I | Patient RD 10 | Patient RD 21 | Patient RD 12 | Patient 23 | Patient RD 14 | Patient RD 25 |
| Maximal affected region (hg18) | Chromosome 15 Deletion (80,367,791-82,944,281) (2.57 Mb) Chromosome 17 Deletion (14,046,599-15,501,445) (1.45 Mb) | Chromosome 5 deletion (7,352,845-8,112,264) (0.759 Mb) | Chromosome X Deletion (0-8,721,625) (8.72 Mb) Chromosome X Duplication (8,721,625-24,779,676) (16.06 Mb) | Chromosome 9 deletion (14,859,861-14,945,988) (86 Kb) Chromosome X Duplication (183 Kb) | Chromosome 12 Duplication (112,766,879-113,047,253) (280 Kb) | Chromosome 12 Duplication (112,525,230-112,859,513) (334 Kb) |
| Minimal affected region (hg18) | Chromosome 15 Deletion (81,011,018-82,932,421) (1.92 Mb) Chromosome 17 Deletion (14,052,640-15,492,596) (1.44 Mb) | Chromosome 5 deletion (7,356,877-8,110,798) (0.754 Mb) | Chromosome X Deletion (814-8,641,567) (8.64Mb) Chromosome X Duplication (8,641,567-24,773,623) (16.13 Mb) | Chromosome 9 deletion chr9 (14,882,957-14,931,672) (48 Kb) Chromosome X Duplication | Chromosome 12 Duplication (112,769,496-113,036,905) (267 kb) | Chromosome 12 Duplication (112,531,958-112,853,000) (321 kb) |
| Inheritance | De novo | Maternal | De novo | Maternal | De novo | Paternal |
| Genes | Multiple (31 and 11) | ADCY2, C5orf49, FASTKD3, MTRR LOC442132 | Multiple (38 and 89) | FREM1 | RBM19 | RBM19 |
| Karyotype | 46,XX,del(15)(q25.2),dup(17)(p12) | 46,XX,del(5)(p15.3.1) | 46,XX,del(X)(p22.31),dup(X)(p22.31;p22.11) | 46,XX,del(9)(p22.3) | 46,XX,dup(12)(q24.13-q24.21) | 46,X,dup(12)(q24.13-q24.21) |

Table 2B | Phenotypes Rotterdam subjects with chromosomal changes that likely have contributed to their diaphragm defects

| | Event 1 | Event 2 | Event 3 | Event 4 | Event 5 | Event 6 |
|---|---|--|--|---------------------------------------|---------------------------------------|---|
| RD # Supp.Table1 | Patient RD 10 | Patient RD 21 | Patient RD 12 | Patient 23 | Patient RD 14 | Patient RD 25 |
| Age | 15 day-old | 1 day-old | 1 day-old | 1 year-old | 3 year-old | 1 year-old |
| Gender | female | female | female | female | female | male |
| Ethnicity | Caucasian Parents | Caucasian Parents | Caucasian Parents | Asian Parents | Caucasian Parents | Caucasian Parents |
| Prenatally identified abnormalities, exposure history and prenatal karyotype | CDH, Severe lung-hypoplasia (LHR 0.7 + liver-up → Tracheal occlusion) 46, XX | CDH, normal chromosomes 46,XX | CDH diagnosed late in gestation, LHR 1.2 + liver-up, no prenatal genetic screening, History multiple spontaneous abortions, Sibling heart defect (VSD) | CDH, normal chromosomes 46, XX | CDH left, normal chromosomes 46,XX | CDH left, LHR 1,65 normal chromosomes 46,XY, Maternal SSRI use, Aunt (paternal side) bilateral hand defect, Nephew (maternal) duplication small intestine |
| Birth History | Vaginal delivery at 38 weeks gestation | Preterm delivery at 36 weeks gestation | Caesarian section at 36,5 weeks gestation | Induced labor at 38.6 weeks gestation | Induced labor at 38.4 weeks gestation | Induced labor at 38.3 weeks gestation |
| Birth Weight, length and OFC | Weight: 2,7 kg | Weight: 2,71kg; Length 49 cm | Weight: 1,84 kg; Length 44 cm; OFC 30,5 cm | Weight: 2,2 kg | Weight: 3,1kg | Weight: 3,2 kg |
| Diaphragm | Left-sided CDH | Left-sided CDH | Left-sided CDH | Left-sided CDH+sac | Left-sided CDH+sac | Left-sided CDH |
| Cardiac | Coarctatio Aortae | No known abnormalities | No known abnormalities | No known abnormalities | Persistent left vena cava superior | No known abnormalities |

| | Event 1 | | Event 2 | | Event 3 | | Event 4 | | Event 5 | | Event 6 | |
|-------------------------------------|---------|--------|--|--|---|--|---|--|---------------|---------------|---------------|---------------|
| RD # | Supp | Table1 | Patient RD 10 | Patient RD 21 | Patient RD 12 | Patient 23 | Patient RD 14 | Patient RD 25 | Patient RD 14 | Patient RD 25 | Patient RD 14 | Patient RD 25 |
| Additional anomalies | | | No known abnormalities | Bilateral dilatation of the ventral basis of the kidneys, Abnormalities of the vertebral bodies, EsophagealCleft-lip palate, atresia type IIIb | Pulmonary atresia, VSD, Syndactily toe 2-3, overlapping toe 4-5, Facial dysmorphisms, Hydronephrosis, Intra- uterine growth retardation | Soft-tissue syn-dactyly toe 2-3, Bifid nose, Additional imaging no evidence for gastro-intestinal or renal anomalies | Mild dysmorphisms: Large ears, Nodule on the proximal interphalangeal articulation of digitus III | Bicuspid aortic valve | | | | |
| Clinical course/ Development | | | a-a ECMO treatment. Died on the 15 th day of life with respiratory insufficiency and pulmonary hypertension | Surgical ligation of fistel within 24 hours, died shortly after surgery because of pulmonary problems | Died 1day after birth because of oxygenation problems | Corrective surgery at day 9, normal motoric, speech-and mental development | Corrective surgery diaphragmatic defect at day 2, complicated by incarcerated hernia day 8 | Corrective surgery diaphragmatic defect at day 2, unremarkable history at 2-year follow-up | | | | |

The following abbreviations are used: LHR Lung to Head Ratio, a-a ECMO arterial-arterial Extra-Corporal-Membrane Oxygenation, VSD Ventricular septum defect

Additional imaging studies in our patient showed no evidence for gastro-intestinal or renal anomalies. Her left-sided CDH -including a sac- was corrected 9 days after birth. One-year follow up showed a normal motoric and developmental pattern.

Events 5 and 6 are partly overlapping duplication events on the long arm of chromosome 12 (12q24) identified in CDH patients RD 14 and RD 25 (Table 2 and Supplemental Table 1). The first patient is a Caucasian female born at 38.4 weeks of gestation. She had a prenatally diagnosed left-sided CDH plus sac. Cardiac evaluation at birth demonstrated a persistent left vena cava superior. Dymorphologic evaluation showed minor dysmorphisms with a prominent forehead, upward slanted palpebral fissures, large ears and a nodule on the proximal interphalangeal articulation of digitus III (Bouchard nodules). SNP array analysis revealed a small, de novo 280 Kb duplication (46, XX, dup (12) (q24.13)(112.768.187-113.042.079) x3), disrupting the coding region of the RNA-binding motif protein 19 (*RBM19*) and situated just proximally of *TBX5* (Figure 1A). Hemizyosity of the latter gene is known to cause a combined phenotype of Holt-Oram (OMIM 142900) and Ulnar-mammary syndromes (OMIM 18450)[28].

The second patient concerned a Caucasian male with mild-complex, left-sided CDH who was born at 38.3 weeks of gestation. The only additional anomaly concerned a bicuspid aortic valve. Pregnancy was complicated by maternal SSRI use. Paternal family history revealed that the proband's aunt was diagnosed with bilateral anomalies of the hands possibly induced by teratogens during pregnancy. A nephew of the proband (maternal side) was diagnosed postnatally with a duplication of the small intestine, which was surgically removed within 2 days. Our patient was identified with a 334 Kb duplication (46, XY, dup (12)(q24.13q24.21)(112.528.59-112.856.256) x3) positioned just proximal of the one of patient-RD 12 and also disrupting the coding region of the *RBM19* gene (Figure 1B). Considering the congenital anomalies in this family: both parents, his nephew and his aunt on maternal side were screened for *RBM19* CNVs. Unfortunately; DNA material of the aunt on paternal side was unavailable. Q-PCR results showed a paternally inherited duplication on 12q24 (Figure 1C), with all other subjects having a normal copy number status for this gene locus. These results might suggest that the limb defects at paternal side are linked to a genetic defect after all and (with reduced penetrance) to the diaphragm hole in our proband.

Somatic CNV patterns in isolated CDH cases

To exclude the possibility of structural variations restricted to the affected diaphragm tissues, we screened for CNVs in diaphragm material of 13 isolated patients and compared this pattern to the blood-derived copy number profile. Results showed no evidence for somatic CNVs nor could we find discrepancies in CNV distribution or Loss Of Heterozygosity (LOH) between the two tissues (Table 3) in any of the subjects that could be related to the diaphragm phenotype.

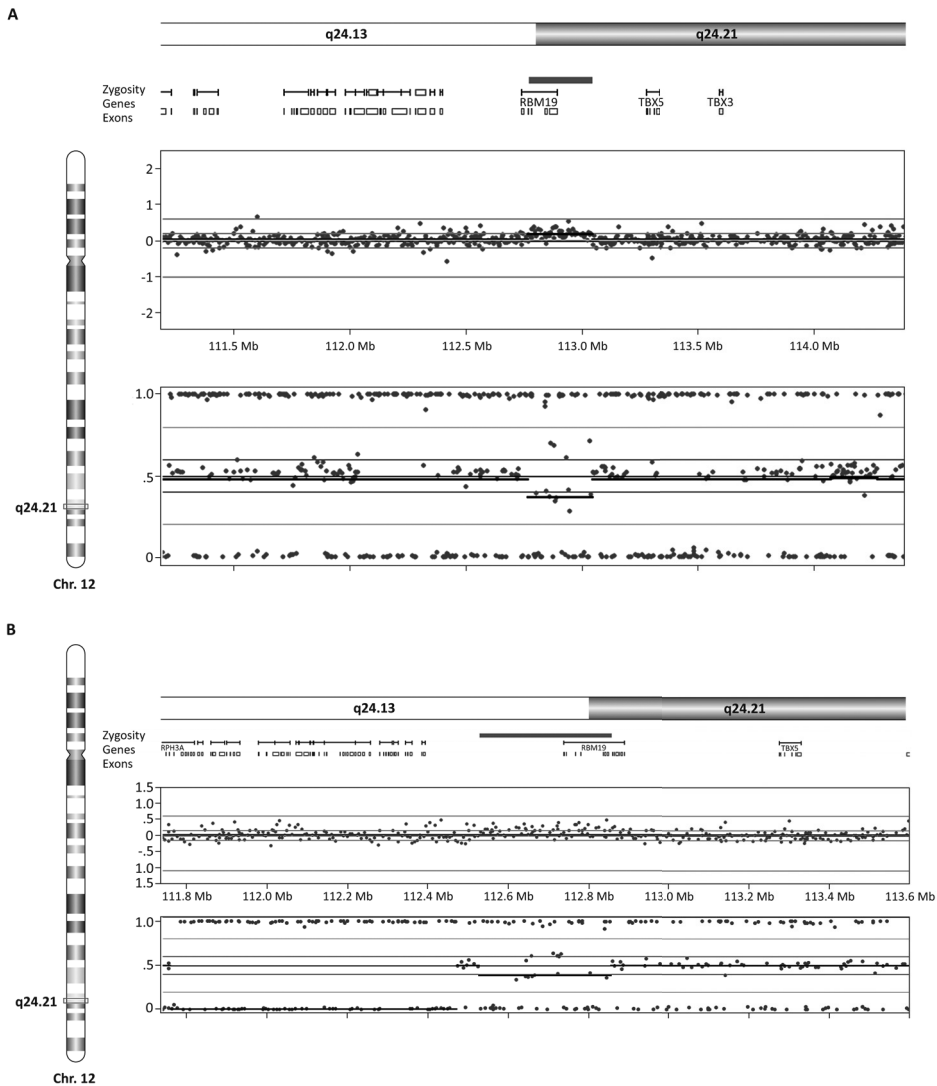


Figure 1 | Results high-resolution SNP array and RT-qPCR analysis events 5 and 6

A: Nexus result of the chromosome 12q24 duplication event in RD patient 14 showing a clear increase in log₂ intensity signal, concomitant with changes in the B-allele frequency (BAF). This event clearly disrupts the coding region of the RBM19 gene.

B: Nexus results of the partly overlapping duplication event in RD patient 25. Analogous to patient 14, this CNV affects the coding region of RBM19, yet is positioned more proximally.

C: Confirmative relative q-PCR results of events 5 (pink bar) and 6 (blue bars). Parental analysis (results not shown) demonstrated that the genomic event of patient RD 14 (event 5) is de novo. In contrast, event 6 is inherited from the father. Green bars represent the results of two non-related healthy controls (see page 246 for color figure).

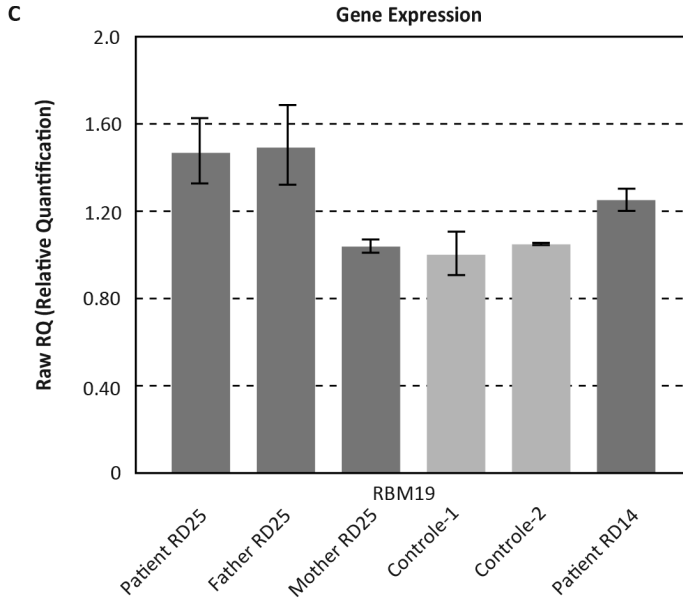


Figure 1 | Continued (see page 246 for color figure)

Table 3 | Germline CNVs detected in blood & diaphragm tissue of 13 CDH patients

| CDH Patient | Chromosomal location (bp) | CNV type | Length (bp) | Genes miRNA | Normal Cohort | Validation |
|-------------|------------------------------|----------|-------------|-------------|---------------|-----------------------------|
| 1-6 | – | – | – | – | – | – |
| 7 | chr22:19,778,080–21,465,347 | CN Gain | 1687268 | 22 | Yes: 7/2026 | FISH, de novo |
| 8 | – | – | – | – | – | – |
| 9 | – | – | – | – | – | – |
| 10 | chr22:17,249,767–17,392,385 | CN Loss | 142619 | 5 | Yes: 14/2026 | Q-PCR, inherited paternally |
| | chr2:57,249,627–57,302,586 | CN Gain | 52960 | 0 | Yes: 25/2026 | Copy Number Polymorphism |
| | chr8:137,774,224–137,917,718 | CN Loss | 143495 | 0 | Yes: 8/2026 | Copy Number Polymorphism |
| 11 | chr15:18,725,221–19,642,760 | CN Loss | 917540 | 7 | Yes: 6/2026 | Copy Number Polymorphism |
| 12-13 | – | – | – | – | – | – |

The following abbreviations are used: CN; Copy Number, Homoz; Homozygous, All Imb; Allelic Imbalance, bp; basepairs, EA; esophageal atresia, CDH; Congenital Diaphragmatic Hernia.

Normal Cohort: CNV detection in blood- or cell-line derived DNA (CHOP, DGV & Decipher)

Discussion

Copy number analysis has proven to be a powerful tool for identifying individual genes and genomic regions that contribute to the development of congenital diaphragmatic hernia (CDH) and associated structural birth defects.

This is the first report on CNV analysis in affected diaphragm material of CDH patients. In addition, this study provides a valuable insight into the occurrence frequency of germline de novo and inherited CNVs by screening the largest mixed CDH cohort (n=117) published to date. In total, 41 unique and/or rare events were established of which sixteen de novo and twenty-five inherited. Six out of 16 de novo CNVs were present in isolated or mild complex (complex-simple) CDH cases. The remainder 10 events were demonstrated in more complex (some of which complex-major) CDH patients and overlapped with previously identified CDH-associated hot spots on chromosome 4pter, 8p23.1, 11q23.1 and 15q26. In contrast, 18 out of 25 inherited CNVs were detected in isolated/mild complex cases with the remainder 7 associated with complex-CDH. Subsequently, these results provide us a few new CDH-candidate regions for both complex as well as isolated CDH and/or fine tune existing phenotype-genotype correlations.

Somatic CNV patterns in isolated CDH cases

Genetic studies usually aim at the identification of germ line mutations as a cause of structural birth defects. Yet, recently it was shown that somatic mosaicism for stochastic CNVs occurs in a substantial percentage of cells, both in normal as well as in diseased cohorts [29-36]. These somatic CNVs might explain phenotypic variability and/or reduced penetrance in physiologic and diseased phenotypes such as CDH. To exclude the possibility of structural variations restricted to the affected diaphragm tissues, we screened for CNVs in this material of a small group of isolated patients. Results indicated that affected tissue-specific CNV is not a major contributor to CDH, although larger tissue collections should be screened to rule out more rarely occurring mutations. Application of high-resolution SNP arrays and next-generation sequencing methods allow for an easier and more sensitive detection of this type of genetic aberrations in the near future and will add up to the (scarce) data generated recently on this topic by some other groups.

The 15q25 microdeletion phenotype includes both diaphragm- as well as heart defects

Wat et al. [37] recently suggested the existence of another candidate region on the distal arm of chromosome 15 associated with diaphragm defects i.e. the 15q25 monosomy syndrome. Its core clinical phenotype is characterized by an increased risk for mental retardation, cryptorchidism, short stature and (possibly) Diamond-Blackfan anaemia. The 2,25 Mb deletion event identified in our CDH patient RD 10 did not allow for refinement of the 15q25-critical interval for diaphragm defects [37], however based on this report a cardiac defect should be added to the list of congenital anomalies associated with this genetic aberration. Additionally, the co-occurring 1,44

Mb de novo deletion on chromosome 17 could theoretically be responsible for this anomaly as well, but is registered in 4 individuals of normal DGV-cohorts.

Disruption of alternative embryonic pathways: the homocystein/folic acid pathway in combined CDH and Esophageal Atresia (EA) phenotypes

Event 2 identified in our complex-CDH patient with VACTERL-associated esophageal atresia (RD 21) shows only 7.5% overlap with CNVs of 4 healthy individuals and includes the *MTRR* gene. Although inherited from a phenotypically normal mother, the importance of the MTRR protein in the homocystein/folic-acid pathway suggests a susceptibility role for this event in our patients' phenotype. *MTRR* encodes a methionine synthase reductase which re-activates methionin synthase (MTR). The latter is a cobalamin-dependent enzyme which catalyses the re-methylation of methionine using *s*-adenosylmethionin as a methyl donor. The eventual product of the re-methylation of methionine is homocystein. Therefore, haploinsufficiency of *MTRR* could theoretically lead to hyper-homocysteinemia. In turn, hyper-homocysteinemia is frequently associated with congenital defects of the heart and the neural tube [38, 39]. Preliminary results from a nested cross-sectional CDH case (n=22)-control (n=28) study from our group did not find significantly different biomarker levels of the methylation pathway in cord-blood [40]. Limpach et al. [41] suggested that homocystein-induced congenital defects are caused by the ability of homocystein to inhibit the conversion of retinal to retinoic acid, thereby providing a link to the well-known RA disruption hypothesis of CDH [42]. Unfortunately, our patient died 1 day postnatally and parents did not permit autopsy or storage of serum blood-and tissue samples. These would have allowed for a more detailed assessment of serum vitamin B12, folic acid, retinol and homocystein levels to provide functional evidence for the putative association with the combined EA- and CDH phenotype.

Chromosome Xp aberrations: is the Holocytochrome C synthase gene a CDH candidate or not?

Various chromosome Xp aberrations are recurrently reported in patients with diaphragm defects, suggesting the importance of one or more genes in this region for diaphragm development. Based on a distinct phenotype of microphthalmia combined with linear skin defects (MLS, OMIM 309801) and CDH, Qidwai et al. [43] recently proposed the Holocytochrome C synthase (*HCCS*) gene as a new Xp22 candidate for diaphragmatic hernia. A few earlier reports on diaphragmatic hernia cases with terminal deletions of Xp22.2-pter [44] backed up this association. However, the deleted region on Xp in female patient RD 12 does not include the *HCCS* gene and positional effects are unlikely due to the large distance of the deletion breakpoint (>1 Mb) to *HCCS*. These results suggest that the proposed role of *HCCS* haploinsufficiency in CDH is not valid or at least not fully penetrant [43]. Obviously, the co-occurring large Xp duplication interferes with the definition of a more precise phenotype-genotype correlation.

FRAS1-related extracellular matrix protein 1 (FREM1): a new CDH candidate gene?

Event 4 concerned a very small deletion on the short arm of chromosome 9 identified in a mild dysmorphic CDH case (RD 23) whose additional symptoms could be assigned to the variable BNAR syndrome (OMIM 608980). The core clinical features of BNAR are usually caused by homozygous missense and frameshift mutations in *FREM1* [26, 27]. *FREM1* protein is known for its overlapping role with *FRAS1*, an extracellular matrix protein that is -to a large extent- functionally interdependent on *FREM1* and affected in patients with Fraser syndrome [OMIM 219000]. However, *Frem1* mice mutants display a considerable wider and milder phenotype and lack the characteristic cryptophthalmos (skin covering the globe of the eye) identified in human and mice Fraser-syndrome patients. Subsequently, Alazami et al. [45] suggested that BNAR represents a milder variant of Fraser syndrome. This idea is supported by data of Slavotinek et al. [46], who recently added the features of Manitoba-Oculo-Tricho-Anal (MOTA) syndrome (OMIM:248450) to the human phenotypic spectrum of the *FREM1-FRAS1* complex.

The occurrence of CDH in our female patient (RD 23) contradicts this idea of a milder *FREM1* phenotype and suggests that haploinsufficiency of this gene opposes an increased risk for the development of diaphragmatic defects. The announcement of a recent new recessive *Frem1* mouse model [47] backs up this idea. In addition, a few human Fraser syndrome patients have been described with CDH in literature [48]. However, true association is only valid after identification of additional CDH patients, since this is the first report of a human *FREM1* case exhibiting CDH. Finally, the suggestive autosomal recessive inheritance modus of *FREM1* associated birth defects is supported by the unaffected phenotype of our patients' mother. Interestingly, her daughter displayed a co-occurring 183 Kb duplication event on chromosome Xq21.1 that included the *ATRX* gene. This extra CNV stresses on the possibility of an additional "second" hit in the same or associated disease pathway causing a recessive phenotype to emerge in offspring of an unaffected carrier-parent (as proposed by Girirajan et al. [49]). However, ingenuity pathway analysis [www.ingenuity.com] showed no links between *FREM1* and *ATRX* and diaphragm defects have not been reported for this gene. Mutations of *ATRX* are known to cause alpha-thalassemia combined with mental retardation.

Haploinsufficiency of RNA-binding motif protein 19 (RBM19) gene predisposes to mildly complex CDH: identification of a unique new CDH hot spot on 12q24

The SNP array technique allows for the identification of genetic aberrations not biased by phenotypic information (genotype-first approach). In this way we identified events 5 and 6 on the long arm of chromosome 12 in two unrelated mild-complex CDH patients (RD 14 and RD 25). This in contrast to the well-known CDH-associated 12p locus that is described in 30% of Pallister-Killian patients (OMIM #601803).

The *RBM19* gene is the most likely causative CDH-candidate in our patients, since both duplications disrupt its coding region. Functional information on the conserved nucleolar protein *RBM19* suggests an important role in *digestive* organ development. Mayer et al. (2003) showed

that the zebrafish variant of *RBM19* (called Nil Per Os) induces organ hypoplasia when knocked-down and causes overgrowth of gastro-intestinal organs when overexpressed [50]. In addition, Zhang et al. [51] recently displayed an important role of *RBM19* in murine pre-implantation development. Interestingly, the relatives of patient RD 25 displayed features (limb and intestinal malformations) that are either related to the same chromosomal anomaly or functionally related to *RBM19* in literature [28, 50]. Mutation screening of this gene in all family members is therefore necessary to rule out second hits in the *RBM19*-associated developmental pathway.

Theoretically, a position effect of the small de-novo duplications in both patients could affect the function of the *TBX5* gene more distally and explain their (mild-cardiac) phenotype. This gene is a member of the Brachyury (T) family of transcription factors, whose mutations cause anomalies of the heart and upper limbs in varying severity. In mice, *Tbx5* transcripts have been demonstrated in lungs, pharynx and thorax body wall. Hiroi et al. [52] found that *TBX5* associates with *NKX2-5* to synergistically promote cardiomyocyte differentiation. Interestingly, Garg et al. [53] demonstrated an interaction between *TBX5* and *GATA4* and implicated that disruption of this association induces human cardiac septal defects. Knowing the important role for *GATA4* in CDH [48, 54], such a process might be suggested for the diaphragm defect in our patients as well. Further functional studies in both patients (and their relatives) will help to answer these questions.

In summary, high-resolution SNP-arrays allow for implementation of the smallest-region of overlap approach at a whole new resolution level and have replaced karyotyping in a diagnostic screening setting. This approach will increase the identified number of small chromosomal areas that harbour genes involved in diaphragm development in both isolated and complex CDH cases, which will improve genetic counselling opportunities to parents. On a population level, the genotype-first approach will enable better stratification of CDH-associated phenotypes in the near future given the wide variability of the size of the diaphragm defect [55]. It may even allow for risk-assessment in terms of severity of pulmonary-arterial hypertension and risk for the development of chronic pulmonary morbidity. However, as suggested by Donahoe and all [56], these molecular approaches need to be integrated with computational and functional analyses in order to truly make significant changes in the care of patients.

Acknowledgements

We are grateful to all parents for their cooperation in this study. Tom de Vries-Lentsch is thanked for help in preparing the figures.

References

1. Torfs, C.P., et al., *A population-based study of congenital diaphragmatic hernia*. *Teratology*, 1992. **46**(6): p. 555-65.
2. Langham, M.R., Jr., et al., *Congenital diaphragmatic hernia. Epidemiology and outcome*. *Clin Perinatol*, 1996. **23**(4): p. 671-88.
3. Sluiter, I., et al., *Congenital diaphragmatic hernia: still a moving target*. *Seminars in fetal & neonatal medicine*, 2011. **16**(3): p. 139-44.
4. Klaassens, M., A. de Klein, and D. Tibboel, *The etiology of congenital diaphragmatic hernia: still largely unknown?* *Eur J Med Genet*, 2009. **52**(5): p. 281-6.
5. Pober, B.R., M.K. Russell, and K.G. Ackerman, *Congenital Diaphragmatic Hernia Overview*, in *GeneReviews*, R.A. Pagon, et al., Editors. 2006: Seattle (WA).
6. Miller, D.T., et al., *Consensus statement: chromosomal microarray is a first-tier clinical diagnostic test for individuals with developmental disabilities or congenital anomalies*. *American journal of human genetics*, 2010. **86**(5): p. 749-64.
7. Klaassens, M., et al., *Prenatal detection and outcome of congenital diaphragmatic hernia (CDH) associated with deletion of chromosome 15q26: two patients and review of the literature*. *American journal of medical genetics*. Part A, 2007. **143A**(18): p. 2204-12.
8. Slavotinek, A.M., et al., *Sequence variants in the HLX gene at chromosome 1q41-1q42 in patients with diaphragmatic hernia*. *Clin Genet*, 2009. **75**(5): p. 429-39.
9. Shaffer, L.G., et al., *The discovery of microdeletion syndromes in the post-genomic era: review of the methodology and characterization of a new 1q41q42 microdeletion syndrome*. *Genetics in medicine : official journal of the American College of Medical Genetics*, 2007. **9**(9): p. 607-16.
10. Wat, M.J., et al., *Chromosome 8p23.1 deletions as a cause of complex congenital heart defects and diaphragmatic hernia*. *Am J Med Genet A*, 2009. **149A**(8): p. 1661-77.
11. Slavotinek, A., et al., *Fryns syndrome phenotype caused by chromosome microdeletions at 15q26.2 and 8p23.1*. *Journal of medical genetics*, 2005. **42**(9): p. 730-6.
12. Chen, C.P., et al., *Prenatal diagnosis of Fryns syndrome associated with a microdeletion at 8p23.1*. *Prenat Diagn*, 2007. **27**(10): p. 967-9.
13. Baynam, G., J. Goldblatt, and I. Walpole, *Deletion of 8p23.1 with features of Cornelia de Lange syndrome and congenital diaphragmatic hernia and a review of deletions of 8p23.1 to 8pter? A further locus for Cornelia de Lange syndrome*. *Am J Med Genet A*, 2008. **146A**(12): p. 1565-70.
14. Ackerman, K.G., et al., *Fog2 is required for normal diaphragm and lung development in mice and humans*. *PLoS Genet*, 2005. **1**(1): p. 58-65.
15. Klaassens, M., et al., *Congenital diaphragmatic hernia associated with duplication of 11q23-qter*. *Am J Med Genet A*, 2006. **140**(14): p. 1580-6.
16. Scott, D.A., et al., *Genome-wide oligonucleotide-based array comparative genome hybridization analysis of non-isolated congenital diaphragmatic hernia*. *Human molecular genetics*, 2007. **16**(4): p. 424-30.
17. Goumy, C., et al., *Retinoid Pathway and Congenital Diaphragmatic Hernia: Hypothesis from the Analysis of Chromosomal Abnormalities*. *Fetal Diagn Ther*, 2010.
18. Brady, P.D., et al., *Recent developments in the genetic factors underlying congenital diaphragmatic hernia*. *Fetal diagnosis and therapy*, 2011. **29**(1): p. 25-39.
19. Wat, M.J., et al., *Genomic alterations that contribute to the development of isolated and non-isolated congenital diaphragmatic hernia*. *Journal of medical genetics*, 2011. **48**(5): p. 299-307.
20. Teshiba, R., et al., *Identification of TCTE3 as a gene responsible for congenital diaphragmatic hernia using a high-resolution single-nucleotide polymorphism array*. *Pediatric surgery international*, 2011. **27**(2): p. 193-8.
21. Srisupundit, K., et al., *Targeted array comparative genomic hybridisation (array CGH) identifies genomic imbalances associated with isolated congenital diaphragmatic hernia (CDH)*. *Prenat Diagn*, 2010. **30**(12-13): p. 1198-206.

22. Machado, I.N., et al., *Copy number imbalances detected with a BAC-based array comparative genomic hybridization platform in congenital diaphragmatic hernia fetuses*. Genetics and molecular research : GMR, 2011. **10**(1): p. 261-7.
23. Van Opstal, D., et al., *Rapid aneuploidy detection with multiplex ligation-dependent probe amplification: a prospective study of 4000 amniotic fluid samples*. Eur J Hum Genet, 2009. **17**(1): p. 112-21.
24. Veenma, D., et al., *Comparable low-level mosaicism in affected and non affected tissue of a complex CDH patient*. PloS one, 2010. **5**(12): p. e15348.
25. Veenma, D.C., et al., *Phenotype-genotype correlation in a familial IGF1R microdeletion case*. Journal of medical genetics, 2010. **47**(7): p. 492-8.
26. Alazami, A.M., et al., *FREM1 mutations cause bifid nose, renal agenesis, and anorectal malformations syndrome*. American journal of human genetics, 2009. **85**(3): p. 414-8.
27. Al-Gazali, L.I., et al., *An autosomal recessive syndrome of nasal anomalies associated with renal and anorectal malformations*. Clin Dysmorphol, 2002. **11**(1): p. 33-8.
28. Borozdin, W., et al., *Contiguous hemizygous deletion of TBX5, TBX3, and RBM19 resulting in a combined phenotype of Holt-Oram and ulnar-mammary syndromes*. American journal of medical genetics. Part A, 2006. **140A**(17): p. 1880-6.
29. Ballif, B.C., et al., *Detection of low-level mosaicism by array CGH in routine diagnostic specimens*. Am J Med Genet A, 2006. **140**(24): p. 2757-67.
30. Bruder, C.E., et al., *Phenotypically concordant and discordant monozygotic twins display different DNA copy-number-variation profiles*. Am J Hum Genet, 2008. **82**(3): p. 763-71.
31. Cheung, S.W., et al., *Microarray-based CGH detects chromosomal mosaicism not revealed by conventional cytogenetics*. Am J Med Genet A, 2007. **143A**(15): p. 1679-86.
32. Iourov, I.Y., S.G. Vorsanova, and Y.B. Yurov, *Chromosomal mosaicism goes global*. Mol Cytogenet, 2008. **1**: p. 26.
33. Iwarsson, E., et al., *A high degree of aneuploidy in frozen-thawed human preimplantation embryos*. Hum Genet, 1999. **104**(5): p. 376-82.
34. Notini, A.J., J.M. Craig, and S.J. White, *Copy number variation and mosaicism*. Cytogenet Genome Res, 2008. **123**(1-4): p. 270-7.
35. Piotrowski, A., et al., *Somatic mosaicism for copy number variation in differentiated human tissues*. Hum Mutat, 2008. **29**(9): p. 1118-24.
36. Youssoufian, H. and R.E. Pyeritz, *Mechanisms and consequences of somatic mosaicism in humans*. Nat Rev Genet, 2002. **3**(10): p. 748-58.
37. Wat, M.J., et al., *Recurrent microdeletions of 15q25.2 are associated with increased risk of congenital diaphragmatic hernia, cognitive deficits and possibly Diamond-Blackfan anaemia*. Journal of medical genetics, 2010. **47**(11): p. 777-81.
38. Smulders, Y.M. and H.J. Blom, *The homocysteine controversy*. Journal of inherited metabolic disease, 2011. **34**(1): p. 93-9.
39. Blom, H.J. and Y. Smulders, *Overview of homocysteine and folate metabolism. With special references to cardiovascular disease and neural tube defects*. Journal of inherited metabolic disease, 2011. **34**(1): p. 75-81.
40. Beurskens, L.W., de Jonge, R., Tibboel, D., Steegers-Theunissen, R.P.M., *A black hole? Epidemiological and molecular biological studies on the etiology of Congenital Diaphragmatic Hernia*, in *Pediatric Surgery department2010*, Erasmus-MC: Rotterdam. p. 163.
41. Limpach, A., et al., *Homocysteine inhibits retinoic acid synthesis: a mechanism for homocysteine-induced congenital defects*. Exp Cell Res, 2000. **260**(1): p. 166-74.
42. Clugston, R.D., et al., *Understanding abnormal retinoid signalling as a causative mechanism in congenital diaphragmatic hernia*. Am J Respir Cell Mol Biol, 2010. **42**(3): p. 276-85.
43. Qidwai, K., et al., *Deletions of Xp provide evidence for the role of holocytochrome C-type synthase (HCCS) in congenital diaphragmatic hernia*. American journal of medical genetics. Part A, 2010. **152A**(6): p. 1588-90.

44. Allanson, J. and S. Richter, *Linear skin defects and congenital microphthalmia: a new syndrome at Xp22.2*. Journal of medical genetics, 1991. **28**(2): p. 143-4.
45. Abdullah, F., et al., *Congenital diaphragmatic hernia: outcome review of 2,173 surgical repairs in US infants*. Pediatric surgery international, 2009. **25**(12): p. 1059-64.
46. Slavotinek, A.M., et al., *Manitoba-oculo-tricho-anal (MOTA) syndrome is caused by mutations in FREM1*. Journal of medical genetics, 2011. **48**(6): p. 375-82.
47. Beck, T., Wat, M., Kim, B.J., Zaveri.H., Justice, M., Lee, B., Scott, D.A. *Frem1 as a model for congenital diaphragmatic hernia (CDH) and bifid nose, renal agenesis, and anorectal malformations syndrome*. in *The American Society of Human Genetics 60th Annual Meeting*. 2010. Washington, DC.
48. Ackerman, K.G., et al., *Gata4 is necessary for normal pulmonary lobar development*. Am J Respir Cell Mol Biol, 2007. **36**(4): p. 391-7.
49. Girirajan, S., et al., *A recurrent 16p12.1 microdeletion supports a two-hit model for severe developmental delay*. Nat Genet. **42**(3): p. 203-9.
50. Mayer, A.N. and M.C. Fishman, *Nil per os encodes a conserved RNA recognition motif protein required for morphogenesis and cytodifferentiation of digestive organs in zebrafish*. Development, 2003. **130**(17): p. 3917-28.
51. Zhang, J., A.J. Tomasini, and A.N. Mayer, *RBM19 is essential for preimplantation development in the mouse*. BMC developmental biology, 2008. **8**: p. 115.
52. Hiroi, Y., et al., *Tbx5 associates with Nkx2-5 and synergistically promotes cardiomyocyte differentiation*. Nat Genet, 2001. **28**(3): p. 276-80.
53. Garg, V., et al., *GATA4 mutations cause human congenital heart defects and reveal an interaction with TBX5*. Nature, 2003. **424**(6947): p. 443-7.
54. Jay, P.Y., et al., *Impaired mesenchymal cell function in Gata4 mutant mice leads to diaphragmatic hernias and primary lung defects*. Developmental biology, 2007. **301**(2): p. 602-14.
55. Lally, K.P., et al., *Defect size determines survival in infants with congenital diaphragmatic hernia*. Pediatrics, 2007. **120**(3): p. e651-7.
56. Donahoe, P.K., K.M. Noonan, and K. Lage, *Genetic tools and algorithms for gene discovery in major congenital anomalies*. Birth defects research. Part A, Clinical and molecular teratology, 2009. **85**(1): p. 6-12.

Chapter 2.2

Complex Congenital Diaphragmatic Hernia in Mice Lacking Chromatin Target of PRMT1

N.Gillemans, D.Szumska, D.Veenma, F.Esteghamat, J.Hou, W.van IJcken, A. de Klein, S.Bhattacharya, D.Tibboel, F.Grosveld, S.Philipsen, and T.van Dijk

Submitted

Supplementary files available on request

Abstract

Congenital diaphragmatic hernia (CDH) is a life-threatening birth defect and is associated with defects in additional organs in 30-40% of the cases. Apart from chromosomal anomalies, the etiology of CDH is still largely unknown. Here we show that mice lacking Chromatin target of PRMT1 (CHTOP) have numerous developmental abnormalities, including the dorsolateral “Bochdalek” type of CDH. CHTOP is a vertebrate-specific chromatin-binding protein that plays a critical role in transcription regulation and has a widespread expression pattern during embryogenesis. CHTOP null mice die *in utero* or shortly after birth; they are reduced in size and display complex cardiovascular malformations. Additionally, they suffer from pulmonary hypoplasia, cleft palate and size reduction of spleen, pancreas, and kidneys. Expression profiling of E9.0 embryos shows aberrant expression of genes involved in mesoderm and vasculature development, as well as a delay in the G2/M-phase of the cell cycle. We further identified a *CHTOP* mutation in a CDH patient that severely affects the interaction between CHTOP and PRMT1, the major protein arginine methyltransferase. Our results demonstrate that CHTOP is essential for vertebrate ontogenesis and that deregulation of CHTOP may play a role in complex CDH syndromes observed in human patients.

Introduction

Congenital diaphragmatic hernia (CDH) is a severe developmental defect occurring in approximately 1 in every 3000 live births [1]. The hallmark of the disorder is a defect in the muscular or tendinous portion of the diaphragm. The incomplete closure of the diaphragm can be variable in size, ranging from a small hole to agenesis of the diaphragm. This allows the abdominal contents, which may include liver, stomach, intestines, and spleen, to protrude into the thoracic cavity, thereby impeding lung growth and development. The resulting pulmonary hypoplasia and postnatal pulmonary hypertension are major causes for the high mortality and morbidity rates associated with CDH (reviewed by [2]). Three types of hernia can be distinguished: the “Bochdalek” form involves the dorsolateral portion of the diaphragm (~70% of the cases), an anterior “Morgagni” form (~27%), and a central form (~2%) [3]. The vast majority of hernias is left-sided (85%), whilst the remainder are right sided (13%) or bilateral (2%) [4]. Apart from the defects in diaphragm and lungs, CDH is accompanied by additional malformations in 30-40% of cases. In this “non-isolated” or “complex” CDH, the cardiovascular system is most commonly affected [5]. Furthermore, CDH has been described as a part of known genetic syndromes for which, in some cases, a single causal gene is identified, such as the *WT1* (“Wilms” Tumour 1) gene in Denys-Drash syndrome and the *GPC3* (glypican-3) gene in Simpson-Golabi-Behmel syndrome [6]. In addition, several rearrangements in specific genetic loci, including interstitial and terminal deletions of 8p23.1 and 15q26, are associated with “complex” CDH. However, whether CDH has a genetic cause for all of these disorders or is merely an incidental occurrence in addition to the other observed malformations, is unclear [7]. Further insight into the genetic etiology of CDH comes from the evaluation of mutant mice. Mice that lack *c-MET*, *MYOD* or *PAX3* display a muscularization defect of the diaphragm, incomplete closure of the diaphragm is observed in null mutants for *Wt1*, *Rara/Rarβ2* (retinoic acid receptor), *Gata4*, and *Coup-TFII/Nr2f2*, while diaphragmatic eventrations are seen in mice that are homozygous for a hypomorphic allele of *Fog2/Zfp2* (reviewed by [8, 9, 10]). Nevertheless, CDH does not display full penetrance in the different mouse models, and mutations in the orthologous genes are rarely found in human CDH patients. Together these observations indicate that CDH is, genetically, a heterogeneous disease, and that multiple factors have to play an important role.

We recently identified Chromatin target of PRMT1 (CHTOP), previously known as Friend of PRMT1 (FOP) and Small protein Rich in Arginine and Glycine (SRAG), encoded by the mouse *2500003M10Rik* and human *C1orf77* genes, respectively [11, 12]. CHTOP is a highly conserved vertebrate-specific protein with no known paralogues. It is a chromatin-associated protein and plays a critical role in transcriptional activation, including estrogen-dependent gene induction in breast cancer cells and globin gene regulation in erythroid cells [11, 13]. CHTOP has no known conserved domains, but its central sequence consists of a glycine-arginine-rich (GAR) domain that contains 26 arginine residues that are flanked by a glycine. GAR regions are a common feature of many RNA-binding proteins (RBPs), but whether CHTOP interacts with RNA is currently unknown. GAR domains can be recognized and modified by members of the protein arginine

methyltransferase (PRMT) family [14]. Indeed, CHTOP was identified in a screen for novel PRMT1-interacting proteins and subsequent experiments have indicated that the GAR region is extensively modified by the enzyme [11]. A role for arginine methylation in regulating protein-protein interactions in gene regulation is well documented [15]. Transcriptional regulators that are controlled by Prmt activity include transcription factors like NIP45 and RUNX1 [16, 17], cofactors like CBP/P300 [18], the nuclear hormone receptor ER α [19], the elongation factor SPT5 [20], as well as histones H3 and H4 (reviewed by [21]).

To study the physiological role of CHTOP, we generated CHTOP -deficient mice. The mutation was induced by gene entrapment in mouse embryonic stem cells. Embryos that do not express CHTOP are reduced in size, display massive edema, and die at the perinatal stage with a complex and heterogeneous phenotype. By using high-throughput multi-embryo magnetic resonance imaging (MRI), we found that all mutant animals suffered from visceral and cardiac malformations (including ventricular and atrial septal defects, double-outlet right ventricle, and right-sided aortic arch), enlarged jugular lymphatic sacs (JLS; all animals), cleft palate (~85% of embryos), and “Bochdalek” type of CDH (~40% of animals). Our results suggest that the malformations are the result of both the deregulated expression of several key regulators of mesoderm differentiation, as well as a general cell cycle defect. Furthermore, we identified a mutation in the *CHTOP* gene in a “complex” CDH patient. The mutation changes an arginine residue within the GAR domain, thereby severely affecting the recruitment of PRMT1. These results indicate that deregulation of CHTOP and/or its associating factors may contribute to syndromes with “complex” CDH in human individuals.

Results

CHTOP is essential for normal embryogenesis

In order to assess the role of CHTOP *in vivo*, a mutant mouse line was established from an embryonal stem cell clone carrying a gene trap insertion in the first intron of the *Chtop* gene (Figure 1A). This insertion could potentially generate a full knockout, as the open reading frame of the *Chtop* gene starts in the downstream exon. Animals heterozygous for the gene trap, from here on referred to as *Chtop*^{+/tr}, were fertile and intercrossed to generate homozygotes (*Chtop*^{tr/tr}). No homozygotes were recovered at weaning during the initial analysis (Figure 1B). Further analysis revealed no *Chtop*^{tr/tr} animals at birth, indicating that a homozygous mutation at the CHTOP locus results in embryonic lethality. At all embryonic stages tested (E9.5 to E16.5) Mendelian ratios of wild-type (*Chtop*^{+/+}), *Chtop*^{+/tr}, and *Chtop*^{tr/tr} embryos were detected by PCR (Figures 1B and 1C). Gross inspection demonstrated growth retardation and severe subcutaneous edema in *Chtop*^{tr/tr} embryos (Figure 1D).

Mouse embryonic fibroblasts (MEFs) were used to examine the effect of the gene trap insertion on CHTOP protein and mRNA levels. CHTOP protein could not be detected in *Chtop*^{tr/tr} cells (Figure 1E, upper panel), while the transcript level was reduced to ~5% (Figure 1E, lower

panel). Expression of CHTOP protein in heterozygous cells was comparable to wild type, while mRNA levels dropped to ~50%. This indicates that the protein level of CHTOP is mainly regulated by protein stability rather than transcription. Furthermore, CHTOP could not be detected by immunohistochemistry in *Chtop^{tr/tr}* embryos (Figure 1F and Supplement Figure 1). In contrast, wild-type littermates displayed a near-ubiquitous expression at this stage of development (E13.5). The intensity of staining varied per tissue, with minimal/no expression in the nuclei of circulating primitive erythrocytes and a proportion of liver cells (Figure 1F). Together, these data show that the gene trap insertion results in complete ablation of CHTOP protein expression and that CHTOP is required for normal embryonic development.

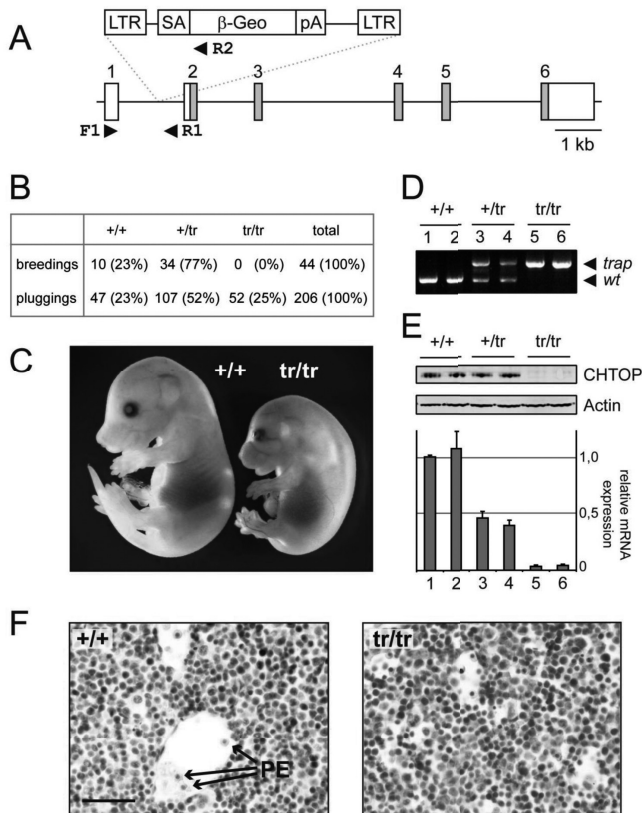


Figure 1 | Generation of *Chtop^{tr/tr}* mice

A: Schematic representation of the *Chtop* genomic locus and the viral genetrapp vector. Exons are indicated, the coding region is shaded. F1, R1, and R2 represent oligonucleotides used for genotyping; LTR = long terminal repeat, SA = splice acceptor, b-Geo = combined selection and reporter gene, pA = poly-A tail. **B:** Genotype analysis of *Chtop^{tr/tr}* intercrosses at weaning (breedings) and embryonic (pluggings) stages. **C:** Wild-type (+/+) and mutant (tr/tr) embryos at E16.5 showing edema and growth retardation in the mutant. **D:** Genotype analysis on yolk sac cells by PCR. **E:** CHTOP protein levels (top panel) and mRNA levels (bottom panel) in embryonic fibroblasts. One of three independent experiments is shown. **F:** Detection of CHTOP protein by immunostaining of fetal liver (E13.5). Circulating primitive erythrocytes (PE) are negative for CHTOP staining. Bar, 100 μ m (see page 247 for color figure).

Multi-embryo imaging reveals multiple developmental abnormalities, including heart defects

The development of edema in various mouse mutants is frequently associated with cardiovascular defects [22, 23]. As traditional histology is labor intensive and loses 3D information necessary for interpretation of complex cardiac malformations, we used high-throughput magnetic resonance imaging (MRI) to analyze embryonic abnormalities [24]. A series of 42 embryos was collected on day 15.5 of gestation, scanned at 43x43x36 μm resolution, and phenotypically scored, with the observer blinded to the genotype. All *Chtop^{tr/tr}* embryos showed edema, bilateral cysts in jugular lymphatic sacs and heart defects (Table 1 and Figure 2A). All embryos had additional abnormalities not directly related to the cardiovascular system, such as small visceral organs (spleen, stomach, pancreas; 13 out of 14 embryos), abnormal right kidney (8 out of 14; Figure 2B), small and abnormal lungs (9 out of 14), cleft palate (12 out of 14), and spinal cord defects (4 out of 14; Table 1). Furthermore, 6 out of 14 embryos displayed congenital diaphragmatic hernia (CDH). None of those anomalies was seen in wild type (11 embryos) or heterozygotes (17 embryos). The combination of defects points to a syndrome with CDH, although it does not fit clearly all the criteria of comparable conditions observed in human patients, such as Fryns syndrome [6]. The cardiovascular defects were pleiotropic and included various lesions, outflow tract -, and aortic arch malformations (Table 2). All mutant hearts had markedly enlarged and dilated right atria (RA) combined with atrial septal defects (ASD), ventricular septal defects (VSD), and an abnormal atrioventricular junction (AVJ). Outflow defects, like common arterial trunk (CAT) and double outlet right ventricle (DORV), were observed in ~50% of *Chtop^{tr/tr}* embryos. Malformations of the aorta were observed in ~40% of the mutant hearts and include overriding aorta, interrupted aortic arch (IAA) and right-sided aortic arch. For 3D reconstruction, a limited number of embryos were re-imaged at a resolution of 25x25x26 μm . Figures 2C (transverse sections) and 2D (3D reconstruction) demonstrate a *Chtop^{tr/tr}* heart with enlarged right atrium, common valve, VSD, DORV, and right-sided aortic arch.

Congenital Diaphragmatic Hernia in *Chtop^{tr/tr}* embryos

Anatomical analysis revealed diaphragmatic hernias in ~40% of *Chtop^{tr/tr}* embryos, with herniation of the liver and stomach into the thoracic cavity (Figure 3A). All hernias were either left-sided or bilateral and located in the dorsolateral region of the diaphragm. An example of a left-sided hernia is shown as a 3D reconstruction (Figure 3B), illustrating the protrusion of the liver and the underdeveloped stomach, thereby competing for space with the left lung. Interestingly, like in humans, impeded development is not restricted to this side of the lung, as demonstrated by the severe hypoplasticity of the contralateral lung and absence of the accessory lobe (Figure 3C).

Diaphragms from *Chtop^{tr/tr}* embryos (E16.5) were thickened around the periphery of the defect compared with the intact contralateral side and wild-type controls (Figure 3D), as observed in nitrofen treated rats [25]. Staining with an antibody specific for smooth muscle actin showed that the diaphragms were well muscularized (Figure 3E). Together, these data confirmed that the diaphragmatic defect did not originate from a myoblast migration defect, as observed

in *c-Met* and *Pax3* null mice [26, 27]. Instead, we observed incomplete fusion of the tissues that form the dorsolateral part of the diaphragm, the pleuroperitoneal fold (PPF) and the body wall component of the diaphragm (Figure 3F and Supplement Figure 2). This was most likely a result of a proliferation defect of the PPF and could be detected from E13.5 onwards (Supplement Figure 3). In conclusion, absence of CHTOP results in a classic Bochdalek-type of CDH in 40% of the animals.

Table 1 | High-throughput high-resolution magnetic resonance microscopy of *Chtop*^{tr/tr} mice (E15.5).

| PHENOTYPE | MP ID | <i>Chtop</i> | | |
|---|--|--------------|-------------|---------------|
| | | +/+ n=11 | +tr n=17 | tr/tr n=14 |
| Small body size | MP: 0001698 | 0 | 0 | 14 |
| Oedema (moderate to massive) | MP: 0001785 | 0 | 0 | 14 |
| Cleft palate | MP: 0000111 | 0 | 0 | 12 |
| Increased spinal cord size (spinal cord folded above the tail) | MP: 0002809 (MP: 0000955 - abnormal SC) | 0 | 0 | 4 |
| Right kidney small and fused to the large left kidney | MP: 0002989 and MP: 0003605 | 0 | 0 | 8 |
| Small spleen | MP: 0000692 | 0 | 0 | 13 |
| Small, abnormally looping stomach | MP: 0002691 and MP: 0000470 | 0 | 0 | 13 |
| Small pancreas (confirmed by histology) | MP: 0004247 | 0 | 0 | 13 |
| Small, abnormal lungs | MP: 0003641 and MP: 0001175 | 0 | 0 | 9 |
| Herniated diaphragm (Congenital Diaphragmatic Hernia) | MP: 0003924 | 0 | 0 | 6 |
| Cystic jugular lymphatic sacks | MP: 0004107 | 0 | 0 | 14 |
| Cardiovascular anomalies | various, see Table2 | 0 | 0 | 14 |

ID = mammalian phenotype ID.

Deregulated gene expression in *Chtop*^{tr/tr} embryos

The type of CDH in *Chtop*^{tr/tr} embryos is identical to CDH observed in *Coup-TFII* null mice and nitrofen-treated rats [28, 25]. As CHTOP can act as a transcriptional coactivator, we first tested whether Coup-TFII or Raldh2, the enzyme inhibited by the herbicide nitrofen, were deregulated in *Chtop*^{tr/tr} embryos [29]. No difference was observed in both the level and pattern of expression for these genes at day 10.5 and 14.5 of gestation as analyzed by immunohistochemistry (IHC; Supplement Figure 4). Next, we performed genome-wide expression profiling of wild type and *Chtop*^{tr/tr} embryos. As the abnormalities observed in *Chtop* null embryos may be the consequences of general and earlier developmental defects, stage-matched embryos were-

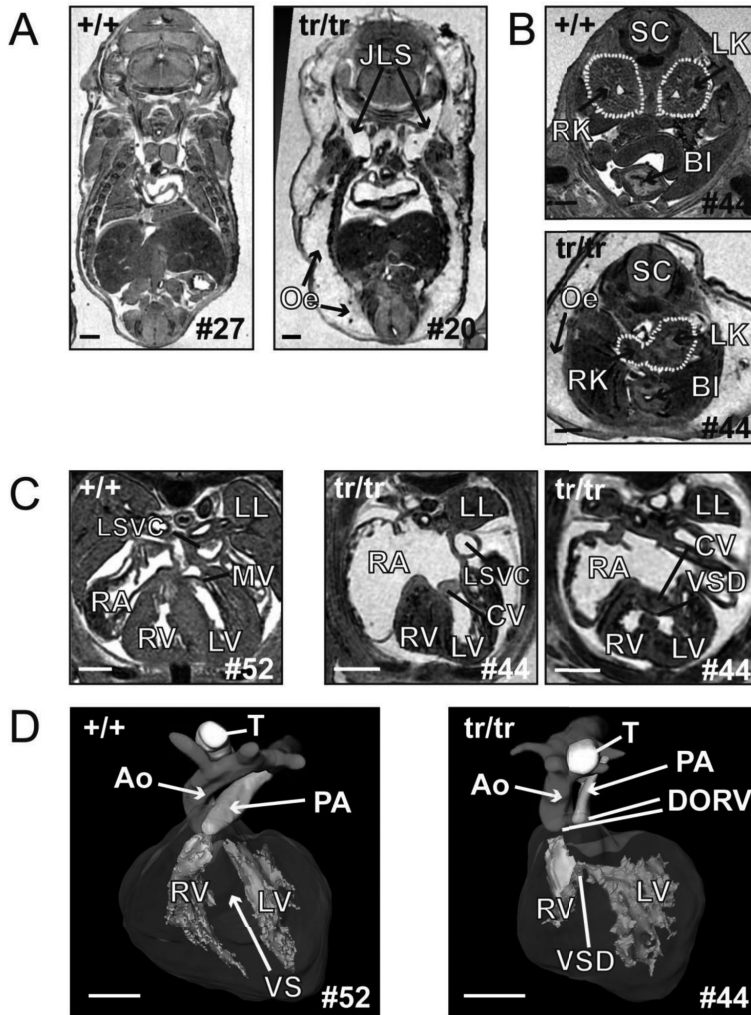


Figure 2 | MRI reveals developmental abnormalities in *Chtop*^{tr/tr} embryos

A: Coronal sections demonstrating oedema (Oe) and cysts in the jugular lymph sacs (JLS). **B-C:** Transverse sections showing small and fused right kidney (RK) and multiple cardiac malformations. Two thoracic sections are shown from the same mutant. Structures indicated are spinal cord (SC), left kidney (LK), bladder (BI), left lung (LL), left superior vena cava (LSVC), right atrium (RA), right ventricle (RV), left ventricle (LV), mitral valve (MV), common valve (CV), and ventricular septal defect (VSD). **D:** 3D reconstruction of the wild-type and mutant hearts clearly demonstrates the VSD, narrowed pulmonary artery (PA), double outlet right valve (DORV), and right-sided aorta (Ao). T = trachea. Bars, 500 μ m (see page 248 for color figure).

collected at the 22-25 somite stage (~E9.0). Total RNA was isolated, labeled and hybridized to Affymetrix Mouse Gene 1.0 ST arrays, allowing whole transcript analysis. Genes that showed ≥ 2 -fold up- or down-regulation are listed in Table S1. As a common mesenchymal defect has been proposed to explain dorsolateral CDH and associated extra-diaphragmatic defects [9, 7], it

is highly interesting that non-supervised pathway analysis revealed mesoderm development as one of the most deregulated processes (Figure 4A). Notably, we observed a marked decrease in expression of the transcription factors *T* (*Brachyury*) and *Tbx6*, genes that are critical for the induction and specification of mesoderm, respectively. We observed considerable variation in the expression values for the individual embryos; therefore we used quantitative PCR followed by correlation analysis for validation. The correlation coefficients for *T* ($r^2=0,93$), *Tbx6* ($r^2=0,78$), *Tcf15* ($r^2=0,89$), *Slit2* ($r^2=0,66$), and *Btk* ($r^2=0,60$) proved the accuracy of these data sets. In line with the IHC data, no change in expression was detected for *Coup-TFII* and *Raldh2*, or for other critical components of the retinoic acid (RA) signalling pathway. Furthermore, we did not find any evidence that the expression of *Wt1*, *Gata4*, and *Fog2* was affected in *Chtop^{tr/tr}* embryos at this developmental stage. As the vasculature develops from mesoderm precursors, it is not surprising that vasculature development appeared deregulated (Figure 4B). Furthermore, we did note an increase of the expression of genes that are associated with the G2/M-phase of the cell cycle, including the cell cycle regulators Cyclin-dependent kinase inhibitor 1A (p21) and Cyclin G1, as well as proteins important for the mitotic spindle (Figure 4C).

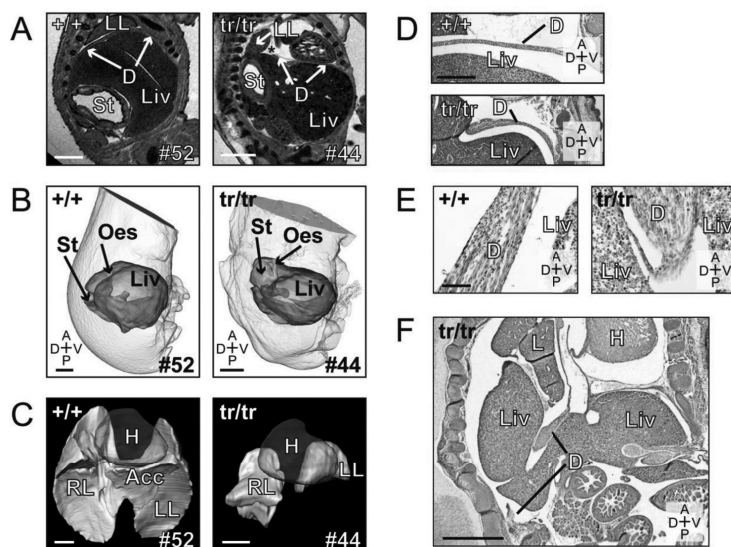


Figure 3 | Congenital Diaphragmatic Hernia in *Chtop^{tr/tr}* embryos

MRI pictures of sagittal sections of wild-type (+/+) and mutant (*tr/tr*) embryos (E15.5). **A:** The mutant displays a „Bochdalek“ type of CDH, with the hernia indicated with *. **B:** 3D reconstruction of the stomach and liver, demonstrating malrotation of the stomach and herniation of the stomach and liver into the thoracic cavity. Scale bar = 0.5 mm. **C:** 3D reconstruction of the lungs, demonstrating hypoplasticity in mutant lungs. **D:** Diaphragm thickening around the diaphragm defect (bottom panel) compared with the normal contralateral side of the diaphragm (top panel). **E:** Muscular cells are present in mutant diaphragms, as indicated by smooth muscle actin immunostaining. **F:** Sagittal section demonstrating dorsolateral CDH, resulting in massive expansion of the liver into the thoracic cavity. Structures indicated are: left lung (LL), right lung (RL), accessory lobe (Acc), diaphragm (D), liver (Liv), stomach (St), oesophagus (Oe), spleen (S), right crus (RC), and heart (H); axes: r – right; l – left; d – dorsal; v – ventral; a – anterior, p – posterior. Bars: 500 mm **A-D**, 100 mm **E**, 1 mm **F** (see page 248 for color figure).

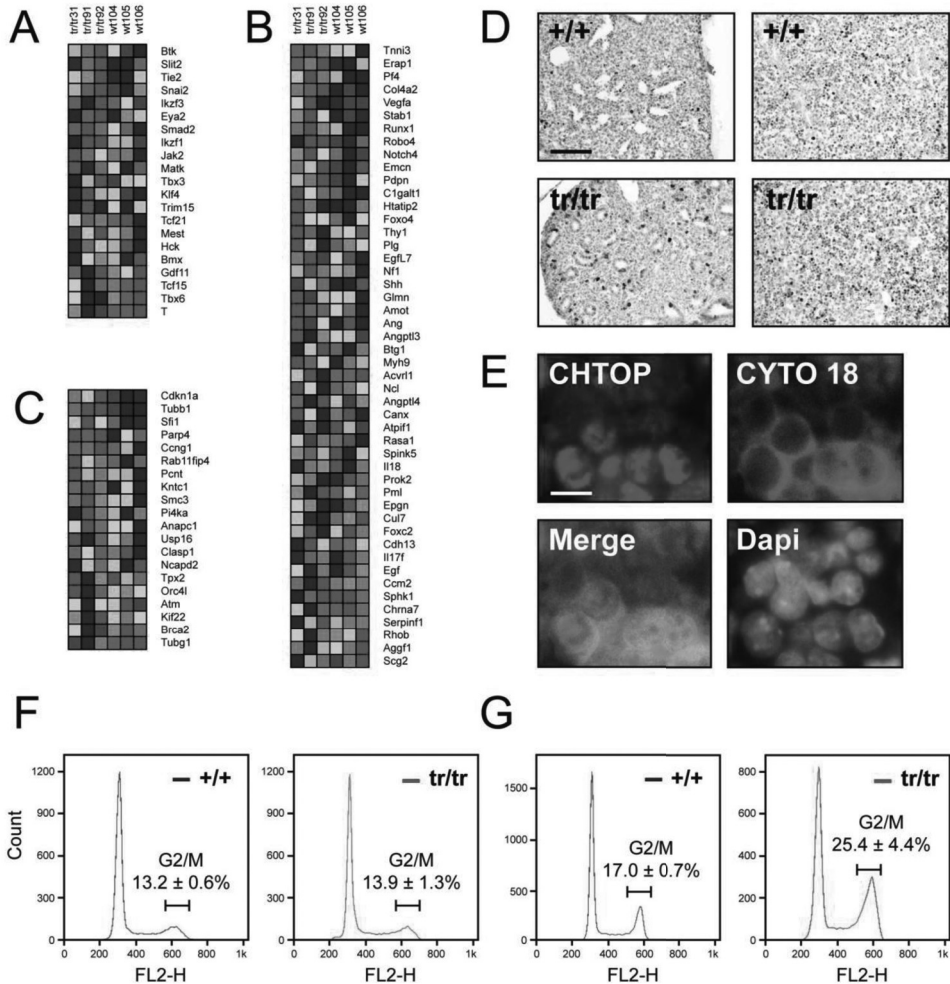


Figure 4 | Deregulated gene expression in *Chtop*^{tr/tr} embryos

Expression profiling was performed on E9.0 embryos (22–25 somite stage). Gene set analysis shows deregulation of: **A:** mesoderm development, **B:** vasculature development, and **C:** the G2/M-phase of the cell cycle. **D:** Immunostaining with an antibody against phosphorylated H3 demonstrates an increase of G2/M cells in mutant lung (left panels) and liver (right panels). One of three independent experiments is shown. **E:** Fetal liver cells (E13.5) with relative high levels of CHTOP (red channel) are hepatic precursors, as demonstrated by their coexpression of cytokeratin 18 (Cyto 18; green channel). DNA was visualized by Dapi staining (blue channel). **F:** FACS analysis shows that wild type and mutant fetal liver derived erythroblasts have similar DNA profiles. In contrast, propidium iodide staining reveals a delay of the G2/M-phase in mutant MEFs **G:** Data are from a single experiment that is representative of three independent experiments. Values represent the mean of 4 littermates ± SD. Bars: 200 μm **D**, 10 μm **E** (see page 248 for color figure).

The possible cell cycle defect was further studied, as it could play a role in the diverse developmental defects observed in *Chtop*^{tr/tr} embryos. Chromosome condensation during mitosis

is associated with phosphorylation of histone H3 at serine 10 (pS10H3) [30]. Staining with an antibody specifically recognizing this modification indeed demonstrates an increase of mitotic cells in various *Chtop*^{tr/tr} tissues (Figure 4D and Supplement Figure 5A). Therefore, we tested whether aberrant proliferation kinetics could be involved in the etiology of CDH. As observed earlier, the fetal liver contained cells with either high or low levels of CHTOP, CHTOPhi and CHTOPlo, respectively (Figure 1F). CHTOPlo cells were rounder, had smaller nuclei combined with less cytoplasm and their chromatin was more condensed compared to CHTOPhi cells, suggesting that CHTOPlo cells were erythroid (precursor) cells, while CHTOPhi represented liver (precursor) cells. Immunofluorescent co-staining with cytokeratin 18, a marker for the hepatic cell lineage [31], confirmed that the CHTOPhi cells represented the hepatic population (Figure 4E). Next, fetal livers from E13.5 embryos were isolated to grow erythroid cultures, while mouse embryonic fibroblasts (MEFs) were cultured from the remaining tissues. Homogenous pro-erythroblast cultures were obtained in serum-free medium and their cell cycle profile was analyzed. No differences in cell cycle dynamics were observed in wild type and *Chtop*^{tr/tr} erythroid cells (Figure 4F). In contrast, primary MEFs from *Chtop*^{tr/tr} had a slower proliferation rate, which was due to an accumulation in G2/M (Figure 4G). While growing the erythroid cells, we noted proliferation of specific adherent cells. The cells were flattened, bi-nucleated and exclusively present in wild-type cultures (Supplement Figure 5B). Although there was not sufficient material to further analyze these cells, the experiments indicate that most cell types have a problem to progress through mitosis when CHTOP expression is perturbed. From E10.0 onwards, the fetal liver grows rapidly as a result of the massive expansion of the erythroid compartment [32]. Erythroid cells, that already have low CHTOP levels, are not affected by the ablation of CHTOP expression. Therefore, expansion of the *Chtop*^{tr/tr} fetal liver is less affected compared to the other embryonic tissues. This may result in the protrusion of the liver into the thoracic cavity before the pleuroperitoneal canals are closed.

CHTOP mutation analysis in CDH patients

To test whether deregulation of CHTOP, located on chromosome 1q21.3, could be involved in the genetics of human CDH, we sequenced parts of the CHTOP locus of 43 patients with complex CDH (see Table S2). The coding region, the splicing boundaries, and the non-coding first exon were fully sequenced (Figure 5A), revealing sequence variation at 7 nucleotide positions. Of these, 5 were observed multiple times and were located outside the coding region (Table S3). The other two were unique and located within the coding region. Both variations resulted in an amino acid change, R175H and R196L, respectively, and could be validated by restriction enzyme analysis (Figure 5B). Nevertheless, the R196L mutation was the only detected variation not previously identified as a single nucleotide polymorphism (SNP). The R196L mutation was also shown in the maternal DNA, indicating that it is not a *de novo* mutation and demonstrating that it is not the sole cause of the clinical features displayed by the affected patient. It should be noted that the mother of patient DS05.1280 and carrier of the R196L mutation, was also

Table 2 | Cardiovascular defects observed in Chtop^{tr/tr} embryos (E15.5)

| EMBRYO ID | VENTRICLES | ATRIA | AVJ | OUTLET | PA | AORTA | OTHER |
|-----------|---------------------------|-----------------|-----------------|--------|---------|--------------|------------------------------------|
| #8 | VSD | both large, ASD | common AV valve | CAT | R-sided | R-sided arch | ~ |
| #18 | VSD, small RV | RA large, ASD | common AV valve | DORV | ~ | IAA | ~ |
| #20 | VSD (muscular) | both large, ASD | common AV valve | CAT | ~ | ~ | ~ |
| #22 | VSD | both large, ASD | common AV valve | CAT | R-sided | R-sided arch | ~ |
| #32 | VSD | RA large, ASD | common AV valve | ~ | ~ | overriding | ~ |
| #34 | VSD | RA large, ASD | common AV valve | ~ | ~ | ~ | ~ |
| #35 | VSD | ASD | common AV valve | ~ | ~ | ~ | ~ |
| #42 | VSD | both large | ~ | ~ | ~ | ~ | ~ |
| #44 | VSD | RA large, ASD | common AV valve | DORV | ~ | R-sided arch | ~ |
| #54 | VSD | ASD | common AV valve | DORV | ~ | ~ | retresophageal R subclavian artery |
| #58 | VSD | both large, ASD | common AV valve | ~ | ~ | ~ | ~ |
| #103 | VSD | both large, ASD | common AV valve | ~ | ~ | IAA | ~ |
| #110 | VSD (outlet and muscular) | ASD | common AV valve | CAT | ~ | ~ | retresophageal R subclavian artery |
| #146 | VSD | ASD | common AV valve | CAT | ~ | ~ | ~ |

VSD = ventricular septal defect (MP:0000281), ASD = atrial septum defect (MP: 0000282), large RA (MP: 0008727), large both atria (dilated; MP: 0003140), abnormal AVJ (common AV valve; MP: 0002745), CAT (MP: 0002633), DORV= double outlet right ventricle (MP: 0000284), R-sided pulmonary artery (PA; MP: 0000486), R-sided AoA (MP: 0004158), IAA (MP: 0004157), overriding Ao (MP: 0000273), Retresophageal RSA (MP: 0004160)

carrier of a balanced translocation t(11;22), resulting in a partial trisomy 11 and 22 in the patient (47,XY,+der(22)t(11;22)(q23.3;q11.2)). Yet, the mother displayed a normal phenotype.

Both the SNP R175H and the mutation R196L were located within the C-terminal part of the GAR domain of CHTOP. As we have shown previously that this region is critical for the interaction with PRMT1, we tested whether the identified variations affected the interaction between CHTOP and PRMT1. The corresponding nucleotides were mutated in murine CHTOP cDNA, after which the tagged constructs were stably expressed in mouse erythroid leukemia (MEL) cells. Exogenous CHTOP was purified from nuclear extracts using paramagnetic streptavidin beads.

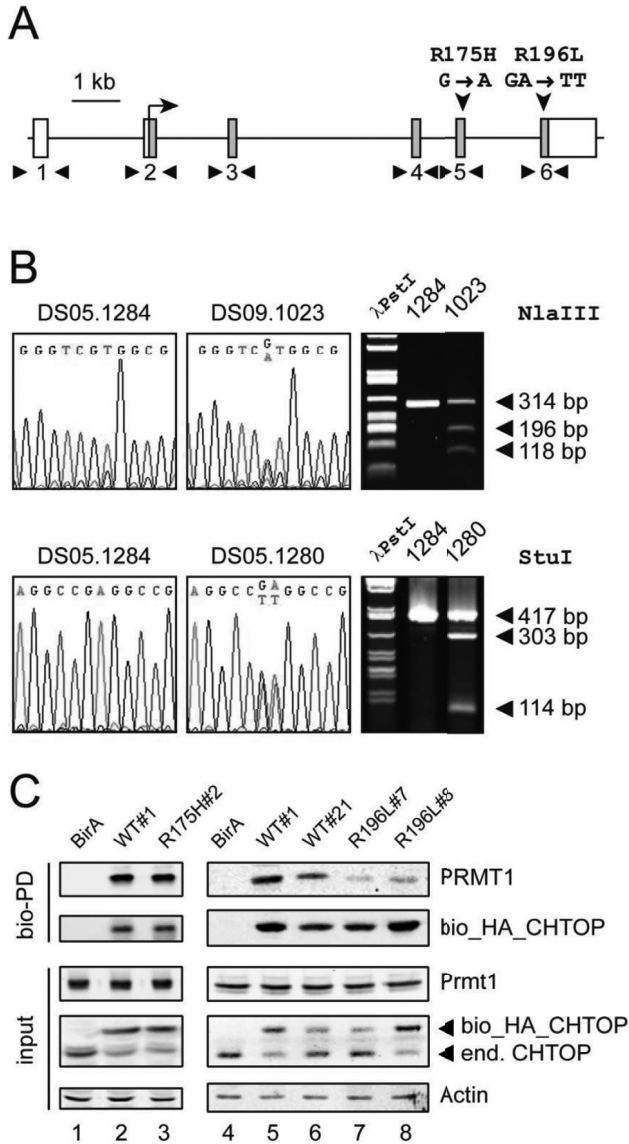


Figure 5 | Detection of CHTOP variations in CDH patients

A: Schematic representation of the human *Chtop* locus. Exons are indicated, the coding region is shaded. Vertical arrowheads indicate the positions of identified variations (R175H and R196L), horizontal arrowheads represent oligonucleotides used for amplification and sequencing. **B:** Identification of the G>A SNP and its validation by *Nla*III digestion (top panels); identification of the GA>TT mutation and its validation by *Stu*I digestion (bottom panels). DS05.1284 = control DNA; DS09.1023 and DS05.1280 = patient DNA **C:** Bio_HA_CHTOP with SNP R175H (left panels) and mutation R196L (right panels) were introduced into MEL cells and tested for their interaction with PRMT1. In contrast to R175H, the R196L mutation greatly reduced the binding to PRMT1. Compare lanes 5 and 8 for relative high ectopic expression of CHTOP, and lanes 6 and 7 for relative low expression. Data are from a single experiment that is representative of three independent experiments (see page 249 for color figure).

No difference in affinity for PRMT1 was observed between wild type CHTOP and CHTOP_R175H (Figure 5C). In contrast, binding of PRMT1 was strongly reduced to CHTOP_R196L, both in high – and low expressing clones (compare lanes 5 and 8, and lanes 6 and 7, respectively). Since arginine methylation plays a role in protein-protein interactions, reduced PRMT1 recruitment is likely to affect additional interactions of CHTOP and/or the methylation status of those additional CHTOP-binding proteins. In conclusion, the first limited screen of 43 CDH patients resulted in the identification of a CHTOP mutation. The CHTOP_R196L mutation severely affects PRMT1 recruitment and may therefore cripple the (epi) genetic functions of CHTOP.

Discussion

Patients with congenital diaphragmatic hernia form a heterogeneous group, both genetically and phenotypically. Malformations in addition to CDH are observed in roughly 30-40% of the patients. With the cardiovascular system most commonly affected, additional clinical findings are highly variable and range from limb and digital anomalies to growth retardation and ear/eye defects [33]. How the different clinical problems relate to each other is currently unclear as the pathogenic mechanisms are largely unknown. Here we describe that *Chtop* null-mutant mice display severe growth retardation and malformation of multiple organs during embryogenesis, including a “Bochdalek” type of hernia. The latter defect resembles the type of CDH induced by the herbicide nitrofen, a powerful inhibitor of retinal dehydrogenase 2 (RALDH2) [34, 29]. Comparable hernias are also observed in *Wt1* null mutant mice, conditionally inactivated *Coup-TFII* mice, *RAR α* and *RAR β 2* double null-mutant mice, and *MyoR* and *Capsulin* double null-mutant mice [25, 28, 35, 26]. Like CHTOP, these are all transcriptional regulators. Although the factors have pleiotropic functions that are only partially overlapping, the common dorsolateral hernia suggests that they interact directly or genetically in the developing diaphragm. Previous studies indicate that abnormal retinoid signalling contributes to the etiology of CDH [36]. In contrast to its role in estrogen receptor (ER α) mediated transcription [11], CHTOP does not appear critical in retinoic acid (RA) signalling. Ablation of the *Raldh2* gene leads to an almost complete block of RA synthesis, resulting in embryonic lethality at E10.5 because of defects in heart, hindbrain, and somites [37]. Also a hypomorphic allele of this gene does not result in a phenocopy of *Chtop*^{tr/tr} mice [38]. Further experiments have to be performed to address whether CHTOP has a subtler role in the RA pathway.

Although the diaphragm consists of different cell types, it is probably completely derived from mesodermal tissue [8]. Consequently, the mesenchymal hit hypothesis has been proposed to explain the association of diaphragmatic and extra-diaphragmatic defects, [39]. This hypothesis posits that: (1) similar signalling pathways are involved in the differentiation of mesenchymal cells in all of the affected organs; and (2) the function of mesenchymal cells in the affected organs is disrupted by genetic or environmental triggers [9]. In line with this viewpoint, our expression profiling data indicates that mesoderm development is one of the major deregulated processes

in the *Chtop^{tr/tr}* animals. Misexpressed genes include *T* (*Brachyury*) and *Tbx6*, transcription factors that play a crucial role in mesoderm specification, somite segmentation, and left-right (L-R) axis determination [40]. It is currently unclear whether these genes are directly regulated by CHTOP, or that their downregulation reflects a general developmental delay. Disorders resulting from failure to establish normal L-R asymmetry include *situs inversus* and heterotaxy. In *situs inversus*, the internal organ arrangement is mirror image of normal anatomy (*situs solitus*). Heterotaxy (*situs ambiguus*) encompasses any abnormal arrangement of internal organs and is usually characterized by congenital anomalies [41]. Many of those, like cardiovascular defects, microgastria, neural tube defects and cleft palate are also observed in *Chtop^{tr/tr}* embryos and in patients with specific CDH-containing syndromes. It should be noted that asplenia or polysplenia, another clinical feature of heterotaxy, is not observed in CHTOP null mice, although *Chtop^{tr/tr}* spleens are strongly reduced in size. Fryns syndrome is a multiple congenital anomaly/mental retardation syndrome [15]. *Chtop^{tr/tr}* mice clearly display a Fryns-like disorder, but whether they might be considered as an animal model for Fryns syndrome is currently uncertain. Perinatal death obscures a detailed analysis of the distal digits and facial appearance, but no obvious limb defects were detected in any of the mutant embryos. The use of a conditional CHTOP knockout strategy may be of help to answer this question.

Chtop^{tr/tr} embryos are growth retarded. In a mixed (129Se-C57BL/6) background, reduced growth is observed from E11.5 onwards. Backcrossing to C57BL/6 worsens the phenotype, resulting in reduced growth from E8.5 onwards. Our results show that this is due to a partial block in mitosis rather than increased apoptosis. Interestingly, erythroid progenitors are less affected compared to other cell types. As a result of massive proliferation of erythroid cells, the fetal liver is rapidly expanding during the developmental stages at which the diaphragm is formed [32, 8]. Because diaphragm development is slowed down in *Chtop^{tr/tr}* mice, the fetal liver may grow beyond the PPF before the primordial diaphragm contributing to the posterolateral part of the diaphragm has completed formed and in this way contribute to the hernia. This mechanism may also explain why CDH is observed in only ~40% of the *Chtop^{tr/tr}* animals, as the relative growth of developing diaphragm and liver will vary between individual embryos.

CDH is, genetically, a heterogeneous disease. Although several genes have been shown to underlie abnormal diaphragm development in mice, only a few CDH-related mutations have been identified in the orthologous genes in humans. Nevertheless, we identified a mutation in the *CHTOP* gene in an initial screen of 43 patients with complex CDH. The mutation could be detected in the maternal DNA, indicating that it is not a *de novo* mutation and demonstrating that it is not the sole cause of the clinical features displayed by the affected patient. Furthermore, it should be noted that the mother was also carrier of a balanced translocation t(11;22), resulting in a partial trisomy 11 and 22 in the patient. This chromosomal anomaly has been associated with CDH previously, although the mechanism remains unclear [42]. The lack of full penetrance of CDH in patients with karyotype 47,XY,+der(22)t(11;22)(q23.3;q11.2) strongly suggest that additional pathogenic mutations are required. The identified mutation changed an arginine residue within the GAR region of CHTOP (R196L), thereby severely reducing the affinity for

PRMT1. Since arginine methylation plays a role in protein-protein interactions, reduced PRMT1 recruitment is likely to affect additional interactions of CHTOP and/or the methylation status of those additional CHTOP-binding proteins. The identification of such proteins will be important to further understand the function of CHTOP and its role in the etiology of CDH.

Materials and methods

Ethics Statement

All work has been approved by the local animal ethics committee.

Generation of mice and genotyping

The 129S2 ES cell clone D044F05 with the gene trap vector rFlpRosabeta γ in the *Chtop* gene was obtained from the German Gene Trap Consortium, now part of the International Gene Trap Consortium (<http://www.genetrapp.org>). The 129S2 ES cell-derived chimeras were generated by injecting C57BL/6 blastocysts. The resulting male chimeras were bred to C57BL/6 females, and agouti offspring were tested for transgene transmission. Animals heterozygous for the gene trap insertion were backcrossed to C57BL/6 mice. Genotyping by PCR was done with DNA isolated from tail biopsies or yolk sac tissue and a mixture of three primers (Table S3).

Analysis of embryos

For MRI analysis, E15.5 embryos were fixed in 4% paraformaldehyde containing 2 mM gadoliniumdiethylenetriamine pentaacetic anhydride (Gd; Magnevist) at 4°C for ~1 week, and then embedded in 1% agarose containing Gd. MRI, data reconstruction and analysis were performed as described [24].

For histology, embryos were dehydrated in a graded ethanol series, cleared in xylene, embedded in paraffin, and sectioned. Serial sections (7 μ m) were collected on slides and stained with eosin and/or hematoxylin. For immunohistochemistry, paraffin sections were permeabilized in 10 mM citric acid (pH 6.0), and blocked with 5% bovine serum albumine (BSA). Primary antibody incubation was performed in blocking solution for 16 hrs at 4°C, followed by peroxidase staining or fluorescent detection. Images were captured using SZX16 and BX40 light microscopes, a DP71 digital camera, and CellD imaging software (all Olympus).

Cell culture

Mouse embryonic fibroblasts (MEFs) and fetal liver-derived erythroid cultures were obtained from E13.5 animals. MEFs were maintained in F10 + Dulbecco modified Eagle medium (DMEM; 50% each; Lonza) supplemented with 10% fetal calf serum (FCS). Erythroid cells were grown in StemPro-34 medium (Gibco), supplemented with human recombinant erythropoietin (1 u/ml; Janssen-Cilag), dexamethasone (10⁻⁶ M; Sigma), and stem cell factor (100 ng/ml). MEL cells were grown DMEM supplemented with 10% FCS.

Cell cycle analysis

Cells were resuspended in PBS, fixed by addition of 9 volumes of 70% ethanol, and stored at 4°C until further analysis. After washing with PBS, the cells were resuspended in 0.5 ml staining solution (0.1% Triton X-100 (Sigma), 20 µg/ml propidium iodide (Invitrogen), and 0.2 mg/ml RNase A in PBS. After incubation for 30 min at RT, cells were stored overnight at 4°C, and analyzed on a BD FACScan cytometer.

Western blotting and antibodies

Western blot analysis was performed as described [11]. Nitrocellulose membranes were blocked in 1% BSA, incubated with appropriate antibodies, and analyzed using the Odyssey Infrared Imaging System (Li-Cor Biosciences). The following primary antibodies were used: CHTOP (KT64) from Absea Biotechnology, HA (sc-7392), Cytokeratin 18 (sc-6259) and Actin (sc-1616) from Santa Cruz, PRMT1 (07-404) and pS10H3 (06-570) from Millipore, COUP-TFII (PP-H7147) from Perseus Proteomics, Smooth muscle actin (1A4) from Thermo Scientific, and RALDH2 was a kind gift of Prof. Peter McCaffery (University of Aberdeen, UK).

Microarray analysis

RNA was extracted from stage-matched embryos (22-25 somites). Microarray analysis was performed as described [43]. The microarray data have been submitted to the NCBI Gene Expression Omnibus database (GSEXXXXX).

Quantitative PCR

Total RNA was extracted using TRI reagent (Sigma-Aldrich). Sequences of the primers used are listed in Sup. Table 3. All reactions involved initial denaturation at 95°C for 5 minutes, followed by 40 cycles of denaturation at 95°C for 30 seconds, annealing at 60°C for 30 seconds, and elongation at 72°C for 30 seconds, using Platinum Taq (Invitrogen) on a C1000 Thermal Cycler (Bio-Rad). Ribonuclease Inhibitor 1 gene transcription was used as a reference for normalization.

Sequencing

Coding regions were amplified by PCR using hybrid primers containing the M13 sequence and an amplicon-specific sequence (Supplement Table 3). PCR products were recovered using NucleoFast 96 PCR clean-up plates (Machery-Nagel), according to manufacturer instructions. Samples were sequenced using M13 primers and a 3730 DNA Analyzer (Applied Biosystems).

Site-Directed Mutagenesis

The mutations mCHTOP_R175H and mCHTOP_R196L were generated using the QuikChange Site-Directed Mutagenesis kit (Stratagene) following the instructions of the provider.

Acknowledgements

We thank Alex Maas, Christel Kockx and the German Gene Trap Consortium for technical assistance and Prof. Peter McCaffery (University of Aberdeen, UK) for the generous gift of the Raldh2 antibody

References

1. Langham MR, Jr., Kays DW, Ledbetter DJ, Frentzen B, Sanford LL, et al. (1996) *Congenital diaphragmatic hernia. Epidemiology and outcome*. Clin Perinatol **23**: 671-688.
2. Sluiter I, van de Ven CP, Wijnen RM, Tibboel D (2011) *Congenital diaphragmatic hernia: Still moving target*. Semin Fetal Neonatal Med **16**: 139-144.
3. Torfs CP, Curry CJ, Bateson TF, Honore LH (1992) *A population-based study of congenital diaphragmatic hernia*. Teratology **46**: 555-565.
4. van Loenhout RB, Tibboel D, Post M, Keijzer R (2009) *Congenital diaphragmatic hernia: comparison of animal models and relevance to the human situation*. Neonatology **96**: 137-149.
5. Stoll C, Alembik Y, Dott B, Roth MP (2008) *Associated malformations in cases with congenital diaphragmatic hernia*. Genet Couns **19**: 331-339.
6. Slavotinek AM (2007) *Single gene disorders associated with congenital diaphragmatic hernia*. Am J Med Genet C Semin Med Genet **145C**: 172-183.
7. Brady PD, Srisupundit K, Devriendt K, Fryns JP, Deprest JA, et al. (2011) *Recent developments in the genetic factors underlying congenital diaphragmatic hernia*. Fetal Diagn Ther **29**: 25-39.
8. Ackerman KG, Greer JJ (2007) *Development of the diaphragm and genetic mouse models of diaphragmatic defects*. Am J Med Genet C Semin Med Genet **145C**: 109-116.
9. Bielinska M, Jay PY, Erlich JM, Mannisto S, Urban Z, et al. (2007) *Molecular genetics of congenital diaphragmatic defects*. Ann Med **39**: 261-274.
10. Beurskens N, Klaassens M, Rottier R, de Klein A, Tibboel D (2007) *Linking animal models to human congenital diaphragmatic hernia*. Birth Defects Res A Clin Mol Teratol **79**: 565-572.
11. van Dijk TB, Gillemans N, Stein C, Fanis P, Demmers J, et al. (2010) *Friend of Prmt1, a novel chromatin target of protein arginine methyltransferases*. Mol Cell Biol **30**: 260-272.
12. Zullo AJ, Michaud M, Zhang W, Grusby MJ (2009) *Identification of the small protein rich in arginine and glycine (SRAG): a newly identified nucleolar protein that can regulate cell proliferation*. J Biol Chem **284**: 12504-12511.
13. van Dijk TB, Gillemans N, Pourfarzad F, van Lom K, von Lindern M, et al. (2010) *Fetal globin expression is regulated by Friend of Prmt1*. Blood **116**: 4349-4352.
14. Zhang X, Cheng X (2003) *Structure of the predominant protein arginine methyltransferase PRMT1 and analysis of its binding to substrate peptides*. Structure **11**: 509-520.
15. Lee DY, Teyssier C, Strahl BD, Stallcup MR (2005) *Role of protein methylation in regulation of transcription*. Endocr Rev **26**: 147-170.
16. Mowen KA, Schurter BT, Fathman JW, David M, Glimcher LH (2004) *Arginine methylation of NIP45 modulates cytokine gene expression in effector T lymphocytes*. Mol Cell **15**: 559-571.
17. Zhao X, Jankovic V, Gural A, Huang G, Pardanani A, et al. (2008) *Methylation of RUNX1 by PRMT1 abrogates SIN3A binding and potentiates its transcriptional activity*. Genes Dev **22**: 640-653.
18. Xu W, Chen H, Du K, Asahara H, Tini M, et al. (2001) *A transcriptional switch mediated by cofactor methylation*. Science **294**: 2507-2511.
19. Le Romancer M, Treilleux I, Leconte N, Robin-Lespinnasse Y, Sentis S, et al. (2008) *Regulation of estrogen rapid signalling through arginine methylation by PRMT1*. Mol Cell **31**: 212-221.
20. Kwak YT, Guo J, Prajapati S, Park KJ, Surabhi RM, et al. (2003) *Methylation of SPT5 regulates its interaction with RNA polymerase II and transcriptional elongation properties*. Mol Cell **11**: 1055-1066.
21. Pal S, Sif S (2007) *Interplay between chromatin remodelers and protein arginine methyltransferases*. J Cell Physiol **213**: 306-315.
22. Shou W, Aghdasi B, Armstrong DL, Guo Q, Bao S, et al. (1998) *Cardiac defects and altered ryanodine receptor function in mice lacking FKBP12*. Nature **391**: 489-492.
23. Tevosian SG, Deconinck AE, Tanaka M, Schinke M, Litovsky SH, et al. (2000) *FOG-2, a cofactor for GATA transcription factors, is essential for heart morphogenesis and development of coronary vessels from epicardium*. Cell **101**: 729-739.

24. Schneider JE, Bose J, Bamforth SD, Gruber AD, Broadbent C, et al. (2004) *Identification of cardiac malformations in mice lacking Ptdsr using a novel high-throughput magnetic resonance imaging technique*. BMC Dev Biol **4**: 16.
25. Clugston RD, Klattig J, Englert C, Clagett-Dame M, Martinovic J, et al. (2006) *Teratogeninduced, dietary and genetic models of congenital diaphragmatic hernia share a common mechanism of pathogenesis*. Am J Pathol **169**: 1541-1549.
26. Babiuk RP, Greer JJ (2002) *Diaphragm defects occur in a CDH hernia model independently of myogenesis and lung formation*. Am J Physiol Lung Cell Mol Physiol **283**: L1310-1314.
27. Li J, Liu KC, Jin F, Lu MM, Epstein JA (1999) *Transgenic rescue of congenital heart disease and spina bifida in Splotch mice*. Development **126**: 2495-2503.
28. You LR, Takamoto N, Yu CT, Tanaka T, Kodama T, et al. (2005) *Mouse lacking COUP-TFII as an animal model of Bochdalek-type congenital diaphragmatic hernia*. Proc Natl Acad Sci U S A **102**: 16351-16356.
29. Mey J, Babiuk RP, Clugston R, Zhang W, Greer JJ (2003) *Retinal dehydrogenase-2 is inhibited by compounds that induce congenital diaphragmatic hernias in rodents*. Am J Pathol **162**: 673-679.
30. Hendzel MJ, Wei Y, Mancini MA, Van Hooser A, Ranalli T, et al. (1997) *Mitosis-specific phosphorylation of histone H3 initiates primarily within pericentromeric heterochromatin during G2 and spreads in an ordered fashion coincident with mitotic chromosome condensation*. Chromosoma **106**: 348-360.
31. Wells MJ, Hatton MW, Hewlett B, Podor TJ, Sheffield WP, et al. (1997) *Cytokeratin 18 is expressed on the hepatocyte plasma membrane surface and interacts with thrombinantithrombin complexes*. J Biol Chem **272**: 28574-28581.
32. Dzierzak E, Speck NA (2008) *Of lineage and legacy: the development of mammalian hematopoietic stem cells*. Nat Immunol **9**: 129-136.
33. Klaassens M, Galjaard RJ, Scott DA, Bruggenwirth HT, van Opstal D, et al. (2007) *Prenatal detection and outcome of congenital diaphragmatic hernia (CDH) associated with deletion of chromosome 15q26: two patients and review of the literature*. Am J Med Genet A **143A**: 2204-2212.
34. Iritani I (1984) *Experimental study on embryogenesis of congenital diaphragmatic hernia*. Anat Embryol (Berl) **169**: 133-139.
35. Mendelsohn C, Lohnes D, Decimo D, Lufkin T, LeMeur M, et al. (1994) *Function of the retinoic acid receptors (RARs) during development (II). Multiple abnormalities at various stages of organogenesis in RAR double mutants*. Development **120**: 2749-2771.
36. Greer JJ, Babiuk RP, Thebaud B (2003) *Etiology of congenital diaphragmatic hernia: the retinoid hypothesis*. Pediatr Res **53**: 726-730.
37. Niederreither K, Subbarayan V, Dolle P, Chambon P (1999) *Embryonic retinoic acid synthesis is essential for early mouse post-implantation development*. Nat Genet **21**: 444-448.
38. Vermot J, Niederreither K, Garnier JM, Chambon P, Dolle P (2003) *Decreased embryonic retinoic acid synthesis results in a DiGeorge syndrome phenotype in newborn mice*. Proc Natl Acad Sci U S A **100**: 1763-1768.
39. Keijzer R, Liu J, Deimling J, Tibboel D, Post M (2000) *Dual-hit hypothesis explains pulmonary hypoplasia in the nitrofen model of congenital diaphragmatic hernia*. Am J Pathol **156**: 1299-1306.
40. Wardle FC, Papaioannou VE (2008) *Teasing out T-box targets in early mesoderm*. Curr Opin Genet Dev **18**: 418-425.
41. Zhu L, Belmont JW, Ware SM (2006) *Genetics of human heterotaxias*. Eur J Hum Genet **14**
42. Holder AM, Klaassens M, Tibboel D, de Klein A, Lee B, et al. (2007) *Genetic factors in congenital diaphragmatic hernia*. Am J Hum Genet **80**: 825-845.
43. Hou J, Aerts J, den Hamer B, van Ijcken W, den Bakker M, et al. (2010) *Gene expression-based classification of non-small cell lung carcinomas and survival prediction*. PLoS One **5**: e10312.

Chapter 2.3

Genomic Alterations that Contribute to the Development of Isolated and Non-Isolated Congenital Diaphragmatic Hernia

M.Wat, D.Veenma, J.Hogue, A.Holder, Z.Yu, J.Wat, N.Hanchard, O.Shchelochkov,
C.Fernandes, A.Johnson, K.Lally, A.Slavotinek, O.Danhaive, T.Schaible,
S-W.Cheung, K.Rauen, V.Tonk, D.Tibboel, A.de Klein, and, D.Scott

J Med Genet (2011 May;48(5):299-307)

Abstract

Background: Congenital diaphragmatic hernia (CDH) is a life-threatening birth defect. Most of the genetic factors that contribute to the development of CDH remain unidentified.

Objective: Identify genomic alterations that contribute to the development of diaphragmatic defects.

Methods: A cohort of 45 unrelated patients with CDH or diaphragmatic eventrations were screened for genomic alterations by array comparative genomic hybridization (aCGH) or SNP-based copy number analysis.

Results: Genomic alterations that were likely to have contributed to the development of CDH were identified in eight patients. Inherited deletions of *ZFPM2* were identified in two patients with isolated diaphragmatic defects and a large de novo 8q deletion overlapping the same gene was found in a patient with non-isolated CDH. A de novo microdeletion of chromosome 1q41q42 and two de novo microdeletions on chromosome 16p11.2 were identified in patients with non-isolated CDH. Duplications of distal 11q and proximal 13q were found in a patient with non-isolated CDH and a de novo single gene deletion of *FZD2* was also identified in a patient with a partial pentalogy of Cantrell phenotype.

Conclusions: Haploinsufficiency of *ZFPM2* can cause dominantly inherited isolated diaphragmatic defects with incomplete penetrance. Our data define a new minimal deleted region for CDH on 1q41q42, provide evidence for the existence of CDH-related genes on chromosomes 16p11.2, 11q23-24 and 13q12 and suggest a possible role for *FZD2* and Wnt signalling in pentalogy of Cantrell phenotypes. These results demonstrate the clinical utility of screening for genomic alterations in individuals with both isolated and non-isolated diaphragmatic defects.

Introduction

Congenital diaphragmatic hernia (CDH) is a life-threatening birth defect that occurs in approximately 1/4000 live births and is defined as a protrusion of abdominal viscera into the thorax through an abnormal opening or defect in that is present at birth [1, 2]. In some cases the herniated viscera are covered by a membranous sac and can be difficult to distinguish from a diaphragmatic eventration in which there is extreme elevation of a part of the diaphragm that is often atrophic and abnormally thin. The majority of CDH cases are sporadic with the recurrence risk for isolated CDH typically quoted as <2% based on a multifactorial inheritance [3]. However, there is a growing body of evidence that small chromosomal anomalies can predispose to the development of CDH [4-10].

The identification of a predisposing genomic change greatly enhances the ability of physicians to provide individualized genetic counseling and to formulate optimal treatment and surveillance plans. This would suggest that screening for genomic changes by array comparative genomic hybridization (aCGH) or SNP-based copy number analysis should be performed on all patients with diaphragmatic defects [10, 11]. However, this practice has not been universally applied.

Efforts to map the locations of all reported chromosomal anomalies associated with CDH have revealed many regions of the genome that are recurrently deleted, duplicated or translocated in individuals with CDH [12, 13]. Each of these genomic regions is likely to harbor one or more CDH-related genes. For some of these regions, a specific gene has been implicated in the development of diaphragmatic defects. Chromosome 8q22q23, for example, is recurrently deleted and translocated in individuals with CDH. This region harbors the zinc finger protein, multitype 2 (*ZFPM2*) gene that has been implicated in the development of diaphragmatic defects based the identification of a de novo truncating mutation in a child with a severe diaphragmatic eventration and the development of similar diaphragmatic defects in mice that are homozygous for a hypomorphic allele of *Zfpm2* [14]. In contrast, chromosome 1q41q42- which is also recurrently deleted in individuals with CDH-harbors a number of genes, none of which have been clearly shown to cause diaphragmatic defects in humans or animal models [15].

In this report we screened a cohort of 45 individuals with diaphragmatic defects for genomic alterations by high-resolution aCGH or SNP-based copy number analysis. Chromosomal anomalies that are likely to have caused or contributed to the development of diaphragmatic defects were identified in eight patients. These findings allow us to define the inheritance pattern of diaphragmatic defects associated with haploinsufficiency of *ZFPM2* and delineate a new minimal deleted region for CDH on 1q41q42. They also provide evidence for the existence of CDH-related genes on chromosomes 16p11.2, 11q23-24 and 13q12 and suggest a possible role for *FZD2* and Wnt signalling in the development of various phenotypes seen in pentalogy of Cantrell [16].

Methodology

Patient accrual

For array studies, informed consent was obtained from a convenience sample of 45 patients with CDH or diaphragmatic eventrations and, when possible, their parents in accordance with IRB-approved protocols. None of these patients have been previously published with the exception of Patient 5 and Patient 7 whose clinical findings were summarized by Shinawi et al. and Fruhman et al. respectively [17, 18].

For sequence analysis of *ZFPM2*, a cohort of 52 patients with CDH and 10 patients with diaphragmatic eventrations were screened for deleterious changes. This cohort consisted of a subset of patients from the array cohort and similarly consented individuals. *ZFPM2* sequence analyses for these individuals have not been previously published.

Array comparative genomic hybridization and SNP-based copy number analyses

In most cases, chromosomal deletions and duplications were identified or confirmed by array comparative genomic hybridization on a research basis using Human Genome CGH 244K or SurePrint G3 Human CGH 1M Oligo Microarray Kits (G4411B, G4447; Agilent Technologies, Santa Clara, CA) prepared according to the manufacturer's protocols and analyzed as previously described using individual sex matched controls with no personal or family history of CDH [7]. Putative copy number changes were defined by two or more adjacent probes at 244K resolution or three or more adjacent probes at 1M resolution with log₂ ratios suggestive of a deletion or duplication when compared to those of adjacent probes.

In two cases – Patient 2 and Patient 6 – causative chromosomal deletions were identified prior to accrual and further aCGH testing was unwarranted based on the molecular data already available. The deletion in Patient 2 was identified using an Illumina CytoSNP bead version 12.2 (Illumina, Inc., San Diego, CA, USA) and the deletion in Patient 6 was identified and defined on a clinical basis using a 105K Combimatrix Molecular Diagnostics array (Combimatrix Molecular Diagnostics, Irvine, CA, USA) hybridized, extracted, and evaluated according to manufacturers' instructions.

Identification of previously reported copy number variants

To determine if putative changes identified by aCGH or SNP-based copy number analysis had been described previously in normal controls, we searched for similar deletions or duplications in the Database of Genomic Variants (<http://projects.tcag.ca/variation/>).

Confirmation of Genomic Changes

Changes that were not identified in the Database of Genomic Variants were confirmed by real-time quantitative PCR with the exception of causative changes identified in Patients 3 and 7, which were confirmed by chromosome analysis and Patients 4 and 6 which were confirmed by FISH analysis.

Quantitative real-time PCR

Quantitative real-time PCR (qPCR) analysis experiments were designed and carried out as previously described [7]. For quantitative real-time PCR analysis within the *ZFPM2* gene experiments were designed in a manner similar to the standard curve method described by Boehm et al. with a region of the *c14orf145* gene serving as a control locus [19].

Chromosome Analyses and FISH Studies

Chromosome analyses were performed for Patients 3 and 7 on a clinical basis by the Molecular Genetics Laboratory at Baylor College of Medicine. FISH analyses were performed for Patient 4 by the Cytogenetic Laboratory at Texas Tech University Health Sciences Center School of Medicine and for Patient 6 by Combimatrix Molecular Diagnostics.

Long-range PCR amplification and sequencing

Long amplification PCR was carried out using the TaKaRa long range PCR system (TaKaRa Bio, Otsu, Shiga, Japan) according to manufacturer's instructions. PCR products were gel-purified, sequenced, and analyzed using Sequencher 4.7 software (Gene Codes Corporation, Ann Arbor, Michigan, USA).

Identification of ZFPM2 sequence changes

Primers were designed to amplify the coding sequence and the intron-exon boundaries of *ZFPM2* and used to amplify patient DNA. Sequence changes in PCR amplified products identified by comparison with control DNA sequences using Sequencher 4.7 software (Gene Codes Corporation, Ann Arbor, Michigan, USA). Hispanic control samples were obtained from the Baylor Polymorphism Resource, a collection of approximately 600 anonymous control samples from major ethnic and racial backgrounds.

Results

Identification of genomic changes in patients with CDH or diaphragmatic eventrations

Forty-five subjects with congenital diaphragmatic hernias or diaphragmatic eventrations of varying severity were screened for chromosomal anomalies by aCGH or SNP-based copy number analysis. Eight subjects carried genomic changes that likely contributed to the development of their diaphragmatic defects. Clinical and molecular data from these subjects are summarized in Table 1.

Table 1 | Summary of data from subjects with chromosomal changes likely to have contributed to diaphragm defects

| | Patient 1 | Patient 2 | Patient 3 | Patient 4 | Patient 5 | Patient 6 | Patient 7 | Patient 8 |
|--|---|---|---|---|--|--|--|---|
| Final Karyotype | 46,XY,del(8) (q22.3q23.1) | 46,XY,del(8) (q23.1q23.1) | 46,XX,del(8) (q22.3q24.23) | 46,XY,del(1) (q41q42.12) | 46,XY,del(16) (p11.2p11.2) | 46,XY,del(16) (p11.2p11.2) | 47,XX+der(13) t(11;13) (q23.2;q12.3) | 46,XY,del(17) (q12.2-q12.2) |
| Minimal/ maximal affected region (hg19) | Chromosome 8 deletion 105,914, 640-106,907, 764 (~993 kb)/ 105,880, 441-106,922, 626 (~1.04 Mb) | Chromosome 8 deletion 106,812, 277-107,420, 029 (~608 kb)/ 106,800, 200-107,511, 467 (~711 kb) | Chromosome 8 deletion 104,516, 737-136,746, 871 (~32.2 Mb)/ 104,508, 082-136,809, 150 (~32.3 Mb) | Chromosome 1 deletion 223,076, 895-225,311, 293 (2.2 Mb)/ 223,073, 839-225,318, 623 (2.2 Mb) | Chromosome 16 deletion 29,652, 999-30,199, 351 (~554 kb)/ 29,350, 831-30,332, 522 (~982 kb) | Chromosome 16 deletion 29,502, 653-30,274, 073 (~771 kb) defined clinically with no minimum or maximum region specified. | Chromosome 11 duplication 112,355, 952-134,927, 114 (26.6 Mb)/ 112,347,267- 134,927,114 (26.6 Mb) | Chromosome 17 deletion 42,633, 066-42,650, 463 (~17.4 kb)/ 42,622,151- 42,657,504 (~35.4 kb) |
| Confirmation Method | Real-time qPCR | Real-time qPCR | Chromosome analysis | FISH | Real-time qPCR | FISH | Chromosome analysis | Real-time qPCR |
| Inheritance | Paternal | Maternal | De novo | De novo | De novo | De novo | Maternal balanced translocation | De novo |
| Age | 4 year-old | 2 day-old | 1 day-old | 2 year-old | 2 year-old | 17 day-old | 8 day-old | 2 year-old |
| Gender | Male | Male | Female | Male | Male | Male | Female | Male |
| Ethnicity | Mixed | Caucasian | Hispanic | Caucasian | Mixed | Caucasian | Hispanic | Caucasian |

| | Patient 1 | Patient 2 | Patient 3 | Patient 4 | Patient 5 | Patient 6 | Patient 7 | Patient 8 |
|---|---|--|---|---|---|--|---|--|
| Prenatally identified abnormalities, exposures, and prenatal karyotype | No abnormalities identified | CDH, intrauterine growth retardation, single umbilical artery, 46,XY | CDH, short extremities, edema/ascites, polyhydramnios, 46,XX,del(8)(q22q24) | No abnormalities identified on two prenatal ultrasounds | CDH, maternal smoking in first trimester | CDH, normal chromosomes 46,XY | CDH, polyhydramnios and intrauterine growth retardation | CDH and omphalocele detected, normal chromosomes 46,XY |
| Birth history | Vaginal delivery at term, vomiting 2 days after birth | Caesarean section at 36 3/7 weeks for abnormal fetal heart rate and decreased movement | Spontaneous vaginal delivery at 34 5/7 wks | Spontaneous vaginal delivery at 37 weeks | Delivery at 37 weeks, after birth he decompensated and required 20 minutes of CPR | Repeat caesarean section at 39 6/7 weeks | Spontaneous vaginal delivery at 37 3/7 weeks | Scheduled caesarean section at 37 1/7 weeks |
| Birth weight, length and OFC | Weight 3.8 kg | Weight: 1.72 kg; length 42 cm; OFC 29.5 cm | No information available | Weight 3.2 kg; length 49.5 cm | Weight estimated at 2.5 kg; length 49 cm; OFC 34 cm. | Weight ~3.5 kg; length 50 cm; OFC 35.5 cm. | No information available | Weight 2.2 kg; length 45 cm, OFC 33 cm |
| Diaphragm | Diaphragmatic eventration | Left-sided CDH | Large left-sided CDH | CDH identified at 11 months | Right-sided CDH | Left-sided CDH | Large left-sided CDH | Anterior medial CDH |
| Cardiac | No known abnormalities | No known abnormalities | No known abnormalities | No known abnormalities | No structural abnormalities noted on ECHO | No structural abnormalities noted on ECHO | Small perimembranous VSD, secundum ASD | Large perimembranous VSD, PFO ASD |

| | Patient 1 | Patient 2 | Patient 3 | Patient 4 | Patient 5 | Patient 6 | Patient 7 | Patient 8 |
|------------------------------------|--|---|--|---|---|--|---|---|
| Additional anomalies | Intestinal malrotation, radioulnar synostosis | No known abnormalities | All extremities were symmetrically short with fixed flexion of the distal upper extremities. | Right cerebral volume loss with ex vacuo dilatation of the right lateral ventricle, diffuse thin cortical mantle, atrophy of right hippocampus, thin corpus callosum, left-sided cryptorchidism with non-attachment to the epididymis | Micro-retrognathia, cleft palate, right inguinal hernia and bilateral post axial polydactyly (paternal) | Hypoplastic, non-articulating thumbs, extra thoracic vertebral pairs of ribs | Clouded corneas, cupped optic nerves, cleft palate, small anterior anus, prominent forehead, large anterior fontanel, posteriorly-rotated low-set ears, micro-retrognathia, wide-spaced hypoplastic nipples, right single palmar crease, tapering fingers, prominent heels. | Coronal craniosynostosis, diminished CNS white matter with thinning of the corpus callosum, omphalocele, bilateral inguinal hernias, left-sided cryptorchidism, |
| Clinical course/development | Only two words at age two. Responded well to speech therapy. Now normal. | Died on the 2 nd day of life with respiratory insufficiency and pulmonary hypertension | Died shortly after delivery | Persistent hypoglycaemia after birth, gross motor, fine motor and language delay, seizures starting at 20 months | No oxygen requirement at 24 months but still receiving supplemental nutrition via g-tube | Died on the 17th day of life with severe respiratory insufficiency and pulmonary hypertension. | Support was withdrawn at 8 days of age. Findings at autopsy included abnormal lung fissures and coronary artery anomalies | At 28 months could walk with a walker, nutritional support via g-tube, ventilator support with acute illness |

CDH = congenital diaphragmatic hernia, OFC = occipital frontal circumference, ASD = atrial septal defect, VSD = ventricular septal defect, ECHO = echocardiogram, CPR = cardiopulmonary resuscitation, CNS = central nervous system, PFO = patent foramen ovale.

Patient 1 is a male of mixed ancestry who was diagnosed at 9 days of age with intestinal malrotation and a large, left-sided diaphragmatic eventration (Figure 1). Later in life, he was diagnosed with left-sided radioulnar synostosis. Despite normal motor development, at 24 months of age he had only two words. However, he made rapid progress with speech therapy and by 31 months of age he was speaking in 4-word sentences. aCGH analysis revealed an ~1 Mb deletion that included only the *ZFPM2* gene on chromosome 8q22.3-23.1 (Figure 1). Quantitative and long-range PCR analysis revealed that the patient's father carried the same deletion (data not shown). A review of his father's medical records did not reveal evidence of a diaphragmatic anomaly despite an extensive evaluation after a severe automobile accident which included an abdominal CT scan. We screened the coding sequence and associated intron exon boundaries of Patient 1's remaining *ZFPM2* allele looking for changes that might account for the difference in phenotype between him and his father but no sequence changes were identified.

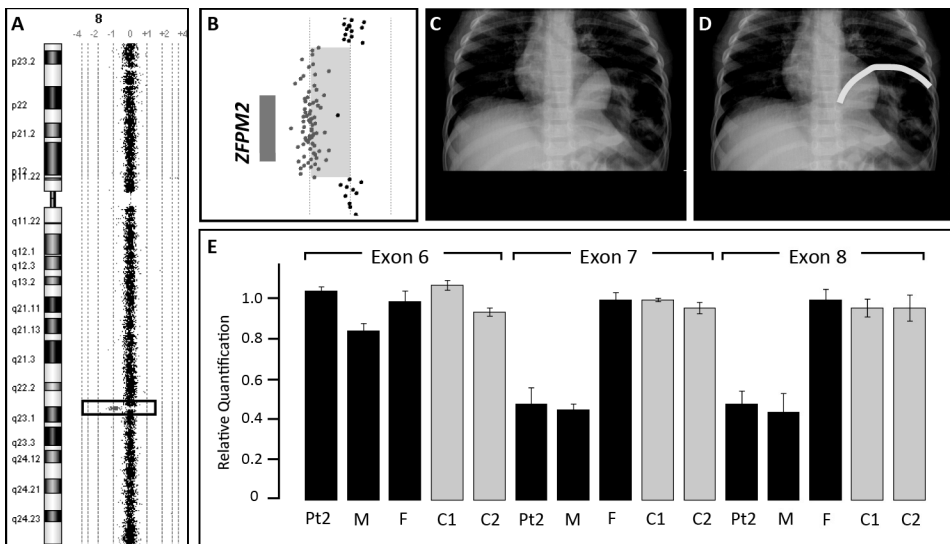


Figure 1 |

A: Array comparative genomic hybridization data from Patient 1 showing an 8q22.3q23.1 single gene deletion of *ZFPM2*. **B:** The relative location of the *ZFPM2* gene in relation to aCGH data from the deletion region in Patient 1 is represented by a gray bar. **C:** A chest radiograph of Patient 1 demonstrating a severe diaphragmatic eventration containing loops of bowel. **D:** The same radiograph shown in panel C with the limits of the diaphragmatic eventration outlined in yellow. **E:** Quantitative PCR analysis demonstrates a normal copy number for *ZFPM2* Exon 6 but a reduced copy number for Exons 7 and 8 in DNA from Patient 2 (Pt2) and his mother (M). Normal copy number values are seen in DNA from Patient 2's father (F) and DNA from two unrelated controls (C1, C2) (see page 249 for color figure).

Patient 2 is a Caucasian male that was diagnosed prenatally with a left-sided CDH. His brother was similarly affected with CDH and died of complications related to his hernia. Except for a single umbilical artery, no additional anomalies were identified after birth. He died at 2 day of age from respiratory insufficiency and pulmonary hypertension. SNP-based copy number analysis

revealed a deletion on chromosome 8q23.1 that included a portion of the 3' coding region of *ZFPM2* and the first coding exon of oxidation resistance gene 1 (*OXR1*) based on mRNA transcript variant 1. Quantitative PCR analysis revealed that exons 7 and 8 of *ZFPM2* were included in the deletion (Figure 1). No sequence changes were identified in the coding sequence and intron/exon boundaries of the remaining allele.

Patient 3 had a de novo ~32 Mb deletion from 8q22.3 to 8q24.23 that overlapped the *ZFPM2* deletions seen in Patient 1 and 2 and also included the *EXT1* and *TRPS1* genes that are associated with Langer-Giedion syndrome (OMIM #150230). This Hispanic female was diagnosed prenatally with a large left-sided posterolateral CDH. Fetal MRI at 34 5/7 weeks also revealed an omphalocele and symmetrically short extremities. Due to severe pulmonary hypoplasia she was placed in neonatal hospice care immediately after birth and died shortly thereafter.

Patient 4 is a Caucasian male who had a normal prenatal course. He was born at 37 weeks gestation and his perinatal course was complicated by persistent hypoglycaemia. A diaphragmatic hernia was identified incidentally on a chest x-ray at 11 months of age during an investigation for failure to thrive. His motor and language development were delayed and he developed seizures at 20 months of age. CNS studies revealed right hemisphere cerebral volume loss with ex vacuo dilatation of the right lateral ventricle with diffuse thin cortical mantle, atrophy in the right hippocampus and a thin corpus callosum. aCGH analysis revealed a de novo 2.2 Mb interstitial deletion of 1q41-1q42.12 (Figure 2).

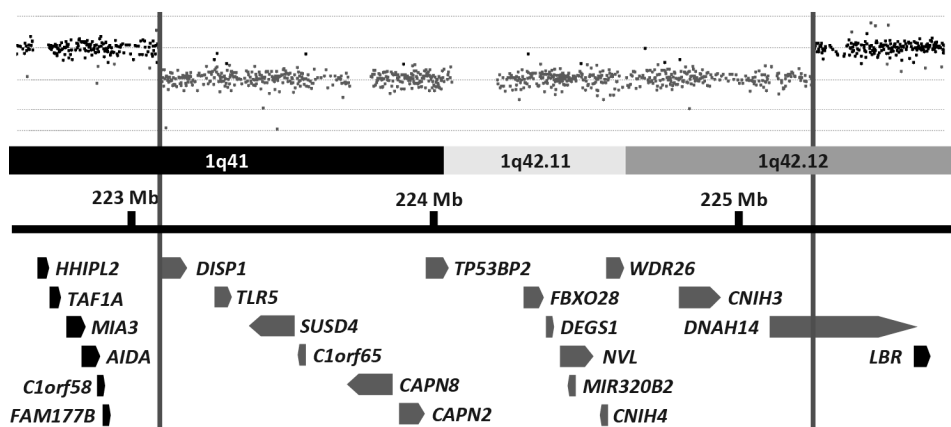


Figure 2 |

Array comparative genomic hybridization data from Patient 4 is shown above a schematic representation of a portion of the 1q41-1q42 region. Genes in this region are represented by block arrows. Red vertical bars mark the limits of the deletion in Patient 4 and delineate the minimal deleted region for congenital diaphragmatic hernia (CDH) in this region of the genome. Genes with all or a portion of their coding sequence inside the minimal deleted region are shown in green (see page 250 for color figure).

Patients 5 and Patient 6 were found to have de novo interstitial deletions of 16p11.2 – a recurrent microdeletion region flanked by low-copy repeats. Patient 5 is a two-year old male of mixed ancestry who had a severe right-sided posterolateral CDH, micrognathia, a U-shaped palatal cleft, paternally inherited autosomal dominant polydactyly, and dysmorphic features consistent with 16p11.2 which were previously described [17]. He continues to need dietary supplementation via G-tube and supplemental oxygen when ill.

Patient 6 was a male infant conceived by intrauterine insemination with non-consanguineous Caucasian parents as donors. A left-sided diaphragmatic hernia was diagnosed prenatally. After birth, both of his thumbs were found to be proximally placed, hypoplastic and non-articulating with the left thumb having a pedunculated appearance. Additional findings included an extra thoracic vertebra and 13 pairs of ribs. He required extra corporal membrane oxygenation within the first day of life, developed severe diffuse edema, and died on the 17th day of life as a result of his severe respiratory insufficiency and pulmonary hypertension.

Patient 7 was born at 37.6 weeks to non-consanguineous Hispanic parents. She had persistent respiratory distress at birth and intubation was complicated by micrognathia and a tongue anomaly. Further evaluation revealed a left-sided CDH, a ventricular septal defect (VSD), and atrial septal defect (ASD), partial cleft palate, small anteriorly placed anus, and dysmorphic features. A marker chromosome was identified by G-banded chromosome analysis and was shown to be the result of an unbalanced maternal translocation between chromosome 13q and 11q resulting in a 47,XX,+der(13)t(11;13)(q23;q12.3) chromosome complement [18]. Her prognosis was deemed poor in light of her multiple anomalies, and she died shortly after support was withdrawn on day of life 8. Additional findings at autopsy included abnormal lung fissures and coronary artery anomalies.

Patient 8 is a two-year old Caucasian male who was diagnosed prenatally with a left-sided anterior CDH, and a large omphalocele. Postnatal cardiac evaluation revealed a large perimembranous VSD and a patent foramen ovale (PFO) versus ASD. Additional anomalies included bilateral inguinal hernias, left-sided cryptorchism and premature fusion of the coronal sutures evident on head CT performed at 7 and 12 months of age. An MRI obtained at 11 months of age revealed diminished bifrontal and bitemporal parenchyma white matter associated with thinning of the corpus callosum, delayed myelination and generous extra-axial CSF spaces. aCGH analysis revealed a de novo 17.4 kb deletion that involved only the frizzled homolog 2 gene (*FZD2*) on chromosome 17q12.2. Amplification of the breakpoint by long-range PCR followed by sequencing revealed that the deletion had occurred between two Alu repeats; an Alu-Sb proximally and an Alu-Sq distally. Matsuzaki et al. has reported deletions of this gene in 3/90 normal Yoruban individuals from Ibadan, Nigeria [20]. However, these changes were not identified by McCarroll et al. who analyzed the same cohort [21]. To determine if the mutations in Patient 8's remaining *FZD2* allele may have contributed to his phenotype, we sequenced the coding region of his remaining *FZD2* allele but did not identify any sequence changes.

Table 2 | Rare inherited changes identified in patients with CDH

| Patient Number | Copy Number Change | Inheritance Pattern | Chromosome | Genes Involved | Minimum/Maximum hg19 | Clinical Synopsis |
|----------------|--------------------|--|------------|-----------------------------|--|--|
| TX-02 | Increase | Paternal | 15q24.2 | <i>COMMD4, NEIL1</i> | 75,605,889-75,644,263 75,600,108-75,648,132 | Female, left-sided CDH, large bronchopulmonary sequestration |
| TX-04 | Increase | Paternal & maternal duplication | 3q26.33 | <i>SOX2, SOX2OT</i> | 181,430,003-181,431,902 181,425,656-181,432,270 | Male, isolated right-sided CDH |
| TX-02 | Increase | Maternal | 5q11.2 | <i>ARL15, HSPB3</i> | 53,450,417-53,759,016 53,443,541-53,765,448 | |
| TX-02 | Increase | Paternal & maternal duplication | 18p11.21 | <i>GNAL, MIPPE1*</i> | 11,872,270-11,878,083 11,863,962-11,884,082 | |
| TX-12 | Decrease | Paternal | 7q32.1 | <i>AHCYL2</i> | 128,988,273-128,996,545 128,978,921-129,002,744 | Male, isolated left-sided CDH |
| TX-14 | Increase | Paternal | 13q21.33 | <i>KLHL1, SCA8, ATXN8OS</i> | 70,673,470-71,577,278 70,666,491-71,594,524 | Male, isolated left-sided CDH |
| TX-23 | Increase | Maternal | 1p31.3 | <i>CACHD1, RAVER2</i> | 65,144,120-65,210,203 65,137,345-65,218,480 | Female, right-sided CDH, ASD, missshaped kidney |
| TX-27 | Decrease | Parents not available | 14q21.1 | <i>FBXO33</i> | 39,884,781-40,262,115 39,875,206-40,301,762 | Female, isolated left-sided |
| TX-28 | Increase | Patient n=4 Mother and father n=3 | 11q13.5 | <i>AQP11, CLNS1A, RSF1</i> | 77,297,657-77,424,591 77,270,540-77,431,584 | Female, left-sided CDH, double outlet right ventricle, VSD |
| TX-36 | Decrease | Not maternal, father not available | 1p12 | <i>HSD3B2</i> | 119,962,240-119,983,891 119,957,963-119,994,447 | Male, isolated left-sided CDH |
| TX-39 | Decrease | Maternal | 16p13.3 | <i>DNASE1, TRAP1</i> | 3,684,132-3,716,095 3,672,598-3,726,606 | Female, left-sided posterior CDH, bicommissural aortic valve |
| TX-42 | Increase | Paternal & maternal Increased copy number | 1q24.3 | <i>DNM3</i> | 171,944,462-171,958,347 171,936,289-171,970,634 | Male, isolated left-sided posterior CDH |
| TX-42 | Decrease | Paternal | 15q21.2 | <i>USP8*, USP50</i> | 50,802,672-50,822,065 50,791,758-50,833,347 | |

| Patient Number | Copy Number Change | Inheritance Pattern | Chromosome | Genes Involved | Minimum/Maximum hg19 | Clinical Synopsis |
|----------------|--------------------|--|------------|--|--|--|
| TX-50 | Decrease | Patient n=0 Parents n=1 | 17q25.1 | <i>TRIM4*</i> | 73,875,459-73,878,627 73,870,461-73,882,792 | Male, isolated left-sided CDH |
| | Increase | Maternal n=2 | Xq27.1 | <i>F9, MCF2, ATP11C, MIR505, CXorf66</i> | 138,594,571-139,089,290 138,556,308-139,102,322 | |
| TX-52 | Decrease | Paternal | 15q23 | <i>AAGAB*, IQCH, C15orf61, MAP2K5</i> | 67,548,229-68,040,596 67,540,042-68,049,656 | Female, right-sided CDH, ASD |
| TX-56 | Increase | Maternal | Xp11.1 | <i>ZXDA</i> | 57,704,902-57,987,522 57,673,005-58,051,706 | Male, right-sided CDH, left-sided inguinal hernia |
| TX-65 | Decrease | Maternal | 7q31.1 | <i>DOCK4</i> | 111,668,580-111,784,369 111,653,357-111,789,489 | Male, left-sided CDH, extra-lobar pulmonary sequestration, |
| TX-72 | Increase | Paternal & maternal Increased copy number | 3q13.31 | <i>GRAMD1C*, ZDHHC23</i> | 113,668,345-113,672,579 113,664,314-113,679,817 | Male, left-sided posterior CDH, |
| TX-73 | Increase | Paternal | 20p12.2 | <i>SNAP25, MKKS, C20orf94, JAG1</i> | 10,223,539-10,902,949 10,213,446-10,937,659 | Male, left-sided CDH, ASD; sibling died shortly after birth with CDH |

* = genes located outside the minimal deleted region but are located, at least partially, inside the maximal deleted region; CDH = congenital diaphragmatic hernia, ASD = atrial septal defect, VSD = ventricular septal defect

Twenty changes not reported in the Database of Genomic Variants were identified in this cohort by aCGH and confirmed by either qPCR and/or FISH analysis (Table 2). In two cases the extent of the copy number variation was larger than that seen in the parents. Patient TX-28 appeared to have four copies of a region on 11q13.5 while her parents each had 3 copies compared to control. Patient TX-50 had no copies of a region on 17q25.1 while his parents each had one copy compared to control. TX-50 also had two copies of a region on Xp27.1, similar to his mother, which could represent a de novo event.

Identifying ZFPM2 sequence changes in patients with CDH and diaphragmatic eventrations

To determine if detrimental sequence changes in *ZFPM2* were a common cause of CDH or diaphragmatic eventrations, we screened the coding region and intron-exon boundaries of this gene in 52 patients with CDH (Table 3) and 10 patients with diaphragmatic eventrations (Table 4). Three non-synonymous changes were identified which had not been previously described in the 1000 Genomes project or dbSNP. A D98N change was identified in a male with an isolated posterior left-sided hernia with a large sac. His mother did not carry a D98N allele but the father was unavailable for analysis. This change was predicted to be possibly damaging by PolyPhen (<http://genetics.bwh.harvard.edu/pph/>) but non-deleterious by SNPs3D (<http://www.snps3d.org/>) [22, 23]. The same change was reported by Bleyl et al. in an individual with bilateral CDH [24]. However, they concluded that the change was likely to be a benign SNP since it was also identified in control samples. A Q889E change was identified in a Hispanic female with a right-sided CDH, ambiguous genitalia and a double vagina. Her mother did not carry the change but the father was unavailable for analysis. This change was predicted to be benign by PolyPhen, non-deleterious by SNPs3D, and was subsequently identified in 5 of 152 (3.3%) Hispanic control chromosomes. A paternally inherited S210T mutation was identified in an African American male with a left-sided CDH and dysmorphic features. This change was predicted to be benign by PolyPhen and non-deleterious by SNPs 3D.

Table 3 | ZFPM2 sequence changes in patients with CDH

| Observed change | Number of Patients (Inheritance Pattern) | Exon | 1000 Genomes*/ dbSNP (Heterozygosity) | Predicted effect (PolyPhen/SNPs3D) |
|-------------------------------|--|------|---|---------------------------------------|
| Non-synonymous changes | | | | |
| D98N | 1 (Non-maternal, father not available) | 3 | No/No | Possibly damaging/ Non-Deleterious |
| S210T | 1 (Paternal) | 6 | No/No | Benign/ Non-Deleterious |
| A403G | 11 | 8 | Yes/Yes (0.341) | Benign/ Non-Deleterious |
| E782D | 10 | 8 | Yes/Yes (0.078) | Benign/ Non-Deleterious |
| Q889E | 1 (Non-maternal father not available) | 8 | No/No – 3.3% Hispanic control chromosomes | Benign/ Non-Deleterious |
| A1055V | 1 (Non-maternal, father not available) | 8 | Yes/Yes (0.146) | Benign/ Non-Deleterious |
| Synonymous changes | | | | |
| P454P | 4 | 8 | Yes/Yes (0.234) | – |
| P592P | 3 | 8 | Yes/Yes (0.101) | – |
| V795V | 2 | 8 | Yes/Yes (0.120) | – |
| Y992Y | 3 | 8 | Yes/Yes (0.104) | – |
| H1069H | 4 | 8 | Yes/Yes (0.234) | – |
| L1123L | 3 | 8 | Yes/Yes (0.156) | – |

* Data accessed on 3/8/2011

Table 4 | ZFPM2 sequence changes in patients with diaphragmatic eventrations

| Observed change | Number of Patients | Exon | 1000 Genomes*/ dbSNP (Heterozygosity) | Predicted effect (PolyPhen) |
|-------------------------------|--------------------|------|---------------------------------------|-----------------------------|
| Non-synonymous changes | | | | |
| A403G | 1 | 8 | Yes/Yes (0.341) | Benign/ Non-Deleterious |
| E782D | 2 | 8 | Yes/Yes (0.078) | Benign/ Non-Deleterious |
| Synonymous changes | | | | |
| P454P | 1 | 8 | Yes/Yes (0.234) | – |
| P592P | 1 | 8 | Yes/Yes (0.101) | – |
| V795V | 2** | 8 | Yes/Yes (0.120) | – |
| H1069H | 1 | 8 | Yes/Yes (0.234) | – |

* Data accessed on 3/8/2011

**Homozygous in one of the patients

Discussion

aCGH and SNP-based copy number analyses are commonly used as a primary screening tool to identify genomic aetiologies in patients with congenital anomalies. Identification of these changes can provide information that physicians can use to hone the prognostic and recurrence risk information given to families and to create individualized therapeutic and surveillance plans for patients.

Haploinsufficiency of ZFPM2 causes autosomal dominant isolated diaphragmatic defects with incomplete penetrance

ZFPM2 is a transcriptional co-factor that forms heterodimers with GATA transcription factors to regulate gene expression during development [25]. The role of ZFPM2 in development of diaphragmatic defects was first demonstrated by Ackerman et al. who showed that mice homozygous for a hypomorphic mutation in *Zfp2* develop diaphragmatic eventrations [14]. In the same publication, they reported a de novo heterozygous R112X mutation in an infant with severe diaphragmatic eventrations and pulmonary hypoplasia who died shortly after birth [14].

Patient 1 is the second child in which haploinsufficiency for ZFPM2 has been seen in association with a severe diaphragmatic eventration. Although Patient 2's deletion affects both the 3' end of ZFPM2 and the first coding exon of OXR1, it is likely that disruption of ZFPM2 underlies the development of CDH in this patient since OXR1 appears to be involved in the prevention of oxidative damage – a process that has not been implicated in the development of diaphragmatic defects [26]. Although DNA is not available on Patient 2's brother, it is likely that he inherited the same deletion from his mother which contributed to his CDH. Alterations in ZFPM2 activity may also be the major, if not the sole, genetic factor that contributed to the development of CDH in Patient 3 and previously reported individuals with CDH with deletions and translocation involving 8q22q23 (Supplemental Table 2) [13]. Since both Patient 1 and Patient 2 inherited their deletions from unaffected parents we conclude that loss-of-function alleles of ZFPM2 are associated with autosomal dominant diaphragmatic defects – CDH or diaphragmatic eventrations – with incomplete penetrance. The identification of the causative genomic changes in Patient 1 and 2, both of whom had only minor anomalies – radioulnar synostosis diagnosed at 2 and half years of age and a single umbilical artery, respectively – provide further evidence that such studies should be considered in individuals who appear to have isolated diaphragmatic defects.

Alterations in ZFPM2 underlie a small fraction of congenital diaphragmatic defects

Screening of the ZFPM2 gene in 52 patients with CDH and 10 patients with diaphragmatic eventrations failed to identify any clearly deleterious changes in the ZFPM2 gene. Similarly, Ackerman et al. did not find deleterious ZFPM2 sequence changes in 29 additional post mortem samples from children with diaphragmatic defects [14]. However, Bleyl et al., screened 96 CDH patients – 53 with isolated CDH, 36 with CDH and additional anomalies, and 7 with CDH and

known chromosomal anomalies – and identified a rare amino acid change, M703L, in a patient with isolated CDH that is predicted to be possibly damaging by PolyPhen and deleterious by SNPs3D (Supplemental Table 3) [24]. These data suggests that severe, deleterious alterations in *ZFPM2* account for only a small portion of diaphragmatic defects. It is unclear, however, whether individual changes, like M703L, increase the risk for CDH and, if so, to what degree.

Delineation of new minimal deleted region for CDH on 1q41q42

Chromosome 1q41q42 has been shown to be recurrently deleted in individuals with CDH. The 1q41q42 minimal deleted region for CDH was previously defined by the maximal region of overlap between a patient reported by Kantarci et al. and a patient described by Van Hove et al. who were subsequently referred to as Patient 7 and Patient 4, respectively, by Shaffer et al. [6, 15, 27]. This interval spanned ~6.3 Mb (220,120,384-226,397,002 hg19) and contained 48 RefSeq genes. The maximal proximal and distal breakpoints of our Patient 4's deletion are located inside the CDH region defined by Shaffer et al. [15]. These breakpoints can be used to define a new minimal deleted region for CDH on chromosome 1q41q42 which spans ~2.2 Mb (223,073,839-225,318,623 hg19) and contains only 15 RefSeq genes (Figure 2). This refined minimal deleted region for CDH does not contain the H2.0-like homeobox (*HLX*) gene which has been considered a candidate gene for CDH based on its expression in the murine diaphragm and the diaphragmatic defects identified in *Hlx*^{-/-} mice [28-30]. Although it is possible that haploinsufficiency of *HLX* can contribute to the formation of diaphragmatic defects in humans, its exclusion from the minimal deleted region for CDH suggests that alterations in *HLX* function are not required for the development of CDH in association with 1q41q42 deletions. The dispatched homolog 1 (*DISP1*) gene has also been considered a candidate gene for CDH and is located within the new minimal deleted interval for CDH. *DISP1* is a membrane spanning protein that plays an essential role in SHH signalling [31]. The potential role of *DISP1* in the formation of CDH is supported by evidence that murine *Disp1* is expressed in the pleuroperitoneal fold (PPF), a structure that is often considered to be the primordial mouse diaphragm and the identification of a somatic Ala1471Gly mutation – predicted to be benign by PolyPhen but “not tolerated” by SIFT (<http://blocks.fhrc.org/sift/SIFT.html>) – in a patient with CDH and other anomalies [32]. However, abnormalities in other SHH signalling proteins have yet to be clearly shown to cause CDH. Truncating mutations (W475X and Y734X) in *DISP1* have been found in two individuals with microforms of holoprosencephaly and their unaffected mothers – consistent with *DISP1*'s role in SHH signalling – but not in individuals with diaphragmatic defects [32, 33]. This suggests that consideration should be given to the possible role of other 1q41q42 genes in the development of CDH. The tumor protein p53 binding protein, 2 (*TP53BP2*) gene could play a role in CDH development by modulating apoptosis and cell proliferation through interactions with other regulatory molecules and has been shown to play a critical role in heart and CNS development in mice [34, 35]. The WD repeat domain 26 (*WDR26*) gene is another candidate gene that is widely expressed and could play a role in the development of CDH by regulating cell signalling pathways and modulating cell proliferation [36, 37].

CDH is recurrently seen in 16p11.2 microdeletion syndrome

Recurrent 16p11.2 microdeletions result in a constellation of defects including developmental delay, cognitive impairment, behavioral problems, seizures and congenital anomalies [17]. Both Patient 5 and Patient 6 have de novo deletions of this region suggesting that CDH should be added to the list of congenital anomalies associated with this microdeletion syndrome.

The T-box 6 gene (*TBX6*) is located on 16p11.2 and encodes a transcription factor that has been shown to play a critical role in important developmental processes including paraxial mesoderm differentiation and left right patterning [38, 39]. As a result, *TBX6* has been hypothesized to contribute to many of the congenital anomalies associated with 16p11.2 [17]. It is possible that haploinsufficiency of *TBX6* also contribute to the development of CDH.

Evidence of CDH-related genes on distal chromosome 11q and proximal chromosome 13q

Patient 7 carried an extra derivative 13 chromosome making her trisomic for a portion of the chromosome 13 extending to 13q12.3 and a portion of chromosome 11 extending from 11q23 to the telomere – 47,XX,+der(13)t(11;13)(q23.2;q12.3). A similar chromosomal complement 47,XY,+der(13)t(11;13)(q21;q14) was seen in a boy with CDH described by Park et al. suggesting that upregulation of genes on distal 11q and/or proximal 13q may play a role in the development of CDH [40]. In support of this hypothesis, duplications of 11q have been recurrently seen in patients with CDH with many cases being associated with an unbalanced 3:1 meiotic segregation of the common t(11;22) translocation – resulting in a 47,XX or XY,+der(22)t(11;22)(q23.3;q11.2) chromosomal complement [13, 41]. Multiple cases of CDH associated with trisomy 13 have also been described providing support for the existence of one or more CDH-related genes on chromosome 13 [13].

The role of FZD2 and Wnt signalling in the development of CDH and defects associated with pentalogy of Cantrell

The cardiac, diaphragmatic and anterior wall defects seen in Patient 8, are similar to those described in pentalogy of Cantrell – a constellation of defects described by Cantrell et al. that includes, a supraumbilical omphalocele, a lower sternal cleft, a defect in the central tendon of the diaphragm, a defect in the pericardium, and an intracardiac anomaly [16]. A de novo deletion of *FZD2* was identified in Patient 8 but similar deletions have been reported in normal individuals from Ibadan, Nigeria [20]. Although this suggests that haploinsufficiency of *FZD2* is unlikely to be the sole cause of this patient's phenotype, several lines of evidence suggest that decreased *FZD2* expression may have contributed to this child's phenotype.

Frizzled genes encode a family of seven transmembrane domain proteins that act as receptors for Wnt signalling proteins [42]. *FZD2* is expressed in a variety of organs during development (Supplemental Table 1) and its protein product has been shown to interact with WNT3A and WNT5A and to signal through both the canonical (Wnt/beta-catenin) and non-canonical (Wnt/Ca⁺⁺ and cyclic GMP) Wnt pathways [43]. In chick embryos, Wnt3a and Wnt5a

modulate the migration of mesodermal precursors and Wnt3a has been shown to control the movement patterns of cardiac progenitor cells [44, 45]. Wnt signalling has also been shown to play a role in the development of CDH and omphalocele in humans. X-linked dominant mutations in *PORCN*, a gene that encodes a protein that modifies Wnt proteins – including WNT3A – for membrane targeting and secretion, have been shown to cause CDH and omphalocele as part of focal dermal hypoplasia (Goltz syndrome; OMIM #305600) [46, 47].

It is possible that deletion of *FZD2*, in combination with other genetic and/or environmental factors, caused dysregulation of these Wnt signalling pathways, leading to the development of the cardiac defects, CDH and omphalocele seen in Patient 8. The potential role of frizzled signalling in developmental processes that require directional tissue movements followed by tissue fusion is supported by the work of Yu et al. who recently showed that mouse frizzled 1 (*Fzd1*) and frizzled 2 (*Fzd2*) genes play an essential and partially redundant role in the correct positioning of the cardiac outflow tract and closure of the palate and ventricular septum [48]. Genetic changes that disrupt these processes may ultimately be found to contribute to other cases of partial or complete pentalogy of Cantrell.

Genomic changes of unknown significance

The majority of the rare genomic changes catalogued in Table 2 are not located within genomic regions that have been shown to be recurrently deleted or duplicated in individuals with CDH and do not affect genes/pathways that have been clearly implicated in the development of diaphragmatic defects. Although the significance of these changes is presently unknown, it is likely that future studies, in humans and animal models, will help to clarify whether these changes increase the risk of developing diaphragm defects.

Acknowledgements

The authors would like to thank the families who participated in this study. We would also like to acknowledge Dr. Brendan Lee who served as a scientific mentor and provided and cared for study patients and Dr. John W. Belmont who provided and cared for study patients.

Funding

This work was supported by National Institutes of Health grants T32-GM007330-33S1 and F30-HL099469-01 (MJW), and KO8-HD050583 and R01-HD065667 (DAS). DV was supported by a Sophia-ErasmusMC grant SSWO 551.

This work was also supported by Award Number P30HD024064 from the Eunice Kennedy Shriver National Institute of Child Health & Human Development. The content is solely the responsibility of the authors and does not necessarily represent the official views of the Eunice Kennedy Shriver National Institute of Child Health & Human Development or the National Institutes of Health. These funding sources had no direct involvement in the study design, the collection, analysis and interpretation of the data, the writing of this report and the decision to submit this manuscript for publication.

License for publication

The Corresponding Author has the right to grant on behalf of all authors and does grant on behalf of all authors, an exclusive licence (or non-exclusive for government employees) on a worldwide basis to the BMJ Group and co-owners or contracting owning societies (where published by the BMJ Group on their behalf), and its Licensees to permit this article (if accepted) to be published in the Journal of Medical Genetics and any other BMJ Group products and to exploit all subsidiary rights, as set out in our licence.

Competing interests

None declared.

Ethics approval

This study was conducted with the approval of the Institutional Review Boards of Baylor College of Medicine, Houston, Texas, USA and Erasmus Medical Center, Rotterdam, the Netherlands.

Contributors

We would also like to acknowledge Dr Brendan Lee who served as a scientific mentor and provided and cared for study patients, and Dr John W Belmont who provided and cared for study patients.

Provenance and peer review

Not commissioned; externally peer reviewed.

References

1. Stege G, Fenton A, Jaffray B. *Nihilism in the 1990s: the true mortality of congenital diaphragmatic hernia*. *Pediatrics* 2003;**112**:532-535.
2. Pober BR. *Overview of epidemiology, genetics, birth defects, and chromosome abnormalities associated with CDH*. *Am J Med Genet C Semin Med Genet* 2007;**145C**:158-171.
3. Edwards JH. *The simulation of mendelism*. *Acta Genet Stat Med* 1960;**10**:63-70.
4. Klaassens M et al. *Congenital diaphragmatic hernia and chromosome 15q26: determination of a candidate region by use of fluorescent in situ hybridization and array-based comparative genomic hybridization*. *Am J Hum Genet* 2005;**76**:877-882.
5. Slavotinek A et al. *Fryns syndrome phenotype caused by chromosome microdeletions at 15q26.2 and 8p23.1*. *J Med Genet* 2005;**42**:730-736.
6. Kantarci S, et al. *Findings from aCGH in patients with congenital diaphragmatic hernia (CDH): a possible locus for Fryns syndrome*. *Am J Med Genet A* 2006;**140**:17-23.
7. Scott DA, et al. *Genome-wide oligonucleotide-based array comparative genome hybridization analysis of non-isolated congenital diaphragmatic hernia*. *Hum Mol Genet* 2007;**16**:424-430.
8. Van Esch H, Backx L, Pijkels E, Fryns JP. *Congenital diaphragmatic hernia is part of the new 15q24 microdeletion syndrome*. *Eur J Med Genet* 2009;**52**:153-156.
9. Wat MJ et al. *Recurrent microdeletions of 15q25.2 are associated with increased risk of congenital diaphragmatic hernia, cognitive deficits and possibly Diamond-Blackfan anaemia*. *J Med Genet* 2010;**47**:777-781.
10. Srisupundit K, et al. *Targeted array comparative genomic hybridisation (array CGH) identifies genomic imbalances associated with isolated congenital diaphragmatic hernia (CDH)*. *Prenat Diagn* 2010;**30**:1198-1206.
11. Scott DA. *Genetics of congenital diaphragmatic hernia*. *Semin Pediatr Surg* 2007;**16**:88-93.
12. Lurie IW. *Where to look for the genes related to diaphragmatic hernia?* *Genetic Counseling* 2003;**14**:75-93.
13. Holder AM, et al. *Genetic factors in congenital diaphragmatic hernia*. *Am J Hum Genet* 2007;**80**:825-845.
14. Ackerman KG, et al. *Fog2 is required for normal diaphragm and lung development in mice and humans*. *PLoS Genet* 2005;**1**:58-65.
15. Shaffer LG, et al. *The discovery of microdeletion syndromes in the post-genomic era: review of the methodology and characterization of a new 1q41q42 microdeletion syndrome*. *Genet Med* 2007;**9**:607-616.
16. Cantrell JR, Haller JA, Ravitch MM. *A syndrome of congenital defects involving the abdominal wall, sternum, diaphragm, pericardium, and heart*. *Surg Gynecol Obstet* 1958;**107**:602-614.
17. Shinawi M, et al. *Recurrent reciprocal 16p11.2 rearrangements associated with global developmental delay, behavioural problems, dysmorphism, epilepsy, and abnormal head size*. *J Med Genet* 2010;**47**:332-341.
18. Fruhman G, et al. *Suspected trisomy 22: Modification, clarification, or confirmation of the diagnosis by aCGH*. *Am J Med Genet A*. 2011;**155**:434-438.
19. Boehm D, Herold S, Kuechler A, Liehr T, Laccone F. *Rapid detection of subtelomeric deletion/duplication by novel real-time quantitative PCR using SYBR-green dye*. *Hum Mutat* 2004;**23**:368-378.
20. Matsuzaki H, Wang PH, Hu J, Rava R, Fu GK. *High-resolution discovery and confirmation of copy number variants in 90 Yoruba Nigerians*. *Genome Biol* 2009;**10**:R125.
21. McCarroll SA, et al. *Integrated detection and population-genetic analysis of SNPs and copy number variation*. *Nat Genet* 2008;**40**:1166-1174.
22. Sunyaev S, et al. *Prediction of deleterious human alleles*. *Hum Mol Genet* 2001;**10**:591-597.
23. Yue P, Melamud E, Moul J. *SNPs3D: candidate gene and SNP selection for association studies*. *BMC Bioinformatics* 2006;**7**:166.
24. Bleyl SB, et al. *Candidate genes for congenital diaphragmatic hernia from animal models: sequencing of FOG2 and PDGFRalpha reveals rare variants in diaphragmatic hernia patients*. *Eur J Hum Genet* 2007;**15**:950-958.

25. Cantor AB, Orkin SH. *Coregulation of GATA factors by the Friend of GATA (FOG) family of multitype zinc finger proteins*. *Semin Cell Dev Biol* 2005;**16**:117–128.
26. Volkert MR, Elliott NA, Housman DE. *Functional genomics reveals a family of eukaryotic oxidation protection genes*. *Proc Natl Acad Sci U S A* 2000;**97**:14530-14535.
27. Van Hove JL, et al. *Fryns syndrome survivors and neurologic outcome*. *Am J Med Genet* 1995;**59**:334-340.
28. Lints TJ, Hartley L, Parsons LM, Harvey RP. *Mesoderm-specific expression of the divergent homeobox gene HLX1 during murine embryogenesis*. *Dev Dyn* 1996;**205**:457-470.
29. Hentsch B, et al. *Hlx homeo box gene is essential for an inductive tissue interaction that drives expansion of embryonic liver and gut*. *Genes Dev* 1996;**10**:70–79.
30. Slavotinek AM, et al. *Sequence variants in the HLX gene at chromosome 1q41-1q42 in patients with diaphragmatic hernia*. *Clin Genet* 2009;**75**:429-439.
31. Ma Y, Erkner A, Gong R, Yao S, Taipale J, Basler K, Beachy PA. *Hedgehog-mediated patterning of the mammalian embryo requires transporter-like function of dispatched*. *Cell* 2002;**111**:63-75.
32. Kantarci S, et al. *Characterization of the chromosome 1q41q42.12 region, and the candidate gene DISP1, in patients with CDH*. *Am J Med Genet A* 2010;**152A**:2493-2504.
33. Roessler E, et al. *Truncating loss-of-function mutations of DISP1 contribute to holoprosencephaly-like microform features in humans*. *Hum Genet* 2009;**125**(4):393-400.
34. Chen Y, Liu W, Naumovski L, Neve RL. *ASPP2 inhibits APP-BP1-mediated NEDD8 conjugation to cullin-1 and decreases APP-BP1-induced cell proliferation and neuronal apoptosis*. *J Neurochem* 2003;**85**:801-809.
35. Vives V, et al. *ASPP2 is a haploinsufficient tumor suppressor that cooperates with p53 to suppress tumor growth*. *Genes Dev* 2006;**20**:1262-1267.
36. Zhu Y, et al. *WDR26: a novel Gbeta-like protein, suppresses MAPK signalling pathway*. *J Cell Biochem* 2004;**93**:579-587.
37. Wei X, et al. *Overexpression of MIP2, a novel WD-repeat protein, promotes proliferation of H9c2 cells*. *Biochem Biophys Res Commun* 2010;**393**:860-863.
38. Chapman DL, Papaioannou VE. *Three neural tubes in mouse embryos with mutations in the T-box gene Tbx6*. *Nature* 1998;**391**:695-697.
39. Hadjantonakis AK, Pisano E, Papaioannou VE. *Tbx6 regulates left/right patterning in mouse embryos through effects on nodal cilia and perinodal signalling*. *PLoS One* 2008;**3**:e2511.
40. Park JP, McDermet MK, Doody AM, Marin-Padilla JM, Moeschler JB, Wurster-Hill DH. *Familial t(11;13)(q21;q14) and the duplication 11q,13q phenotype*. *Am J Med Genet* 1993;**45**:46–48.
41. Klaassens M, et al. *Congenital diaphragmatic hernia associated with duplication of 11q23-qter*. *Am J Med Genet A* 2006;**140**:1580-1586.
42. Wang HY, Liu T, Malbon CC. *Structure-function analysis of Frizzleds*. *Cell Signal* 2006;**18**:934-941.
43. Sato A, Yamamoto H, Sakane H, Koyama H, Kikuchi A. *Wnt5a regulates distinct signalling pathways by binding to Frizzled2*. *EMBO J* 2010;**29**:41-54.
44. Sweetman D, Wagstaff L, Cooper O, Weijer C, Münsterberg A. *The migration of paraxial and lateral plate mesoderm cells emerging from the late primitive streak is controlled by different Wnt signals*. *BMC Dev Biol* 2008;**8**:63.
45. Yue Q, Wagstaff L, Yang X, Weijer C, Münsterberg A. *Wnt3a-mediated chemorepulsion controls movement patterns of cardiac progenitors and requires RhoA function*. *Development* 2008;**135**:1029-1037.
46. Wang X, et al. *Mutations in X-linked PORCN, a putative regulator of Wnt signalling, cause focal dermal hypoplasia*. *Nat Genet* 2007;**39**:836-838.
47. Dias C, et al. *A nonsense PORCN mutation in severe focal dermal hypoplasia with natal teeth*. *Fetal Pediatr Pathol* 2010;**29**:305-313.
48. Yu H, Smallwood PM, Wang Y, Vidaltamayo R, Reed R, Nathans J. *Frizzled 1 and frizzled 2 genes function in palate, ventricular septum and neural tube closure: general implications for tissue fusion processes*. *Development* 2010;**137**:3707-3717.

Chapter 2.4

Copy Number Detection in Discordant Monozygotic Twins of Congenital Diaphragmatic Hernia (CDH) and Esophageal Atresia (EA) Cohorts

D.Veenma, E.Brosens, E.de Jong, C.van de Ven, C.Meeuwissen,
T.Cohen-Overbeek, M.Boter, H.Eussen, H.Douben, D.Tibboel and A.de Klein

Eur J Hum Genet. 2012 Mar;20(3):298-304. doi: 10.1038/ejhg.2011.194.

Abstract

The occurrence of phenotypic differences between monozygotic twins is commonly attributed to environmental factors, assuming that monozygotic twins have a complete identical genetic make-up. Yet, recently several lines of evidence showed that both genetic and epigenetic factors could play a role in phenotypic discordance after all. A high occurrence of copy number variation differences was observed within monozygotic twin pairs discordant for Parkinson disease, thereby stressing on the importance of post-zygotic mutations as disease-predisposing events.

In this study, the prevalence of discrepant copy number variations was analysed in discordant monozygotic twins of the Esophageal Atresia and Congenital Diaphragmatic Hernia cohort in the Netherlands. Blood-derived DNA from 11 pairs (seven Esophageal Atresia and four Congenital Diaphragmatic Hernia) was screened using high-resolution SNP arrays. Results showed an identical copy number profile in each twin pair. Mosaic chromosome gain or losses could not be detected either with a detection threshold of twenty percent. Some of the germ-line structural events demonstrated in five out of eleven twin pairs could function as a susceptible genetic background. For example, the 177Kb loss of chromosome 10q26 in CDH pair-3 harbours the *TCF7L2* gene (*Tcf4* protein), which is implicated in the regulation of muscle fiber type development and maturation.

In conclusion, discrepant copy number variations are not a common cause of twin discordancy in these investigated congenital anomaly cohorts.

Introduction

Monozygotic (MZ) twin comparisons have been used for many decades to specify contributions of both nature (heredity) and nurture (environment) [1]. Normally the study design is based on the presumption that monozygotic twins come from one fertilized egg and therefore have complete identical genetic make-ups. Yet, recently several lines of evidence suggested that genetic and epigenetic factors could play a role in MZ phenotypic variances after all [2-6]. Using a BAC array platform, Bruder et al. [6] demonstrated that discordance in their monozygotic Parkinson's disease (PD) twin cohort of nine individuals could be the result of Copy Number Variation (CNV) differences. However, Baranzini et al. [7] could not reproduce this high intra-twin pair variability of structural variants using both array and next-generation sequencing in three twin pairs discordant for Multiple Sclerosis.

We investigated whether discrepant CNVs could cause discordance in MZ twin pairs of the Dutch Esophageal Atresia (EA [MIM 189960]) and Congenital Diaphragmatic Hernia (CDH [MIM 142340]) cohort. Blood-derived DNA from 11 (7 EA and 4 CDH) pairs of MZ twins was screened using high-resolution SNP arrays.

EA generally presents at birth with a defective formation of the esophagus with or without a fistulous tract to the trachea. Although not lethal in most cases, long-term morbidity plays a significant role in these patients. CDH is a more severe birth defect characterized by defective formation of the diaphragm, lung hypoplasia and pulmonary hypertension. Despite medical advances mortality for isolated cases is 20% and for none-isolated cases up to 60%. Both EA and CDH are presumed to have a multifactorial etiology and the identification of chromosomal aberrations and knockout animal models provide strong evidence for a genetic component [8]. In contrast, both anomalies present with low twin concordance rates, 10.7% and 15.6% for EA and CDH respectively, and sibling recurrence rates are low (1-2%) as well. Shaw-Smith [9] already pointed out that the incidence of twinning in EA is 2.6 times higher than statistically expected. 206 pairs are described in literature up until now, however information on zygosity is less thorough [9-16]. Orford et al. [15] stated that at least 80% of reported EA twins are same-sex pairs. In total, 22 out of these 206 twin pairs are concordant for the EA phenotype. In literature, 77 twin pairs have been described for CDH of which 53 were recognized as monozygotic [17-20]. 12 pairs were concordant for the CDH phenotype.

The rationale of this study was to investigate whether CNVs in the affected twin sibling could account for phenotypic discordance of either Esophageal Atresia or Congenital Diaphragmatic Hernia MZ twin siblings. Although results showed no such proof, germ-line structural events were detected and these could represent a susceptible genetic background as seen in other genetic anomalies. Results are discussed in the context of earlier MZ twin reports.

Materials and methods

Ethics statement

Research involving human participants has been approved by the “Medical Ethical Committee (METC) at Erasmus-MC, which specifically approved for blood withdrawal of both twins and their parents. Informed consent forms were obtained for the index case and his/her parents at once and for the healthy twin separately.

Patients

The 11 affected twin samples were collected from the congenital anomaly cohort in Rotterdam (Erasmus MC Sophia’s Hospital, the Netherlands) in which 541 EA- and 626 CDH- patients are currently registered. Of these, 22 CDH patients (14 dizygotic, five MZ, three not tested) and 35 EA patients (six dizygotic, nine MZ, 20 not tested) were the result of a twin pregnancy. Included were those twin samples with a written parental informed consent, quality material of both siblings and confirmed monozygosity by STR profiling (AmpFISTR identifier PCR amplification kit, Applied Biosystems, Foster City, CA). Another exclusion criterion was the identification of a genetic abnormality, most commonly an aneuploidy.

DNA isolation

Automated DNA extraction from peripheral blood (or skin fibroblasts in case of two affected CDH twins) was performed using local standard protocols. DNA quality and concentration were checked with the Quant-iT™ PicoGreen® dsDNA Kit (Invitrogen Corporation, Carlsbad, California, USA).

Whole-genome high-resolution SNP array

SNP analysis was carried out using the Illumina HumanCytoSNP-12 bead chip version 2.2 (Illumina, San Diego, CA, USA). This chip includes 220,000 of the most informative SNPs en markers with a median physical distance of 6.2 Kb. DNA samples were processed according to the manufacturer’s protocol. The call rate of this array batch was above 0.98, except for 1 sample.

SNP array analysis

Data for each bead chip were self-normalized in Genomestudio GT® (Illumina, San Diego, CA, USA) using information contained within the array. Copy number estimates for each individual sample were determined by comparison to a common reference set of 200 CEU samples from the HapMAP project [www.hapmap.org/downloads/raw_data] (supplied by Illumina, manifest files) and visualized in the Nexus software program (version five, Biodiscovery, El Segundo, CA, USA) as log₂ ratios. Analysis settings were as follow: both SNP-FASST and SNP-Rank segmentation methods were executed independently with significance thresholds ranging from 1×10^{-4} to 1×10^{-6} and log-ratio thresholds of 0.18 and -0.18 for duplication and deletions respectively. The maximum contiguous probe spacing was 1000 Kbp and the minimum number of probes per segment was

set to three, limiting CNV detection to sizes above 18.6 Kb. Subsequently, only CNVs above 50 Kb were validated. Paired analysis for deletions and duplications was performed in each affected twin versus its healthy co-twin. As described recently high-resolution (SNP) arrays are suitable for detection of both germ-line and mosaic CNVs [21-25]. Mosaic copy number aberrations are hallmarked by a concomitant change of log₂ intensity signal and a shift in b-allele frequency. The detection limit (sensitivity) of the Nexus SNP-FASST algorithm for mosaic CNVs is 20 percent using a heterozygous imbalance threshold of 0.45 [22]. To review functionality of each putative CNV at once, occurrence frequencies in a qualified normal pediatric cohort of 2026 individuals [26] (CHOP [<http://cnv.chop.edu/>]) and in the DGV [<http://www.tcag.ca>] were uploaded in the Nexus program as well. Since these populations display various ethnic backgrounds, comparison to an in-house normal reference set was performed as well. Additionally, possible intra-twin pair genotype differences (with respect to all SNP-markers presented on the array) were evaluated in Genomestudio GT[®] using the paired analysis settings.

Validation using Fluorescent In-Situ Hybridization and relative-quantitative PCR analysis

Confirmation of each CNV with quantitative real time PCR and/or FISH was executed in the twin-siblings and their parents according to local standard protocols with minor modifications [22, 27]. For FISH, BAC clones were selected from the UCSC genome browser [<http://genome.ucsc.edu/>], purchased at BACPAC resources centre (Oakland, California, USA) and labelled (Random Prime labelling system Invitrogen Corporation, Carlsbad, California, USA) with Bio-16-dUTP or Dig-11-dUTP (Roche applied science, Indianapolis, USA). After validation on control metaphases, the chromosome 22 BAC clones RP11-62K15 and RP1-66M5 were used for confirmation in EA-pair-I.

Primer pairs for quantitative real-time PCR were designed from unique sequences within the minimal deleted or duplicated regions of each copy number change using Primer Express software v2.0 (Applied Biosystems, Carlsbad, California, USA). The nucleotide-nucleotide BLAST algorithm at NCBI [<http://www.ncbi.nlm.nih.gov/BLAST/>] was used to confirm that each PCR amplification product was unique. Quantitative PCR analyses were performed using an ABI7300 Real-time PCR system in combination with KAPA-SYBR fast master mix (KapaBiosystems, Woburn, MA, USA). Experiments were designed with a region of the *C14ORF145* gene serving as a control locus as previously described [27].

Results

Clinical characterization and monozygosity screening of twin pairs

Clinical features of each twin pair are summarized in Table 1. Briefly, seven out of 11 pairs were discordant for the phenotype of EA (Table1A) and four out of 11 for CDH (Table 1B). Four out of eleven EA-affected patients harbored (major) additional anomalies. Considering CDH; there is a

variable expression of left and right CDH with all persons (as expected) featuring lung hypoplasia. We are dealing with an isolated CDH cohort since most anomalies in pairs 3 and 4 are minor. Finally, zygosity status of each twin pair was confirmed (data not shown) by STR profiling using the commercially available STR identifier kits of Applied Biosystems.

Table 1A | Clinical features EA Cohort.

| Pair | GA | Birth order | | Obstetric history | EA | Fistel | Type of additional anomalies |
|------|-------|-------------|----------------|---|----|--------|---|
| EA | (wks) | (Patient) | (Healthy twin) | | | | |
| EA1 | 37,3 | 1 | 2 | Breech presentation | + | + | Dysmorphic Auricular tags, Cleft uvula Abnormal dermatoglyphics Heart ASD Lung Lunghypoplasia right Neurologic/skeletal Scoliosis Fusion of vertebrae Hemivertebrae IUGR |
| EA2 | 36 | 2 | 1 | Breech presentation Maternal medication: sintrom | + | + | Heart VSD Lung Lunghypoplasia |
| EA3 | NA | NA | NA | NA | + | + | Heart Cardiac situs Dextrocardia healthy twin |
| EA4 | NA | NA | NA | NA | + | - | - |
| EA5 | 33,5 | 1 | 2 | Breech presentation Fever durante partu | + | + | Dysmorphic Triangular face, Deep set eyes, Palpebral fissures slant down Small mandible Thin fingers, hypoplastic thumbs Proximal placement of thumb Hypoplastic or absent radii Sacral hemangioma healthy twin |
| EA6 | 34,4 | NA | NA | Polyhydramnios Maternal medication: corticosteroids | + | + | Heart VSD Tricuspid incompetence |
| EA7 | | NA | NA | - | + | + | - |

Table 1B | Clinical features CDH Cohort.

| Pair CDH | GA (wks) | Birth order | | Obstetric history | CDH | Type of additional anomalies |
|-------------|-------------|-------------|----------------|---|-------|--|
| | | (Patient) | (Healthy twin) | | | |
| CDH1 | 35,3 | 2 | 1 | Sectio Caesarea Breech presentation | left | – |
| CDH2 | 33,4 | 1 | 2 | Sectio Caesarea >24hrs ruptured membrane | left | – |
| CDH3 | 38,5 | 2 | 1 | – | right | Urogenital Inguinal hernia Hydrocele testis |
| CDH4 | 34,1 | 2 | 1 | Sectio Caesarea | left | Dysmorphic Small mandibula IUGR |

The following abbreviations are used: ASD; Atrial Septal defect, CDH; Congenital Diaphragmatic Hernia, EA; esophageal atresia, GA; Gestational Age, IUGR; Intra Uterine growth Retardation, VSD; Ventricular Septal Defect. Unfortunately, for a few EA subjects detailed clinical data is unavailable

Paired CNV analysis of discordant monozygotic twins

Results of the paired CNV analysis of each MZ twin couple are summarized in Table 2 showing no evidence of pathogenic CNV discordance in both congenital anomaly cohorts. In order to detect mosaic (somatic) aberrations, specific attention was paid to b-allele frequency changes as well. In the EA cohort a total of ten germline CNVs were identified. Seven concerned common Copy Number Polymorphisms (CNP) defined by the occurrence of the CNV in at least five individuals of qualified normal pediatric cohorts in literature. The remaining three events were present in both the twin and at least one healthy parent and are therefore less likely to be pathogenic as well. For example, the 666 Kb sized chromosome 22q deletion in EA pair-1 (Figure 1) was found both in the healthy twin and his mother and partly overlaps with CNVs catalogued in control cohorts.

Existence of inherited CNVs was detected in the CDH cohort as well. A total of three CNVs were distinguished of which two are not prevalent in normal cohorts. All three events were present in the healthy twin as well. Figure 2 represents the 177Kb loss of chromosome 10q26 in CDH pair-3 and harbors the *TCF7L2* gene (*Tcf4* protein), which is mainly known for its involvement in blood glucose homeostasis as a result of Wnt signalling changes.

Not ruled out in this study are the presence of balanced genomic alterations and small (<50kb) or very-low mosaic (<20%) chromosome aberrations beyond the detection level of our experimental approach.

Table 2 | Inherited CNVs detected in MZ twins of the Rotterdam congenital anomaly cohort.

| EA pair (bp) | Chromosomal location (bp) | CNV type | Length (bp) | Gene symbols | Discordant twin | Normal Pediatric Cohort # | Validation |
|--------------|------------------------------|----------|-------------|--------------------------|-----------------|-------------------------------------|---|
| 1 | chr22:46,163,818-46,870,578 | CN Loss | 666192 | FLJ46257 (hypothetical) | yes | yes (0/2026, 0/370, overlap 25 DGV) | FISH, inherited maternally |
| 2 | chr7:75,420,580-75,471,147 | CN Loss | 50567 | POR, STYXL1, TMEM120A | yes | yes (0/2026, 0/370, overlap 2 DGV) | q-PCR, inherited (both parents heterozygous deletion) |
| 3 | chr6:162,638,827-162,840,229 | CN Gain | 201402 | PARK2 | yes | yes: 5/2026 | q-PCR, inherited maternally |
| | chr17:41,522,684-41,646,903 | CN Gain | 124219 | KIAA1267 | yes | yes: 69/2026 | Copy Number Polymorphism |
| | chr18:1,895,191-1,960,898 | CN Loss | 65707 | - | yes | yes: 26/2026 | Copy Number Polymorphism |
| 4 | chr14:19,283,777-19,479,370 | CN Gain | 195593 | OR4K1, OR4K2, OR4K5, etc | yes | yes: 35/2026 | Copy Number Polymorphism |
| 5 | chr12:7,892,014-8,027,862 | CN gain | 135848 | SLC2A14, SLC2A3 | yes | yes: 39/2026 | Copy Number Polymorphism |
| 6 | chr12:31,146,084-31,303,651 | CN gain | 157567 | DDX11 | yes | yes: 20/370 | Copy Number Polymorphism |
| | chr2:89,728,406-89,885,025 | CN gain | 156619 | | yes | yes: 14/2026 | Copy Number Polymorphism |
| | chr8:2,322,561-2,577,455 | CN gain | 254894 | | yes | yes: 32/2026 | Copy Number Polymorphism |
| 7 | - | - | - | - | - | - | - |

| CDH pair (bp) | Chromosomal location | CNV (type) | Length (bp) | Gene symbols | Discordant twin | Normal Cohort # | Validation |
|---------------|-------------------------------|------------|-------------|------------------|-----------------|-------------------------------------|-----------------------------|
| 1 | - | - | - | - | - | - | - |
| 2 | - | - | - | - | - | - | - |
| 3 | chr10:114,660,279-114,838,014 | CN Loss | 177735 | TCF7L2 [22] | yes | no | q-PCR, inherited maternally |
| 4 | chr4:86,595,913-87,070,050 | CN Loss | 474137 | ARHGAP24 [23-24] | yes | yes (0/2026, 0/370, overlap 27 DGV) | q-PCR, inherited maternally |
| | chr4:57,743,262-57,795,280 | CN Gain | 52018 | - | yes | yes (2/2026, 0/370, overlap 15 DGV) | Copy Number Polymorphism |

The following abbreviations are used: CN; Copy Number, bp; basepairs, EA; Esophageal Atresia, CDH; Congenital Diaphragmatic Hernia.# Normal Cohort; CHOP [<http://cmv.chop.edu/>] and DGV [<http://tcag.ca.uk&Decipher>; [<http://decipher.sanger.ac.uk/application/>].Percentage of overlap with CNVs in control databases are designated if not 100% aligned.

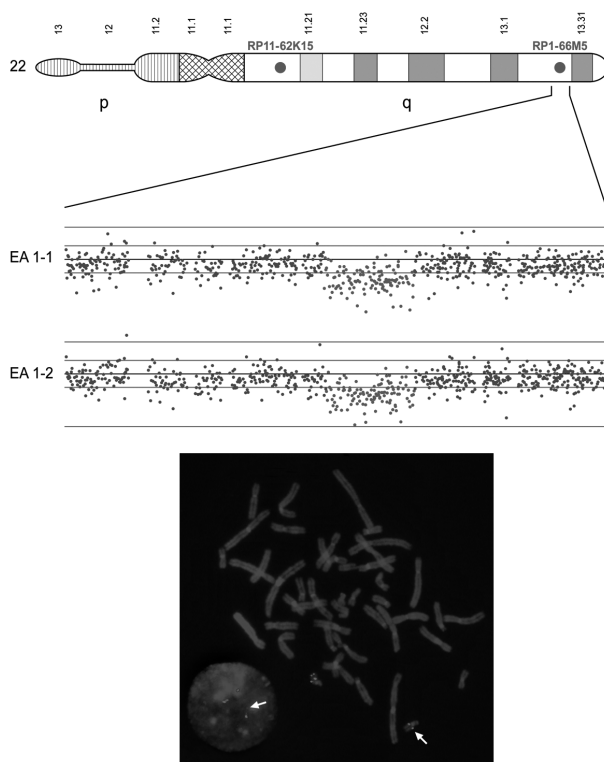


Figure 1 | SNP and Fluorescent In-Situ Hybridization results of inherited chromosome 22-CNV in EA pair-I

Nexus results (Top) of the 666 Kb deletion on chromosome 22q13.3 in both individuals of EA pair-I showing a clear drop in log₂ intensity signal validated by FISH (Bottom) on metaphase chromosomes of the affected EA twin-1. Probes: control: RP11-62K15 (green) and target: RP11-66M5 (red). Parental analysis (results not shown) demonstrated that this genomic event is inherited from the mother and therefore less likely pathogenic. In addition, no gene is allocated to this region neither are any miRNA transcripts hampering the identification of functional elements in this region as well (see page 250 for color figure).

SNP genotype analysis monozygotic twin cohorts

SNP genotype differences between the affected and unaffected twin siblings were evaluated for each SNP on the Illumina® bead chip. After removal of less accurately called SNPs, genotyping analysis showed concordance for almost all SNPs ($n=299671$) within each MZ pair. A total of five SNPs in three EA-pairs were dissimilar and three SNPs in two CDH pairs (Table 3). CDH pair-3 showed discrepancy for 99 SNPs, which could be attributed to less overall genotyping accuracy and therefore was not analyzed further. Until now, only rs2824374 (which is closely linked to the *CXADR* gene) could be associated with embryonic (mal) development, however literature only reports on effects to the kidneys and cochlea [28, 29]. None of the other identified discordant intra-twin SNP loci are directly linked to a phenotype.

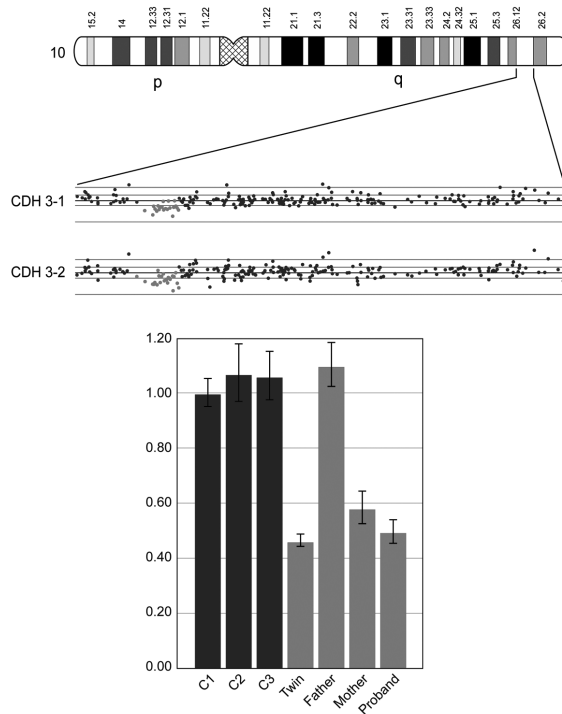


Figure 2 | SNP and relative Q-PCR results of inherited chromosome 10-CNV in CDH pair-3.

Nexus result (Top) of the chromosome 10q26 deletion event in CDH pair-3 showing a clear drop in log₂ intensity signal, which was confirmed by relative q-PCR (bottom) in the affected proband, the unaffected twin and the mother (see page 250 for color figure).

Table 3 | Discordant SNPs in MZ twin pairs of the Rotterdam Congenital anomaly cohort.

| Pair EA | Discordant SNPs | Chromosomal location (dbSNP build 130) (bp) | Gene symbols |
|---------|-----------------|---|---------------------|
| 1 | rs11573502 | chrX:24888693-24889193 | POLA1 |
| 2 | - | - | - |
| 3 | - | - | - |
| 4 | rs10125846 | chr9:2821641-2822141 | KIAA0020 |
| | rs1744767 | chr20:35200380-35200880 | LOC140699 isoform 3 |
| | rs438895 | chr1:8260692-8261192 | |
| 5 | - | - | - |
| 6 | - | - | - |
| 7 | rs1576026 | chr9:25,453,089-25,453,589 | - |

| Pair CDH | Discordant SNPs | Chromosomal location (dbSNP build 130) (bp) | Gene symbols |
|----------|--|---|---|
| 1 | rs17730982 rs2824374 | chr8:134851934-134852434 chr21:17879252-17879752 | CXADR; possible involvement kidney & cochlear development [25,26] |
| 2 | – | – | – |
| 4 | rs6571064 | chr6:103400463-103400963 | – |
| 3 | Not evaluated; SNP Quality rate < 0.95 | – | – |

The following abbreviations are used:bp; basepairs, EA; Esophageal Atresia, CDH; Congenital Diaphragmatic Hernia.

Discussion

A high occurrence of copy number variants that differed between siblings discordant for Parkinson's disease was recently suggested [6]. However, intra-twin pair variability for germ-line CNVs could not be detected in our subset of EA and CDH MZ twins. Within the limitations of the used experimental approach, structural variants in mosaic form (above 20%) could neither be demonstrated. Application of next-generation sequencing methods will allow for an easier and more sensitive calling of the smallest mosaic aberrations in the near future and will add up to the (scarce) data generated recently on this topic by some other groups [30-33].

Various causes could account for the discrepancy in CNV findings between our congenital anomaly twin cohort and the Parkinson cohort. First of all: an age factor. The rather high prevalence of mosaic CNVs in PD twins could have been generated during lifetime. This was suggested by a small study of the group of Dumanski et al. [34, 35], who identified mosaic aberrations in a wide-range of tissues of three phenotypically normal individuals. This hypothesis would imply that age-accumulated (tissue-specific) CNV events could play a role in diseases developing symptoms later in life. Consequently, they are expected to contribute less to congenital disorders. Secondly, differences in CNV prevalence between our study and the Parkinson study could be based on methodological differences such as choice of platform. Although Bruder et al. [6] presented confirmative evidence for a few of their CNVs using a different platform, detailed confirmation of most CNVs was lacking. On the other hand, structural DNA variation might play a minor role in EA- and CDH- pathophysiology, suggesting that in these congenital cohorts the focus should be widened on environmental and epigenetic factors. Two recent studies [2, 7] revealed a (significant) proportion of epigenetic variability between MZ twins in investigated tissues. However, in the Multiple Sclerosis twin cohort study these changes could not account for disease discordance. A similar study for EA, CDH or other congenital anomalies is difficult to perform, since the target tissues cannot be obtained from the healthy co-twin for obvious reasons. Structural variations restricted to the affected esophagus and diaphragm tissue could represent another cause for twin discordancy, yet was not excluded in this monozygotic cohort due to unavailability of the affected material.

Finally, although our results showed no prove for CNV contribution to phenotypic MZ-discordance, germ-line structural events were detected in both cohorts and these events could represent a so-called susceptible genetic background. In five out of eleven twin pairs germline CNVs were identified. These were rarely detected in a specific pediatric normal population [26] and/or our in-house control cohort and could therefore represent an increased susceptibility to congenital anomalies by means of a dosage responsive- or position- effect. For example, the 177Kb loss of chromosome 10q26 in CDH pair-3 might be of functional importance. A recent report demonstrated *Tcf4* (alias *Tcf7l2*) expression in connective tissue fibroblasts during development and suggested its role in the regulation of muscle fiber type development and maturation [36]. Additionally, certain polymorphisms and mutations in *TCF7L2* are linked to an increased risk of type 2 diabetes³⁷. This implies that loss of one functional *TCF7L2* allele might be associated with (super) normal glucose tolerance. Indeed we observed evidence of increased serum glucose (a Glucose of 12.2 mmol/l was identified within 24 hours postnatal) in the affected individual of twin pair 3. However, also 1 normal glucose level (Glucose 3.6 mmol/l) was determined within the same time window and since this patient was critically ill and died shortly thereafter no absolute conclusions can be drawn from these results. The healthy twin had an unremarkable medical record so far. Similarly, the haploinsufficient *ARHGAP24* gene in CDH pair-4 (encoding a vascular, cell-specific GTPase-activating protein) could confer genetic susceptibility for CDH by means of its function in modulating angiogenesis and through its interaction with filamin-A [37, 38]. Girirajan et al. [39] recently demonstrated that a second hit may elicit a severe phenotype in offspring of healthy CNV-carriers. Hypothetically this second hit can constitute another CNV in the same or associated disease pathway as well as a pathogenic SNP. These results underline the importance of archiving all genomic events (also those with a “benign” nature at first sight) in a freely accessible database such as initiated by the ISCA consortium [<https://www.iscaconsortium.org>]. Detailed and unbiased phenotyping is crucial for the understanding of the more complex genotype-phenotype correlations as well.

In summary, we investigated whether the existence of discrepant CNVs could be causal to the phenotypic discordance in MZ twin pairs of the Esophageal Atresia and Congenital Diaphragmatic Hernia cohort in Rotterdam and found no such proof. Prospective collection of DNA material in various MZ twin cohorts is warranted to evaluate the possibility of such genetic factors contributing to human phenotypic variability in general and to twin-discordance specific. We feel that the use of high-resolution SNP arrays and sequencing based methods are more suitable in these designs than BAC arrays. Finally, phenotypic correlations can only be made after proper analysis in normal cohorts as well.

Acknowledgments

The authors would like to thank all patients, specifically all twins and their parents for making this study possible. Also, we thank Tom de Vries-Lentsch for his help in preparing the figures.

Conflict of interest statement

This study was funded by the Sophia's Children's Hospital Foundation for Medical Research, Rotterdam, The Netherlands (SSWO 493 and 551). The funders had no role in study design, data collection and analysis, decision to publish, or preparation of the manuscript.

References

1. Hall, J.G., *Twinning*. Lancet, 2003. **362**(9385): p. 735-43.
2. Kaminsky, Z.A., et al., *DNA methylation profiles in monozygotic and dizygotic twins*. Nat Genet, 2009. **41**(2): p. 240-5.
3. Kimani, J.W., et al., *X-chromosome inactivation patterns in monozygotic twins and sib pairs discordant for nonsyndromic cleft lip and/or palate*. Am J Med Genet A, 2007. **143A**(24): p. 3267-72.
4. Machin, G.A., *Some causes of genotypic and phenotypic discordance in monozygotic twin pairs*. Am J Med Genet, 1996. **61**(3): p. 216-28.
5. Streit, A. and R.J. Sommer, *Genetics: Random expression goes binary*. Nature. **463**(7283): p. 891-2.
6. Bruder, C.E., et al., *Phenotypically concordant and discordant monozygotic twins display different DNA copy-number-variation profiles*. Am J Hum Genet, 2008. **82**(3): p. 763-71.
7. Baranzini, S.E., et al., *Genome, epigenome and RNA sequences of monozygotic twins discordant for multiple sclerosis*. Nature, 2010. **464**(7293): p. 1351-6.
8. Holder, A.M., et al., *Genetic factors in congenital diaphragmatic hernia*. Am J Hum Genet, 2007. **80**(5): p. 825-45.
9. Shaw-Smith, C., *Esophageal atresia, tracheo-esophageal fistula, and the VACTERL association: review of genetics and epidemiology*. J Med Genet, 2006. **43**(7): p. 545-54.
10. Sunagawa, S., et al., *Dichorionic twin fetuses with VACTERL association*. J Obstet Gynaecol Res, 2007. **33**(4): p. 570-3.
11. Depaepe, A., H. Dolk, and M.F. Lechat, *The epidemiology of tracheo-esophageal fistula and esophageal atresia in Europe*. EUROCAT Working Group. Arch Dis Child, 1993. **68**(6): p. 743-8.
12. Farquhar, J., R. Carachi, and P.A. Raine, *Twins with esophageal atresia and the CHARGE association*. Eur J Pediatr Surg, 2002. **12**(1): p. 56-8.
13. Khan, R.A. and K.L. Narashimhan, *Discordance in twins for esophageal atresia with tracheoesophageal fistula*. Indian J Pediatr, 2009. **76**(3): p. 334-5.
14. Ohno, K., et al., *Esophageal atresia with tracheoesophageal fistula in both members of monozygotic twins*. Pediatr Surg Int, 2008. **24**(10): p. 1137-9.
15. Orford, J., et al., *Esophageal atresia in twins*. Pediatr Surg Int, 2000. **16**(8): p. 541-5.
16. Trobs, R.B., et al., *Congenital esophageal atresia discordant for tracheo-esophageal fistula occurring in a set of dizygotic twins*. Eur J Pediatr Surg, 2006. **16**(4): p. 260-4.
17. Donahoe, P.K., K.M. Noonan, and K. Lage, *Genetic tools and algorithms for gene discovery in major congenital anomalies*. Birth Defects Res A Clin Mol Teratol, 2009. **85**(1): p. 6-12.
18. Lau, S.T., et al., *Fraternal twins with Morgagni hernias*. J Pediatr Surg, 2005. **40**(4): p. 725-7.
19. Machado, A.P., et al., *Concordance for bilateral congenital diaphragmatic hernia in a monozygotic dichorionic twin pair - first clinical report*. Fetal Diagn Ther. **27**(2): p. 106-9.
20. Pober, B.R., et al., *Infants with Bochdalek diaphragmatic hernia: sibling precurrence and monozygotic twin discordance in a hospital-based malformation surveillance program*. Am J Med Genet A, 2005. **138A**(2): p. 81-8.
21. Conlin, L.K., et al., *Mechanisms of mosaicism, chimerism and uniparental disomy identified by single nucleotide polymorphism array analysis*. Hum. Mol. Genet., 2010. **19**(7): p. 1263-75.
22. Veenma, D., et al., *Comparable low-level mosaicism in affected and non affected tissue of a complex CDH patient*. PloS one, 2010. **5**(12): p. e15348.
23. Shaffer, L.G., et al., *Targeted genomic microarray analysis for identification of chromosome abnormalities in 1500 consecutive clinical cases*. The Journal of pediatrics, 2006. **149**(1): p. 98-102.
24. Ballif, B.C., et al., *Detection of low-level mosaicism by array CGH in routine diagnostic specimens*. American journal of medical genetics. Part A, 2006. **140**(24): p. 2757-67.
25. Xiang, B., et al., *Analytical and clinical validity of whole-genome oligonucleotide array comparative genomic hybridization for pediatric patients with mental retardation and developmental delay*. American journal of medical genetics. Part A, 2008. **146A**(15): p. 1942-54.

26. Shaikh, T.H., et al., *High-resolution mapping and analysis of copy number variations in the human genome: a data resource for clinical and research applications*. Genome research, 2009. **19**(9): p. 1682-90.
27. Scott, D.A., et al., *Genome-wide oligonucleotide-based array comparative genome hybridization analysis of non-isolated congenital diaphragmatic hernia*. Human molecular genetics, 2007. **16**(4): p. 424-30.
28. Excoffon, K.J., et al., *The Coxsackievirus and Adenovirus Receptor: a new adhesion protein in cochlear development*. Hear Res, 2006. **215**(1-2): p. 1-9.
29. Raschperger, E., et al., *The coxsackie and adenovirus receptor (CAR) is required for renal epithelial differentiation within the zebrafish pronephros*. Dev Biol, 2008. **313**(1): p. 455-64.
30. Razzaghian, H.R., et al., *Somatic mosaicism for chromosome X and Y aneuploidies in monozygotic twins heterozygous for sickle cell disease mutation*. Am J Med Genet A, 2010. **152A**(10): p. 2595-8.
31. Hasler, R., et al., *Genetic control of global gene expression levels in the intestinal mucosa: a human twin study*. Physiol Genomics, 2009. **38**(1): p. 73-9.
32. Notini, A.J., J.M. Craig, and S.J. White, *Copy number variation and mosaicism*. Cytogenet Genome Res, 2008. **123**(1-4): p. 270-7.
33. Yurov, Y.B., et al., *Aneuploidy and confined chromosomal mosaicism in the developing human brain*. PLoS One, 2007. **2**(6): p. e558.
34. Piotrowski, A., et al., *Somatic mosaicism for copy number variation in differentiated human tissues*. Hum Mutat, 2008. **29**(9): p. 1118-24.
35. De, S., *Somatic mosaicism in healthy human tissues*. Trends Genet April 13. [Epub ahead of print], 2011.
36. Mathew, S.J., et al., *Connective tissue fibroblasts and Tcf4 regulate myogenesis*. Development, 2011. **138**(2): p. 371-84.
37. Nakamura, F., et al., *Molecular basis of filamin A-FILGAP interaction and its impairment in congenital disorders associated with filamin A mutations*. PLoS One, 2009. **4**(3): p. e4928.
38. Su, Z.J., et al., *A vascular cell-restricted RhoGAP, p73RhoGAP, is a key regulator of angiogenesis*. Proc Natl Acad Sci U S A, 2004. **101**(33): p. 12212-7.
39. Girirajan, S., et al., *A recurrent 16p12.1 microdeletion supports a two-hit model for severe developmental delay*. Nature genetics, 2010. **42**(3): p. 203-9.

Chapter 2.5

Comparable Low-Level Mosaicism in Affected and Non-affected Tissue of a Complex CDH Patient

D.Veenma, N.Beurskens, H.Douben, B.Eussen, P.Noomen, L.Govaerts, E.Grijseels, M.Lequin, R.de Krijger, D.Tibboel, A.de Klein, and D.van Opstal

PLOS One (2010 Dec 21; 5(12): e15348)

Supplementary files available on request

Abstract

In this paper we present the detailed clinical and cytogenetic analysis of a prenatally detected complex Congenital Diaphragmatic Hernia (CDH) patient with a mosaic unbalanced translocation (5;12). High-resolution whole genome SNP array confirmed a low-level mosaicism (20%) in uncultured cells, underlining the value of array technology for identification studies. Subsequently, targeted Fluorescence In-Situ Hybridization in postmortem collected tissues demonstrated a similar low-level mosaicism, independently of the affected status of the tissue. Thus, a higher incidence of the genetic aberration in affected organs as lung and diaphragm cannot explain the severe phenotype of this complex CDH patient.

Comparison with other described chromosome 5p and 12p anomalies indicated that half of the features presented in our patient (including the diaphragm defect) could be attributed to both chromosomal areas. In contrast, a few features such as the palpebral downslant, the broad nasal bridge, the micrognathia, microcephaly, abnormal dermatoglyphics and IUGR better fitted the 5p associated syndromes only.

This study underlines the fact that low-level mosaicism can be associated with severe birth defects including CDH. The contribution of mosaicism to human diseases and specifically to congenital anomalies and spontaneous abortions becomes more and more accepted, although its phenotypic consequences are poorly described phenomena leading to counseling issues. Therefore, thorough follow-up of mosaic aberrations such as presented here is indicated in order to provide genetic counselors a more evidence based prediction of fetal prognosis in the future.

Introduction

CDH and somatic (chromosomal) mosaicism

Congenital Diaphragmatic Hernia (CDH) is a severe birth defect characterized by defective formation of the diaphragm, lung hypoplasia and pulmonary hypertension. Its overall prevalence is 1/3000 live births and the majority are left sided. Associated anomalies (i.e. non-isolated cases with or without an abnormal karyotype) are involved in 60% of cases. The mortality rate is still high: 10-20% for isolated and up to 40% for non-isolated cases. CDH is increasingly detected by structural ultrasound in the second trimester of pregnancy showing features like a mediastinal cardiac shift away from the side of the defect and an intra-thoracic stomach bubble [1]. From a clinical point of view, early detection enables counseling by a pediatric surgeon and/ or clinical geneticist. Parents may opt for a termination of pregnancy and in case of continuation; obstetric and postnatal management can be optimized with referral to a specialized tertiary centre with ECMO (Extra Corporal Membrane Oxygenation) facilities.

The presumed multifactorial etiology of CDH is still poorly understood. Yet, the identification of human chromosomal “hot spots” presents strong evidence for a genetic component [2-3]. Because chromosomal aberrations are detected in 10-20% of the cases, regular cytogenetic analysis by GTG-band karyotyping and FISH are highly recommended in each patient [3]. In addition, performance of high-resolution whole genome array could be valuable, especially in case of additional malformations such as in the cardiovascular system, genito-urinal tract and central nervous system [4]. Furthermore, CDH may be part of a defined syndrome, the most well recognized one being Fryns (OMIM 229850 with over 80% of the patients showing CDH, though its locus remains elusive. Finally, CDH caused by tissue-limited mosaicism, specifically of tetrasomy 12p, is rather common within the Pallister-Killian syndrome (PKS)(OMIM 601803 [5]). However, in literature only a few other types of mosaic abnormalities have been described in association with CDH [6-10]. Difficulties in detecting (low-level) mosaicism and the former absence of practical, high-resolution whole genome screening techniques could partly account for these low incidences.

Mosaicism is defined as “the presence of a mixture of cells of different genetic composition in a single organism” [11-12]. Advances in molecular cytogenetic techniques have allowed for a systematic whole genome screening of genetic aberrations among others in mosaic form. Results indicated that such mosaicism probably exists at a higher frequency than expected [12-13]. To date, published studies on this topic both included screens of diseased and (although very few) phenotypically normal individuals and focused on single nucleotide mutations/polymorphisms [14-15] as well as structural chromosomal aberrations/ variations [16-23]. It is accepted that the phenotypic consequences of these somatic mutations depend on the type of cells involved, the nature of the initial mutation and its timing. Somatic mosaicism is also known to produce often a milder phenotype than in its non-mosaic form, allowing for survival of some disorders/aneuploidies that would otherwise result in lethality. Germ-line and somatic mosaicism are thus acknowledged as important factors contributing to phenotypic variability [11]. Nonetheless,

in general the significance of somatic mosaicism usually remains under-appreciated and performance of detailed postmortem follow-up of the aberrations in multiple tissues is done only rarely. Consequently, real understanding whether and how chromosomal mosaicism has the potential to mediate tissue-specific dysfunction in affected (and phenotypic normal) individuals largely remains elusive.

In this case report we present the detailed clinical and molecular cytogenetic analysis of a low-mosaic unbalanced translocation (5;12) identified in a complex-CDH patient. The identification of this specific chromosome aberration with high resolution whole genome SNP array on umbilical cord blood shows the value of array technology for identification studies, also in cases of low mosaicism. Furthermore, we hypothesized in the patients' affected tissues a higher contribution of abnormal cells, which was assessed by FISH analysis in several tissues. Finally, results of phenotype-genotype correlations of each characteristic in this patient are presented.

Material and Methods

Routine Cytogenetic and targeted FISH analysis

Ethics approval was provided by the Medical Ethics Committee of the Erasmus Medical Centre, Rotterdam, The Netherlands. A written informed consent was obtained from all participants in this study.

Sixteen ml of amniotic fluid (AF) was cultured using the in situ method in BD Falcon Culture slides (VWR, Amsterdam, The Netherlands) and subsequently used for both GTG-banded karyotyping and fluorescence in situ hybridization (FISH). Karyotyping of the parents was executed on GTG banded metaphase spreads obtained from peripheral blood cultures. Karyograms were reported according the ISCN rules. Fetal skin and umbilical cord tissue were cultured according to standard techniques and used for FISH analysis in a postnatal diagnostic setting.

FISH experiments were performed according to standard protocols with minor modifications and analyzed with an Axioplan 2 Imaging microscope (Zeiss, Sliedrecht, The Netherlands). Images were captured using Isis software (MetaSystems, Altlußheim, Germany). BAC clones were selected from the UCSC genome browser (UC Santa Cruz, Santa Cruz, CA, <http://genome.ucsc.edu/cgi-bin/hgGateway>, assembly March 2006) and purchased from BACPAC Resources (Oakland, CA). BAC probes (Table S1) were subsequently validated on control metaphases. Targeted whole chromosome paints 5 and 12 and probes of the Cri-du-Chat/Cornelia-de-Lange region were commercially available from Eurodiagnostics (Arnhem, Netherlands) and Cytocell (<http://www.cytocell.com/products/aquarius/micro/cri.asp>) respectively.

MLPA

DNA was isolated from 2x2 ml of uncultured AF using the Chemagenic Magnetic Separation Module I (Chemagen, Baesweiler, Germany). MLPA analyses were performed using the SALSA

P036 and P070 kits of MRC-Holland (Amsterdam, the Netherlands). These kits contain probes for all subtelomeric p-and-q arm regions of all chromosomes. In addition, a specific aneuploidy sensitive kit (P095) and a mental retardation focused kit harbouring 6 probes in the 5p15 telomeric region were executed. MLPA reactions were performed using the manufacturer's protocol with minor modifications [24] and amplification products were separated and quantified as described previously [25]. Dosage ratio values of <0.7 and >1.3 were used as boundaries for deletions and duplications respectively with use of specific calculated cut-off values in case of kit P095.

High resolution SNP array

High-resolution whole genome analysis was performed on umbilical-cord blood derived DNA, using the Illumina Quad610 genotyping bead chip (Illumina, San Diego, CA, USA) according to the manufacturer's protocol. This array contains 598 821 SNP probes distributed genome wide and an additional 21 890 intensity-only probes in regions where SNP coverage is poor. Image intensities were extracted using the Illumina's BeadScan software. Data for each BeadChip were self-normalized in Beadstudio GT (version 3.0+) using information contained within the array (<http://www.illumina.com/applications>). CNVs were detected by comparison to the common Illumina-reference set of 87 CEU samples specific for the Q610 array and visualized in Nexus (version 4.1) software as log₂ ratios (<http://www.biodiscovery.com/index/nexus>). The analysis settings were as follow: SNP rank segmentation with a significance threshold of 1×10^{-6} and log-ratio-thresholds of 0.2 and -0.2 for duplication and deletion respectively. Mosaic changes were assessed by looking for aberrations in probe intensities along with a shift in genotype frequencies of the SNP probes (measured by b-allele frequencies).

FISH on paraffin embedded tissue of multiple samplings and placental cryo-sections

Interphase FISH was performed on 4 μm thick paraffin embedded tissue sections. The tissue sections were placed on poly-L-Lysine coated slides. After deparaffinization using xylene, slides were processed in 1M NaSCN for 10 min at 80°C. Next, pepsin digestion was optimized for each specific tissue type and slides were dehydrated in alcohol. Denaturation of the probes was carried out for 2 min at 95°C. Hybridization was performed at 37°C for 14-16 h. The slides were then washed in posthybridization wash buffers at 55°C and 42°C for 3x5 min and counterstained with DAPI. Signals were counted in at least 100 cells. Results were expressed as the percentage of chromosome 5p signal (RP11-7M4, green) to control probe signal (RP11-90P7, red, Table S1). Internationally accepted cut-off values of $>15\%$ of the nuclei with one signal to identify deletions were adapted from the available tumor tissue literature [26]. The expected percentage in a normal case is 100%; which means that there is no gene deletion. Placental nuclear suspensions were harvested as described before [27] and fixated in methanol/acetic acid. FISH was performed according to local protocols.

Results

Patient report, Cytogenetic analysis and MLPA

A 22-year old Moroccan patient was referred to our tertiary centre for follow up and genetic counseling of a CDH detected in her unborn child by 20-weeks structural ultrasound in her first pregnancy. The medical history was unremarkable. There was no family history of congenital anomalies; however she and her partner were consanguineous in the 2nd line. Ultrasound examination revealed a defect in the left posterolateral diaphragm and herniation of intestine, stomach and liver. Fetal biometry measurements were on the 2nd percentile. Prognosis concerning lung hypoplasia seemed critical with a lung head ratio of <1.0 (0.61 at 21 3/7 weeks) and an intrathoracic liver [28]. Amniocentesis was performed at 20 weeks and 2 days.

Routine cytogenetic analysis confirmed the clinical suspicion of a chromosomal abnormality and revealed a high-mosaic deletion of chromosome 5 in cultured amniocytes which was confirmed by FISH with probes specific for chromosome 5: the karyotype on cultured AF cells was 46,XX,del(5)(p13.3) [27]/46,XX [4] (Table 1 and Table S1). Both parents had a normal karyotype. Based on the paint result an unbalanced translocation was suspected. Therefore MLPA with subtelomeric kits P036 and P070 was performed on DNA isolated from uncultured amniotic fluid cells. Surprisingly, results did not reveal such an anomaly showing normal relative probe signals for all probes including the one on 5p. MLPA using kit P096 which includes 6 probes within the Cri-Du-Chat (CDC) critical region, showed a normal result as well, most probably indicating a much lower level of mosaicism in uncultured AF cells compared to cultured cells.

Table 1 | Detection of mosaicism using molecular cytogenetic studies

| Detection | | | |
|-----------|----------------------|-----------|------------------|
| Period | Method | Tissue | Mosaic level (%) |
| Prenatal | GTG-band/FISH | AF-c | 87 |
| | MLPA | AF | normal |
| Postnatal | FISH | FUM | 43 (38*) |
| | | DER | 35 (23*) |
| | SNP array | UC-bl | 20 |
| | FISH ParafinEmbedded | Heart | 24 |
| | | Liver | 32 |
| | | Diaphragm | 26 |
| | | Lung | 29 |
| | | Kidney | 28 |
| | FISH Frozen | Placental | 13 |
| DER | | 36 | |

AF: Amniotic Fluid, AF-c: Amniotic Fluid-cultured
 DER: skin, FUM: Fibroblast culture Umbilical cord
 UC-bl: Umbilical Cord Blood; *metaphase

Based on the ultrasound and cytogenetic findings, the parents decided to terminate the pregnancy at 23.1 weeks of gestation. A female fetus was delivered vaginally and postmortem physical examination showed a normally proportioned but intra-uterine growth (length) restricted fetus; weight (490 gr: normal: 524 +/- 116 gr), crown-rump length (17.5 cm; normal 20.8 +/- 1.9 cm) and foot-length 3.5 cm (normal: 4.2 +/- 0.5 cm). Dysmorphological features were significant for the following: convex eye globes, abnormal palpebral (down) slant, hypertelorism, wide nasal bridge, flat philtrum, thin upperlip, micro-and-retrognathia and nuchal wideness. Abnormal external ear development on both sides and aberrant posterior rotation of the ears were noted as well. Concerning the extremities, a palmar crease on the right was seen and also an abnormal positioning of the anus with short perineum and sacral dimple. Inspection of the internal organs presented a large left diaphragmatic defect of the Bochdalek type with herniation of stomach, duodenum and parts of colon, liver and spleen. Further, this fetus showed severe lung hypoplasia (right 2.1gr, left 1.2 gr; lung-body ratio $\ll 0.015$) and left kidney-agenesis with compensatory right kidney hyperplasia. Finally, autopsy demonstrated normal morphology of all remaining organs and no structural aberrations of the brain on postmortem MRI.

The prenatally identified mosaicism 46,XX,del(5)(p13.3) in cultured amniotic fluid cells was confirmed by postmortem cytogenetic analysis in umbilical cord and skin tissue, yet in a much lower frequency than expected (Table 1). Because the suspicion of an unbalanced translocation persisted, yet not confirmed by MLPA on uncultured cells, a whole genome SNP array was applied.

High-Resolution SNP-array

High-resolution whole genome SNP array on DNA from umbilical cord blood confirmed the 5p deletion and indeed identified a coexisting chromosome 12p13.2 duplication by using information of both log₂ intensities and B-allele frequency as described recently (Figure 1) [29]. These array results were subsequently confirmed by FISH using chromosome 12 paint in addition to a 12p13.32 probe on cultured AF (Figure 2). So, ultimately the patients karyotype could be summarized as 46,XX,der(5)t(5;12)(p13.2;p12.3).arr 12p12.3(rs7136701- rs10845353)x3,5p13.2(rs1108867-rs16903304)x1 (NCBI Build 36/hg18 [30]). Considering the mosaic rate, B-allele ratios of the array suggested a different level of mosaicism in the umbilical cord blood as present in the cultured AF cells. The estimated percentage of mosaicism based on these array results was 20%.

FISH on different paraffin embedded tissues and cryosections of placenta

Considering the big difference between mosaic rates of cultured amniocytes and umbilical cord blood as well as uncultured AF-cells, we hypothesized that the genetic aberration rate could be high in affected tissues (such as lungs, kidneys and diaphragm) and lower in normal ones (heart, liver). Therefore we screened 7 different paraffin embedded tissues sections with FISH using specific BAC clones. Results are summarized in Table 1; showing no significant differences however in the levels of mosaicism between normal and affected tissue. The derivative chromosome 5

was detected in 24-36% of the cells overall, confirming the array-based estimated percentage of mosaicism. Finally, to assess a co-existing placental mosaicism we also screened frozen sections of placental tissue after nuclear isolation revealing mosaicism in 10% of the nuclei.

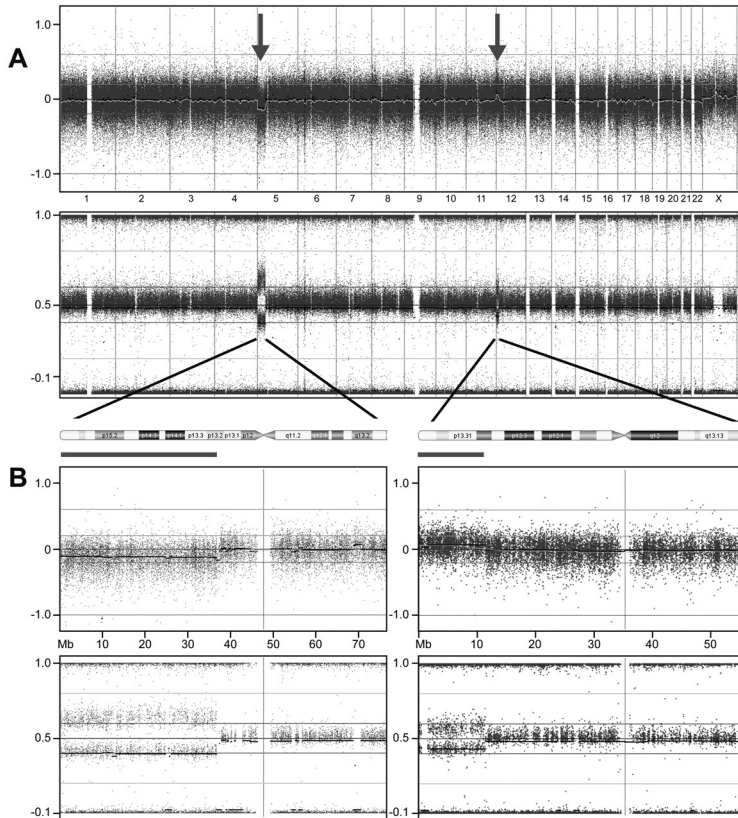


Figure 1 | Results High-resolution SNP array using uncultured umbilical cord blood material

A: Whole genome array: Log₂ intensity (Top) and B-Allele Frequencies BAF (Bottom). Top: Y-axis: Relative Copy Number State. X-axis: autosomes number 1-22 and the two sex chromosomes.

Displayed are the relative and normalized log₂ intensities of all available SNPs on the array across the patients' genome. At the beginning of chromosome 5 a slight drop of log₂ intensity is visible representing the deletion of part of the short arm of chromosome 5 in a low-mosaic state. Similarly, the mosaic 12p duplication is depicted as a small peak of log₂ intensity at the beginning of chromosome 12. Bottom: confirmation of aberrations by the more clearly visible changes in BAF. **B:** Enlarged views of the results of chromosome 5 (left) and 12 (right) showing both the log₂ intensity window as well as the BAF results (see page 251 for color figure).

Genotype-Phenotype comparison

Structural aberrations of chromosome region 5p (clinically recognized as the Cri-du-Chat syndrome or as the Cornelia de Lange syndrome) and 12p (featuring as PK syndrome or a pure

mosaic trisomy 12p) are both associated with CDH. Yet, for chromosome 5p diaphragmatic hernia has only been associated with Brachmann-de-Lange patients and not with those featuring Cri-du-Chat. Subsequently, the diaphragmatic candidate region on 5p most likely overlaps with the critical region of CdLS, taking into account that CdLS patients are genetically heterogenous as well. Hulinsky et al. [31] identified a child with both CDH and CdLS which had a pure interstitial deletion of 5p [del(5)(p13.1;p14.2)]. Results of the comparison with this patient, and for all other characteristics in our patient compared to those described in literature (for both regions) [32-37] are summarized in Table S2. Based on these comparisons half of the features present in our patient could be attributed to both chromosomal areas. Exceptions to this were: the palpebral downslant, the broad-nasal bridge, the retro- and micro-gnathia, microcephaly, abnormal dermatoglyphics and IUGR, which better fit the 5p associated syndromes.

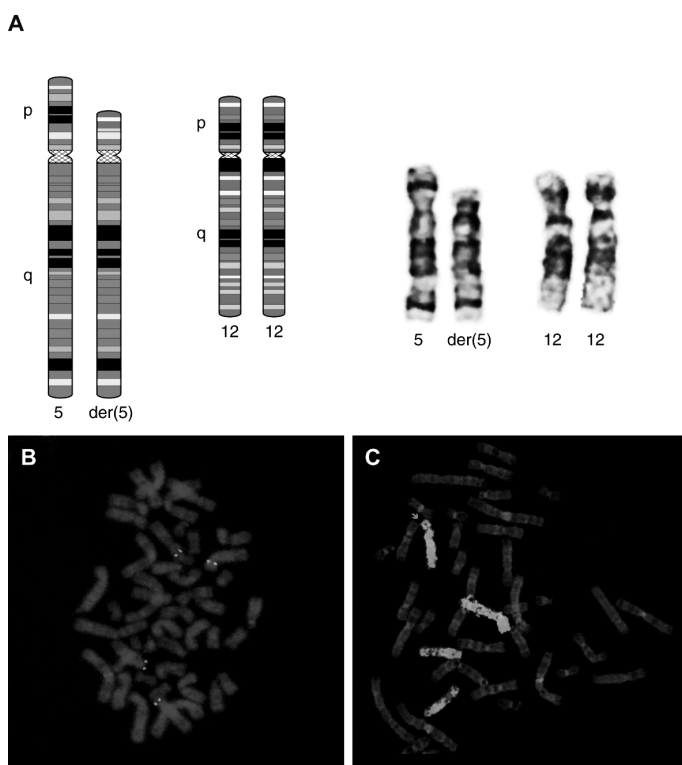


Figure 2 | Fluorescent In-Situ Hybridization results using cultured amniotic fluid and skin material

A: Left: Schematic representation of the unbalanced der(5)t(5;12)(p13.2;p12.3) and its normal chromosome 12 counterpart. Right: Partial Karyotype of the patient showing both the normal and abnormal chromosome 5 and both normal chromosomes 12. **B:** Fluorescent In-Situ Hybridization (FISH) on a metaphase spread of 1 umbilical cord-fibroblast-cell presenting 1 copy of BAC clone RP11-7M4 (Green) on the normal chromosome 5 and 3 of clone RP11-62P15 (red) on both chromosomes 12 and the der(5). **C:** Whole-Chromosome Paint FISH results of 1 AF-cell showing duplication of part of the short arm of chromosome 12 (WCP12: red) at the expense of part of 1 copy of chromosome 5 (WCP5:green) (see page 251 for color figure).

Discussion

In this case report we present the detailed clinical and cytogenetical analysis of a unique low-mosaic der (5) t(5;12) aberration identified in a CDH patient with multiple congenital anomalies. Classification of the true chromosome abnormality was possible only after performance of a high-resolution whole genome SNP array on uncultured umbilical cord blood. Application of this technology in the identification of mosaic aberrations was reviewed very recently [29]. Although mosaic abnormalities are increasingly considered to be important factors in (spontaneous) abortions [38], congenital anomalies [22, 39-42] and in phenotypic variability, analysis of multiple tissues in prenatal cases is done only rarely. In addition, data on chromosomal mosaicism frequencies in phenotypically normal individuals, with the exception of studies in reproductive tissues [13], is sparse as well [11, 21]. While the clinical significance of the aberrant cell line was quite obvious in our patient due to the presence of major associated birth defects, this is not always the case. Therefore, the recent availability of more sensitive and easier applicable techniques will lead to increased detection of low-mosaic aberrations at a prenatal stage and subsequently lead to more genetic counseling problems. Extensive follow-up of mosaic aberrations in affected cohorts as well as research of the incidence in the normal population is indicated in order to provide genetic counselors a more evidence based prediction of fetal prognosis in the future.

Phenotypic variability at the tissue level correlated to mosaic frequency?

Because the mosaic aberration was present in both placenta- and embryonic material we suggest that the translocation (and subsequent loss of the “other” balanced translocation product) occurred as a very early mitotic event in an initially normal diploid zygote. More specifically, this may have occurred at least before differentiation of trophoblast and inner cell mass in the 16-cell stage. To explain the phenotypic variability at the tissue level, we speculated that the malformations of lungs, diaphragm and kidneys would associate with a much higher level of mosaicism than the normally developed tissues of heart and liver. This would thus mirror a situation in which the post zygotic mutation arose in an important lung-and diaphragm specific precursor cell population and time window. However, such a linear correlation between level of mosaicism and tissue pathophysiology could not be confirmed in our case. Associations between the severity of the (whole) clinical phenotype and the percentage of abnormal cells are generally known for the most common autosomal aneuploidy (trisomy 21), yet the mechanism by which this aneuploidy results in the complex heterogeneous phenotype cannot be attributed to mosaicism alone and is therefore still under discussion [43-44]. Differences in default gene-expression profile requirements between tissues, and subsequently variable susceptibility for loss or gain of different chromosome areas could account for the tissue specific pathology in multi-system diseases in general and in mosaic states as well.

Finally, uncultured tissues are in general better able to reveal true chromosomal mosaicism frequencies as compared to cultured tissues, since culturing may introduce a selection bias that

distorts the percentages of abnormal cells. However we were not able to detect the low-mosaicic der(5) in uncultured AF-cells using MLPA, yet did detect a high-mosaicic der(5) in cultured AF cells. From this it can be concluded that the level of mosaicism in uncultured cells was probably too low to be detected with MLPA. These kind of discrepancies have been described in some areas of tissue-specific mosaicism, like mosaic trisomy 20 [45]. However, in the present case there were no clues at all for tissue limited mosaicism as explained above.

Mosaic unbalanced translocation (5;12) and CDH

Chromosomal abnormalities are detected in 9.5%-34% of prenatally diagnosed CDH cases [46]. The most common identified aneuploidy is trisomy 18 and smaller structural rearrangements (microdeletions/duplications) of the distal arms of chromosome 1q, 8p and 15q are relatively common in complex-CDH subjects as well. However, structural abnormalities of almost all chromosomes in association with diaphragm defects have been described in literature, including those of the short arms of chromosomes 5 and 12 [London medical Databases version 1.0.19]. Unfortunately, the candidate genes responsible for malformation of the diaphragm remain to be determined for both these regions, yet literature suggests that the candidate region for diaphragm defects on 5p most likely overlaps with the CdLS critical region only. In 2004 Krantz et al. [33] described a child with classical symptoms of CdLS and a balanced, de novo t(5;13)(p13.1;q12.1) thereby disrupting the NIPBL gene. However, this child did not show a diaphragm defect. In contrast, Hulinsky et al. [31] did identify a child with the CdLS phenotype, CDH and a pure interstitial deletion of 5p (del(5)(p13.1;p14.2)). Whether NIPBL is indeed the causative gene for CdLS associated diaphragm defects needs to be determined. In our own CDH cohort we have 1 patient with both the CdLS-phenotype and a mutation in exon 9 of the NIPBL gene. However, since CDH is only rarely associated with CdLS (5%) and routine NIPBL mutation screening is only recently been put into standard practice, more specific cases featuring both need to be determined. It is also possible, that a combination of CDH and CdLS is often lethal and therefore rarely notified. Low-mosaicism in our case may have caused changes in the (severity) of the CdLS phenotype as repeatedly suggested in literature.

We also compared our patients remaining characteristics to the features described in literature for both genomic areas. Based on this comparison half of the features presented in our patient could be attributed to both chromosomal areas, while some were more associated with the 5p region. Hulinsky et al. [31] suggested that some of the atypical CdLS characteristics in their patient (hypoplastic kidneys, adrenal gland abnormalities and multiple cysts) are caused by haploinsufficiency of other 5p13.1- p14.2 genes. However, retrospective analysis of our patients' MRI did not show evidence for cysts and adrenal gland defects. Moreover, renal abnormalities (primarily vesicouretral reflux and cysts) are described for CdLS after all. Since our case is not a pure monosomy and very early prenatal dysmorphology hampers identification of some clinical features, direct comparison between this literature case and our patient remains troublesome.

Focusing on CDH and genetic mosaicism: the earlier mentioned Pallister-Killian syndrome is the most common CDH-associated syndrome caused by tissue-limited mosaicism. In a small study

more than ten years ago, Donnenfeld et al. [47] tried to evaluate the overall percentage of tissue-specific mosaicism among fetuses with prenatally diagnosed diaphragmatic hernia and found in one out of 13 fetuses a mosaic isochromosome 12p. However, the diagnostic techniques used in this study were limited and the number of investigated patients low. Only a few other case-reports on CDH and genetic mosaicism have been published since, featuring the chromosomes Y and 16. None have described a mosaic der 5 t(5;12).

Mosaicism and detection with high-resolution SNP array

In general it is very difficult to estimate the true incidence and significance of genetic mosaicism in human congenital anomalies. The application of high-resolution SNP arrays allows for an easier and more sensitive detection of this type of genetic aberrations for several reasons. First, SNP arrays are shown to be able to detect levels of mosaicism as low as 5% using the B-allele frequency as a more sensitive measurement compared to the more difficult detection of subtle down- or up crease of log R ratios (which only can be used in Oligo based arrays). Second, the possible use of low amounts of DNA from any kind of (uncultured) tissue diminishes the technical failures due to the in-vitro cell culturing process [29]. So, the wide application of these methodologies in diagnostic and research settings will increase our knowledge and ability to diagnose patients with chromosomal mosaicism and allow for better genotype-phenotype correlations.

Acknowledgements

The authors would like to thank the patient and all family members who cooperated in this study and T. de Vries-Lentsch for assistance with manuscript preparation.

References

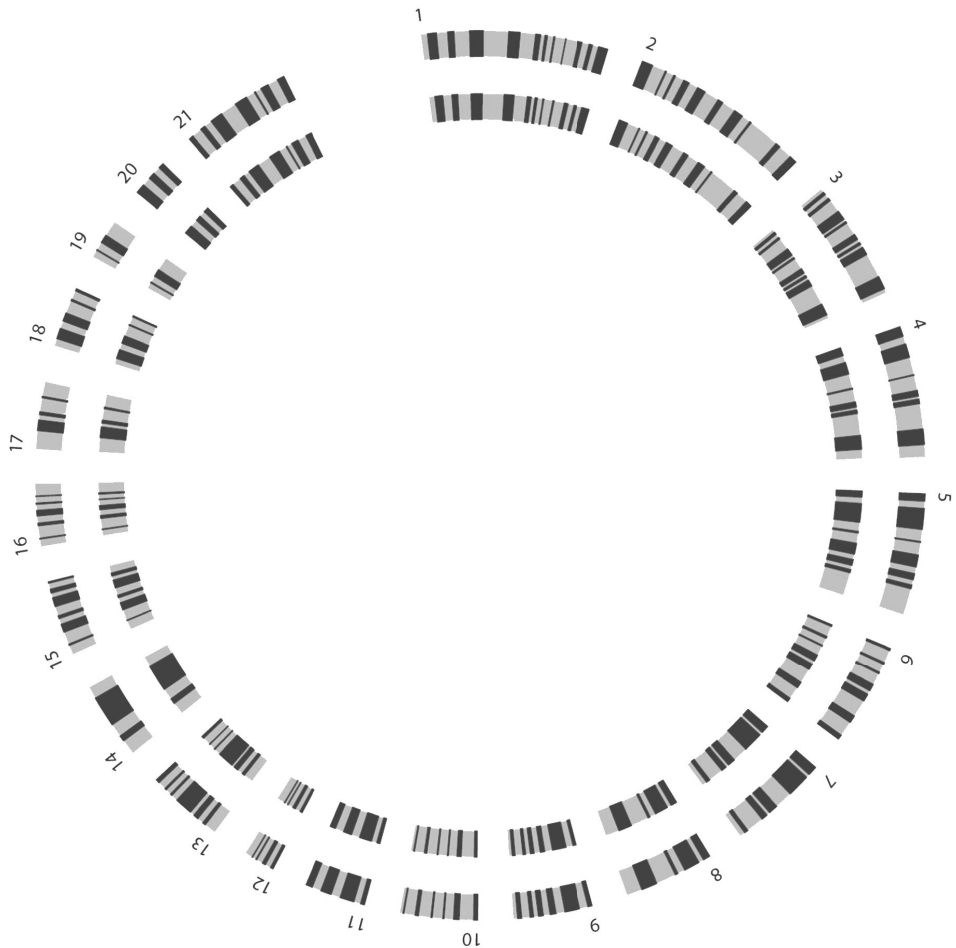
1. Garne E, Loane M, Dolk H, De Vigan C, Scarano G, et al. (2005) *Prenatal diagnosis of severe structural congenital malformations in Europe*. *Ultrasound Obstet Gynecol* **25**: 6-11.
2. Holder AM, Klaassens M, Tibboel D, de Klein A, Lee B, et al. (2007) *Genetic factors in congenital diaphragmatic hernia*. *Am J Hum Genet* **80**: 825-845.
3. Klaassens M, de Klein A, Tibboel D (2009) *The etiology of congenital diaphragmatic hernia: still largely unknown?* *Eur J Med Genet* **52**: 281-286.
4. Scott DA, Klaassens M, Holder AM, Lally KP, Fernandes CJ, et al. (2007) *Genome-wide oligonucleotide-based array comparative genome hybridization analysis of non-isolated congenital diaphragmatic hernia*. *Hum Mol Genet* **16**: 424-430.
5. Bergoffen J, Punnett H, Campbell TJ, Ross AJ, 3rd, Ruchelli E, et al. (1993) *Diaphragmatic hernia in tetrasomy 12p mosaicism*. *J Pediatr* **122**: 603-606.
6. Ahn HY, Shin JC, Kim YH, Ko HS, Park IY, et al. (2005) *Prenatal diagnosis of congenital diaphragmatic hernia in a fetus with 46,XY/46,X,-Y,+der(Y)t(Y;1)(q12;q12) mosaicism: a case report*. *J Korean Med Sci* **20**: 895-898.
7. Chen CP, Shih JC, Chern SR, Lee CC, Wang W (2004) *Prenatal diagnosis of mosaic trisomy 16 associated with congenital diaphragmatic hernia and elevated maternal serum alpha-fetoprotein and human chorionic gonadotrophin*. *Prenat Diagn* **24**: 63-66.
8. Nowaczyk MJ, Ramsay JA, Mohide P, Tomkins DJ (1998) *Multiple congenital anomalies in a fetus with 45,X/46,X,r(X)(p11.22q12) mosaicism*. *Am J Med Genet* **77**: 306-309.
9. Li C (2010) *A prenatally recognizable malformation syndrome associated with a recurrent post-zygotic chromosome rearrangement der(Y)t(Y;1)(q12;q21)*. *Am J Med Genet A* **152A**: 2339-2341.
10. Takahashi H, Hayashi S, Miura Y, Tsukamoto K, Kosaki R, et al. (2010) *Trisomy 9 mosaicism diagnosed in utero*. *Obstet Gynecol Int* 2010.
11. Yousoufian H, Pyeritz RE (2002) *Mechanisms and consequences of somatic mosaicism in humans*. *Nat Rev Genet* **3**: 748-758.
12. Erickson R (2010) *Somatic gene mutation and human disease other than cancer: An update*. *Mutation Research in press*.
13. Iourov IY, Vorsanova SG, Yurov YB (2008) *Chromosomal mosaicism goes global*. *Mol Cytogenet* **1**: 26.
14. Ng SB, Turner EH, Robertson PD, Flygare SD, Bigham AW, et al. (2009) *Targeted capture and massively parallel sequencing of 12 human exomes*. *Nature* **461**: 272-276.
15. Wheeler DA, Srinivasan M, Egholm M, Shen Y, Chen L, et al. (2008) *The complete genome of an individual by massively parallel DNA sequencing*. *Nature* **452**: 872-876.
16. Ballif BC, Rorem EA, Sundin K, Lincicum M, Gaskin S, et al. (2006) *Detection of low-level mosaicism by array CGH in routine diagnostic specimens*. *Am J Med Genet A* **140**: 2757-2767.
17. Bruder CE, Piotrowski A, Gijsbers AA, Andersson R, Erickson S, et al. (2008) *Phenotypically concordant and discordant monozygotic twins display different DNA copy-number-variation profiles*. *Am J Hum Genet* **82**: 763-771.
18. Cheung SW, Shaw CA, Scott DA, Patel A, Sahoo T, et al. (2007) *Microarray-based CGH detects chromosomal mosaicism not revealed by conventional cytogenetics*. *Am J Med Genet A* **143A**: 1679-1686.
19. Lestou VS, Desilets V, Lomax BL, Barrett IJ, Wilson RD, et al. (2000) *Comparative genomic hybridization: a new approach to screening for intrauterine complete or mosaic aneuploidy*. *Am J Med Genet* **92**: 281-284.
20. Notini AJ, Craig JM, White SJ (2008) *Copy number variation and mosaicism*. *Cytogenet Genome Res* **123**: 270-277.
21. Piotrowski A, Bruder CE, Andersson R, de Stahl TD, Menzel U, et al. (2008) *Somatic mosaicism for copy number variation in differentiated human tissues*. *Hum Mutat* **29**: 1118-1124.
22. Bergman Y (1999) *Allelic exclusion in B and T lymphopoiesis*. *Semin Immunol* **11**: 319-328.

23. Yurov YB, Iourov IY, Vorsanova SG, Liehr T, Kolotii AD, et al. (2007) *Aneuploidy and confined chromosomal mosaicism in the developing human brain*. PLoS One **2**: e558.
24. Schouten JP, McElgunn CJ, Waaijer R, Zwijnenburg D, Diepvens F, et al. (2002) *Relative quantification of 40 nucleic acid sequences by multiplex ligation-dependent probe amplification*. Nucleic Acids Res **30**: e57.
25. Van Opstal D, Boter M, de Jong D, van den Berg C, Bruggenwirth HT, et al. (2009) *Rapid aneuploidy detection with multiplex ligation-dependent probe amplification: a prospective study of 4000 amniotic fluid samples*. Eur J Hum Genet **17**: 112-121.
26. van Dekken H, Pizzolo JG, Reuter VE, Melamed MR (1990) *Cytogenetic analysis of human solid tumors by in situ hybridization with a set of 12 chromosome-specific DNA probes*. Cytogenet Cell Genet **54**: 103-107.
27. Vindelov LL, Christensen IJ, Nissen NI (1983) *A detergent-trypsin method for the preparation of nuclei for flow cytometric DNA analysis*. Cytometry **3**: 323-327.
28. Jani J, Peralta CF, Benachi A, Deprest J, Nicolaides KH (2007) *Assessment of lung area in fetuses with congenital diaphragmatic hernia*. Ultrasound Obstet Gynecol **30**: 72-76.
29. Conlin LK, Thiel BD, Bonnemann CG, Medne L, Ernst LM, et al. (2010) *Mechanisms of mosaicism, chimerism and uniparental disomy identified by single nucleotide polymorphism array analysis*. Hum Mol Genet **19**: 1263-1275.
30. Shaffer L.G. SML, Campbell, L.J., editor (2009) *ISCN 2009: An International System for Human Cytogenetic Nomenclature (2009): Recommendations of the International Standing Committee on Human Cytogenetic Nomenclature S.Karger AG (Switzerland)*. 138 p.
31. Hulinsky R, Byrne JL, Lowichik A, Viskochil DH (2005) *Fetus with interstitial del(5)(p13.1p14.2) diagnosed postnatally with Cornelia de Lange syndrome*. Am J Med Genet A **137A**: 336-338.
32. Deardorff MA CD, Krantz ID (2005) *Gene reviews Cornelia de Lange Syndrome*. In: Pagon RA BT, Dolan CR, Stephens K, editor. Seattle.
33. Krantz ID, McCallum J, DeScipio C, Kaur M, Gillis LA, et al. (2004) *Cornelia de Lange syndrome is caused by mutations in NIPBL, the human homolog of Drosophila melanogaster Nipped-B*. Nat Genet **36**: 631-635.
34. Segel R, Peter I, Demmer LA, Cowan JM, Hoffman JD, et al. (2006) *The natural history of trisomy 12p*. Am J Med Genet A **140**: 695-703.
35. Zumkeller W, Volleth M, Muschke P, Tonnies H, Heller A, et al. (2004) *Genotype/phenotype analysis in a patient with pure and complete trisomy 12p*. Am J Med Genet A **129A**: 261-264.
36. Kondoh T, Shimokawa O, Harada N, Doi T, Yun C, et al. (2005) *Genotype-phenotype correlation of 5p-syndrome: pitfall of diagnosis*. J Hum Genet **50**: 26-29.
37. Mainardi PC, Perfumo C, Cali A, Coucourde G, Pastore G, et al. (2001) *Clinical and molecular characterisation of 80 patients with 5p deletion: genotype-phenotype correlation*. J Med Genet **38**: 151-158.
38. Vorsanova SG, Kolotii AD, Iurov I, Kirillova EA, Monakhov VV, et al. (2005) *[Diagnosis of numerical chromosomal aberrations in the cells of spontaneous abortions by multicolor fluorescence in situ hybridization (MFISH)]*. Klin Lab Diagn: 30-32.
39. Iwarsson E, Lundqvist M, Inzunza J, Ahrlund-Richter L, Sjoblom P, et al. (1999) *A high degree of aneuploidy in frozen-thawed human preimplantation embryos*. Hum Genet **104**: 376-382.
40. Valduga M, Philippe C, Bach Segura P, Thiebaugeorges O, Miton A, et al. (2010) *A retrospective study by oligonucleotide array-CGH analysis in 50 fetuses with multiple malformations*. Prenat Diagn **30**: 333-341.
41. Wells D, Delhanty JD (2000) *Comprehensive chromosomal analysis of human preimplantation embryos using whole genome amplification and single cell comparative genomic hybridization*. Mol Hum Reprod **6**: 1055-1062.
42. Zhang YX, Zhang YP, Gu Y, Guan FJ, Li SL, et al. (2009) *Genetic analysis of first-trimester miscarriages with a combination of cytogenetic karyotyping, microsatellite genotyping and arrayCGH*. Clin Genet **75**: 133-140.

43. Laffaire J, Rivals I, Dauphinot L, Pasteau F, Wehrle R, et al. (2009) *Gene expression signature of cerebellar hypoplasia in a mouse model of Down syndrome during postnatal development*. BMC Genomics **10**: 138.
44. Reymond A, Marigo V, Yaylaoglu MB, Leoni A, Ucla C, et al. (2002) *Human chromosome 21 gene expression atlas in the mouse*. Nature **420**: 582-586.
45. Van Opstal D, van den Berg C, Galjaard RJ, Los FJ (2001) *Follow-up investigations in uncultured amniotic fluid cells after uncertain cytogenetic results*. Prenat Diagn **21**: 75-80.
46. Kunz J, Schoner K, Stein W, Rehder H, Fritz B (2009) *Tetrasomy 12p (Pallister-Killian syndrome): difficulties in prenatal diagnosis*. Arch Gynecol Obstet **280**: 1049-1053.
47. Donnenfeld AE, Campbell TJ, Byers J, Librizzi RJ, Weiner S (1993) *Tissue-specific mosaicism among fetuses with prenatally diagnosed diaphragmatic hernia*. Am J Obstet Gynecol **169**: 1017-1021.

Chapter 3

Disrupted RA Signalling in CDH: Gene-Expression & Patho-Epigenetic Mechanisms in 15q26 Monosomy Patients and a Nitrofen Rodent Model



Chapter 3.1

Spatial Positioning of CDH Candidate Genes in a 15q26 Deleted Fibroblast Patient Model

D.Veenma, L.Joosen, W.van Cappellen, M.van de Corput, B.Eussen, D.Tibboel and A.de Klein

Manuscript in preparation

Summary

The pathogenetic mechanisms causing diaphragm- and lung- defects in patients with congenital diaphragmatic hernia (CDH) are largely unknown. In this study, we investigated the three-dimensional clustering of candidate “diaphragm” genes (*NR2F2*, *ZFPM2* and *GATA4*) as a prerequisite for proper co-expression and normal development. Failure of this epigenetic process might contribute to CDH in a certain subclass of complex patients displaying chromosomal rearrangements. Structural aberrations may have an impact on the radial distribution of the chromosome segments on which these genes reside. We used 15q26-deleted human fibroblast nuclei as a CDH study model. Since juxta-positioning of genes could be dependent on a certain stimulus, gene clustering was also analyzed after a 48 hours induction period with retinoic acid.

Nuclear positions were assessed using quantitatively 2D and 3D in-situ hybridization techniques and compared to the relative positions in sex-matched control nuclei. Results showed that the coordinated expression of these three CDH candidate genes was independent of nuclear co-association. Moreover, the *NR2F2* alleles were almost exclusively located within their chromosome territory, without evidence for relocation upon disease or upon RA induction. However, a significantly different nuclear positioning was demonstrated for the partial chromosome segment 15q on which the remaining functional *NR2F2* allele in patients is located. Whether this change has a functional impact on gene expression levels in this chromosomal region remains to be determined.

In conclusion, coordinated expression of the CDH candidate genes *NR2F2*, *ZFPM2* and *GATA4* is independent of nuclear co-association in complex 15q26 monosomy patients. Subtle gene expression effects might be elicited by the changes in 15q sub-chromosomal nuclear topology.

Introduction

Children born with Congenital Diaphragmatic Hernia (CDH, OMIM 142340) suffer from severe respiratory distress caused by a classical “set” of features: a defect in the muscular or tendinous portion of the diaphragm, pulmonary hypoplasia, and pulmonary hypertension. CDH has a worldwide occurrence frequency of one in 3000 live born infants and mortality rates vary between 20-60% [1]. Moreover, this birth defect is associated with significant short- and long-term morbidity among survivors [2]. CDH patients can either present with an isolated defect or with CDH as part of a complex phenotype, meaning that in the latter group the defect is accompanied by other congenital anomalies as well [3]. Ultrasound detection in the first pregnancy trimester now enables prenatal genetic counseling and optimized care in specialized hospitals, however the presumed multifactorial causes of CDH are still largely unknown. Some valuable insights into its genetic susceptibility were recently provided by the application of molecular cytogenetic techniques to patients’ DNA. Using these techniques, over 20 recurrently deleted or duplicated regions – including on chromosome band 15q26, 8p23.1 and 8q22-q23 – were identified in complex cases [4]. These structurally aberrant regions are thought to harbor genes important for both diaphragm development and Retinoic Acid (RA) signalling and include: the nuclear receptor subfamily 2, group F2 gene (*NR2F2*, OMIM 107773), the transcription factor encoding gene GATA binding protein 4 (*GATA4*, OMIM 600576) and the zinc finger protein, multitype 2 gene (*ZFPM2*, OMIM 603693). Involvement of these three specific genes in diaphragm development is further implicated by their corresponding (conditional) knockout mice models, which display CDH in a proportion of the offspring [5-7]. Moreover, all three genes were recently shown to be expressed at specific developmental stages of rodent diaphragm development [8] and detrimental changes were identified for *ZFPM2* in isolated human CDH individuals [6, 9]. An effort to identify similar mutations for either *NR2F2* or *GATA4* have failed so far and imply that haploinsufficiency of these genes alone is insufficient to cause CDH in humans. Therefore, other genetic (i.e. the additive effect of two or more genes in the deleted region) or epigenetic mechanisms might be at play for the 15q26 and 8p23.1 monosomy phenotype. In this study we searched for such alternative epigenetic factors using a 15q26 deleted-Retinoic Acid (RA) modulated cell culture model. The 15q26 deletion is the most common and strongly CDH associated chromosomal hot spot described to date [10]. Disruption of RA signalling is suggested in the pathogenesis of CDH based on numerous studies in both humans [11-13] and animals (Vitamin-A deficient and teratogen-induced models) [14-17].

A central theme in the regulation of gene expression is the binding of transcription factors to specific sites along the DNA. Since these sites can be several hundreds of kilobases away from a target gene promoter [18], the chromatin strand forms loops to bring these sites together in a so-called “transcriptional hub”. Preferential long-range interactions between gene-loci have been identified as well, mainly in-cis and on the same chromosome [19, 20] but also in-trans and between different chromosomes [21-24]. These specific combinations of gene associations might be explained for by the necessity for genes to share common transcriptional resources

[25, 26]. Besides allocation of resources, accumulation of genes at a certain factory may provide the cell a mechanism by which it could coordinate the expression of genes of a common pathway [26]. This coordinated gene expression is especially important during embryonic development in which groups of genes have to be expressed in a strictly spatial- and temporal-controlled manner. Following this, we hypothesized the three-dimensional clustering of crucial “diaphragm” genes as a prerequisite for proper co-expression and normal diaphragm development and a perturbation of this process in patients with a diaphragm defect and one functional *NR2F2* allele (i.e. having a 15q26 monosomy). In other words, we investigated the possibility of disturbance of inter-chromosomal interactions of three important CDH candidate genes (*NR2F2*, *GATA4* and *ZFPM2*) in human CDH fibroblast cell lines harboring a 15q26 deletion. Since juxta-positioning of these genes could be dependent on a certain stimulus, we studied three-dimensional clustering with and without RA induction. As a second objective, we considered an abnormal nuclear positioning of *NR2F2* relative to its chromosome territory (CT) in patient cell lines. It has been suggested that certain loci escape the repressive environment of their CT in order to be expressed fully during a certain developmental/differentiation stage or as part of the cellular response to a certain environmental stimulus [27-31]. Thirdly, the effect of loss of the distal arm of chromosome 15 on nuclear sub-chromosomal topology was analyzed in light of a possible association to more large-scale gene-expression level changes [32].

Material and methods

Cell cultures

A skin fibroblast biopsy (DFP1) was harvested from a complex CDH patient with a known 15q26.2q26.3 deletion as the result of an unbalanced translocation event with chromosome 3 as previously described [33]. A control human sex-matched fibroblast culture (DFC1) was kindly provided by the department of Biochemistry (Erasmus MC, the Netherlands). Detailed analysis of other pathogenic structural anomalies was ruled out by SNP array analysis (HumanCytoSNP-12 v2.1, Illumina, Inc. San Diego, USA) showing in detail the boundaries of the deletion at high-resolution. The control cell line showed no pathogenic copy number variations. Both cell lines were maintained in HAMF10 medium with 12.5% Fetal Bovine serum (Biowhittaker, CA, USA) and 1% Penicillin/ Streptomycin. Culturing for 3D FISH analysis was performed on 18 mm thick cover slips (Harvard Apparatus, Massachusetts, USA) in separate 6-well cell culturing plates (BD Biosciences-TM; 6-well Multiwell TM, plate) at 37°C in a humidified atmosphere containing 5% CO₂ until 90% confluence. Medium was changed every 2-3 days and the day before harvesting. To study the effects of RA on CDH candidate gene dynamics, cells were grown for 48 hours in medium supplemented with either 0 or 10 μmol/l of All-Trans Retinoic Acid (ATRA) (Sciencelab. com, inc, Houston, Texas, USA) diluted in DMSO.

Fluorescent In-situ Hybridization (FISH)

DNA from BAC clones that included the *NR2F2* (RP11-784A9 or RP11-46C2), *ZFPM2* (RP11-1029P14) and *GATA4* (RP11-802F15) genes were selected from the UCSC genome browser (UC Santa Cruz, Santa Cruz, CA, <http://genomw.ucsc.edu/>, assembly March 2006) and purchased from BACPAC Resources (Oakland, CA, USA). Direct labelling was executed as described before [34] (Random Prime labelling system Invitrogen, Invitrogen Corporation, Carlsbad, CA, USA) with Alexa Fluor Dye 488 and 594. Fluorochrome Cy5 was incorporated following the Agilent array CGH labelling kit (Agilent technologies, Santa Clara, United States). Probe signal intensity and position were validated on control metaphases. Whole chromosome paints of chromosome 8 and 15 (directly labelled with FITC or Texas red) and partial paints of sub-chromosomal territories 8p, 8q and 15q (fluorochromes Cy5 or Cy3) were obtained from Metasystems GmbH (Altlussheim, Germany). Combinations of 4-6 ul of each labelled DNA product were used per FISH experiment, with 2 ul of Cot-1 DNA adding to a maximum volume of 18 ul with hybridisation mix.

2D FISH on interphase cells was performed according to local standard protocols [35].

Specific numbers of analyzed 2D nuclei were respectively; unstimulated control (n=108), unstimulated CDH (n=116), RA-stimulated control (n=97) and RA-stimulated CDH (n=70).

3D FISH experiments were slightly adapted from a published protocol by Cremer et al. [36]. Briefly, coverslips were washed twice with 1xPBS at 37°C and fixed in 4% Paraformaldehyde/PBS (PH 7.0) for exactly 10 minutes at room temperature (RT). During the last minute a few droplets of 0.5% Triton X-100/PBS was added for permeabilization. After fixation, cells were washed 3 times for 3 minutes (RT) in 0.01% Triton X-100/PBS, incubated for 10 minutes (RT) at 0.5% Triton X-100/PBS and then incubated with RNase/2xSCC for 1 hour at 37°C to minimize RNA background. After subsequent washes in PBS for 3 times 10 minutes, cells were incubated in 0.1M HCL for 5' at RT, and washed twice in 2xSCC for 1 min. Finally; coverslips were equilibrated (at least overnight) in 50% formamide/2xSCC (pH 7.2).

For hybridization the slides were taken out of the formamide solution, drained very briefly before appliance of the appropriate hybridization mixture (containing the specific mixture of probes) and finally covered carefully (without pressure) with a superfrost slide (Menzel-Glaser, Saabruckener, Germany). Denaturation was performed at 75°C for exactly 2 minutes following hybridization for 2-3 days in a 37°C incubator. Then, slides were rinsed briefly in 2xSCC, washed stringently 3 times for 3 minutes in 0.1% Tween-20/2xSCC at RT and washed again in 1xPBS for 1'. Finally, DAPI staining (1: 10.000) combined with Vectashield H-100 mounting medium was applied and sealed with colorless nailpolish on standard Menzel microscope slides.

Microscopy and analysis

2D slides were examined with an Axioplan 2 Imaging microscope (Carl Zeiss, Jena, Germany) equipped with Plan-Neofluor oil-immersion objectives and a multicolor band-pass filter set.

3D image stacks were acquired using a Zeiss LSM 510 Meta confocal laser-scanning microscope (Carl Zeiss, Jena, Germany) equipped with a 63x plan-apochromat oil NA 1.4 DIC objective. The pinhole diameter was set to 1 airy unit. DAPI, Alexa 488 and Alexa594

fluorochromes were excited with a 405nm diode laser, a 488nm Argon laser and a 561nm He/Ne laser respectively and detected using a multi-track imaging mode using the beam splitters HFP 405/488/561, NFT 565, NFT 650 and filters BP 350-450, BP 505-550, LP 585. Eight bit images were acquired using a 2 times line averaging, and had a 512 x 512 pixel frame size and a 48 x 48 pixel size using an optical sectioning of 120nm. The point-spread function was determined by scanning green en red fluorescent beads with a diameter of 100nm (Duke scientific). The chromatic shift was determined by scanning multicolored fluorescent beads (Tetraspeck beads; Invitrogen) with a diameter of 500 nm. The empirically obtained point spread function (PSF) was used for deconvolving the image stacks with the classic maximum of likelihood algorithm that is implemented in the Huygens Deconvolution software package 3.0 (Scientific Volume Imaging, Hilversum, the Netherlands). After deconvolution, image stacks were corrected for chromatic shift. Subsequently, images from 50-150 nuclei were analyzed individually for each experiment using optimized fixed threshold and seed parameters to segment the fluorescent spots.

By determining the center of mass (COM) of each object in 3D the distances between two objects were calculated. Furthermore, the distance of the RP11-46C2 probe to the nearest surface of a larger structure (CT or nuclear membrane) was determined. In addition, overlapping intensities of two objects in different channels was evaluated by determining the level of intersecting voxels. Significance in the data-distributions was assessed using the non-parametric Mann-Whitney U test/Kolmogorov-Smirnov Test. A p-value of $p < 0.05$ was considered significant. Excluded from the analysis were all nuclei that seemed to have been damaged during the experiment procedure or not captured fully.

Results

Association frequency of three CDH candidate genes in control- and 15q26 haploinsufficient fibroblast nuclei

To test our hypothesis that known CDH candidate genes *NR2F2*, *GATA4* and *ZFPM2* – which are located on different chromosomes – interact within the nucleus, we performed 2D multicolor FISH analysis in a control fibroblast cell line (DFC1). 2D FISH enables faster image analysis compared to 3D techniques, although it slightly exaggerates interphase distances [37]. The second objective was to determine whether loss of 1 functional *NR2F2* allele in 15q26 deleted-patient fibroblast cultures (DFP1) influenced the spatial organization of these gene loci relative to each other.

Visual inspection of 2D images revealed six respectively five distinct and separate hybridization signals; both alleles of *GATA4* (red), *ZFPM2* (green) and *NR2F2* (purple) in the DFC1 cells (Figure 1A) and loss of one *NR2F2* FISH signal in the DFP1 cells (Figure 1C). We did not detect any obvious physical association between the analyzed genes in either control nuclei or in cells from 15q26 CDH patients. Since it is possible that the absence of these hypothesized interactions is the result of lack of a certain stimulus, we re-analyzed these processes after 48 hours exposure

of cells to 10 $\mu\text{mol/L}$ of retinoic acid (RA). Similarly, total absence of nuclear co-localization was determined in both DFC1 cells and DFP1 nuclei (Figure 1B and D).

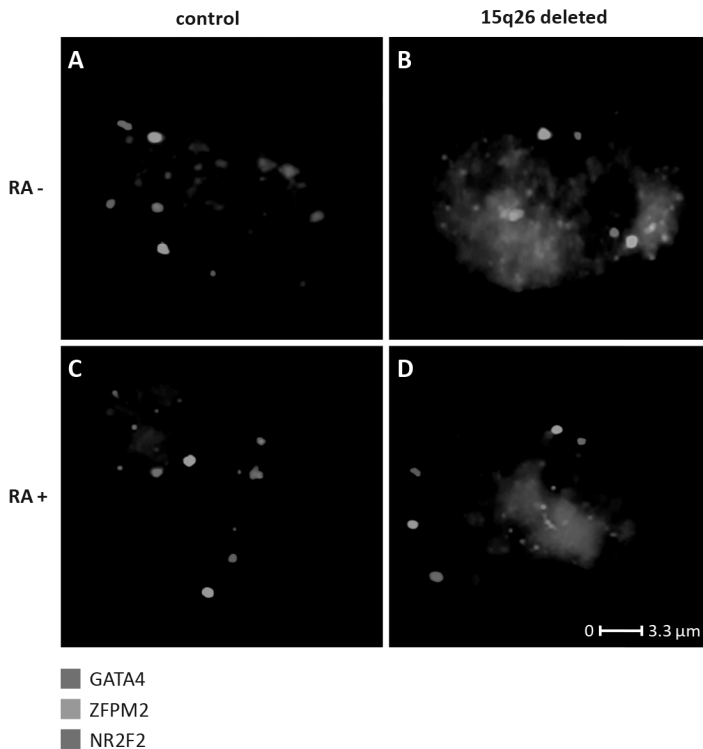


Figure 1 | Nuclear organization of CDH candidate genes in interphase fibroblast nuclei.

Representative 2D FISH images of distances between putative CDH genes *NR2F2*, *GATA4* and *ZFPM2* are shown and analyzed based on multicolor signals of BAC clones RP11-784A9, RP11-241B23 and RP11-1029P14 respectively. FISH spots of the three genes in Control (A and C) and 15q26-deleted CDH patient cells (B and D) and in an unstimulated (A and B) and RA-stimulated (C and D) condition. No co-localization of CDH-candidate genes was detected in both cell lines.

Bar = 3.3 μm . (red = *GATA4*, green = *ZFPM2*, purple = *NR2F2*, gray = nuclear DAPI counter stain) (see page 252 for color figure).

Nuclear positioning of *NR2F2* with respect to its chromosome territory 15

The frequency with which the *NR2F2* gene sits outside of its chromosome territory (CT) 15 was assessed next. Percentages of overlap were obtained by determining the percentage of intersecting voxels between the *NR2F2* allele-signals and their respective CT15 signals in the other channel. Only cells with a total absence of overlap (intersecting voxels = 0%) were considered as outside the chromosome backbone. In DFC1 nuclei 96% of both *NR2F2* alleles showed almost complete overlap with its respective CT15 (Table 1 and Figure 2). The average

percentage of intersecting *NR2F2* allele- and CT15- voxels was 77%, indicating that both alleles are positioned at the periphery of their chromosome territory, which is in line with their distal chromosomal 15 position. Subsequently, we evaluated whether this relative position could be affected by RA addition. Results showed no large relocation of the *NR2F2* alleles upon RA treatment in control cells, although a slightly larger percentage of alleles (9%) sat outside CT15. Finally, to exclude a possible role of malpositioning of *NR2F2* in a disease state, repositioning of this gene with and without RA was analyzed in DFP1 as well. Percentages of overlap were 94% and 92% in unstimulated and RA stimulated patient cells respectively (Table 1) indicating there is no difference in *NR2F2* positioning in 15q26 monosomy cell lines.

Table 1 | Percentages of overlap between *NR2F2* and its respective chromosome territory in control cells (DFC1) and CDH-15q26 deleted patient (DFP1) nuclei with and without RA

| | Control (DFC1) | 15q26-CDH patient (DFP1) |
|---------------|----------------|--------------------------|
| Unstimulated | 96% (156) | 94% (54) |
| RA-Stimulated | 91% (105) | 92% (61) |

In parentheses the absolute number of nuclei analysed

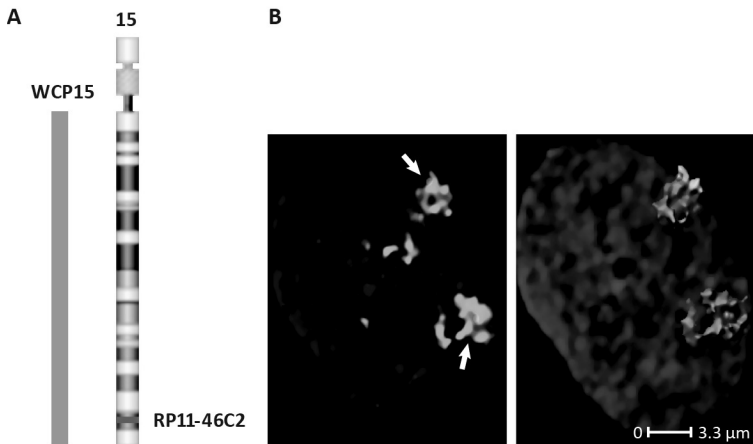


Figure 2 | *NR2F2* localization relative to its chromosome territory 15

A: Schematic diagram depicting the used FISH probes RP11-46C2 (red) and whole-chromosome territory 15 (CT15) paints (green) to analyze the position of the *NR2F2* alleles relative to their CT15. **B:** Representative FISH image of the nuclear position of chromosome territory 15 and the *NR2F2* alleles relative to each other in a control nucleus. (B, left) Visualization of an unprocessed xy-projection image. (B, right) Deconvolved and 3D volume rendered image showing a preferred territory surface position of *NR2F2* for one allele, and a complete CT interior position of the other allele. Both alleles show an almost complete overlap with their respective CTs and show no signs of relocalisation. Nuclei are stained with DAPI (blue). Bar = 3.3 μm (see page 252 for color figure).

Nuclear organization of partial CTs 15q and 8p in 15q26 deleted and control cell lines

To evaluate a possible impact of loss of the distal arm of chromosome 15 on nuclear organization, we compared the relative nuclear positions of partial chromosomal territories (pCT) 15q and 8p in DFP1 versus DFC1. Distances were measured in interphase nuclei analyzing the hybridization signals between 8p and 15q homologues, between the 15q partially deleted and its heterologous 8p counterparts and the relative distance of all these CT regions to the nuclear center. Distances were normalized for nuclear volume differences determined by the total number of DAPI voxels for each nucleus separately. The partially deleted pCT15 could be distinguished easily from its normal pCT15 counterpart in DFP1 based on its smaller pCT15 voxel volume.

Results showed that nuclear positioning of the partially deleted pCT15 was unaffected in DFP1 versus DFC1. The relative distance between homologues pCT8 signals and between heterologous deleted pCT15 and pCT8 signals were unaffected by patient status as well. However, further analysis did show a nuclear repositioning of the normal pCT15 in DFP1 compared to its normal partner in DFC1 with an increased internal location of the structural normal pCT15 in CDH fibroblasts (Figure 3).

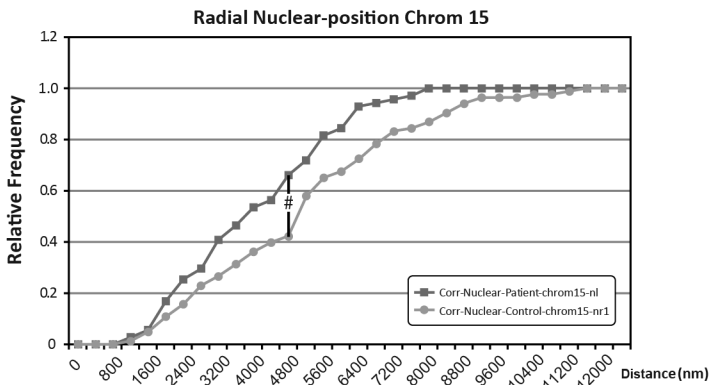


Figure 3 | Nuclear position of partial CT15q in control and CDH 15q26-deleted cell lines

This cumulative frequency graph shows the radial position of partial Chromosome Territory 15 (CT15) in control (dark green) and CDH-15q26 deleted (red) fibroblast nuclei. It only represents the position of the normal, untranslocated pCT15 in patient DFP1 and its normal pCT15 counterpart in control DFC1. Distances are corrected for nuclear volume.

Distribution differences were calculated using the Wilcoxon-Mann-Whitney test (see # $p = 0,003$). In each experiment 150 nuclei were analyzed (see page 253 for color figure).

Discussion

The pathogenetic mechanisms causing diaphragm- and lung- defects in patients with congenital diaphragmatic hernia (CDH) are largely unknown. Some valuable insights were provided by the identification of over 20 recurrently deleted and duplicated regions in the genome of complex CDH individuals [4]. Yet, which mechanisms and gene candidates are responsible for the induction of diaphragm defects in patients harboring these structural aberrations remains largely elusive. We hypothesized that nuclear co-association of candidate “diaphragm” genes or reallocation of the strong 15q26 CDH candidate *NR2F2* are prerequisite for proper co-transcription and normal diaphragm development. Failure of this process might contribute to CDH in patients displaying chromosomal rearrangements. To analyze whether co-localization and re-allocation are indeed altered in cells from a CDH patient with only one functional *NR2F2* allele, 15q26 deleted and Retinoic Acid (RA) stimulated fibroblast nuclei (DFP1) were used as a study model. Interaction frequencies in non-deleted, sex-matched fibroblast nuclei were used as controls (DFC1). Although skin fibroblasts are for obvious reasons not fully representative of developing diaphragm material, both cell lines do share a mesodermal origin and both have the machinery for RA metabolism [38].

Spatial arrangements were studied using a multicolor 2D FISH technique. A physical interaction between the CDH genes *NR2F2*, *GATA4* and *ZFPM2* could not be demonstrated, also not after RA stimulation. These results held for both DFP1 and DFC1 nuclei and implied that coordinated expression during diaphragm development was independent of nuclear co-association. These experiments cannot rule out the existence of more rapid and transient co-localization events, because FISH protocols were applied after a 48-hours window of RA induction. However, expression studies of the group of Greer et al. [8] show mRNA and protein levels of the investigated genes throughout (E10-E14) rodent diaphragm development. Postnatal obtained dermal fibroblasts may display fundamental differences in timing and occurrence of clustering events as compared to early embryological diaphragm material [20, 27]. Yet, our 2D FISH studies showed no proof for nuclear co-association in diaphragm-biopsy derived nuclei of *isolated* CDH patients (results not shown). Only animal models will enable developmental stage specific analysis, but require preferential interactions to be evolutionary conserved [39]. Alternatively, iPSC approaches using human cell lines might be more appropriate to truly solve this timing issue [40].

Numerous groups recently reported on the association between gene (re) positioning relative to the chromosomal backbone and transcription status changes during certain developmental processes or upon differentiation [30, 31, 41-44]. We followed the physical behavior of the *NR2F2* gene in DFC1 cells and compared them to those in DFP1, before and after RA induction. Results showed that *NR2F2* sits almost exclusively within its chromosome territory, both in control and in patient nuclei. This status was hardly affected by RA stimulation, although a slightly larger percentage of alleles sat outside CT15. This could be caused by fluctuation in the size of the CT itself as a response to RA or considered as a true movement away from the

CT. Irrespective of this, our relocation-proportions are by far not comparable to the percentages of relocation described in literature (40-60%) [42, 45, 46] and therefore unlikely to have a major impact on gene expression. Moreover, skepticism about a direct link between re-localization events as a prerequisite for transcription initiation and/or prolongation was stated recently; one study demonstrated that relocation behavior is more closely determined by chromosomal context than by transcriptional activity [39]. Furthermore, up until now only one paper [27] has proofed the causal relationship between gene expression regulation and gene repositioning.

Finally, we investigated the impact of the chromosomal rearrangement on the radial distribution of the chromosome segments on which the CDH candidate genes reside. Human fibroblast nuclei are known to have a chromosome-size correlated CT distribution [47]. In addition, CT15 tends to associate centrally with other acrocentric chromosomes by means of its nuclear organizing region [47, 48]. In general, mean distances between homologous acrocentric chromosomes are short, but not significantly different from other small centrally located CTs implying a “restricted space” effect on CT ordering. In this context, loss of band 15q26.1-q26.3 (and the joining of only a small segment of band 3q29) in DFP1 may exert a significant shift on the remaining pCT15 and (generally) on CT topology of the nuclear interior. This chromosomal rearrangement-induced reorganization of the nucleus could in turn effect gene expression.

Our results showed that nuclear positioning of the partially deleted pCT15 was unaffected in DFP1 versus DFC1 nuclei. Yet, surprisingly the normal un-translocated pCT15 exhibited a more central location in DFP1. The unchanged position of the translocated pCT15 is in agreement with results from Tanabe et al. [49]. This group studied the impact of (evolutionary originated) chromosomal rearrangements on the topological arrangement of chromosome segments across various higher primates. The data set was generated using gene-density ordered cell-types and focused on CTs18 (gene-poor) and CT19 (gene-dense). Some tumor-focused studies have been published on this subject as well, with variable and inconclusive outcomes [50, 51]. In contrast, Harewood et al. [32] recently demonstrated repositioning in gene-density ordered cells of a derivative chromosome 11-CT as the result of a balanced translocation with chromosome 22. Intriguingly, they further showed evidence for large-scale changes in gene-expression levels as a consequence of the alterations in CT topology. Similarly, the more central positioning of the normal pCT15 in our patients' nuclei might have an impact on gene-expression levels: it is generally accepted that the nuclear interior is a particularly competent environment for transcription. Allele-specific expression assays (both in balanced and unbalanced translocation carriers) are required to distinct such influences from the impact of the translocation event itself. Alternatively, it is possible that transcription level changes such as in the study of Harewood, are only present in case of more “extreme” repositioning of a CT locus i.e. from a lamina-associated position to the nuclear interior and vice-versa.

In this study we investigated whether – in a certain subclass of complex CDH patients- disruption of the nuclear organization of CDH candidate loci (and their chromosome segments) underlies the pathophysiology of this congenital anomaly. Although no evidence was found for dependence of coordinated expression on nuclear gene co-association, we did find a significant

nuclear repositioning of one of the partial chromosome segments on which a candidate gene resides. Whether this change only reflects the chromosomal rearrangement or has a functional implication on gene expression levels remains to be determined.

Acknowledgements

We thank Tom de Vries Lentsch for help in preparing the figures and the Department of Biochemistry of Erasmus MC for providing the human control dermal fibroblast cell line.

References

1. Sluiter, I., et al., *Congenital diaphragmatic hernia: Still a moving target*. Seminars in fetal & neonatal medicine, 2011.
2. Peetsold, M.G., et al., *The long-term follow-up of patients with a congenital diaphragmatic hernia: a broad spectrum of morbidity*. *Pediatr Surg Int*, 2009. **25**(1): p. 1-17.
3. Dott, M.M., L.Y. Wong, and S.A. Rasmussen, *Population-based study of congenital diaphragmatic hernia: risk factors and survival in Metropolitan Atlanta, 1968-1999*. Birth defects research. Part A, Clinical and molecular teratology, 2003. **67**(4): p. 261-7.
4. Holder, A.M., et al., *Genetic factors in congenital diaphragmatic hernia*. *Am J Hum Genet*, 2007. **80**(5): p. 825-45.
5. You, L.R., et al., *Mouse lacking COUP-TFII as an animal model of Bochdalek-type congenital diaphragmatic hernia*. *Proc Natl Acad Sci U S A*, 2005. **102**(45): p. 16351-6.
6. Ackerman, K.G., et al., *Fog2 is required for normal diaphragm and lung development in mice and humans*. *PLoS Genet*, 2005. **1**(1): p. 58-65.
7. Ackerman, K.G., et al., *Gata4 is necessary for normal pulmonary lobar development*. *Am J Respir Cell Mol Biol*, 2007. **36**(4): p. 391-7.
8. Clugston, R.D., W. Zhang, and J.J. Greer, *Gene expression in the developing diaphragm: significance for congenital diaphragmatic hernia*. *American journal of physiology. Lung cellular and molecular physiology*, 2008. **294**(4): p. L665-75.
9. Wat, M.J., Veenma, D.C.M., *Genomic alterations that contribute to the development of isolated and non-isolated congenital diaphragmatic hernia*. *J med Genet*, 2011.
10. Klaassens, M., et al., *Prenatal detection and outcome of congenital diaphragmatic hernia (CDH) associated with deletion of chromosome 15q26: two patients and review of the literature*. *American journal of medical genetics. Part A*, 2007. **143A**(18): p. 2204-12.
11. Beurskens, L.W., et al., *Retinol status of newborn infants is associated with congenital diaphragmatic hernia*. *Pediatrics*, 2010. **126**(4): p. 712-20.
12. Goumy, C., et al., *Retinoid Pathway and Congenital Diaphragmatic Hernia: Hypothesis from the Analysis of Chromosomal Abnormalities*. *Fetal Diagn Ther*, 2010.
13. Major, D., et al., *Retinol status of newborn infants with congenital diaphragmatic hernia*. *Pediatr Surg Int*, 1998. **13**(8): p. 547-9.
14. Babiuk, R.P., B. Thebaud, and J.J. Greer, *Reductions in the incidence of nitrofen-induced diaphragmatic hernia by vitamin A and retinoic acid*. *Am J Physiol Lung Cell Mol Physiol*, 2004. **286**(5): p. L970-3.
15. Clugston, R.D., et al., *Understanding abnormal retinoid signalling as a causative mechanism in congenital diaphragmatic hernia*. *Am J Respir Cell Mol Biol*, 2010. **42**(3): p. 276-85.
16. Nakazawa, N., et al., *Altered regulation of retinoic acid synthesis in nitrofen-induced hypoplastic lung*. *Pediatr Surg Int*, 2007. **23**(5): p. 391-6.
17. Wilson, J.G., C.B. Roth, and J. Warkany, *An analysis of the syndrome of malformations induced by maternal vitamin A deficiency. Effects of restoration of vitamin A at various times during gestation*. *Am J Anat*, 1953. **92**(2): p. 189-217.
18. Kleinjan, D.A. and V. van Heyningen, *Long-range control of gene expression: emerging mechanisms and disruption in disease*. *American journal of human genetics*, 2005. **76**(1): p. 8-32.
19. Simonis, M., et al., *Nuclear organization of active and inactive chromatin domains uncovered by chromosome conformation capture-on-chip (4C)*. *Nat Genet*, 2006. **38**(11): p. 1348-54.
20. Schoenfelder, S., et al., *Preferential associations between co-regulated genes reveal a transcriptional interactome in erythroid cells*. *Nat Genet*, 2010. **42**(1): p. 53-61.
21. Lomvardas, S., et al., *Interchromosomal interactions and olfactory receptor choice*. *Cell*, 2006. **126**(2): p. 403-13.
22. Osborne, C.S., et al., *Active genes dynamically colocalize to shared sites of ongoing transcription*. *Nat Genet*, 2004. **36**(10): p. 1065-71.

23. Osborne, C.S., et al., *Myc dynamically and preferentially relocates to a transcription factory occupied by Igh*. PLoS Biol, 2007. **5**(8): p. e192.
24. Spilianakis, C.G. and R.A. Flavell, *Long-range intrachromosomal interactions in the T helper type 2 cytokine locus*. Nat Immunol, 2004. **5**(10): p. 1017-27.
25. Fraser, P. and W. Bickmore, *Nuclear organization of the genome and the potential for gene regulation*. Nature, 2007. **447**(7143): p. 413-7.
26. Schoenfelder, S., I. Clay, and P. Fraser, *The transcriptional interactome: gene expression in 3D*. Curr Opin Genet Dev, 2010. **20**(2): p. 127-33.
27. Amano, T., et al., *Chromosomal dynamics at the Shh locus: limb bud-specific differential regulation of competence and active transcription*. Dev Cell, 2009. **16**(1): p. 47-57.
28. Ballester, M., et al., *The nuclear localization of WAP and CSN genes is modified by lactogenic hormones in HC11 cells*. J Cell Biochem, 2008.
29. Chambeyron, S., et al., *Nuclear re-organisation of the Hoxb complex during mouse embryonic development*. Development, 2005. **132**(9): p. 2215-23.
30. Volpi, E.V., et al., *Large-scale chromatin organization of the major histocompatibility complex and other regions of human chromosome 6 and its response to interferon in interphase nuclei*. J Cell Sci, 2000. **113** (Pt 9): p. 1565-76.
31. Williams, R.R., et al., *Neural induction promotes large-scale chromatin reorganisation of the Mash1 locus*. J Cell Sci, 2006. **119**(Pt 1): p. 132-40.
32. Harewood, L., et al., *The effect of translocation-induced nuclear reorganization on gene expression*. Genome Res, 2010. **20**(5): p. 554-64.
33. Klaassens, M., et al., *Prenatal detection and outcome of congenital diaphragmatic hernia (CDH) associated with deletion of chromosome 15q26: two patients and review of the literature*. Am J Med Genet A, 2007. **143A**(18): p. 2204-12.
34. van de Corput, M.P. and F.G. Grosveld, *Fluorescence in situ hybridization analysis of transcript dynamics in cells*. Methods, 2001. **25**(1): p. 111-8.
35. Eussen, B.H., et al., *A familial inverted duplication 2q33-q34 identified and delineated by multiple cytogenetic techniques*. European journal of medical genetics, 2007. **50**(2): p. 112-9.
36. Cremer, M., et al., *Multicolor 3D fluorescence in situ hybridization for imaging interphase chromosomes*. Methods Mol Biol, 2008. **463**: p. 205-39.
37. Kocanova, S., et al., *Activation of estrogen-responsive genes does not require their nuclear colocalization*. PLoS Genet, 2010. **6**(4): p. e1000922.
38. Goumy, C., et al., *Fetal skin fibroblasts: a cell model for studying the retinoid pathway in congenital diaphragmatic hernia*. Birth Defects Res A Clin Mol Teratol, 2010. **88**(3): p. 195-200.
39. Brown, J.M., et al., *Association between active genes occurs at nuclear speckles and is modulated by chromatin environment*. J Cell Biol, 2008. **182**(6): p. 1083-97.
40. Maherali, N. and K. Hochedlinger, *Guidelines and techniques for the generation of induced pluripotent stem cells*. Cell stem cell, 2008. **3**(6): p. 595-605.
41. Chambeyron, S. and W.A. Bickmore, *Chromatin decondensation and nuclear reorganization of the HoxB locus upon induction of transcription*. Genes Dev, 2004. **18**(10): p. 1119-30.
42. Christova, R., et al., *P-STAT1 mediates higher-order chromatin remodelling of the human MHC in response to IFNgamma*. J Cell Sci, 2007. **120**(Pt 18): p. 3262-70.
43. Finlan, L.E., et al., *Recruitment to the nuclear periphery can alter expression of genes in human cells*. PLoS Genet, 2008. **4**(3): p. e1000039.
44. Kosak, S.T., et al., *Subnuclear compartmentalization of immunoglobulin loci during lymphocyte development*. Science, 2002. **296**(5565): p. 158-62.
45. Brown, J.M., et al., *Coregulated human globin genes are frequently in spatial proximity when active*. J Cell Biol, 2006. **172**(2): p. 177-87.
46. Mahy, N.L., et al., *Spatial organization of active and inactive genes and noncoding DNA within chromosome territories*. J Cell Biol, 2002. **157**(4): p. 579-89.

47. Bolzer, A., et al., *Three-dimensional maps of all chromosomes in human male fibroblast nuclei and prometaphase rosettes*. PLoS Biol, 2005. **3**(5): p. e157.
48. Heride, C., et al., *Distance between homologous chromosomes results from chromosome positioning constraints*. J Cell Sci, 2010. **123**(Pt 23): p. 4063-75.
49. Tanabe, H., et al., *Evolutionary conservation of chromosome territory arrangements in cell nuclei from higher primates*. Proc Natl Acad Sci U S A, 2002. **99**(7): p. 4424-9.
50. Cremer, M., et al., *Inheritance of gene density-related higher order chromatin arrangements in normal and tumor cell nuclei*. J Cell Biol, 2003. **162**(5): p. 809-20.
51. Meaburn, K.J. and T. Misteli, *Locus-specific and activity-independent gene repositioning during early tumorigenesis*. J Cell Biol, 2008. **180**(1): p. 39-50.

Chapter 3.2

Expression Profiling with and without Retinoic Acid (RA) in 15q26-Deleted Congenital Diaphragmatic Hernia Fibroblasts: Relative Cellular RA Deficiency

D.Veenma, E.Brosens, M.Peters, M. Jhamai, C.Wouters, M.Pescatori, R.Rottier, A.Kremer, D.Tibboel and A.de Klein

Manuscript in preparation

Supplementary files available on request

Abstract

Patients with Congenital Diaphragmatic Hernia (CDH) form a heterogeneous group, both genetically and phenotypically. In this study we searched for new genetic insights in the etiology of this birth defect applying a CDH-Retinoic Acid (RA) modulated cell culture model. We used fibroblast cultures of patients with deletions in the most frequent and strongest CDH associated chromosomal hot spot described in humans: the 15q26 region. Our output-measures contained the transcriptome profiles of RNA isolated from two 15q26 monosomy cases versus two sex-matched controls after a 48-hour period of exposure to four different RA concentrations. Differential expression patterns at default were analyzed in detail as well. We speculated that overstimulation with RA would unmask a relative RA-deficiency in the patient group.

Results showed that some of the key components of RA homeostasis, Cellular Retinoic Acid Binding Protein type I (CRABPI) and Cytochrome P450 subunit 26A1 (CYP26A1), were profoundly up-regulated after RA stimulation in patient cell lines only. In addition, new light was shed on existing ideas of 15q26-candidate genes: only the genes *TTC23* and *LRRRC28* – and not the strong candidate *NR2F2* - were significantly down-regulated in the patient group. Results further pointed out several new early mesenchymal (*NR5A2*, *EDNRA*, *GPC4*) and lung vascular (*RGS4*, *ANPEP*, *CNN1*) candidate genes, underlining a concomitant effect on both lung- and mesenchyme (diaphragm) development.

In conclusion, this study emphasizes that RA-signalling disruption in complex 15q26-associated CDH is subtle and involves not only an altered expression of genes from the deleted area but also involves key factors of the RA pathway and of mesenchymal- and lung-development. The “patho-phenotypic” potential of the 15q26 monosomy can therefore not be fully explained by simple haploinsufficiency of genes in the smallest-region of overlap. Finally, the diaphragmatic- and pulmonary defects of CDH in these cases could be causally linked on a cellular and molecular level.

Introduction

Congenital Diaphragmatic Hernia (CDH) is a severe birth defect characterized by a hole in the posterolateral part of the diaphragm and affects 1 in 3000 live births. Ventilator support and pharmaceutical treatment of the co-occurring pulmonary hypoplasia and -hypertension are insufficient in respectively 20% of isolated cases and 60% of complex ones, leading to early perinatal death [1]. The hypothesized multifactorial and heterogenic etiology of CDH has been the subject of extensive patient-oriented and animal-model based research. Some valuable insights into its genetic susceptibility were recently provided by the application of molecular cytogenetic techniques to patients' DNA [2-4]. Chromosomal aberrations are currently detected in 20-30% of the human cases and some of these recurrent, structural anomalies point to CDH associated loci and genes (*NR2F2*, *ZFPM2*, *GATA4*) involved in the Retinoic Acid (RA) signalling pathway. The most common chromosomal hot spot is the distal 15q monosomy (*OMIM 142340*) [2].

Literature reports over 30 persons with CDH and an interstitial or terminal deletion of the long arm of chromosome 15q [2, 5, 6]. Although rare by itself, a defect of the diaphragm is the cardinal clinical finding in this microdeletion syndrome, suggesting a causative role of haploinsufficiency of 1 or more 15q26 genes in respiratory muscle maldevelopment [7]. Other features include a typical facial appearance, distal digital hypoplasia, and abnormalities of the eyes, urogenital, C.N.S. and cardiovascular system.

The *NR2F2* gene is the most obvious CDH-associated, 15q-candidate (*OMIM 107773*) based on conditional knock out mice studies demonstrating a posterolateral diaphragmatic defect after tissue-specific ablation of *Nr2f2* [8]. Unfortunately, a concomitant search for additional pathologic human *NR2F2* mutations – or mutations in other genes from the deleted region – failed to identify any [9]. However, high penetrance of CDH in 15q26-cases remains hard proof for the importance of distal 15q genes and/or regulatory elements in diaphragm development. This assumption is supported by mRNA- and protein expression-results at various developmental stages in the rodent CDH-model [10].

The association between RA signalling-disruption and CDH is extensively discussed in literature [11, 12]. Briefly, in the early fifties, abnormalities -among which diaphragmatic defects- observed in animals fed on a Vitamin A Deficient diet (VAD) formed the first clue for the importance of RA in diaphragm development [13]. Since then several studies provided arguments for this theory showing: 1) reduced CDH incidence after reintroduction of Vitamin A in the VAD and teratogenic RA-models [14-16] 2) the occurrence of CDH, albeit with markedly reduced penetrance, in (partial) knock-out models of RA-pathway genes [8, 17-20], 3) expression of RA pathway genes in the primordial diaphragm of in-vitro RARE perturbation studies with and without RA [15], 4) the recurrent identification in human CDH-patients of mutations in chromosomal regions that harbor crucial RA pathway genes [21] 5) mutations of the cellular retinol-binding protein-receptor (*STRA6*) in complex human phenotypes featuring diaphragmatic defects [22, 23] and finally, our recent paper confirming the association in human cases between CDH and low retinol or low retinol-binding protein levels independent of maternal status [24, 25].

In this study we searched for new genetic insights in the etiology of CDH using a cell-culture based model. We speculated that deleted genes in the 15q26 chromosomal area are crucial for both diaphragm development and RA signalling. Secondly, we hypothesized that overstimulation of 15q26 deleted fibroblast cultures with RA could mimic a normal “healthy” transcriptome or at least elicit different effects as compared to control fibroblasts. Dermal fibroblasts form an excellent model system to analyze the different components of the RA signalling pathway in CDH, since they have the same mesodermal origin as diaphragm tissue and express all the necessary metabolic components of this pathway [11]. Output measures concerned the transcriptome profiles of RNA isolated from two 15q26 monosomy patients versus two sex-matched controls after a 48-hour exposure to four different RA-concentrations. Differential expression patterns at default were analyzed in detail as well. Results showed that this “complex phenotype approach” is able to shed new light on existent knowledge of 15q26- as well as RA-candidates. In addition, it pointed to several new, embryologically early expressed mesenchymal – and lung vascular-candidate genes. Finally, the most deregulated expression levels at default directed to several genes that might contribute to the co-occurring anomalies of the 15q26 monosomy phenotype.

Material and Methods

Patient samples

In this study we used three different sources of patient material. Firstly, RA-stimulation and whole transcriptome analysis were performed in Dermal Fibroblast Cells (DFC) obtained from two CDH patients displaying a cytogenetically confirmed distal chromosome 15q deletion. These deletions resulted from a parental balanced translocation $t(3;15)(3q29;q26)$ in case of female **DFC1** and a de novo unbalanced $t(4;15)(q35;q26)$ for male **DFC2** (Figure 1). Control samples included two dermal fibroblast cultures of anonymous healthy individuals of both sexes (female **DFC3** and male **DFC4**), which were kindly provided by the Department of Biochemistry (Erasmus MC, Rotterdam, Netherlands). Secondly, we cultured and RA-stimulated diaphragm fibroblasts from three male isolated-CDH patients, which enabled us to distinguish (by targeted RT-qPCR) between differential expression as a consequence of 15q26 monosomy only or as a result of CDH. These diaphragm cells - obtained during corrective surgery after separate informed consent – were processed according to standard procedures of dermal fibroblast culturing. Finally, lung-material of five unrelated isolated-CDH cases – who died within 48 hours after birth as previously described [26]- was used as an additional input for the array-confirmative RT-qPCR experiments. Exclusion of (additional) large copy number events was accomplished in all samples by SNP array.

Cell culture

Cells were cultured in 75 cm² culture flasks (BD Biosciences Falcon™, San Jose, CA, USA) at incubator settings of 37°C and 5% CO₂, using HAMF10 medium supplemented with 12.5% Fetal Bovine Serum (Biowhittaker, CA, USA) and 1% penicillin-streptomycin. Culture medium was

refreshed every 2-3 days and additionally the day before harvesting. Cultures were exposed at 75% confluence to medium containing 0.25, 0.5, 1.0 or 5.0 $\mu\text{mol/l}$ of RA (Sciencelab.com, Inc., Houston, Texas) diluted in DMSO. For each cell line two controls were collected: one without DMSO and RA and one with only DMSO. After 48 hours medium was removed and cells were rinsed with DPBS (GIBCO®/ Invitrogen, Carlsbad, CA, USA). Subsequently, cells were trypsinised with TrypLE™ Express (Invitrogen, Carlsbad, CA, USA) for exactly 5 minutes, centrifuged for 5 min at 200g and finally suspended and stored in RNAlater Stabilization Reagent at -80°C (Qiagen, Inc., Hilden, Germany).

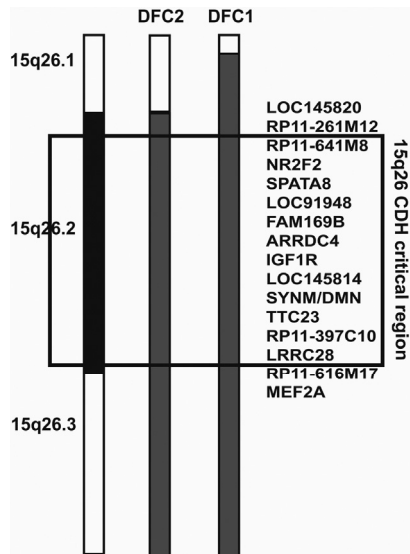


Figure 1 | Overlapping deletions of patient samples DFC1 and DFC2 on chromosome 15q26 and the minimal deleted region for diaphragm defects.

Figure 1 presents a schematic overview of the 15q26 deletion events in CDH dermal fibroblast cultures DFC1 and DFC2. In both patients this deletion results from an unbalanced translocation: $46,XX,der(15)t(3;15)(q29;q26.1)$ in case of DFC1 and $46,XY,der(15)t(4;15)(q35.1;q26.1)$ for DFC2. The demarcated region indicates the “critical” 15q26 region associated with diaphragm defects as described in literature.

DNA and RNA isolation and Quality control

DNA and RNA were isolated from all different cell sources using the Qiagen DNeasy and RNeasy kit according to the manufacturer’s protocol (Qiagen, Inc., Hilden, Germany). DNA concentrations and quality were checked by Quant-iT™ PicoGreen® dsDNA kit (Invitrogen, Carlsbad, CA, USA). RNA quality was assayed with the Agilent 2100 bio analyser and complement Agilent RNA 6000 Nano kit (Agilent Technologies, Inc., Santa Clara, California).

SNP and Expression Array

Variations in genotype and whole transcriptome were measured using the Illumina SNP (12-Human CytoSNP DNA Analysis-) and Expression (HumanHT-12 Expression-) BeadChips according to the manufacturers' protocol (Illumina, Inc., San Diego, USA). SNP and expression data were further processed (as described before [6] using the manufacturers' compatible Genome- and Bead-Studio programs.

Expression array data analysis

Figure S1 depicts a summary of our analysis flow-chart. Briefly, intensity signal data from each human HT-12 Expression BeadChip was subtracted and normalized using quantile normalization without background subtraction [27, 28]. Genes showing minimal variation across the total set of arrays were excluded from the analysis. More specifically, probes whose expression differed by at least $P > 0.05$ in over 80% of all DFC-samples were retained (in total 19.268 out of 47.000 probes). All experiments met specific Genechip QC criteria and data generated in this study have been deposited in the Gene Expression Omnibus with accession number XXXXXX. Global gene expression differences at default (Patient DFC 1/2 versus Control DFC 3/4) and genes up- or down-regulated after retinoic acid stimulation were identified using Partek Genomic Suite software (Partek Incorporated, St. Louis, Missouri, USA). Ingenuity Pathway Analysis software (Ingenuity Systems Inc. Redwood City, CA) and Genomatix software (München, Germany) were used to establish the cellular functions affected by diseased state or retinoic acid exposure. Anni [29] and Endeavour [<http://homes.esat.kuleuven.be>] were used for text-mining and gene prioritization.

Quantitative RT-PCR

Two μg of each total RNA sample was reversely transcribed to cDNA using the iScript cDNA synthesis kit (Bio-Rad, Hercules, CA). An ABI7300 Real-time PCR system was used in combination with KAPA-SYBR fast master mix (KapaBiosystems, Woburn, MA, USA). Reactions were performed in triplet and designed in a manner similar to the standard curve method described by Boehm et al. [30] with a region of the GAPDH gene serving as a control locus. Primers (depicted in Table S1) from the unique cDNA sequences of various target genes were designed using Primer Express software v2.0 (Applied Biosystems).

Results

RA toxicity

RA toxicity was determined using patient cell line DFC1 and control DFC3. Output measures included cell-morphology by haematoxylin-eosin staining and proliferation rate, which was periodically inspected 3, 15, 24, 48, 72 and 135 hours after RA exposure at a concentration range between 0 to 100 $\mu\text{mol/l}$. Results showed a growth-inhibiting effect 72 hours after exposure, at RA-concentrations above 1.00 $\mu\text{mol/l}$ irrespective of the origin of the cells. Although statistically

not significant, we noticed at default a slightly reduced growth rate for DFC1 as compared to DFC3. The morphological aspect of both cell lines was similar and unaffected, both in unstimulated as well as in stimulated conditions up to 100 $\mu\text{mol/l}$ of RA for 48 hours.

Based on these toxicology data, we exposed dermal fibroblasts of two 15q26 monosomy cases (DFC 1/2) and two sex-matched controls (DFC 3/4) for 48 hours to medium containing 0, 0.25, 0.5, 1.0 and 5.0 $\mu\text{mol/l}$ of RA diluted in DMSO. Total RNA of each of these conditions - including a sample for each cell line without either DMSO or RA - was isolated and hybridized to Illumina human HT-12 Expression Beadchips allowing whole transcriptome analysis.

Quality and Clustering of transcriptome data

To examine correlations in the transcriptome data we performed principle component analysis (PCA). Figure S2A depicts the results of the first four principal components, demonstrating that DFC-control- and DFC-diseased-groups are distinctly separated. For reasons of practicability, fibroblasts were stimulated and harvested in two culture batches, which unfortunately was recognized as a substantial source of variation (Figure S2B) and therefore removed by the Partek software (Figure S2C). PCA results also indicated that the global expression patterns at default were quite similar for the 0 RA-0 DMSO group as compared to the 0 RA+DMSO group, stressing on a small effect for the solvent DMSO. Finally, PCA showed that for each individual cell culture its 6 samples were closely clustered together with a clearly visible effect of RA-treatment in the same direction.

ANOVA

Statistically significant changed genes were identified by analysis of variance (ANOVA) with FDR-corrected p-values of < 0.01 using diseased status, cell line and cell line*diseased status as possible factors of variation. ANOVA was performed for the default situation (DFC1/2 versus DFC 3/4) and after RA-treatment in patient dermal fibroblasts using a concentration of 1.0 $\mu\text{mol/l}$ (DFC1/2 versus DFC1/2 with RA-1.0). Based on the expression levels of some known RA-responsive genes [31], this RA dosage was independently recognized as the concentration at which the strongest RA effect was present. The patient-specific RA-induced gene list was then divided into two categories: The first one includes genes whose expressions already differed from controls at default. The second category includes those genes that were not differentially expressed in default but were significantly up (or down) regulated by RA in patient cultures only. Figure 2 presents a summary of the overall results.

Default expression deregulation

First we questioned whether the genome-wide expression profiles of control and diseased samples were similar in default or not. This contrast between normal vs. patient yielded 378 differentially expressed genes (Figure 2 and Table S2), excluding those genes that were up or down-regulated as a consequence of DMSO treatment in either cell line ($n=33$). Next, we examined the default gene list on six specific items as presented in Table 1. New interesting

candidates were filtered out by text mining- and gene prioritization approaches paying specific attention to those in our top-20 (as presented in Table 2). In addition, non-supervised pathway analysis demonstrated that the cell cycle process (cell cycle transition point regulators and cellular assembly or organization genes) was one of the major deregulated processes (Table 1). Below, we briefly review the most remarkable default results.

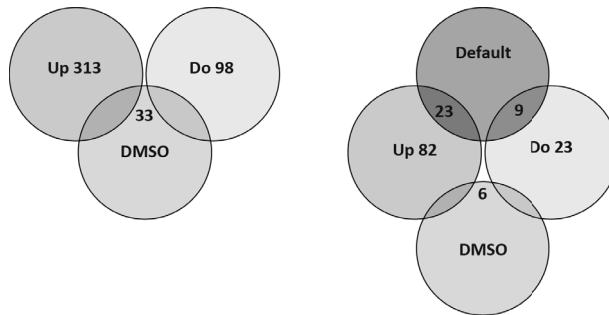


Figure 2 | Overview of differential expressed gene numbers

Overall results of the total number of statistically significant changed genes in 15q26 monosomy dermal fibroblasts as compared to controls using ANOVA analysis with FDR corrected p-values of <0.01 . On the left: results of default transcriptome differences between the two groups. On the right: expression level differences between patients and controls of genes, which showed a significant response to RA-treatment in patient fibroblasts at a concentration of 1.0 $\mu\text{mol/L}$.

Abbreviations: UP means relative up-regulation in the patient group, DOWN means relative down-regulation in the patient group, DMSO stands for gene expression changes as a consequence of the RA-solvent DMSO.

Two genes of the 15q26 CDH “critical region”, that is TetraTriCopeptide repeat domain 23 (*TTC23*) and Leucine Rich Repeat Containing 28 (*LRRC28*), were significantly down-regulated in both patients as compared to controls. In contrast, CDH-candidate *NR2F2* displayed a strong up regulation, however this effect was only significant in DFC1. None of the genes in the duplicated regions on chromosome 3 or 4 were identified as differentially expressed and overall there was no enrichment of genes in the chromosomal regions affected by structural variation. Moreover, genes encoding proteins involved in RA signalling or metabolisms were not significantly altered at default. The following seven genes formerly associated – directly or indirectly – with CDH in literature were distinguished. From the TOP-20 list this included Glycopican 4 (*GPC4*, CDH associated with Simpson-Golabi-Behmel syndrome), Endothelin Receptor type A (*EDNRA*) [32] and Insulin-like Growth Factor Binding Protein 5 (*IGFBP5*) [33]. The remainder encompassed: Collagen, type I, Alpha 1 (*COL1A*, CDH associated with Ehlers-Danlos, OMIM 130000), Capsulin (*TCF21*) [34-36], Kruppel-like factor 2 (*KLF2*) [37] and ParaThyroid Hormone 1 Receptor (*PTH1R*) [38, 39].

Table 1 | Enrichment analysis and filtering differential expressed gene lists on specific items

| Items | Orientation diff.expression | Gene count DEFAULT | Gene symbol DEFAULT | Gene count DIFF-RA CDH-CTRL | Gene symbol DIFF-RA CDH-CTRL |
|--|--------------------------------|-----------------------|---|--------------------------------|--|
| Cell (cycle) process, cell division & assembly | | Up & Down (39) | Selection Genomatrix: CCND1,GTSE1,CDC34, CCND1, BCAT1, CKS2, MAD2L1,NEK6,GASZL1, CDKN3, CDC25B, SGOL2, CCNA2, SESN1, CDCA3,CDK10, MYH10, NEDD9, PBK, NCAPG, PTTG1,CEP55, CDa8. | Up (32) | 26s Proteasome, Alp, Ap1, Caspase,CDC25B, CD44, collagen, Collagen type I, YWHAQ, TXN,Cyclin A, DLC1, Estrogen Receptor, HSPB1, TWIST1,IGFBP5/6, Integrinα, ITGA2/4, ITGA11, Jnk, KRAS, KRT18, LIPG, Mimp, NCOA7, NFKB, P38 MAPK, Pdgf, PPM1D, Raf, RBCK1, S100A4, P-value(Ingenuity) : 2,50*E-07-1,94*E-02 |
| 15q26 critical region | UP | - | - | Down (11) | CDT1, UHRF1,ITGB3, UHRF1, AURKA, PLK4 AURKA, TRIP13, PTPRB,CCDC99, TRIP13, P-value (Ingenuity): 4,20*E-04-3,17*E-02 |
| Patients' duplicated chromosomal area's | Down | 2 | TTC23, LRRC28 | - | - |
| | UP | - | - | 1 | ANKRD37 |
| | Down | - | - | - | - |
| RA signalling | UP | - | - | 3 | CRABP-I, CYP26A1, NCOA7 |
| | Down | - | - | - | - |
| CDH associated genes literature | UP | 7 | GPC4, EDNRA,IGFBP5, TCF21, PTH1R, KLF2, COL1A1 | 2 | IGFBP5, GPC4 |
| | Down | - | - | 1 | EDNRA |
| New (top) genes, genes prioritized | - | selection | RG54, MYH10, NR5A2, KLF11, ACAN, CAV1, HOXB6, DLX3/1 MEF2D, MUSK | selection | RG54,KRT18,TWIST, HBEFG, DLC1, CD44, IGA11/4, IGB3/2 |

DEFAULT: Differentially Expressed between Patients and Controls at default; DIFF-RA CDH-CTRL: Differentially Expressed upon RA stimulation in Patients and with statistically significant expression differences between patients and controls; RA: Retinoic Acid; CDH: Congenital Diaphragmatic Hernia; UP: Up-regulated; Down: Down-regulated; Genomatrix: Genomatrix software (Munche, Germany); ^: >4 = significant; Ingenuity: Ingenuity Pathway Analysis (IPA) software (Ingenuity Systems Inc. Redwood City, CA)

Table 2 | Array results TOP-20 differential expressed genes

| Default UP Diff. expressed | Rank p-value | Default DOWN Diff. expressed | Rank p-value | RA-induced UP Diff. expressed | Rank p-value | RA-induced DOWN Diff. expressed | Rank p-value | Default 15q26 | Rank p-value | RA induced 15q26 | Rank p-value |
|-------------------------------|-----------------|---------------------------------|-----------------|----------------------------------|-----------------|------------------------------------|-----------------|------------------|-----------------|---------------------|-----------------|
| RGS4 | 1 | C3orf26 | 1 | RGS4 | 1 | EDNRA* | 1 | ST8SIA2 | - | ST8SIA2 | - |
| MYH10* | 2 | NCAPG | 2 | HRASLS3 | 2 | GRP | 2 | RGMA | - | RGMA | - |
| SELS | 3 | HS.539760 | 3 | NCOA7 | 3 | BST1* | 3 | CHD2 | - | CHD2 | - |
| KCNIP3 | 4 | HJURP | 4 | IGFBP5* | 4 | SGCD | 4 | IGF1R | - | IGF1R | - |
| GPC4* | 5 | KCNS3 | 5 | GPC4* | 5 | RPESP | 5 | NR2F2 | - | NR2F2 | - |
| SELS | 6 | HSD3B7 | 6 | CRABP1* | 6 | WDR51A | 6 | ARRDC4 | NA | ARRDC4 | NA |
| GRP | 7 | C8orf34 | 7 | GOLGA3 | 7 | HAS3 | 7 | MCTP2 | NA | MCTP2 | NA |
| SGCD | 8 | P2RY6 | 8 | SSTR1 | 8 | IMPAD1 | 8 | DMN | - | DMN | - |
| EDNRA* | 9 | C3orf14 | 9 | CDC25B | 9 | PPP1R14C | 9 | | | | |
| CSRP1 | 10 | C9orf40 | 10 | KRT18* | 10 | NOPE | 10 | ZFPM2 | - | ZFPM2 | - |
| RPL23AP7 | 11 | TTC23 | 11 | LOC646723 | 11 | TRIP13 | 11 | GATA4 | - | GATA4 | - |
| SSTR1 | 12 | ZMYND8 | 12 | WARS | 12 | PLK4 | 12 | | | | |
| SH3D19 | 13 | HS.105618 | 13 | HS.128753 | 13 | LIPG | 13 | CNV other | | CNV other | |
| ANPEP* | 14 | KLHL7 | 14 | KCNIP3 | 14 | HBEGF* | 14 | ANKRD37 | - | ANKRD37 | 58 |
| HAS3 | 15 | C19orf40 | 15 | WARS | 15 | FAM83D | 15 | | | | |
| CUTL1 | 16 | CENPA | 16 | HS.57079 | 16 | HYLS1 | 16 | | | | |
| CNN1* | 17 | ABCC13 | 17 | DBI | 17 | GENPK | 17 | | | | |
| SGCD | 18 | IFT57 | 18 | LOC649366 | 18 | DPH3 | 18 | CRABP1* | - | CRABP1* | 6 |
| PLEKHG2 | 19 | CENPK | 19 | S100A4 | 19 | TPMT | 19 | NCOA7 | - | NCOA7 | 4 |
| SH3KBP1 | 20 | CPEB1 | 20 | CD44* | 20 | SENP1M | 20 | CYP26A1* | - | CYP26A1* | 67 |

| Default UP Diff. expressed | Rank p-value | Default DOWN Diff. expressed | Rank p-value | RA-induced UP Diff. expressed | Rank p-value | RA-induced DOWN Diff. expressed | Rank p-value |
|-------------------------------|-----------------|---------------------------------|-----------------|----------------------------------|-----------------|------------------------------------|-----------------|
| BST1* | 21 | | | | | | |
| IGFBP5* | 23 | | | | | | |
| NRSAZ* | 51 | LRRC28 | 45 | DLC1 | 51 | | |
| DLX3 | 94 | | | TWIST1 | 52 | | |
| DLX1* | 256 | | | | | | |
| SPRY1 | 174 | | | | | | |
| TCF21* | 258 | | | | | | |

* Filtered & Prioritized by multiple testing correction and Endavour [<http://homes.esat.kuleuven.be>]

Blue colored Genes associated in literature with major anomalies of the 15q26 phenotype

Red colored Genes putatively related to the specific lung defects in 15q26 monosomy patients

Default up Differentially up-regulated Genes in patients versus controls at default

Default DOWN Differentially down-regulated Genes in patients versus controls at default

UP Genes up-regulated in patient samples upon RA and differentially expressed compared to Controls RA-induced

DOWN Genes down-regulated in patient samples upon RA and differentially expressed compared to Controls.

NA No probes

Available on array.

As gene expression values also varied within the group of 15q-monosomy patients (DFC-culture 1 and 2), we performed quantitative RT-PCR for a few selected candidates. Results are summarized in Table 3 showing full confirmation of array outcomes. To distinguish between expression differences as a consequence of 15q26 monosomy only or as a cause of CDH, we additionally screened the mRNA levels of these selected genes in cultured diaphragm material derived from three non-related isolated CDH patients (Table 3). Expression alterations were specific for the 15q26-deleted condition in case of *EDNRA*, *NR5A2*, *TTC23* and *LRRC28*. In contrast, *RGS4*, *GPC4* and *IGFBP5* were altered in all three isolated CDH patients. Finally, *RGS4* was tested in lung material of five non-related CDH patients and was strongly up-regulated in three of them.

Since diaphragm defects constitute only part of the complex phenotype displayed by children with 15q26 monosomies [2], it is not surprising that several of the (TOP) default up-regulated genes are directly- or indirectly associated in literature with major anomalies of: the cardiovascular- (*MYH10*, *GPC4*, *CSRP1*, *HAS2*, *CNN1*, *TCF21*), urogenital (*MYH10*, *GPC4*, *SPRY1*, *TCF21*), craniofacial (*EDNRA*, *GPC4*, *DLX1*, *TCF21*), C.N.S (*MYH10*, *KCNIP3*, *DLX1*) and musculoskeletal (*GPC4*, *DLX1*, *TCF21*) system. These genes are hallmarked blue in Table 2. A brief overview of their embryonic function is presented in Table S3. Genes putatively related to the specific lung defects in 15q26 monosomy patients are highlighted in red and include Regulator of G protein signalling 4 (*RGS4*) [40], *IGFBP5* [41], *EDNRA*, *GPC4*, Alanyl-membrane aminopeptidase (*ANPEP*), *CNN1* and *TCF21* [34]. Interestingly, *NR5A2* was selected by endeavor gene prioritization and is known as an early embryonic developmental factor with a crucial role in mesodermal genesis [42, 43]. RT-qPCR analysis in isolated samples showed normal *NR5A2* expression levels indicating a 15q26 specific aberrant expression.

Gene expression differences after RA-treatment

In the second part of this study we assumed that a relative deficiency in RA signalling is the primary derailed mechanism underlying the 15q26 -diaphragm- phenotype. We reasoned that RA (over) stimulation could compensate for this deficiency and return whole transcriptome levels to (nearly) normal or could unravel patients' pathologic response to RA in case of RA-responsive genes. Analogous to the default comparison, we examined RA-treated expression profiles on the six items as summarized in Table I.

Overall results are shown in Figure 2 (and Table S4) presenting 82 significantly up- and 23 significantly down-regulated genes upon RA-treatment in 15q26 monosomy cultures (DFC 1 and 2) that in turn were differentially expressed between the patient- and control (DFC 3 and 4) group. Of these, 23 RA-up and 9 RA-down-regulated genes (among others *RGS4*, *GPC4*, *IGFBP5*) were present in the default comparison, implying that the patients' response to RA is similar to controls or intensified mRNA-differences with controls. In agreement with our null-hypothesis, RA elicited a compensating reaction in patients for the TOP-default differentially expressed genes *EDNRA*, *HAS3* and *BST1*, however failed to correct their mRNA-levels to normal. In contrast, the remainder set of TOP-default genes, that is *MYH10*, *CSRP1*, *ANPEP*, *CNN1* and the 15q26 CDH-critical genes *TTC23* and *LRRC28* did not respond to RA in patients. This was confirmed

Table 3 | RT-qPCR results of selection of differential expressed genes

| Default Diff. expressed | Rank p-value | Array Result | | Quantitative q-PCR result | | Conclusion | |
|------------------------------|-----------------|--------------|-----------------------|---------------------------|---------------------|--------------|--|
| | | Normal | 15q26 | Normal (n=2) | 15q26 (n=2) | | Isolated CDH (n=3) |
| RGS4 | 1 | + | UP | + | UP | UP | CDH specific; CDH-lung 3/5 UP |
| GPC4* | 5 | + | UP | + | UP | UP, except 1 | CDH specific |
| SGCD | 8 | + | UP | - | - | - | Not reproduced, also in DOWN list; probably polymorphism array probe |
| EDNRA* | 9 | + | UP | + | UP | +/- | 15q26 specific |
| IGFBP5* | 23 | + | UP | + | UP | UP | CDH specific |
| NR5A2* | 51 | + | UP | + | UP | +/- | 15q26 specific |
| 15q26-Default | | | | | | | Reference[10]; Gene expression in rodent primordial diaphragm |
| TTC23 | 11 | + | DOWN | + | DOWN | +/- | 15q26 specific; Default + minimally RA-responsive |
| LRRC28 | 45 | + | DOWN | + | DOWN | +/- | 15q26 specific |
| NR2F2 | - | - | - | + | UP (DFC1) | UP | Patients don't match; other mechanism? |
| RA induced | | | | | | | Conclusion |
| Diff. expressed | Rank p-value | Array Result | | Quantitative q-PCR result | | Conclusion | |
| | | Normal | 15q26 | Normal | 15q26 | | Isolated CDH |
| EDNRA* | 1 | DEFAULT | (insufficiently) DOWN | DEFAULT + | insufficiently DOWN | not tested | 15q26 specific |
| RA pathway-RA induced | | | | | | | Conclusion |
| Diff. expressed | Rank p-value | Array Result | | Quantitative q-PCR result | | Conclusion | |
| | | Normal | 15q26 | Normal | 15q26 | | Isolated CDH |
| CRABP1* | 6 | + | UP | + | UP | +/- | 15q26 specific |
| CYP26A1* | 67 | + | UP | - | - | - | assay not possible |

* Filtered & Prioritized by multiple testing correction and Endavour [<http://homes.esat.kuleuven.be>]

Blue colored: Genes associated in literature with major anomalies of the 15q26 phenotype

Red colored: Genes putatively related to the specific lung defects in 15q26 monosomy patients

Default: Differentially Expressed between Patients and Controls at default

RA: induced Genes up or down-regulated in patient samples upon RA and differentially expressed compared to controls

by RT-qPCR analysis for *TTC23* (Table 3). In case of *NR5A2* – highlighted at default by gene-prioritization – mRNA levels continued to be relatively lower in patient samples irrespective of RA stimulation. In case of *EDNRA* – the gene associated with CDH in literature – RT-qPCR analysis pointed to a 15q26 specific RA-effect.

Considering the hypothesized insensitivity of 15q26 cases to RA-stimulation, we also looked at RA-responsive genes whose mRNA levels were not significantly different between the two groups at default. Three members of the RA signalling pathway – including two of its key-players: that is Cellular Retinoic Acid Binding Protein I (CRABPI) and Cytochrome-P450 Protein 26A1(CYP26A1) -could be attributed to this group. Verification of array results with Q-PCR confirmed that CRABPI was relatively up-regulated in patients only. Unfortunately due to abundant SNP-Polymorphisms, we could not develop an appropriate assay for CYP26A1 (Table 3). ANKyrin Repeat Domain 37 (*ANKRD 37*) on chromosome band 4q35.1 was relatively up-regulated in patients upon RA as well, which could result from the duplication of this chromosomal area in *DFC2*. Since no embryonic function is allocated to this gene and since it is mainly expressed in tissues not associated with the 15q26 phenotype, a clear correlation to CDH is unlikely [Biobase Knowledge library, GmbH, Wolfenbuettel, Germany].

Finally, analogous to the default situation, cell growth and proliferation constituted a significant theme in the RA-induced lists, however only with partly overlapping gene members (*Cdc25B*, *Ccna2*; controlling G2/M phase transition).

Discussion

Patients with CDH form a heterogeneous group both genetically and phenotypically. Chromosomal aberrations are now detected in 20-30% of human cases and some of these recurrent, structural anomalies point to CDH associated loci and genes (*NR2F2*, *ZFPM2*, *GATA4*) involved in the RA signalling pathway [21, 44]. In this study we hypothesized that genes in the 15q26 region – the most frequent and strongest CDH-associated chromosomal hot spot in humans – are important for both diaphragm development as well as for RA-signalling. We suggested that RA-treatment could normalize aberrant default gene expression profiles of 15q-deleted dermal fibroblasts. In addition, these cell cultures could be instrumental for the delineation of the molecular pathways disrupted in the co-occurring lung defects.

In the default state, 378 genes were differentially expressed between control- and 15q26 deleted- dermal fibroblasts. Some of these genes encoded proteins previously associated with CDH in literature (Table 1); others could be connected to the co-occurring anomalies of the 15q26 monosomy phenotype. Below we briefly discuss point by point the candidate genes highlighted in our enrichment analysis (Table 1).

From the CDH 15q26 “critical region” (Figure S1) only two significantly down-regulated gene transcripts were identified, *TTC23* and *LRR28* (Figure S1). This result does not coincide with the hypothesized dosage-response mechanism for genes in this region. In other words, there was

no enrichment of distal 15q genes in patients versus controls overall, implicating that a putative phenotypic effect of this region is exerted through alternative genetic disruption mechanisms (at least in the investigated cell lines). Recently several groups stressed on the occurrence of expression level changes of genes in the boundary-regions of CNVs and also on the importance of long-range position effects of CNVs [45, 46]. These studies imply that identification of the true 15q-CDH-causative gene might be less straightforward than previously expected, which is supported by our data. Because no *TTC23* mRNA levels were detected in an embryonic rodent diaphragm model, a causative role for this gene in CDH is less likely [10]. In contrast, *LRRC28* mRNA expression was shown throughout diaphragm development in the same study, however immuno-histochemical validation was not performed due to lack of commercial antibodies. Since the function of this gene is not understood, it is difficult to speculate on its role in CDH. *NR2F2* - the strongest hypothesized 15q CDH-candidate – displayed aberrant gene expression levels irrespective of RA-stimulation in one out of two patients. Surprisingly, this gene presented with an opposite expression response based on the haplo-insufficient mechanism that is generic to all 15qter deletion cases (whether they are a consequence of a pure monosomy or not). In general, expression responses in the opposite direction are seen in 10% of the total number of transcripts situated in a copy number variant [45]. An increase of NR2F2 protein in DFC1 could lead to competition for dimerization with the nuclear RA-receptor and thereby exert a RA-diminishing effect (Figure 3). Interestingly, *NR5A2* – highlighted in the default list by gene-prioritization - is also linked to inhibition of RA signalling and might enhance NR2F2s' repression of the nuclear RA-pathway [50] (Figure 3). Moreover, NR5A2 is known for its crucial role in mesodermal genesis early during embryonic development [42, 43] and could provide a link to the mesenchymal hit hypothesis of CDH [51]. The dissimilar *NR2F2* mRNA responses within the patient group could be caused by a difference in translocation type and/or by a difference in 15q26 deletion size. Recently a 15q26 monosomy CDH case was described without deletion of the *NR2F2* gene [47] emphasizing that additional genetic factors have to play a role in its associating diaphragmatic defects.

Proliferation kinetics in mesenchymal-derived primordial diaphragm cells – and possibly also in their associating lung cells [48] – is thought to be disrupted in CDH [16]. Therefore it is highly interesting that non-supervised pathway analysis revealed the cell cycle process as one of the major deregulated processes in 15q26-deleted dermal fibroblasts (Table 1). These putative defects in cell rate should be studied further using immunohistochemistry staining with mitotic-specific antibodies.

The significantly different default levels in DFC 1 and 2 of genes such as *NR5A2*, *HAS3*, *CNN1*, *EDNRA*, *GPC4* and *ANPEP* (Table 2), emphasize on the involvement of *early developmental* master regulators in diaphragm development. Default results also pointed to several new lung vascular (*RGS4*, *ANPEP*, *CNN1*) factors. We speculate that in the 15q monosomy cases, the same genetic disturbances target similar cell types (mesenchymal origin) and cell-processes (cell proliferation) of both lung- and diaphragm development. Concerning these co-occurring lung abnormalities, we briefly discuss the TOP-differentially expressed genes *EDNRA* and *RGS4*.

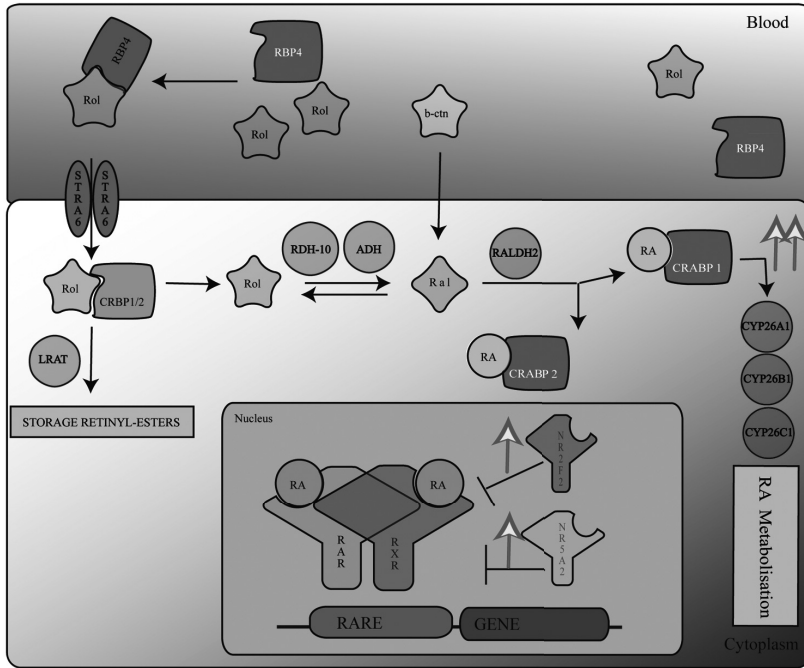


Figure 3 | RA metabolism and RA signalling in 15q26 fibroblasts

The intracellular processing of Retinoic Acid (RA) involves two different pathways. Firstly, RA can be transported to CYP26-proteins by CRABP1 and will then be metabolized into polar substances. Secondly, it can bind to CRABP2 and be transported to the nucleus. In the nucleus RA can bind to the Retinoic Acid Receptor (RAR)/Retinoid X Receptor (RXR) heterodimer, which in turn binds to a Retinoic Acid Response Element (RARE) located in the promoter area of specific genes. This complex can activate/inhibit transcription.

CRABP1 has a higher affinity for RA compared to CRABP2. Therefore, up regulation of CRABP1 in 15q26 deletion-patients favors RA metabolism over nuclear RA signalling. CYP26A1 was expressed at a higher level in the patient group as well. Elevated levels of NR2F2 (in DFC1) and NR5A2 might further reduce nuclear RA signalling.

Rol, retinol; RBP, retinol binding protein; STRA6, stimulated by retinoic acid 6; CRBP, cellular retinol binding protein; RaI, retinaldehyde; ADH, alcohol dehydrogenase; RALDH, retinaldehyde dehydrogenase; CYP26, cytochrome P450 26 enzymes; RAR, retinoic acid receptor; RXR, retinoid X receptor; RARE retinoic acid response element. B-ctn, beta-carotene; LRAT, Lecithin retinol acyltransferase, NR2F2; Nuclear receptor 2, subfamily F2; NR5A2, Nuclear Receptor 5, subfamily A2.

Expression alterations of *EDNRA* at default were specific for DFC 1 and 2. This gene was strongly down-regulated upon RA-treatment, however failed to return its mRNA levels to normal. We speculate that *EDNRA* might have a dual role in the 15q-monosomy phenotype by disrupting both craniofacial development as well as lung development. *Ednra*^{-/-} embryos die at birth from severe craniofacial defects resulting from disruption of neural crest cell patterning and differentiation [52]. Moreover, a small study using a chemically induced CDH rodent model, demonstrated altered *EDNRA* levels in lung tissue [34]. In lung material of cystic fibrosis patients, polymorphisms in *EDNRA* were associated with aberrant smooth muscle cell proliferation rates [53]. Regulator of G protein signalling 4 (*RGS4*) is also associated with lung ontogenesis. Albig

and colleagues [40] demonstrated that RGS4 overexpression delayed and altered lung epithelial cell tubulation by selectively inhibiting G protein-mediated p38 MAPK activation. This in turn, reduces epithelial cell proliferation, migration and expression of vascular endothelial growth factor (*VEGF*). Similarly, it abrogated endothelial cell angiogenic sprouting. Default levels of RGS4 mRNA were up-regulated in both dermal- as well as diaphragm- patient cultures. In addition, we tested the expression of this gene in lung material of five non-related, isolated CDH patients and found that it was strongly up-regulated in three of them. As a potential new early contributor of CDH lung pathophysiology, immunohistochemistry confirmation of RGS4 is warranted.

Genes encoding proteins involved in the RA-signalling cascade were not significantly different expressed between the two groups at default. This could suggest that only subtle disruptions of RA-signalling play a role in 15q26 associated diaphragm maldevelopment. This principle may also apply to CDH patients in general and is reflected in results from literature; only few complex human CDH cases [21, 22] have been directly ascribed to major genetic defects in crucial RA genes. No such key RA-mutations are identified in isolated CDH cases so far. Alternatively, the hypothesized relative RA-deficiency may only become apparent in periods of transient high-demand for RA [15].

To test the hypothesis of subtle RA-disturbances in 15q-deleted patients, we stimulated dermal fibroblasts from two 15q26 monosomy cases (and its two sex-matched controls) with four different concentrations of RA. Consequently, only deregulations positioned in the metabolic and/or downstream nuclear components of the retinoid pathway will be picked up by this approach. In line with this view, a key component of RA homeostasis, Cellular Retinoic Acid Binding Protein type 1 (*CRABP1*) was profoundly up-regulated after stimulation in 15q deleted cell lines. This effect was proven to be 15q-specific by quantitative RT-PCR comparison to isolated CDH cases. Another key component of RA metabolism, *CYP26A1* was increased as well, while none of the critical 15q26-deleted genes were significantly induced or repressed in response to RA. More specifically, there was a relative up-regulated expression of RA-components that function to increase the intracellular metabolism of RA at the cost of downstream nuclear RA-signalling under conditions of high RA-load (Figure 3). A relative RA-deficiency and consequent misbalance in RA-induced transcription regulation (possibly of developmental genes) might be the result. This RA-stimulation experiment mimics the well-known and transient increased demand for retinoic acid specifically in the trunk of the embryo at the critical period of diaphragm development [49]. Further experiments using dermal fibroblasts or amniotic cells of a large cohort of isolated CDH patients have to be performed to address whether subtle RA-insensitivity plays a role in these cases as well. Targeted disruption of the synthesizing part of the RA-signalling “arm” should be executed to check whether an absolute hypo-vitaminose could be of influence instead. Finally, since Clugston et al. [15] demonstrated that CRABPI is only expressed in the cytoplasm of neural crest cells of the primordial rodent diaphragm, it is crucial to investigate these specific patterns during human diaphragm development. In contrast, CRABPII was expressed abundantly throughout the rodent primordial diaphragm.

In conclusion, the diaphragmatic- and pulmonary defects of CDH could be causally linked on a cellular and molecular level. Our study suggests that RA-signalling disruption in complex 15q26-associated CDH is subtle and involves not only an altered expression of genes from the deleted region but also key factors of the RA pathway and of mesenchymal- and lung- development. Finally, simple haploinsufficiency of genes in the smallest region of overlap cannot fully explain the patho-phenotypic potential of the 15q26 monosomy.

References

1. Sluiter, I., et al., *Congenital diaphragmatic hernia: Still a moving target*. Seminars in fetal & neonatal medicine, 2011. **5**(2): p. 245.
2. Klaassens, M., et al., *Prenatal detection and outcome of congenital diaphragmatic hernia (CDH) associated with deletion of chromosome 15q26: two patients and review of the literature*. Am J Med Genet A, 2007. **143A**(18): p. 2204-12.
3. Scott, D.A., et al., *Genome-wide oligonucleotide-based array comparative genome hybridization analysis of non-isolated congenital diaphragmatic hernia*. Human molecular genetics, 2007. **16**(4): p. 424-30.
4. Wat, M.J., et al., *Genomic alterations that contribute to the development of isolated and non-isolated congenital diaphragmatic hernia*. Journal of medical genetics, 2011. **48**(5): p. 299-307.
5. Biggio, J.R., Jr., et al., *Congenital diaphragmatic hernia: is 15q26.1-26.2 a candidate locus?* American journal of medical genetics. Part A, 2004. **126A**(2): p. 183-5.
6. Veenma, D.C., et al., *Phenotype-genotype correlation in a familial IGF1R microdeletion case*. J Med Genet, 2010. **47**(7): p. 492-8.
7. Slavotinek, A.M., *Gene reviews: Fryns syndrome*, in *Fryns Syndrome* B.T. Pagon RA, Dolan CR, et al, Editor 2010: Seattle.
8. You, L.R., et al., *Mouse lacking COUP-TFII as an animal model of Bochdalek-type congenital diaphragmatic hernia*. Proc Natl Acad Sci U S A, 2005. **102**(45): p. 16351-6.
9. Slavotinek, A.M., et al., *Array comparative genomic hybridization in patients with congenital diaphragmatic hernia: mapping of four CDH-critical regions and sequencing of candidate genes at 15q26.1-15q26.2*. European journal of human genetics : EJHG, 2006. **14**(9): p. 999-1008.
10. Clugston, R.D., W. Zhang, and J.J. Greer, *Gene expression in the developing diaphragm: significance for congenital diaphragmatic hernia*. Am J Physiol Lung Cell Mol Physiol, 2008. **294**(4): p. L665-75.
11. Goumy, C., et al., *Fetal skin fibroblasts: A cell model for studying the retinoid pathway in congenital diaphragmatic hernia*. Birth Defects Res A Clin Mol Teratol.
12. Greer, J.J., R.P. Babiuk, and B. Thebaud, *Etiology of congenital diaphragmatic hernia: the retinoid hypothesis*. Pediatr Res, 2003. **53**(5): p. 726-30.
13. Wilson, J.G., C.B. Roth, and J. Warkany, *An analysis of the syndrome of malformations induced by maternal vitamin A deficiency. Effects of restoration of vitamin A at various times during gestation*. Am J Anat, 1953. **92**(2): p. 189-217.
14. Babiuk, R.P., B. Thebaud, and J.J. Greer, *Reductions in the incidence of nitrofen-induced diaphragmatic hernia by vitamin A and retinoic acid*. Am J Physiol Lung Cell Mol Physiol, 2004. **286**(5): p. L970-3.
15. Clugston, R.D., et al., *Understanding Abnormal Retinoid Signalling as a Causative Mechanism in Congenital Diaphragmatic Hernia*. Am J Respir Cell Mol Biol, 2009.
16. Clugston, R.D., W. Zhang, and J.J. Greer, *Early development of the primordial mammalian diaphragm and cellular mechanisms of nitrofen-induced congenital diaphragmatic hernia*. Birth Defects Res A Clin Mol Teratol. **88**(1): p. 15-24.
17. Ackerman, K.G., et al., *Fog2 is required for normal diaphragm and lung development in mice and humans*. PLoS Genet, 2005. **1**(1): p. 58-65.
18. Jay, P.Y., et al., *Impaired mesenchymal cell function in Gata4 mutant mice leads to diaphragmatic hernias and primary lung defects*. Dev Biol, 2007. **301**(2): p. 602-14.
19. Norden, J., et al., *Wt1 and retinoic acid signalling in the subcoelomic mesenchyme control the development of the pleuropericardial membranes and the sinus horns*. Circ Res. **106**(7): p. 1212-20.
20. Mark, M., N.B. Ghyselinck, and P. Chambon, *Function of retinoic acid receptors during embryonic development*. Nucl Recept Signal, 2009. **7**: p. e002.
21. Holder, A.M., et al., *Genetic factors in congenital diaphragmatic hernia*. Am J Hum Genet, 2007. **80**(5): p. 825-45.
22. Chassaing, N., et al., *Phenotypic spectrum of STRA6 mutations: from Matthew-Wood syndrome to non-lethal anophthalmia*. Hum Mutat, 2009. **30**(5): p. E673-81.

23. Segel, R., et al., *Pulmonary hypoplasia-diaphragmatic hernia-anophthalmia-cardiac defect (PDAC) syndrome due to STRA6 mutations--what are the minimal criteria?* Am J Med Genet A, 2009. **149A**(11): p. 2457-63.
24. Beurskens, L.W., et al., *Retinol status of newborn infants is associated with congenital diaphragmatic hernia.* Pediatrics. **126**(4): p. 712-20.
25. Major, D., et al., *Retinol status of newborn infants with congenital diaphragmatic hernia.* Pediatr Surg Int, 1998. **13**(8): p. 547-9.
26. Rajatapiti, P., et al., *Spatial and temporal expression of glucocorticoid, retinoid, and thyroid hormone receptors is not altered in lungs of congenital diaphragmatic hernia.* Pediatric research, 2006. **60**(6): p. 693-8.
27. Illumina, I., *GenomeStudio™ Gene Expression Module v1.0 User Guide*, 2004-2008, Illumina, Inc.
28. Illumina, I., *BeadStudio Normalization Algorithms for Gene Expression Data Technical Note*, 2007 Illumina.
29. Jelier, R., et al., *Anni 2.0: a multipurpose text-mining tool for the life sciences.* Genome Biol, 2008. **9**(6): p. R96.
30. Boehm D, Herold S, Kuechler A, Liehr T, Laccone F. *Rapid detection of subtelomeric deletion/duplication by novel real-time quantitative PCR using SYBR-green dye.* Balmer, J.E. and R. Blomhoff, *Gene expression regulation by retinoic acid.* J Lipid Res, 2002. **43**(11): p. 1773-808.
31. Dingemann, J., et al., *Upregulation of endothelin receptors A and B in the nitrofen induced hypoplastic lung occurs early in gestation.* Pediatr Surg Int, 2010. **26**(1): p. 65-9.
32. Rutenstock, E., et al., *Downregulation of insulin-like growth factor binding protein 3 and 5 in nitrofen-induced pulmonary hypoplasia.* Pediatr Surg Int, 2010. **26**(1): p. 59-63.
33. Burgos, C.M., et al., *Gene expression analysis in hypoplastic lungs in the nitrofen model of congenital diaphragmatic hernia.* J Pediatr Surg, 2010. **45**(7): p. 1445-54.
34. Lu, J.R., et al., *Control of facial muscle development by MyoR and capsulin.* Science, 2002. **298**(5602): p. 2378-81.
35. Miyagishi, M., T. Nakajima, and A. Fukamizu, *Molecular characterization of mesoderm-restricted basic helix-loop-helix protein, POD-1/Capsulin.* International journal of molecular medicine, 2000. **5**(1): p. 27-31.
36. Lukosiute, A., et al., *Down-regulation of lung Kruppel-like factor in the nitrofen-induced hypoplastic lung.* European journal of pediatric surgery, 2011. **21**(1): p. 38-41.
37. Doi, T., et al., *Prenatal treatment with retinoic acid activates parathyroid hormone-related protein signalling in the nitrofen-induced hypoplastic lung.* Pediatr Surg Int, 2011. **27**(1): p. 47-52.
38. Doi, T., et al., *Disturbance of parathyroid hormone-related protein signalling in the nitrofen-induced hypoplastic lung.* Pediatr Surg Int, 2010. **26**(1): p. 45-50.
39. Albig, A.R. and W.P. Schiemann, *Identification and characterization of regulator of G protein signalling 4 (RGS4) as a novel inhibitor of tubulogenesis: RGS4 inhibits mitogen-activated protein kinases and vascular endothelial growth factor signalling.* Molecular biology of the cell, 2005. **16**(2): p. 609-25.
40. Kaminski, N., et al., *Global analysis of gene expression in pulmonary fibrosis reveals distinct programs regulating lung inflammation and fibrosis.* Proc Natl Acad Sci U S A, 2000. **97**(4): p. 1778-83.
41. Gu, P., et al., *Orphan nuclear receptor LRH-1 is required to maintain Oct4 expression at the epiblast stage of embryonic development.* Molecular and cellular biology, 2005. **25**(9): p. 3492-505.
42. Labelle-Dumais, C., et al., *Nuclear receptor NR5A2 is required for proper primitive streak morphogenesis.* Developmental dynamics : an official publication of the American Association of Anatomists, 2006. **235**(12): p. 3359-69.
43. Klaassens, M., A. de Klein, and D. Tibboel, *The etiology of congenital diaphragmatic hernia: still largely unknown?* Eur J Med Genet, 2009. **52**(5): p. 281-6.
44. Ricard, G., et al., *Phenotypic consequences of copy number variation: insights from Smith-Magenis and Potocki-Lupski syndrome mouse models.* PLoS biology, 2010. **8**(11): p. e1000543.
45. Henrichsen, C.N., E. Chaignat, and A. Reymond, *Copy number variants, diseases and gene expression.* Human molecular genetics, 2009. **18**(R1): p. R1-8.

46. Mosca, A.L., et al., *Refining the critical region for congenital diaphragmatic hernia on chromosome 15q26 from the study of four fetuses*. *Prenat Diagn*, 2011.
47. van Loenhout RB, T.I., Fox EK, Huang Z, and P.M. Tibboel D, Keijzer R, *The pulmonary mesenchymal tissue layer is defective in an in vitro recombinant model of nitrofen-induced lung hypoplasia*. *Am J Pathol*, 2011(Accepted Sept 6th 2011).
48. Takahashi, Y.I., J.E. Smith, and D.S. Goodman, *Vitamin A and retinol-binding protein metabolism during fetal development in the rat*. *The American journal of physiology*, 1977. **233**(4): p. E263-72.
49. Kruse, S.W., et al., *Identification of COUP-TFII orphan nuclear receptor as a retinoic acid-activated receptor*. *PLoS biology*, 2008. **6**(9): p. e227.
50. Bielinska, M., et al., *Molecular genetics of congenital diaphragmatic defects*. *Ann Med*, 2007. **39**(4): p. 261-74.
51. Ruest, L.B. and D.E. Clouthier, *Elucidating timing and function of endothelin-A receptor signalling during craniofacial development using neural crest cell-specific gene deletion and receptor antagonism*. *Developmental biology*, 2009. **328**(1): p. 94-108.
52. Darrah, R., et al., *EDNRA variants associate with smooth muscle mRNA levels, cell proliferation rates, and cystic fibrosis pulmonary disease severity*. *Physiological genomics*, 2010. **41**(1): p. 71-7.

Chapter 3.3

***NR2F2* Promoter Interactions in Diaphragm Development: Chromosome Conformation Capture-Sequencing (4C-Seq) in a Rodent Model of Congenital Diaphragmatic Hernia (CDH)**

D.Veenma , R.Palstra, T.Brands, E.de Wit, M.Vermeij, C.Cockx, R.Brouwer,
B.Eussen, I.Sluiteer, R.Rottier, W.van IJcken, W.de Laat , D.Tibboel and A.de Klein

Manuscript under review by co-authors

Supplementary files available on request

Abstract

The pathogenetic mechanisms causing diaphragm- and lung-defects in patients with congenital diaphragmatic hernia (CDH) are largely unknown. Several human and knockout mice studies provided strong evidence for involvement of the *NR2F2* gene, which encodes an orphan nuclear transcription factor that is implicated in embryonic retinoic-acid (RA) signalling and is crucial for mouse organogenesis. We used chromosome conformation capture sequencing technology (4C-seq) to map the genome-wide interaction pattern of *NR2F2* in four different tissues of the nitrofen rodent CDH-model.

4C data in control rodent embryonic day E17 (E17) demonstrated that, despite differences in the activation level of the *NR2F2* gene, the spatial environment of the *NR2F2* locus was grossly similar across all samples. The gene-poor *NR2F2* region interacted mainly with other gene poor regions. Subtle differences for specific interactions were demonstrated in lungs and diaphragm upon nitrofen induction and pointed to new CDH candidate genes such as *PPP2R1A*. Its protein PP2A is known for its role in fetal kidney development and has an expression pattern similar to the CDH gene *WT1*. RT-qPCR analysis confirmed active transcription in rodent E17 lung and diaphragm and showed that expression levels decreased upon nitrofen-treatment.

Analysis of the most abundant interaction partners of *NR2F2* across all 4C samples identified one specific domain on chromosome 14 which harboured the developmentally involved *PCDH7* and *UGDH* genes. In general, *NR2F2*-interaction partners were mainly involved in cell- growth and -death, both key processes in embryogenesis. Finally, the OCT1 protein was recognised as the common regulatory source of *NR2F2* promoter interactions by computational analysis of transcription factor bindings sites.

In conclusion, using 4C technology we identified new CDH candidate genes that might function with *NR2F2* during diaphragm development.

Introduction

Congenital diaphragmatic hernia (CDH) is a severe birth defect characterized by defective formation of the diaphragm, pulmonary hypoplasia and pulmonary hypertension. It accounts for 8% of all major congenital defects and has a mortality rate of 20-60% [1]. CDH is presumed to have a multifactorial aetiology, yet its individual contributing factors are still largely unknown [2]. Using molecular cytogenetic techniques, chromosomal aberrations are now detected in 20-30% of human cases and some of these recurrent, structural anomalies point to CDH associated loci and genes (*NR2F2*, *ZFPM2*, *GATA4*) involved in the Retinoic Acid (RA) signalling pathway [3-5]. Various animal studies – using nutritional, teratogenic and genetic knockout approaches – already emphasized on this putative link between disrupted vitamin-A signalling and diaphragm defects (the “retinoid hypothesis”) [6-9]. Moreover, at the epidemiological level, our group recently confirmed in human cases the association between CDH and low serum retinol or retinol-binding protein levels, independent of maternal vitamin-A status [10].

The *Nuclear Receptor subfamily 2, group member F2 (NR2F2)* gene encodes an orphan nuclear transcription factor that is expressed abundantly in the mesenchymal compartment of developing organs. It is known for its crucial role in mouse embryogenesis (reviewed by Lin et al. [11]) and was recently implicated in embryonic stem cell state maintenance and -differentiation [12]. Germ-line inactivation of *Nr2f2* in mice (alias *Couptf-II*) causes embryonic lethality with defects in angiogenesis and heart development [13]. In contrast, *Nr2f2* heterozygous mice are viable, but display defects in mesoderm-derived tissues including fat, muscle and the reproductive tract. An important function for this gene in diaphragm development is implicated by conditional knock out studies showing a postero-lateral diaphragmatic defect – the most common type of CDH – in offspring after tissue-specific ablation of *Couptf-II* in foregut mesenchyme [14]. *NR2F2* is also expressed at various developmental stages of *rodent* diaphragm development [15]. Interestingly, several studies demonstrated a direct role for *NR2F2* in RA signalling [16, 17], thereby underlining a possible link between *NR2F2* malfunctioning and the “retinoid hypothesis” of CDH. Moreover, *NR2F2* is positioned in the most frequent CDH associated chromosomal hot spot described in humans to date: the 15q26 monosomy [18]. In this study we hypothesized that a changed nuclear environment of *NR2F2* is involved in CDH pathogenesis. To test this theory we applied chromosome conformation capture technology (4C) to embryonic tissues of both wild type and nitrofen CDH-induced rat embryos. 4C allows for screening the genome in an unbiased manner for DNA regions that are in close contact in the three-dimensional nuclear space to a region of interest, in our case the promoter region of *NR2F2* [19].

Analysis of the spatial organisation of the interphase nucleus by means of complementary microscopy-3D FISH studies and chromosome conformation capture technology revealed the occurrence of a complex three-dimensional network of chromosomal interactions [20-23]. These interactions were shown to occur between target genes and distant regulatory units – both in-cis and in-trans – and are hypothesized to affect – or reflect – gene expression regulation at multiple levels. Coordinated expression and interaction of multiple – functionally similar –

genes mediated by transcription factors has been suggested also [24, 25]. Therefore, knowledge of *NR2F2*'s DNA association partners during embryogenesis both in a healthy control state as well as upon interference with RA signalling, may provide better insights into the pathogenetic mechanisms of CDH. To accomplish this, we used the 4C technique and mapped the genome-wide interaction patterns of *NR2F2* in several tissues of a teratogenic RA-signalling disrupting rat CDH-model. Administration of the herbicide nitrofen® (2,4-dichlorophenyl-p-nitrophenyl) during pregnancy induces congenital anomalies including diaphragm defects in offspring [26]. Inhibition of the intracellular RA synthesizing enzyme, retinaldehyde dehydrogenase 2 (RALDH2) has been hypothesized as its mechanism of action [27]. We reasoned that disruption of vitamin-A signalling in nitrofen treated offspring would induce a global change in the interaction pattern of the *NR2F2*-promoter as compared to untreated embryos, especially in those tissues affected by CDH i.e. the diaphragm and lungs. Interactions of *NR2F2* in heart- and liver served as non-CDH specific controls. 4C results showed that the spatial environment of the *NR2F2* locus was grossly similar for all tissues investigated implicating that the majority of identified interactions are non-functional. In contrast, subtle changes were shown upon nitrofen induction and pointed to several new putative interaction partners of *NR2F2*. The corresponding transcriptional responses of these loci – as analysed by RT-qPCR – suggest that these changes might be of functional importance in the development of the CDH-affected organs.

Material and methods

Tissue collection

Pregnant Sprague-Dawley rats were ordered from Harlan laboratories® (Horst, the Netherlands) and shipped at embryonic day E7 of gestation (term = day E21). Nitrofen-treatment and fetal delivery at embryonic day E17 were executed as previously described [28].

The Animal Welfare committee of Erasmus MC in Rotterdam (the Netherlands) approved for tissue dissection (protocol number 138-09-09). Subsequently, we obtained the residue tissue of lung, heart, liver and diaphragm.

Two independently dissected Sprague-Dawley nests were used in each group; control and nitrofen-treated respectively. In case of nitrofen administration we only included tissue of those embryos that displayed a diaphragm defect, yielding 8 and 13 adequate embryos respectively. For controls the number of pups encompassed 14 and 15 respectively. In addition, biological replicates were generated for nitrofen induced-lung and -diaphragm tissues in a separate and third isolation.

4C technology

The 4C-seq assay was performed as previously described [19, 29] with minor modifications. Briefly, pooled rodent tissue collections of heart, lung, diaphragm and liver were collagenase treated for 1 hour and meshed for production of a single cell suspension. These suspensions

were then fixed with 2% formaldehyde in PBS for 10 min at room temperature. The reaction was quenched by adding ice-cold glycine in a final concentration of 125 mM, followed by a quick wash with cold PBS. Each tissue-pellet was subsequently placed into ice-cold cell lysis buffer (50mM Tris-pH 7.5, 150mM NaCl, 5mM EDTA, 0.5% Nonidet P40, 1% Triton-X100, 1x Complete protease inhibitor) and cells were disrupted by repetitively pipetting up and down several times. Finally, nuclei were centrifuged for 5 minutes with 1800 rpm at 4°C and supernatant was re-moved afterwards. Pellets were instantly freezed in liquid nitrogen and stored at -80°C for less than 3 months.

Frozen pellets of dissected embryos were pooled and used as input for the 4C-procedure. The restriction enzyme Bgl-II (Roche applied science, Almere, the Netherlands) was used to digest the chromatin. Linked Bgl-II fragments were preferentially ligated under dilute conditions followed by de-crosslinking and purification of DNA. The resulting BglII 3C library was digested with NLA-III four-base restriction enzyme (Roche) and 4C circular DNA molecules were generated by ligation under dilute conditions. Next, DNA fragments that interacted specifically with the *NR2F2* promoter were PCR amplified using *NR2F2* promoter specific divergent primers (Forward primer (plus strand) = 5' TGC AAG TCG ATT GTC TGG CTT 3', Reverse primer (plus strand) = 3' CCG CCT CAA AAA GTG CCT CA 5'). These primers were linked to adaptor-sequences (Illumina Inc., San Diego, USA) necessary for sequencing in addition to a four base index code for multiplexing several samples in one lane. PCR reactions were performed directly on the circularized 4C templates in a strictly linear fashion using the Expand Long Template PCR system (Roche applied science, Almere, the Netherlands). Finally, end products of 6 PCR reactions were pooled and purified using the QIA quick nucleotide removal system (Qiagen Benelux B.V., Venlo, the Netherlands).

4C-sequencing

5 pM of purified 4C-library per sample were sequenced on the Illumina Hiseq 2000 platform (Illumina Inc., San Diego, USA) generating 101 basepair reads. Images were recorded and analysed by the complementing Illumina Genome Analyzer Pipeline (GAP). Sequences were mapped against the rodent genome – build Baylor 3.4, November 2004 – using the ELAND alignment software (Illumina Inc., San Diego, USA).

The proportional distribution of reads identified in each tissue sample can be found in Table SI, depicting both the percentage of peaks mapping to chromosome 1 and to the remainder of the genome. Next, we determined the absolute amount of sequence reads per Bgl-II fragment, which were then normalised for sequence depth to allow inter-sample comparisons. To test for reproducibility two biological replicate libraries of nitrofen treated-lung and -diaphragm tissue were run and analysed on the Illumina Hiseq2000 platform.

Statistical analysis of 4C-seq data

4C data was analysed using the R programme language [<http://www.R-project.org>] and a slightly adjusted standardized 4C-seq analysis pipeline as recently described [34]. Briefly, this analysis workflow is based on the assumption that reliable interactions can only be detected as

genomic clusters of multiple restriction fragments with increased signals [30]. Moreover, since the coverage declines as a function of the distance from the viewpoint, it needs to be normalised for the background coverage. For this purpose, Z-scores were calculated for a given window of fragment ends l , and of size w , analogous to Splinter et al. [31]. Similarly, non-random 4C signals in-cis were identified using a false discovery rate (FDR) of 0.01 after randomly permutating the data set 100 times. For the trans interactions, an FDR threshold of 0.01 was determined based on 1000 random permutations of the data for every chromosome at a window size of 500. Since this window size is usually arbitrarily chosen, the identification of interacting regions is limited to a certain size. To circumvent this problem, the group of de Wit et al. also developed a multi-scale algorithm that evaluates the statistical significance at all possible window sizes resulting in so-called DNA-interacting domainograms (DID). In this way, statistically significant interactions can be visualised at all scales. In addition, to identify the exact boundaries of the interacting regions in the domainograms, the “dynamic programming algorithm” [32, 33] was applied. The resulting most specific hits in each sample were then visualized using custom made tracks in the UCSC browser [<http://genome.ucsc.edu/>] and an in-house 3D visualization tool [34].

Correlation analysis between tissue samples

The hypothesized differences between diseased (nitrofen-treated) tissues and controls, were calculated using the Spearman’s coefficient of rank correlation (r) between a total set of Z scores of two 4C experiments, analogous to Splinter et al. [31].

Down-and up-stream enrichment analysis of DIDs

Table S2 presents an overview of the general characteristics of the significant interacting domains in each sample determined using several annotation tracks downloaded from the University of California at Santa Cruz (USCS) Table browser. Ingenuity Pathway Analysis (IPA) software (Ingenuity Systems Inc. Redwood City, CA) was used to identify enriched cellular functions putatively executed by the *NR2F2* promoter region and its interacting DNA elements. Upstream promoter analysis of genes in close proximity of *NR2F2* was performed using ExplainTm (Biobase GmbH, Wolfenbuettel, Germany). Statistically significant enriched binding sites were defined by a yes versus no ratio above three (yes/no>3.0) and p-values less than 0.001 according to the manufacturer’s instructions.

RNA isolation and NR2F2 expression analysis using relative RT-PCR

RNA extraction was performed using the Qiagen-mini RNAeasy kit according to the manufacturers instructions (Qiagen Benelux B.V., Venlo, the Netherlands). For each tissue type, total RNA was prepared using as input material of 5-6 embryos at embryonic stage E17. Subsequently, 1 microgram of total RNA was converted to cDNA by a commercially available kit (iScript, Bio-Rad Laboratories, Inc, Hercules, California, USA).

Primer pairs (Table S3) for quantitative RT-PCR were designed at the intron-exon junctions of the rodent *NR2F2*-sequence (Primer Express software v2.0, Applied Biosystems, Carlsbad, California, USA). Reactions were performed in triplet according to the standard curve method as described by Boehm et al. [35], using an ABI7300 Real-time PCR system in combination with KAPA-SYBR fast master mix (KapaBiosystems, Woburn, MA, USA) and 0.6 μ l of each cDNA product per well. A region of the *S18R* gene served as a control locus. RT-PCR experiments for the *NR2F2* interacting genes; *PCDH7*, *UGDH* and *PPP2R1A* as well as for *OCT1*, were executed in the same way.

Results

4C technology was applied to four types of tissue (diaphragm, lung, heart and liver) obtained from all available offspring of two healthy Sprague-Dawley nests at embryonic day E17. To enable a detailed study of the putative conformational differences of the *NR2F2* promoter in nitrofen-induced CDH, this procedure was repeated after administration of nitrofen at embryonic day E9. 4C assays allow for screening the genome in an unbiased manner for DNA regions that are in close contact in the three-dimensional nuclear space to a region of interest. 4C PCR end products were run on an Illumina HiSeq2000 platform and analysed using the 4C-sequence specific analysis pipeline adopted from Splinter et al. [31].

NR2F2 transcriptional levels at rodent stage E17

To replicate and validate earlier reported *NR2F2* expression in lung- and diaphragm- material of healthy Sprague-Dawley offspring [36], we first performed quantitative PCR analysis of this gene at embryonic day E17. Levels were compared to those determined in control -heart and -liver tissue. Additionally, adult spleen RNA was isolated from the maternal rat and used as a known low *NR2F2*-expressed control [www.genecards.org]. Results demonstrated that in day E17-control livers, *NR2F2* was expressed at a similar level as adult spleen and therefore employed as an internal low-expressed embryonic control in subsequent experiments (data not shown). The relative mRNA expression levels of *NR2F2* in each healthy tissue are illustrated in Figure 1 and compared to the levels upon nitrofen treatment. *NR2F2* is expressed at significantly higher levels in control diaphragm and lung as compared to heart and liver (Mann-Whitney U test; $p < 0.001$). Nitrofen induces a small reduction of *NR2F2* in heart and liver (0.90 and 0.94 relative fold change respectively), whereas the *NR2F2* response in diaphragm is reduced considerably (0.45 fold). Interestingly, lung tissue showed an opposite, albeit mild dosage response (1.17 fold) upon nitrofen treatment.

The rodent E17 NR2F2-interaction pattern in controls

Visual inspection of all significant long-range DNA interactions across chromosome 1 – using the earlier published domainograms of the group of van Steensel et al. [32] – showed that the global interaction pattern of *NR2F2* in-cis is similar for all investigated tissues. Two examples are

depicted in Figure 2A and represent control -diaphragm and -liver interactome. The same holds true for *NR2F2*'s long-range interactions with other chromosomes and is presented in the circos plots for diaphragm and liver in healthy offspring tissue (Figure 2B). However, minor differences in the interaction efficiency (i.e. frequency as indicated by arrows) of a subset of DNA-association partners may be suggested by these domainogram data as well. Table S4 illustrates as an example, all the significant domains including DID z-scores and gene symbols of the diaphragm control sample.

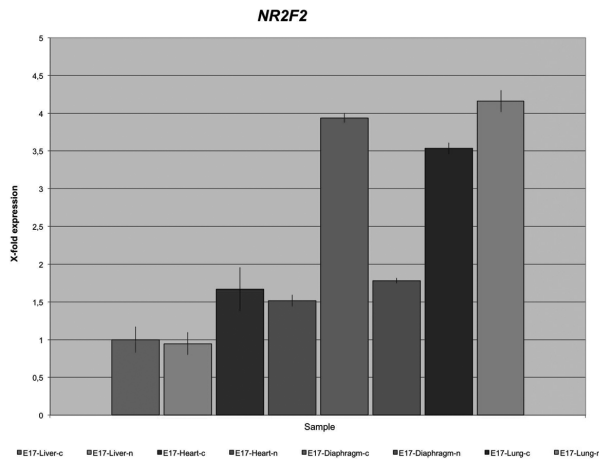


Figure 1 | Relative mRNA expression levels of *NR2F2*

Illustration of relative mRNA expression levels of *NR2F2* detected by real-time Q-PCR in four different tissues (liver, heart, diaphragm, lung) of a rodent-CDH model with (n; nitrofen) and without nitrofen (c;control). Tissues of five-six pups were harvested and pooled at embryonic day E17. Levels in control-liver (dark red) were used as an internal control. (see page 253 for color figure)

Collectively, this data shows that the *NR2F2* promoter region is engaged in many specific long-range DNA interactions across the bait-chromosome (in-cis), but also displays inter-chromosomal contacts (in-trans). Since the *NR2F2* gene is located in a gene-poor region on rat chromosome 1, we expected its global interaction profile to be characterized by other gene-poor regions. General features of the *NR2F2*-interacting DNA domains per tissue type are summarised in Table S2 and indeed showed that this gene mainly associates with other gene poor regions. The number of Refseq genes/Mb varied between 4-10, while a gene density of 35 genes/Mb has been described for gene rich areas in the human genome [37]. The average gene density of the rodent genome is 6.22 per one Mb of DNA and comparable to the one in humans (6,33/Mb). A relative low overall GC content per sample (~40%) supported these numbers. Furthermore, there was a difference in size between the in-cis interacting regions captured by our *NR2F2*-specific 4C (<1Mb) as compared to those in-trans (~10Mb). This is similar to what has recently been observed for the X chromosome [31].

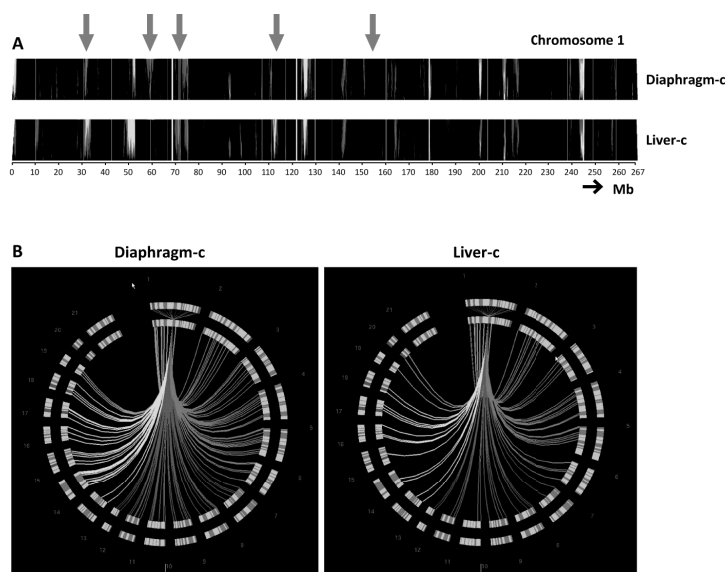


Figure 2 | Domainograms of *NR2F2* in rodent E17-control tissues

A: in-cis interactions in control-diaphragm (Top) and control-liver tissue (Below) showing an overall similar genomic 3D environment, although minor differences (arrows) in the interaction efficiency of a subset of interaction partners may be suggested by these representations.

B: Circos plot depicting the interactions of *NR2F2* with other chromosomes in control-diaphragm (Left) and control-liver tissue (Right), again demonstrating grossly similar patterns. Each line represents a trans interaction. Chromosomes are plotted around the circle. Colours indicate the chromosomes that were contacted in each quadrant (see page 253 for color figure).

NR2F2-interaction profiles in nitrofen-induced CDH-tissues

The main objective of this study was to investigate whether interference with RA signalling – using the teratogen nitrofen – could induce global changes in the DNA association partners of the *NR2F2* promoter, specifically in those tissues affected in CDH patients i.e. the diaphragm and lungs. Detailed analysis of the general characteristics of these nitrofen-induced 4C data (Table S2), revealed a slight increase in the size of the cis-interacting domains in the nitrofen-induced diaphragm tissue, whereas the trans-domains were more prominent in the nitrofen-lungs. Moreover, the ratio of inter-over intra-chromosomal captures decreased in the nitrofen-lungs, suggesting that the *NR2F2* promoter is positioned relatively more at the periphery of its chromosome territory in control lungs as compared to nitrofen-treated lungs.

In contrast to our hypothesis, 4C-nitrofen results demonstrated that for each individual sample type the overall genomic environment is similar in the nitrofen-induced tissue as compared to its healthy control. In other words, the interaction pattern for both the bait chromosome and for the remainder genome was almost identical between diseased and control samples. Examples of such comparisons are summarised in Figure 3, showing the domainograms of chromosome 1 and 14 in respectively diaphragm (Figure 3A,B) and lung (Figure 3C,D) tissue,

with and without nitrofen. In addition, duplo experiments of lung nitrofen-treated samples are illustrated. Spearman's rank correlation analysis was applied to statistically validate this similarity as summarised in Table S5.

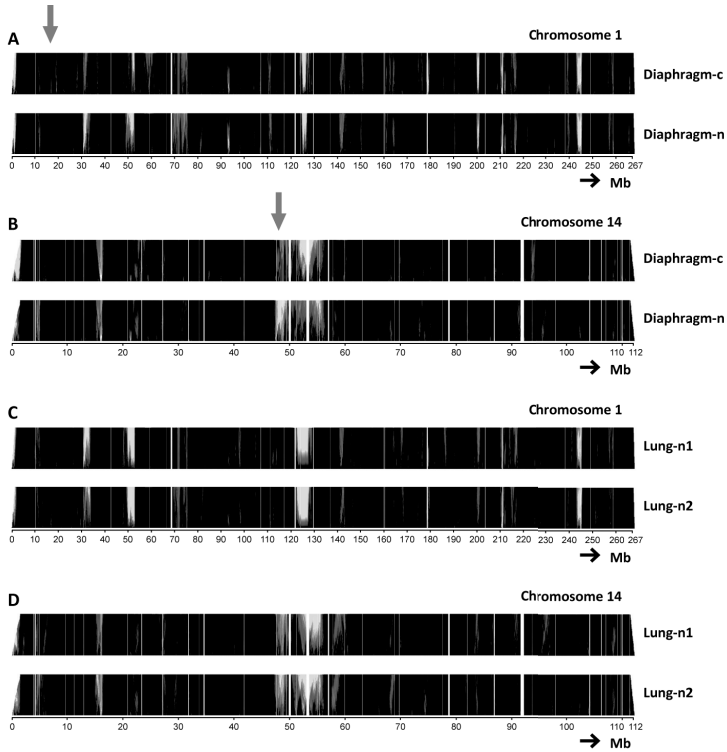


Figure 3 | Domainograms of rodent *NR2F2* upon nitrofen-induction at E17

Comparing the in-cis **A**: and in-trans (using chromosome 14) interactions **B**: in control-diaphragm (Top) and nitrofen-treated diaphragm (Below) tissue respectively showing an overall similar genomic 3D environment although, very subtle differences (arrow) in the interaction efficiency (i.e. frequency) occurred in these subsets also. **C/D**: Similar as in A/B for duplo experiments of nitrofen-lung-induced tissues; index 1 (Top) and index 2 (Below) (see page 254 for color figure).

Although gross chromosomal reorganisation was ruled out, our control-disease comparisons also indicated the occurrence of more subtle changes in the composition and frequency of a subset of interaction partners. For this, we specifically searched for disappearing or newly occurring contacts in respectively the nitrofen-lung and nitrofen-diaphragm samples as compared to its healthy controls. Results are summarised in Table 1, in which the putative significance of the “changing” interacting domain is reflected in its calculated DID Z-score. Focusing on the *TOP-30* interacting domains (marked by an asterisk), we demonstrated respectively 1 nitrofen-diaphragm

and 8 nitrofen-lung domains that harbour developmentally important genes such as *FZD4*, *ALG8* and *WNT11*. Interestingly, the in nitrofen-diaphragm tissue disappearing in-cis domain on chromosome 1 (marked yellow in Table 1) overlapped with one out of seven significant in-cis domains that disappeared in the nitrofen-lungs also. These corresponding results suggest that this domain might contain genes or regulatory units that are involved in the pathogenesis of CDH via disrupted RA signalling, especially since no such changes were identified for the non-CDH affected tissues (heart/liver). Similar to the locus of *NR2F2*, this domain on chromosome 1q12 is characterized by a gene-desert and contained only 1 annotated Refseq gene, *Protein phosphatase 2 regulatory subunit A alpha (PPP2R1A)*. The *Vom1r* cluster embodies a collection of rodent specific pseudogenes of pheromone receptors. The transcriptional activity of the *PPP2R1A* gene was confirmed in lung and diaphragm tissue using RT-qPCR (Figure 4). Moreover, its levels dropped (0.69 and 0.71 relative fold change respectively) in response to nitrofen-treatment.

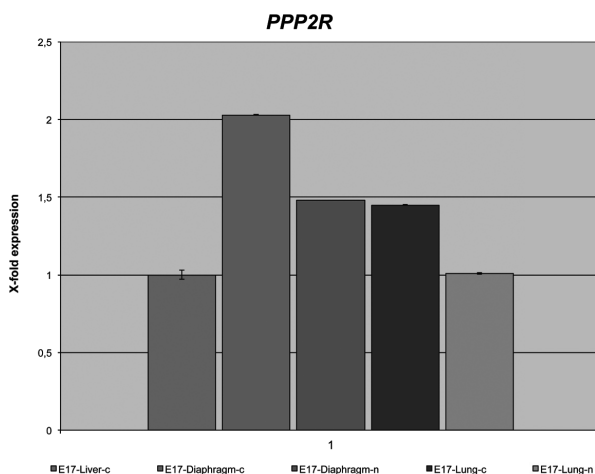


Figure 4 | Relative mRNA expression levels of *PPP2R1A*

Illustration of relative mRNA expression levels of *NR2F2* detected by real-time Q-PCR in CDH affected (diaphragm, lung) tissues of a rodent-CDH model with (n; nitrofen) and without nitrofen (c; control). Tissues of five-six pups were harvested and pooled at embryonic day E17. Levels in control-liver (dark red) were used as an internal control (see page 255 for color figure).

Finally, we filtered genes in the affected lung- and diaphragm domain table on specific items as presented in Table 2 using the software program Ingenuity Pathway Analysis (IPA). Results showed no overlap for genes associated with CDH in literature. Genes encoding proteins involved in RA signalling or metabolism were absent too. Pathway analysis showed no enrichment for lung- or diaphragm specific developmental cascades.

Table 1 | Significantly different interacting domains in affected tissues Congenital Diaphragmatic Hernia

| Diaphragm | | | | | | |
|---------------------------------|-----------|-----------|------------------|-------|---|--|
| chrom | start | end | Size domain (bp) | score | other tissues displaying the interacting domain | Number Gene Ids (refseq) of genes |
| Disappearing contacts | | | | | | |
| chr1 | 18620721 | 18782889 | 162168 | 39 | - | 0 no genes found |
| chr1 | 57765855 | 58908287 | 1142432 | 683* | Controle Lung | 14 Ppp2r1a , Vom1r9 , Vom1r10 , Vom1r11 , Vom1r12 , Vom1r13 , Vom1r14 , Vom1r15 , Vom1r16 , V1rf4 , etc. |
| chr1 | 257929685 | 258296974 | 367289 | 30 | all other Nitrofen samples | 1 Ins1 |
| chr10 | 8954 | 3967815 | 3958861 | 23 | all other samples, except controle lung | 15 Bfar , Pla2g10 , RGD1305733 , Abcc1 , RGD1305823 , Myh11 , Nde1 , Mir484 , Lkap , Rrn3 , Ntan1 , Pdxdc1 , RGD1305537 , Cpped1 , Snx29 |
| Newly appearing contacts | | | | | | |
| chr1 | 31855729 | 33497292 | 1663860 | 166 | all other samples, except nitrofen heart | 0 no genes found |
| chr2 | 205170820 | 211935178 | 6764358 | 98 | all other samples | 9 Vav3 , Ntng1 , Prmt6 , Hmox3 , Amy2 , Amy1a , Rnpc3 , Olfm3 , S1pr1 |
| chr3 | 373 | 3671666 | 3671293 | 80 | all other samples | 43 LOC499742 , Spopl , Hnmt , Tbpl2 , Il1f9 , Il1f6 , Il1f8 , Il1f5 , Il1f10 , Il1rn , Psd4 , Pax8 , Cacna1b , Ehmt1 , Arrdc1 , Noxa1 , Nrarp , etc |
| chr5 | 28599396 | 46084898 | 17485502 | 76 | all other samples | 28 Necab1 , Calb1 , Decr1 , Nbn , Ripk2 , Mmp16 , Cpne3 , Fam82b , Wwp1 , Slc7a13 , Atp6v0d2 , Ttpa , Ggh , Nkain3 , Ccnc , Usp45 , Sfrs18 , etc. |
| chr7 | 37915546 | 45704538 | 7788992 | 84 | all other samples | 14 Tmtc3 , Cep290 , RGD1307947 , LOC500827 , Mgat4c , Nts , Rassf9 , Aix1 , Slc6a15 , Tmtc2 , RGD1310270 , Ccdc59 , Ppfia2 , RGD1307051 |
| chr15 | 89162474 | 99858668 | 20 | 98 | all other samples | 13 Ndfip2 , Spry2 , Trim52 , Slitrk1 , Slitrk6 , Slitrk5 , Mir17-1 , Mir18a , Mir19a , Mir20a , Mir19b-1 , Mir92a-1 , Gpc5 |
| chr19 | 20736969 | 27950872 | 7213903 | 81 | all other samples, except nitrofen liver | 81 Cbln1 , Siah1a , Lomp2 , Abcc12 , Phkb , Itfg1 , Neto2 , Dnaja2 , Gpt2 , RGD1308706 , LOC100363129 , Mylk3 , Orc6l , Vps35 , Olr1666 , Man2b1 , etc. |

* TOP-30 Interacting domains

| Lung | | | | | | |
|------------------------------|-----------|-----------|------------------|---|---------------------|---|
| chrom | start | end | Size domain (bp) | other tissues displaying the interacting domain | Number of genes | Gene Ids (refseq) |
| Disappearing contacts | | | | | | |
| chr1 | 58060817 | 58949114 | 888297 | 3238* | Controlle Diaphragm | 11 Ppp2r1a , Vom1r12 , Vom1r13 , Vom1r14 , Vom1r15 , Vom1r16 , V1rf4 , Vom1r17 , Vom1r19 , Vom1r20 , Vom1r21 |
| chr1 | 90378749 | 90748974 | 370225 | 4954* | - | 3 RGD1310358, Ccne1 , Plekhf1 |
| chr1 | 145540859 | 146383375 | 842516 | 9532* | - | 4 Tmem135 , Fzd4 , Prss23 , Me3 |
| chr1 | 154309238 | 154736524 | 427286 | 6829* | - | 6 Gab2 , Kctd21 , Alg8 , Ndufc2 , Thrsp , Ints4 |
| chr1 | 155937546 | 156456594 | 519048 | 7979* | - | 5 Prkrii , Wnt11 , RGD1561870, Uvr , Dgat2 |
| chr1 | 185187786 | 185938822 | 751036 | 2963* | - | 18 Xpo6 , Sbk1 , Lat , Spns1 , Nfatc2ip , Cd19 , Rabep2 , Tufm , Atxn2l , Eif3c , Cln3 , Apob48r , Nupr1 , Ccdc101 , Sult1a1 , Giyd2 , Coro1a , Mapk3 |
| chr1 | 189805970 | 189942610 | 136640 | 1522* | - | 3 Ate1 , Nsmce4a , Tacc2 |
| chr3 | 156348518 | 162132757 | 5784239 | 454 | - | 36 Elmo2 , Slc13a3 , Slc2a10 , Eya2 , Zmynd8 , Sulf2 , Prex1 , Tp53rk , Arfgef2 , Cse1 , Stau1 , Ddx27 , Znfx1 , Kcnb1 , Ptgis , B4galnt5 , etc. |
| chr6 | 106352817 | 111168617 | 4815800 | 460 | - | 54 Dpf3 , Dcaf4 , Zfyve1 , Rbm25 , Psen1 , Numb , RGD1307704, Acot2 , Acot1 , Acot4 , Acot3 , Acot5 , Dnal1 , Pnma1 , RGD1306119, Ptgr2 etc. |
| chr7 | 134301126 | 140555689 | 6254563 | 511 | - | 100 Ano6 , Slc38a1 , Slc38a2 , Slc38a4 , Amigo2 , Fam113b , Rpap3 , Endou , Rapgef3 , Slc48a1 , Vdr , Tmem106c , Col2a1 , Pfkm , Asb8 , etc. |
| chr9 | 33056817 | 36528018 | 3471201 | 341 | - | 26 Ccdc115 , Imp4 , Ptpn18 , Tesp1 , Cfc1 , Tesp2 , Plekhb2 , Hs6st1 , Uggt1 , Neur13 , Arid5a , RGD1309220, Lman2l , Cnmm3 , Ankrd23 , etc. |
| chr9 | 56276239 | 59500878 | 3224639 | 568 | - | 35 RGD1306941, RGD1311269, MGC94335 , Spats2l , Kctd18 , Aox1 , Aox3 , Aox4 , Aox3l1 , Bzw1 , Cik1 , Ppil3 , Nif3l1 , Orc2l , etc. |
| chr14 | 14401386 | 18514773 | 4113387 | 787 | - | 26 Mrpl1 , Cnot6l , Cxcl13 , RGD1561226, Cng2 , Ccni , Sept11 , Shroom3 , Stbd1 , Scarb2 , Nup54 , Art3 , Cxcl11 , Cxcl10 , etc. |

| Lung (Continued) | | | | | | |
|---------------------------------|----------|-----------------|------------------|---|-----------------|---|
| chrom | start | end | Size domain (bp) | other tissues displaying the interacting domain | Number of genes | Gene ids (refseq) |
| Disappearing contacts | | | | | | |
| chr17 | 14709685 | 18313602 | 3603917 | 440 | 49 | Pitx1, Catsper3, Txnrc15, Ddx46, Camlg, B4galt7, Tmed9, Fam193b, Ddx41, Mir3542, Dok3, Polim7, Dbn1, Prr7, Grk6, F12, etc. |
| chr18 | 36935789 | 48984591 | 12794349 | 618 | 26 | Jakmip2, Spink1, Spink3, Scgb3a2, RGD1563060, Spink5, Spink5I2, Spink6, RGD1559536, Myot, Dcp2, Mcc, Kcnn2, Trim36, Pgg1b, etc. |
| chr18 | 61317675 | 64744415 | 3426740 | 908 | 29 | Nedd4l, LOC502176, Mir3591, Mir122, Znf532, RGD1304731, Sec11c, Grp, Lman1, Cplx4, Rax, Pmaip1, Mcc4r, etc. |
| Newly appearing contacts | | | | | | |
| chr1 | 48771938 | 49842497 | 1070559 | 1110* | 5 | [Milt4, Vom2r7, Vom1r1, Vom2r8, RGD1564755] |
| chr2 | 96535563 | 110403295 | 13867732 | 619 | 24 | [Pkia, Pxmp3, Zfx4, Hnf4g, Ythdf3, Mir124-2, Bhlhe22, Cyp7b1, Armc1, Mfrr1, Pde7a, Dnajc5b, RGD1562890, Trim55, Crh, etc. |
| chr9 | 4617 | 4583327 | 4578710 | 160 | 11 | Slc5a7, Sult1c3, LOC301165, Sult1c2, Sult1c2a, RGD1564811, Rab5a, Efhb, Kcnn8, Satb1, Tbc1d5 |
| chr9 | 23861897 | 30646225 | 6784328 | 315 | 4 | Bai3, Phf3, Ptp4a1, Lgsn |
| chr11 | 37912498 | 43182779 | 6230304 | 435 | 41 | C2cd2, Znf295, Arl6, Mina, Gabrr3, Olr1528, Olr1529, Olr1530, Olr1531, Olr1532, Olr1533, Olr1535, etc. |
| | | | | | 516 | |
| | | | | | 39 | |

* TOP-30 Interacting domains calculated based on DID z_score

The NR2F2 interactome across all investigated tissues: downstream analysis

Next, we determined the overlapping DIDs across *all* samples, in order to distinguish the most specific and abundant DNA interactions of the *NR2F2*-E17 promoter region independent of tissue type and nitrofen induction. Results showed respectively 7 regions in-cis and 48 in-trans that significantly interacted with *NR2F2* in all tissues investigated (as summarised in Table 3). Genes in this overall *NR2F2*-interacting domain list were then examined and filtered on specific items, analogous to the genes in the CDH affected tissue-list (Table 2). The following four genes formerly associated – directly or indirectly – with CDH in literature were identified: *GLI2* [38], *TBL1X* (X-linked CDH), *ICAM1* [39] and *KLF2* [40] corresponding to domains on respectively chromosome 13, X, 8 and 16. No RA-signalling factor was present in this list, neither were any other strong CDH candidate genes (*ZFPM2*, *GATA4*, *WT1* and *LRP2*) known from literature. Non-supervised pathway analysis demonstrated that the cellular functions, cell growth and cell death, were the major processes executed/controlled by the genes in contact with *NR2F2* (Table 2). Moreover, in agreement with the extensive evidence of *NR2F2* functioning as a metabolic factor [11], the endocrine developmental pathway was the most represented network.

Table 2 | Enrichment analysis/Filtering genes in NR2F2 interacting domains

| Items | Gene count NR2F2-General | Gene symbol NR2F2-General |
|---|-----------------------------|---|
| CDH associated genes Literature | 4 | <i>Gli2</i> , <i>TBL1X</i> <i>ICAM1</i> , <i>KLF2</i> |
| RA signalling/RAR activation | – | – |
| Top Molecular&cellular functions: cellular growth &cell death; Ingenuity | 338/273 | P val 7,41E-09 - 1,26E-02/4,36E-07 - 1,38E-02 |
| Top Networks: Endocrine System Development and Function; Ingenuity | 33 | Score 33: <i>ANGPTL4</i> , <i>AP1M1</i> , <i>Ap2alpha</i> , <i>BRD4</i> , <i>BST2</i> , <i>CHERP</i> , <i>CHTF8</i> , <i>DCPS</i> , <i>Dgk</i> , <i>DGKA</i> , <i>DNM2</i> , <i>Dynamin</i> , <i>EPS15L1</i> , <i>F2</i> , <i>FNBP4</i> , <i>GGCX</i> , <i>GNA11</i> , <i>HMG20B</i> , <i>IER2</i> , <i>ILF2</i> , <i>ILF3</i> , <i>PACSN3</i> , <i>PRPF40A</i> , <i>RAB8A</i> , <i>RBM10</i> , <i>SERPINB8</i> , <i>SERPINB10</i> , <i>SF3A2</i> , <i>SF3B4</i> , <i>SLC2A3</i> , <i>SUGP1</i> , <i>SV2A</i> , <i>TCERG1</i> , <i>WBP4</i> , <i>YES1</i> |
| New (top) genes, genes prioritized by endeavour | – | In preparation |

NR2F2-General; Genes in interacting-NR2F2 domains across all samples
Ingenuity; Ingenuity Pathway Analysis (IPA) software (Ingenuity Systems Inc. Redwood City, CA)
Endeavour; <http://homes.esat.kuleuven.be>
RA; Retinoic Acid
CDH; Congenital Diaphragmatic Hernia
P-val; P-value

Ranking the interacting genomic regions (based on their DID z-score) per sample revealed that the promoter region of *NR2F2* captured a subset of interaction partners very efficiently across all samples. This was most obvious for a locus on chromosome 14 (Supp .Table S6, red coloured)

that harboured 18 genes in total of which the *PCDH7* and *UGDH* gene are the most interesting. Since co-localisation with *NR2F2* may only be functional in case of active transcription, we performed RT-qPCR using target specific primer sets for these two preferential contacted genes and confirmed their activity in all tissues investigated (results not shown).

The NR2F2 interaction pattern across all investigated tissues: upstream analysis

To identify transcription factors that might control the genes in the *NR2F2*-interacting dataset (n=2015 in total), we used the data analysis system ExPlain™. First we filtered out all 508 olfactory receptor genes, because the proteins they encode are located specifically in the cilia of the olfactory sensory neurons and have no obvious association with our tissue types. Transcription factor binding sites (TFBSs) in our remaining target gene set (n=1507) were compared to the frequencies of these sites in a so-called background gene set constituting of non-*NR2F2*-interacting rodent house keeping genes (n=399). Results showed that the *NR2F2*-interactome was exclusively enriched for the transcription factor OCT1, which suggests that this protein might be involved in the expression regulation of *NR2F2* and its associating gene partners at rodent embryonic stage E17. RT-qPCR analysis confirmed *OCT1* expression in RNA extracted from our rodent CDH model, both in wild type as well as in nitrofen-exposed tissues. Yet, transcription levels varied widely between samples, with very low levels in lung-control samples (results not shown).

Discussion

The pathogenetic mechanisms causing diaphragm- and lung- defects in patients with congenital diaphragmatic hernia (CDH) are largely unknown. Several human and knockout mice studies provided strong evidence for involvement of the *NR2F2* gene [14, 18], which encodes an orphan nuclear transcription factor that is implicated in embryonic RA-signalling and is crucial for mice organogenesis [11, 16]. However, most of its specific gene regulatory networks during development remain to be identified.

Similar to the well-known and abundant expression of *NR2F2* during mouse organogenesis [11], our RT-PCR analysis showed that this gene was transcribed in all four (i.e. diaphragm, lung, heart and liver) investigated embryonic rat tissues. Responses of *NR2F2* upon nitrofen in CDH affected tissue were in line with data from literature [36]. The different mRNA levels at embryonic day E17 suggested a continuing role for this gene in the development of the diaphragm and lungs, whereas its role was subdued in the almost completed heart and liver organs. This result is reflected in the variability of the nitrofen-induced fold changes of the corresponding tissues.

The impact of the -dynamic- spatial configuration of the human genome on gene expression regulation is well recognised [41]. However much debate continues whether chromosomal interactions as a means to share common regulatory resources during specific differentiation and developmental programs is a general concept of gene-transcription regulation or merely

a mechanism to fine-tune transcription in exceptional cases [42, 43]. Despite these issues, DNA spatial patterns identified at a certain developmental stage are thought to reflect the genome's functional output at that specific time-window. Moreover, such blueprints might serve as markers to identify diseased states [44, 45]. Therefore, identification of the subnuclear environment of the *NR2F2* gene in embryonic tissues of healthy rodent offspring as well as upon chemical interference with RA signalling will provide novel epigenetic insights into the role of *NR2F2* in diaphragm- and lung organogenesis. To accomplish this we used 4C technology. Interactions in heart-and liver served as non-CDH specific controls. Transcriptional responses of its associating DNA partners were measured by quantitative RT-PCR.

Application of 4C technology to healthy rodent E17 control tissue demonstrated that, despite the identified variability in *NR2F2* activity, the spatial environment of the *NR2F2* locus was grossly similar. Moreover, the global interaction profile of the *NR2F2* gene, which is located in a gene-desert on rodent chromosome 1, was characterized by other gene-poor regions. These results are in agreement with recent 4C papers [42, 46], which showed that the subnuclear environment of a certain DNA region is mainly dictated by its chromosomal context i.e. the properties of both the region itself and of its proximal regions on the linear DNA strand, and thus mainly independent of transcriptional status. Yet, occurrence of more subtle differences in the efficiency and composition of identified preferential contacts – in a population of cells at any point in time - was suggested also by these reports. This, in turn may boost or reduce existing expression levels of the preferred interacting genes leading to variegated gene expression in the tissue as a whole [42]. These subtle effects on gene transcription might consequently be crucial during certain embryonic time windows, for example during diaphragm development. Indeed, our data indicated the existence of mild interaction-differences between 4C samples. These differences are reflected in the dissimilarity of the intensity of the domains between samples as visualised in our domainograms (Figure 2 and 3) and in the diversity of ranks per domain per sample. To validate these mild changes confirmatory 3D FISH experiments should be executed, although co-associations are expected to occur in only a low proportion of the cells. A recently proposed adaptation to the 4C protocol, which is more sensitive to pick up all the functionally relevant interactions, might also be considered [43].

Summarised, although the global spatial environment of the *NR2F2* locus was heavily constrained by its chromosomal context – and independent of both its transcriptional tissue levels and of nitrofen treatment – the degree of this constrain might fluctuate. Therefore, we investigated whether minor changes in the composition of the interacting domains occurred upon exposure to the chemical nitrofen and specifically for CDH-affected tissues. Indeed, one domain on chromosome 1q12 fulfilled these criteria, suggesting that it contains DNA elements that are important for both the development of the lungs and the diaphragm and is possibly involved in RA signalling. Next, Refseq annotation analysis positioned only 1 gene within this 1.1 Mb domain; the *PPP2R1A* gene. The protein Ppp2R is a member of the serine-threonine phosphatase family that plays an essential regulatory role in cell growth, differentiation, and apoptosis and is altered in breast and lung carcinomas [OMIM *605983]. *PP2A* is important

in fetal kidney growth and differentiation [47] and has an expression pattern similar to that of the Wilms tumor suppressor gene *WT1*, which is a strong CDH candidate also. Our RT-qPCR analysis confirmed that this gene is actively transcribed in rodent E17 lung and diaphragm tissue. Moreover, levels in its corresponding nitrofen-treated tissues dropped, supporting its proposed functional role in CDH. The use of combined RNA/DNA 3D FISH studies must further provide evidence for this.

Despite this remarkable result, careful interpretation is mandatory for three reasons. Firstly, Clugston et al. recently suggested that the initial perturbation event of diaphragm development occurs much earlier – i.e. at stage E13.5 in embryonic rodent development - than previously expected [48]. Therefore, application of 4C technology to pick up chromatin reorganisation at this stage should be considered, although limited by an even lower amount of available diaphragm material. For this, Tolhuis et al. [33] implemented an extra amplification step to their 4C protocol. Secondly, cell quantity requirements were not completely fulfilled for duplo control-lung and control-nitrofen diaphragm samples, which might have mildly influenced the identification of long-range interactions, especially those in trans. Thirdly, although much used in CDH-related studies, the nitrofen-CDH model has a few limitations. First, this model cannot be uniquely categorized to CDH, since nitrofen induces other congenital anomalies among which heart defects. Penetrance of CDH is not complete, with typical occurrence rates between 60-90%. And then, the precise mechanism by which nitrofen induces reduction of retinoic acid signalling is not clear: is it purely based on inhibition of the rate-limiting enzyme controlling retinoic acid synthesis (RALDH2) or not? Therefore, a recent developed RAR alpha specific mice model for CDH might be considered [49].

Since large-scale three-dimensional differences were absent across all investigated tissue types, we focused on the overlapping interacting domains. Such domains will point to the most abundant interaction partners of the *NR2F2* promoter at rodent embryonic stage E17 and shed new light on its functional roles. Fifty-six regions in total, containing over 2000 genes (of which 508 so-called olfactory receptor genes) interacted with *NR2F2* in all 4C samples. Unsupervised downstream pathway analysis showed that these genes were mainly involved in cell- growth and -death, both key processes in embryogenesis. Enrichment analysis using several bio-informatic filtering tools only identified four genes associated with CDH in literature and no member of the RA-signalling pathway neither any other strong CDH candidates. More subtle variations in the efficiency of these four *NR2F2* interacting- CDH-candidate gene-containing domains between CDH-related and non-related tissues were ruled out. These results might be explained by our specific search for the more abundant roles of the *NR2F2* promoter in the overlapping DID gene list. Alternatively, it could mean that the specific roles of the abundant *NR2F2*-interacting genes in lung and diaphragm development are not yet discovered or that in general most DNA-DNA interactions are non-functional. In this respect, it is highly interesting that the most efficient interaction partner of *NR2F2* was a locus on chromosome 14 which harboured the *PCDH7* and the *UGDH* gene among others. Both these genes are putative new CDH candidates, although no exclusive association can be appointed to these genes, since long-range interactions usually

occur between regions that are not confined to single genes or gene promoters. Protocadherin 7 (PCDH7) is a member of the cadherin protein superfamily, which constitutes membrane-associated glycoproteins that mediate calcium dependent cell-cell adhesion. *PCDH7* was recently implicated in the pathogenesis of RETT syndrome [50], but is expressed in lung and heart tissue also [OMIM *602988]. Interestingly, both *NR2F2* [11] and members of the cadherin protein family are known to play a major role in the regulation of Epithelial-Mesenchymal-Transition (EMT) during organogenesis. Moreover, EMT was recently suggested to contribute to primordial diaphragm tissue [51], and is a well-known process during lung development. The enzyme UDP-glucose dehydrogenase (UGDH)[OMIM *603370], converts UDP-glucose to UDP-glucuronate, which in turn is a critical component of glycosaminoglycans, hyaluronan and heparan sulphates. In this way, UGDH exerts its role in tissue development and cell-migration and -proliferation. Garcia-Garcia et al. [53] showed that in *Ugdh* deficient mice (alias lazy mesoderm mutation (Izme) mice) gastrulation is arrested with defects in mesoderm-migration. Failure of the latter process is implicated in CDH. Because co-localisation of these loci with *NR2F2* may only be functional in case of active transcription, we performed RT-qPCR. Results showed that both genes were indeed transcribed in all tissues investigated including rodent lungs and diaphragm.

Finally, we performed upstream analysis of the E17-NR2F2-specific interactome and demonstrated that transcription factor binding sites of the protein OCT1 were exclusively enriched in the promoters of the genes in this list. This analysis suggests that OCT1 [OMIM *602607] is involved in the expression regulation of *NR2F2* and its associating gene partners at this specific developmental window. In general, OCT proteins are defined by their ability to interact with a DNA sequence known as the “octamer motif”. Its member OCT1 is widely expressed in embryonic tissues and *Oct1* deficient mice die during embryogenesis over a wide developmental window (E12.5-E18.5) [54]. OCT1 shares significant homology with OCT4 and regulates some common target genes, however cannot substitute OCT4s’ role in the generation of pluripotency. Interestingly, OCT1 has a role in mediating the RA signalling pathway [55]. RT-qPCR analysis confirmed *OCT1* expression in RNA extracted from our rodent CDH model, both in wild type as well as in nitrofen-exposed tissues, albeit with significantly lower levels in control lungs. Further experiments using CHIP technology have to be performed to confirm the binding of OCT1 to the promoter of *NR2F2*. Furthermore, an experimental design in which conditional OCT1-removal during mesoderm genesis leads to a subsequent significant reduction in the interaction frequency of the *NR2F2* associating genes must be executed.

In conclusion, application of 4C technology in a wild type and RA-signalling interrupted, CDH rodent model showed that despite the identified differences in the activation-level of the *NR2F2* gene, the spatial environment of the *NR2F2* locus is grossly similar across all investigated tissues. In contrast, subtle differences for specific interactions were demonstrated upon nitrofen-treatment, pointing to new CDH candidate genes such as *PPP2R1A*. Moreover, increased knowledge of the most abundant interaction partners of *NR2F2* across all 4C samples identified one specific domain on chromosome 14 and the Oct1 protein as the common regulatory source of the *NR2F2* interactome.

References

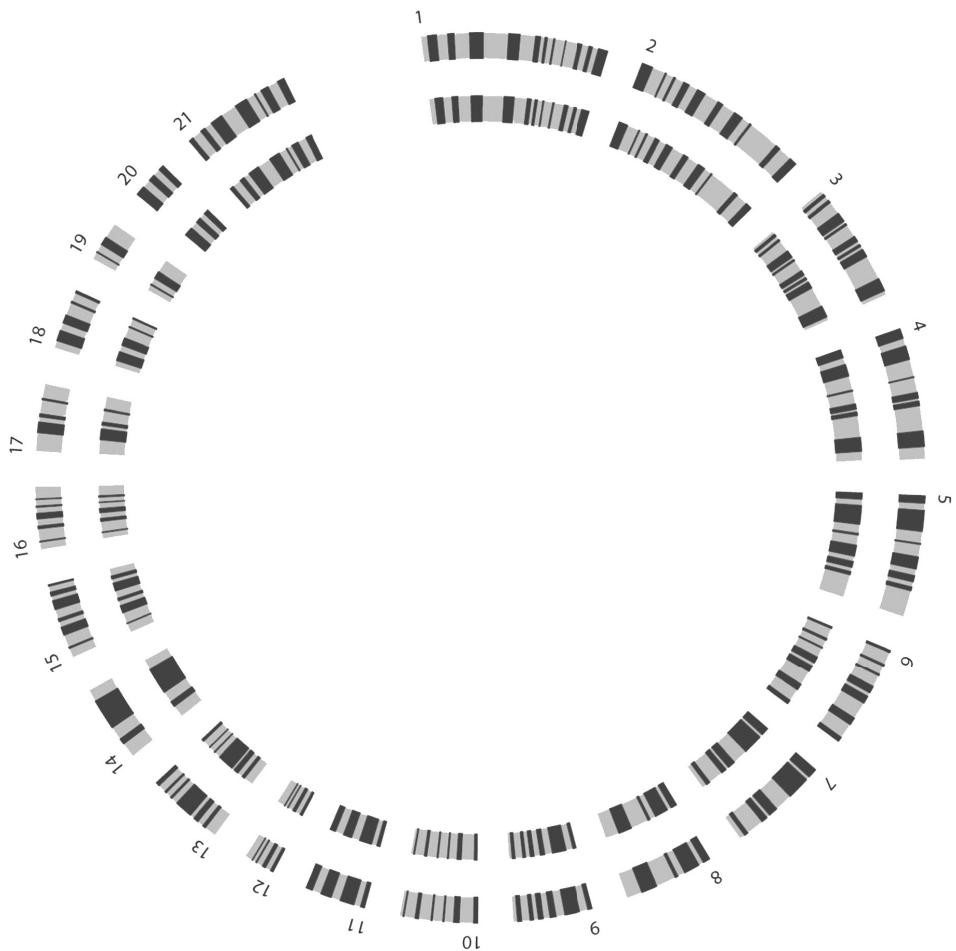
1. Sluiter, I., et al., *Congenital diaphragmatic hernia: still a moving target*. Seminars in fetal & neonatal medicine, 2011. **16**(3): p. 139-44.
2. Klaassens, M., A. de Klein, and D. Tibboel, *The etiology of congenital diaphragmatic hernia: still largely unknown?* Eur J Med Genet, 2009. **52**(5): p. 281-6.
3. Brady, P.D., et al., *Recent developments in the genetic factors underlying congenital diaphragmatic hernia*. Fetal diagnosis and therapy, 2011. **29**(1): p. 25-39.
4. Gallot, D., et al., *Congenital diaphragmatic hernia: a retinoid-signalling pathway disruption during lung development?* Birth Defects Res A Clin Mol Teratol, 2005. **73**(8): p. 523-31.
5. Holder, A.M., et al., *Genetic factors in congenital diaphragmatic hernia*. Am J Hum Genet, 2007. **80**(5): p. 825-45.
6. Beurskens, N., et al., *Linking animal models to human congenital diaphragmatic hernia*. Birth Defects Res A Clin Mol Teratol, 2007. **79**(8): p. 565-72.
7. Clugston, R.D., et al., *Teratogen-induced, dietary and genetic models of congenital diaphragmatic hernia share a common mechanism of pathogenesis*. Am J Pathol, 2006. **169**(5): p. 1541-9.
8. Clugston, R.D., et al., *Understanding Abnormal Retinoid Signalling as a Causative Mechanism in Congenital Diaphragmatic Hernia*. Am J Respir Cell Mol Biol, 2009.
9. van Loenhout, R.B., et al., *Congenital diaphragmatic hernia: comparison of animal models and relevance to the human situation*. Neonatology, 2009. **96**(3): p. 137-49.
10. Beurskens, L.W., et al., *Retinol status of newborn infants is associated with congenital diaphragmatic hernia*. Pediatrics, 2010. **126**(4): p. 712-20.
11. Lin, F.J., et al., *Coup d'Etat: an orphan takes control*. Endocrine reviews, 2011. **32**(3): p. 404-21.
12. Rosa, A. and A.H. Brivanlou, *A regulatory circuitry comprised of miR-302 and the transcription factors OCT4 and NR2F2 regulates human embryonic stem cell differentiation*. The EMBO journal, 2011. **30**(2): p. 237-48.
13. Pereira, F.A., et al., *The orphan nuclear receptor COUP-TFII is required for angiogenesis and heart development*. Genes & development, 1999. **13**(8): p. 1037-49.
14. You, L.R., et al., *Mouse lacking COUP-TFII as an animal model of Bochdalek-type congenital diaphragmatic hernia*. Proc Natl Acad Sci U S A, 2005. **102**(45): p. 16351-6.
15. Clugston, R.D., W. Zhang, and J.J. Greer, *Gene expression in the developing diaphragm: significance for congenital diaphragmatic hernia*. Am J Physiol Lung Cell Mol Physiol, 2008. **294**(4): p. L665-75.
16. Vilhais-Neto, G.C., et al., *Rere controls retinoic acid signalling and somite bilateral symmetry*. Nature, 2010. **463**(7283): p. 953-7.
17. Pinaire, J., et al., *The retinoid X receptor response element in the human aldehyde dehydrogenase 2 promoter is antagonized by the chicken ovalbumin upstream promoter family of orphan receptors*. Archives of biochemistry and biophysics, 2000. **380**(1): p. 192-200.
18. Klaassens, M., et al., *Prenatal detection and outcome of congenital diaphragmatic hernia (CDH) associated with deletion of chromosome 15q26: two patients and review of the literature*. Am J Med Genet A, 2007. **143A**(18): p. 2204-12.
19. Simonis, M., et al., *Nuclear organization of active and inactive chromatin domains uncovered by chromosome conformation capture-on-chip (4C)*. Nat Genet, 2006. **38**(11): p. 1348-54.
20. de Laat, W. and F. Grosfeld, *Inter-chromosomal gene regulation in the mammalian cell nucleus*. Curr Opin Genet Dev, 2007. **17**(5): p. 456-64.
21. Schneider, R. and R. Grosschedl, *Dynamics and interplay of nuclear architecture, genome organization, and gene expression*. Genes Dev, 2007. **21**(23): p. 3027-43.
22. Sexton, T., et al., *Gene regulation through nuclear organization*. Nat Struct Mol Biol, 2007. **14**(11): p. 1049-1055.

23. Schoenfelder, S., I. Clay, and P. Fraser, *The transcriptional interactome: gene expression in 3D*. *Curr Opin Genet Dev*, 2010. **20**(2): p. 127-33.
24. Fraser, P., *Transcriptional control thrown for a loop*. *Curr Opin Genet Dev*, 2006. **16**(5): p. 490-5.
25. Fraser, P. and W. Bickmore, *Nuclear organization of the genome and the potential for gene regulation*. *Nature*, 2007. **447**(7143): p. 413-7.
26. Kluth, D., et al., *Nitrofen-induced diaphragmatic hernias in rats: an animal model*. *Journal of pediatric surgery*, 1990. **25**(8): p. 850-4.
27. Mey, J., et al., *Retinal dehydrogenase-2 is inhibited by compounds that induce congenital diaphragmatic hernias in rodents*. *The American journal of pathology*, 2003. **162**(2): p. 673-9.
28. van der Horst, I.W., et al., *Expression and function of phosphodiesterases in nitrofen-induced congenital diaphragmatic hernia in rats*. *Pediatric pulmonology*, 2010. **45**(4): p. 320-5.
29. Simonis, M. and W. de Laat, *FISH-eyed and genome-wide views on the spatial organisation of gene expression*. *Biochim Biophys Acta*, 2008. **1783**(11): p. 2052-60.
30. Simonis, M., J. Kooren, and W. de Laat, *An evaluation of 3C-based methods to capture DNA interactions*. *Nature methods*, 2007. **4**(11): p. 895-901.
31. Splinter, E., et al., *The inactive X chromosome adopts a unique three-dimensional conformation that is dependent on Xist RNA*. *Genes & development*, 2011. **25**(13): p. 1371-83.
32. de Wit, E., F. Greil, and B. van Steensel, *High-resolution mapping reveals links of HP1 with active and inactive chromatin components*. *PLoS genetics*, 2007. **3**(3): p. e38.
33. Tolhuis, B., et al., *Interactions among Polycomb domains are guided by chromosome architecture*. *PLoS Genet*, 2011. **7**(3): p. e1001343.
34. Knoch, T.A., et al., *The GLOBE 3D Genome Platform - towards a novel system-biological paper tool to integrate the huge complexity of genome organization and function*. *Studies in health technology and informatics*, 2009. **147**: p. 105-16.
35. Boehm, D., et al., *Rapid detection of subtelomeric deletion/duplication by novel real-time quantitative PCR using SYBR-green dye*. *Human mutation*, 2004. **23**(4): p. 368-78.
36. Doi, T., K. Sugimoto, and P. Puri, *Up-regulation of COUP-TFII gene expression in the nitrofen-induced hypoplastic lung*. *Journal of pediatric surgery*, 2009. **44**(2): p. 321-4.
37. Splinter, E., et al., *The inactive X chromosome adopts a unique three-dimensional conformation that is dependent on Xist RNA*. *Genes Dev*, 2011. **25**(13): p. 1371-83.
38. Kim, P.C., R. Mo, and C. Hui Cc, *Murine models of VACTERL syndrome: Role of sonic hedgehog signalling pathway*. *Journal of pediatric surgery*, 2001. **36**(2): p. 381-4.
39. Takayasu, H., et al., *Impaired alveolar epithelial cell differentiation in the hypoplastic lung in nitrofen-induced congenital diaphragmatic hernia*. *Pediatric surgery international*, 2007. **23**(5): p. 405-10.
40. Lukosiute, A., et al., *Down-regulation of lung Kruppel-like factor in the nitrofen-induced hypoplastic lung*. *European journal of pediatric surgery : official journal of Austrian Association of Pediatric Surgery [et al] = Zeitschrift fur Kinderchirurgie*, 2011. **21**(1): p. 38-41.
41. Baker, M., *Genomics: Genomes in three dimensions*. *Nature*, 2011. **470**(7333): p. 289-94.
42. Noordermeer, D., et al., *Variiegated gene expression caused by cell-specific long-range DNA interactions*. *Nature cell biology*, 2011. **13**(8): p. 944-51.
43. Schoenfelder, S., et al., *Preferential associations between co-regulated genes reveal a transcriptional interactome in erythroid cells*. *Nat Genet*, 2010. **42**(1): p. 53-61.
44. Meaburn, K.J., et al., *Primary laminopathy fibroblasts display altered genome organization and apoptosis*. *Aging Cell*, 2007. **6**(2): p. 139-53.
45. Meaburn, K.J., et al., *Disease-specific gene repositioning in breast cancer*. *J Cell Biol*, 2009. **187**(6): p. 801-12.
46. Hakim, O., et al., *Diverse gene reprogramming events occur in the same spatial clusters of distal regulatory elements*. *Genome Res*, 2011. **21**(5): p. 697-706.
47. Ruteshouser, E.C., L.K. Ashworth, and V. Huff, *Absence of PPP2R1A mutations in Wilms tumor*. *Oncogene*, 2001. **20**(16): p. 2050-4.

48. Clugston, R.D., W. Zhang, and J.J. Greer, *Early development of the primordial mammalian diaphragm and cellular mechanisms of nitrofen-induced congenital diaphragmatic hernia*. Birth Defects Res A Clin Mol Teratol, 2010. **88**(1): p. 15-24.
49. Clugston, R.D., et al., *Understanding abnormal retinoid signalling as a causative mechanism in congenital diaphragmatic hernia*. Am J Respir Cell Mol Biol, 2010. **42**(3): p. 276-85.
50. Miyake, K., et al., *The protocadherins, PCDHB1 and PCDH7, are regulated by MeCP2 in neuronal cells and brain tissues: implication for pathogenesis of Rett syndrome*. BMC neuroscience, 2011. **12**: p. 81.
51. Norden, J., et al., *Wt1 and retinoic acid signalling in the subcoelomic mesenchyme control the development of the pleuropericardial membranes and the sinus horns*. Circulation research, 2010. **106**(7): p. 1212-20.
52. Walsh, E.C. and D.Y. Stainier, *UDP-glucose dehydrogenase required for cardiac valve formation in zebrafish*. Science, 2001. **293**(5535): p. 1670-3.
53. Garcia-Garcia, M.J. and K.V. Anderson, *Essential role of glycosaminoglycans in Fgf signalling during mouse gastrulation*. Cell, 2003. **114**(6): p. 727-37.
54. Kang, J., A. Shakya, and D. Tantin, *Stem cells, stress, metabolism and cancer: a drama in two Acts*. Trends in biochemical sciences, 2009. **34**(10): p. 491-9.
55. Wang, J. and A. Yen, *A novel retinoic acid-responsive element regulates retinoic acid-induced BLR1 expression*. Mol Cell Biol, 2004. **24**(6): p. 2423-43.

Chapter 4

General Discussion



Adapted from:

“Developmental and Genetic aspects of Congenital Diaphragmatic Hernia”

D.Veenma, A.de Klein and D.Tibboel

Paediatric Pulmonology 2012, in press

General Discussion

Despite progress in prenatal diagnosis and postnatal therapy, congenital diaphragmatic hernia (CDH) still carries high mortality and considerable short- and long-term morbidity. Further clinical improvement could be accomplished by standardising care in an international setting and harmonising complication registration in a collective database. Therefore, the recent foundation of the European CDH consortium and the international CDH study group are very welcome [1, 2]. In addition, research efforts are directed at the very early embryonic processes and factors that lead to CDH. More knowledge on these issues could lead to new treatment modalities (especially for pulmonary hypertension) and perhaps even prevention strategies. In this respect, awareness of the sub-microscopic molecular changes in CDH has already led to individualised genetic counselling. So far, however, this genetic knowledge applied only to a few complex CDH cases and has not yet changed therapy guidelines.

The studies in this thesis aimed to identify new genetic factors in both isolated and complex CDH patients. We considered germ-line and somatic (CNV-)mutations and searched for alternative epigenetic causes as well. The next section first describes the pitfalls in CNV-phenotype ascertainment. I then address the difficulties of research focusing on the impact of the spatial configuration of the human genome on gene expression regulation. Finally, I elaborate on the current views of diaphragm embryology, identify its lacunas, and provide recommendations for future research.

4.1 The clinical context of Copy Number Variations (CNV) in general and for CDH specifically: Methodological considerations

The use of genome-wide array techniques on material from diseased individuals has brought the need to distinguish likely pathogenic CNVs from likely benign CNVs and stresses on the importance of CNV-screening in phenotypically normal cohorts [3]. Although risk assessment of CNVs has drastically improved, we should be reluctant to associate them directly with disease phenotypes. For we are still dealing with 1) differences in CNV prevalence between certain diseased cohorts, 2) confounding in CNV calling across the genome, 3) different mechanisms to convey phenotypes, and 4) incomplete penetrance. These features will briefly be summarised below.

CNV prevalence varies between diseased cohorts

The genome wide frequency of de novo CNVs is estimated to be 1.2×10^{-2} with an average CNV size ranging from 62 Kb to 10Mb [4, 5]. Interestingly, the latest CNV correlation studies showed enrichment of large de novo CNVs in certain diseased cohorts, e.g. neuro-developmental and autoimmune disorders. The de novo CNVs in these patients also affected genes more often than

CNVs identified in normal cohorts [4, 6, 7]. This discovery suggests a clinically important variability in the genetic contribution of CNVs to disease aetiology across different populations.

It is not yet known whether this finding holds true for CDH patient cohorts as well.

The sensitivity of arrays to detect structural variations is unequal across the genome

The increased number of total probes on the latest generation of arrays has dramatically improved its genomic resolution. Still, certain portions of the genome – such as the telomeric regions – remain less covered and might be more susceptible to certain disruption mechanisms [8]. Moreover, most of the small exonic changes go undetected. Consequently, in general there is confounding in the ascertainment of a phenotype to a CNV. Further improvement of array coverage, both in terms of spacing and number, will reduce this bias [9]. But then, future application of whole-genome sequencing techniques will likely outgrow the advancements in array techniques. In the case of rare CNVs (such as in isolated CDH), only sample size will then remain as a discovery-limiting step. Moreover, several research groups have studied the relative contributions of CNVs and Single Nucleotide Polymorphisms (SNPs) to expression phenotypes [10]. Although CNVs cover on average a much larger percentage of the genomic DNA strand, they contributed far less than SNPs to variations in mRNA transcript levels [10]. This finding points to the current biased focus on CNVs as disease causing variants only. Thus there is every reason to develop more complex, combinatorial genetic analysis methods, especially for multi-genic diseases such as (isolated-) CDH.

Identification of the true CNV causative gene(s) is less straightforward than proposed

CNVs may induce phenotypes by gene-interruption, position- and dosage-effects, and unmasking of a recessive coding region mutation [11-14]. However, the commonly used smallest-region-of-overlap (SRO) approach presumes that only genes within the affected chromosomal area exhibit gene-expression alterations, thereby ignoring possible other disruption mechanisms. Altered gene expression levels have been found in the boundary regions of CNVs and it was suggested that even long-range position effects may be important [15, 16]. Identifying the true causative factor(s) might therefore be not as easy as thought. The large size of most of the identified rearrangements, which contain multiple genes, is another impediment. These concerns are reflected in our expression array results of Chapter 3 (article 2). In contrast to the hypothesized dosage-response mechanism for deleted genes in the CDH 15q26 critical region, we identified only two significantly down-regulated gene transcripts. Moreover, the strongest hypothesized CDH-candidate – *NR2F2* – displayed an opposite expression response in some patients, emphasizing that simple haploinsufficiency of this gene cannot fully explain diaphragm defects associated with 15q26 monosomy. It seems, therefore, that we must resort to functional studies (ideally in an embryonic, tissue-specific and species-specific context) to confirm the link between the candidate gene(s) involved and the specific phenotype.

Recently, the suspected dose-dependent influence of a subset of CNVs on gene-expression (and subsequently on phenotype) was studied throughout mice development [17]. A changing influence of certain brain-specific CNVs was seen, adding another level of complexity to the interpretation of CNV-phenotype correlations.

Incomplete penetrance

Most of the established CNV events to date are inherited from a phenotypically normal parent, and are of a benign/non-pathogenic nature [18]. Recently, a dominant digenic disease model was proposed for a subgroup of severe developmental delay cases, implicating that inherited CNVs could represent an important disease-specific susceptible background [19, 20]. In this two-hit dominant model the independent effect of two gene-modifiers adds up to create a phenotype of developmental delay. It differs from the two-hit-one gene model for autosomal-recessive diseases, in which both alleles of one gene-locus become non-functional by two separate hits/mutations. The dominant digenic model also suggests that two or more hits within the same developmental pathway can have a more severe impact on phenotypes. CNV approaches will therefore greatly benefit from basic cell biologic pathway knowledge. CNV analysis in our own CDH cohort of 121 patients, including 4 MZ twins discordant for CDH (chapter 2), yielded 27 (22%) inherited CNVs. Thirteen of those were rare in a specific paediatric normal population and in our in-house adult control cohort. Moreover, the regions affected by these CNVs included several genes putatively involved (based on GO terms and the corresponding knock-out mice phenotype) in the diaphragm phenotype. Finally, new statistical analysis methods are needed to identify the proportions of disease variability caused by epistatic mechanisms and/or gene-environmental interaction-mechanisms. Such designs may also reveal to what extent certain CNVs can compensate for disease-inducing, loss-of-function rearrangements (as shown recently in a phenotypically normal 22q11.2 carrier [21]).

Standardised phenotyping and early genetic screening as crucial steps in genotype-phenotype ascertainment

Since genetic research and (prenatal) counselling for congenital disorders moves towards a genotype-first approach, standardised phenotyping and registration in widely accessible databases becomes more and more important. This could be achieved with the use of standardised lists of dysmorphic features and with the application of 3D camera techniques [22, 23] for a more unbiased dysmorphic analysis. Early postnatal CNV detection in combination with long-term clinical follow up also opens up the possibility of mapping the influence of CNVs on the longitudinal development of certain disease phenotypes [24].

Genetic screening approaches will most likely be revolutionised in another way. Non-invasive extraction of sufficient amounts of good quality fetal DNA from maternal blood is already feasible [25-28]. Aside from the economical implications, high-throughput (and even genome-wide) screening of all pregnant women will soon become possible. Such population based screening will help assign CNVs of unknown functional significance and give a more

realistic estimation of CNV prevalence in all human foetuses. The latter could be relevant, as CNV prevalence likely depends on developmental stage and age. In addition, it will allow for genetic screening of spontaneous abortions of which most genetic material is currently lost. For CDH research this could be valuable, since CDH is an important cause of stillbirths and abortions.

Structural variations in the CDH cohort

The first extensive overview in 2007 [29] made clear that many non-isolated CDH cases were attributable to sub-microscopic chromosomal anomalies. We, in collaboration with other research groups, presented a genome-wide map of CDH-specific recurrent CNVs that overlapped with the positions of Vitamin-A pathway genes. This indicated that disruption of the retinoid-signalling pathway may be involved in CDH aetiology. This first overview was recently complemented by array data of four different groups [30-33]. Patient numbers, phenotypes and timing of array analysis varied widely between these studies: The smallest study concerned 12 prenatal cases, the largest 79 isolated cases (summarised in Table 1). Different array techniques were applied, precluding a meta-analysis on screening effectiveness.

In chapter 2 we describe the genome-wide copy number screen of 117 “Rotterdam” CDH subjects with isolated or complex CDH of varying severity. In total, 41 unique and/or rare events (35% of the patients) were established of which 16 were de novo and 25 were inherited. Remarkably, 5 out of the 16 de novo CNVs were present in isolated CDH cases; the remainder 11 in more complex cases. The latter partly overlapped with previously identified CDH-associated hot spots. Results are presented in Figure 1.

In summary, an emerging theme in these published CNV data sets and ours (Chapter 2) is the low prevalence of *overlapping* de novo CNVs in nonrelated, isolated cases in contrast to the microdeletion/duplication “hot spots” demonstrated in several complex CDH subgroups.

The chance of identifying an overlapping event may be particularly low because isolated cases represent a heterogeneous population in which de novo mutations in many different genes can result in the same basic phenotype. Moreover, isolated cases are more likely to result from a complex inheritance pattern in which combinations of genetic modifiers and environmental factors affect the final phenotype. Identification of these individual (genetic) factors requires specific high-resolution, genome-wide molecular approaches both on a DNA and a chromatin level and in very large patient cohorts. Alternatively, researchers might come up with additional phenotypic characteristics (such as all details of the diaphragmatic defect) to create genetically more homogenous subgroups. Chromatin data will provide the missing link to the various – presumably non-specific - predisposing environmental factors. Therefore, to fully understand the complex nature of CDH, more research initiatives should focus on epigenetic mechanisms. In this thesis we describe an epigenetic study on the influence of the spatial configuration of the human genome on gene expression regulation of CDH candidate genes (chapter 3). Other tissue specific epigenetic mechanisms such as DNA methylation and histone modification can be analysed in prospectively collected frozen diaphragm tissue of both cases and controls.

Table 1 | Overview CNV studies CDH cohort

| Reference | Patient Numbers | Patient Type | | Array platform | Results | | inherited, but absent/low in database normal individuals |
|---------------------------|---------------------------------------|--------------|---------|--|---------|-----------|--|
| | | Isolated | Complex | | de novo | inherited | |
| 29 | Literature overview of patients -2007 | | | 1 - (mainly) Lower resolution | | | |
| 30 | 45 | + (NS) | + (NS) | 2 - Human Genome CGH 244K Sureprint G3 Human CGH 1 M 105 K Combimatrix Molecular Diagnostics | 6 | 20 | 18 |
| 31 | 12 * | 1 | 11 | 2 - Constitutional Chip® 4.0 | NS | NS | |
| 32 | 28 | 24 | 4 | 3 - CytoSNP 370K, 550K and 660K | NS | NS | 2 |
| 33 | 79 * | 79 | 0 | 2 - Targeted Oligo array, 15K | | | 3 |
| Veenma et al, this thesis | 117 | 67 | 50 | 3 - CytoSNP Quad 610 and 12.2, Affy 250K) | 16 | 25 | 13 |

NS Exact numbers not specified

* Timing of screening prenatal instead of postnatal

1 Array platform-BAC

2 Array platform-oligo

3 Array platform-SNP

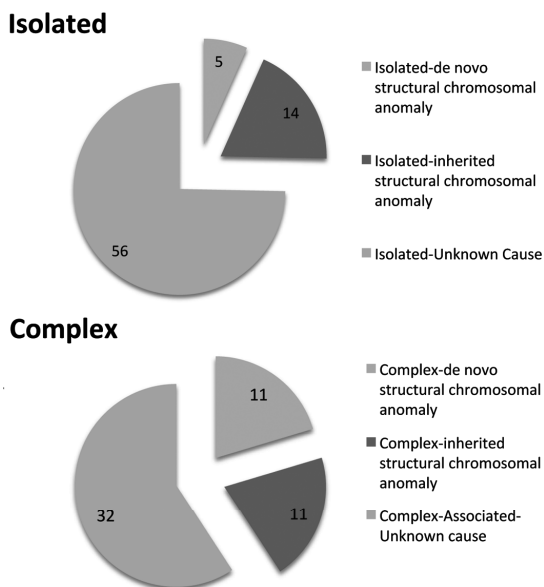


Figure 1 | Circular plots of genome-wide copy number screen results of 117 “Rotterdam” CDH subjects

Patients are classified depending on the absence (isolated CDH, $n=67$) or presence (complex, $n=50$) of additional birth defects. The blue colour represents the number of patients with a causative de novo structural chromosomal anomaly. Depicted in red is the proportion of patients identified with an inherited structural aberration, and green representing a remainder CDH subgroup with a yet unidentified (genetic) cause. Inherited CNVs could confer susceptibility to CDH after all, since they hardly occurred in two normal control populations. Remarkably, 5 out of 16 de novo CNVs were present in isolated CDH cases (see page 256 for color figure).

4.2 Current perspectives on the role of spatial organization on gene expression regulation: Methodological considerations of 3D multicolor FISH and 4C technology data

In chapter 3, chromosome conformation capture technology revealed a complex three-dimensional network of - not necessarily functional - chromosomal interactions in four different tissues of the nitrofen rodent CDH-model. The occurrence of specific combinations of DNA associations might be explained by the necessity for genes to share common transcriptional resources [34, 35]. Accumulation of genes at a certain transcriptional factory may provide the cell a mechanism by which it can coordinate the expression of genes of a common pathway. Such coordinated transcription is especially important during embryonic development in which groups of genes have to function in a strictly spatial- and temporal-controlled manner in the embryo. In line with this view, we first investigated (using the targeted 3D multicolor FISH technique) the three-dimensional clustering of crucial “diaphragm” genes (*NR2F2*, *ZFPM2* and

GATA4) as a prerequisite for their proper co-expression during normal diaphragm development. Coordinated transcription of these three CDH candidate genes proved independent of nuclear co-association. In the light of recent evidence, our hypothesis might now be considered naïve. First of all, the influence of this specific epigenetic control mechanism on gene-expression levels is less than previously speculated [34, 36, 37]. Secondly, physical proximity of loci does not imply a function of that interaction [35]. Thirdly, specific gene association events occur in specific developmental time windows. Below we briefly summarize these and other concerns on the functional implications of chromosomal interactions that have been reviewed extensively in the literature [38-49].

Intra-chromosomal looping between a distant regulatory element (even up to 1 Mb from the gene) and a gene has been well established [43, 47-51]. It is not yet known whether factors at the level of the linear DNA - such as activity of gene-neighbors, frequency of neighbors, position of repeats and of regulatory elements - would overrule the impact of the three-dimensional position effect on expression regulation. The same goes for factors at the level of chromatin folding, influenced by histone- and DNA-modifications and the position of nucleosomes. Much debate continues on reports of inter-chromosomal interactions as well. Such in-trans interactions may occur between a gene and a putative regulatory site (enhancer, promoter, insulator) or between coordinately expressed genes of a certain pathway [52-57]. Fine-tuning of gene expression by spatial positioning may only be relevant for certain cell types or processes such as cytokine-receptor choice, imprinting, differentiation during development, or for a cell's response to environmental stimuli [58]. The radial positioning of a gene and its long-range interactions are in general not conserved across species. In addition, specific radial (re)positioning is no absolute requirement for gene-expression initiation and/or prolongation: expression-levels of relocated genes are often unchanged and relocation is rather a consequence of chromosomal context/chromatin neighborhood. At this time of writing, only one paper [52] proved the causal relationship between gene expression regulation and co-localization of a gene locus (*SHH*) and its distant regulatory element. Moreover, skepticism about functionality was fuelled by reports on active transcription factors inside chromosome territories, suggesting there is no absolute requirement for CTs to intermingle or for genes to loop out. Furthermore, the methods used in the first reports on this type of events were based on less stringent definitions on co-localization and the use of 2D-FISH techniques only. In addition, the radial positioning process is probably dynamic and stochastic as current co-association studies (using 3D FISH and the more cell population based method 4C) only show association in limited proportions of cells at any one time (range of 5-15%). As an explanation, in each cell at any one time, a certain gene has associations with only a fraction of its preferential partners thereby benefitting (but not essential for transcription!) from the cooperative associations [37, 59]. In contrast, whether directly causative or merely reflecting a different state, nuclear spatial organization seems to change in a subset of cells at a certain developmental stage or as a response to external stimuli and may eventually lead to fine-tuning of certain gene expression programs. Therefore, studying nuclear

organization might help identify key factors in developmental processes, as demonstrated by our 4C results in Chapter 3.

4.3 Embryology of the Diaphragm, its remaining issues and Molecular-Genetic Pathways in CDH pathophysiology

The diaphragm consists of different cell types (myoblasts, neuronal- and supportive-cells) but is probably completely derived from mesodermal tissue. The so-called mesenchymal hit hypothesis postulates that defects in the posterolateral diaphragm at rodent embryonic stage E10-E14 originate from failure of mesenchyme derived Pleuro Peritoneal Fold (PPF) cells to form properly and to provide a migration platform for the diaphragm muscle precursor cells. In humans this transient mesodermal PPF can be demonstrated between the 4-5th week of gestation. Even though these insights were a real step forward in understanding CDH pathophysiology, many issues remain to be resolved. For we are still dealing with an unknown 1) origin and characterization of PPF cells, 2) nature of the primary disrupted cellular process in PPFs, 3) etiology of left prevalence in humans, 4) putative role of the liver, 5) nature of the retinoid pathway aberrations and finally 6) an ongoing debate on whether lung defects are caused separately from the diaphragm defects in CDH or not. All these issues will be addressed below. Additionally a hypothetical framework in which the diaphragmatic- and pulmonary defects of CDH could be causally linked on a cellular and molecular level will be presented.

Remaining challenges in CDH pathophysiology

1) PPF cell origin and markers?

The first major challenge in CDH research will be the discrimination of future PPF cells from the large bulk of lateral plate mesoderm that arises at the dorsal side of the intra-embryonic coelom of each somite. A related question is the following: does the body wall tissue that contributes to this cell pool originate from several or only one (truncal) somite? In other words, which mesodermal cell marker(s) can uniquely identify the cells contributing to the future PPF and what is the origin of this amuscular structure? The amuscular component of the PPF is somewhat unique in ways not understood and clearly differs from the mesenchymal substrate in other muscles since the defect is limited to the diaphragm and perhaps some muscular structures of the lung.

2) Primary defect in PPF?

The second challenge is to unravel the disrupted basic cellular processes in the population of PPF cells. Is it failure of migration of PPF cells – in analogy with a neural crest like behavior or migrating precursor muscle cell behavior – or is there a defect in the proliferation/apoptosis balance that underlies the shortage of PPF cells? Clugston et al. [60] recently showed that decreased proliferation is the primary mechanism of action of nitrofen at teratogenic doses in

the PPF of rodents. Interestingly, the same cellular processes have recently been implicated in the pathophysiology of the lung [61]. However, because the nitrofen model has its limitations, these findings must be confirmed in other CDH-induced animal models. In addition, the group of John Greer demonstrated that PPF cells are very unlikely to derive from the neural crest in contrast to earlier suggestions [62-64]. In a transgenic mouse (*Wnt1-Cre/R26R*) model, which labels neural crest derived tissue, only Schwann cell precursors migrating from the phrenic axons were marked.

Another cellular pathway that might be implicated emerged from studies of the involvement of Wilms' Tumor 1 (*WT1*) and retinoic acid (*RA*) signalling in liver morphogenesis and more recently in PPF formation at the level of the subcoelomic cardiac mesenchyme [65, 66]. These studies showed that mesenchyme cells must delaminate from the subcoelomic body wall tissue (most probably epithelium) in order to contribute to the PPF at the cardiac level and to the septum transversum at the diaphragm level. Consequently, through disruption of the Epithelial-Mesenchymal-Transition (EMT) pathway of lateral body wall cells there may not be enough mesenchymal cells contributing to these structures. We hypothesize a similar process in pleuro-peritoneal fold formation. Changes in the expression levels of the most important factors of EMT signalling (such as *SNAI1/Snail1*, *SNAI2/Slug* and *CDH1-and CDH2* genes which are responsible for the switch from E-CADHERIN to N-CADHERIN) are currently under investigation by the group of John Greer (personal communication).

3) Left-sided prevalence: chemical or mechanical causative factors?

A third remaining issue is: how can we explain the predominance of left-sided defects in human CDH? Is there as shown for rodents [67], a developmental stage-dependent variation in susceptibility to left- or right-sided defects in humans?

Rodents predominantly exhibited left-sided defects in case of toxic RAR α -inhibiting substance administrations at embryonic days E8-E9 and right-sided defects at E11-E13. It is not known whether this temporal aspect of CDH susceptibility is reflected in an asymmetrical left-right spatial pattern of crucial diaphragm signalling molecules. This finding also suggests that these hypothesized patterns are more easily disturbed on the left side than on the right, or, alternatively, that on the right side there are more redundant – compensating – signalling pathways. In this respect, it is interesting to recall that in the conditional *coup-tfII* knockout mice model, COUP-TFII expression at day E11.5 was slightly higher on the left side of the post-hepatic mesenchymal plate (PHMP) than on the right [68]. This asymmetric expression of COUP-TFII was recently demonstrated across the left-right axis of the presomitic mesoderm of the mouse trunk as well and interestingly resulted in asymmetric RA signalling [69]. Alternatively, CDH might be viewed as a subtype of laterality disorder (called heterotaxy or situs ambiguous). Several dozens of laterality genes that are differentially expressed on the two sides of vertebrates have been described [70]. Moreover, key factors in body axis formation were recently associated with less severe cardiac phenotypes [71]. The existence of various complex CDH associated syndromes that present with various midline defects already supports a laterality view for a proportion of the

non-isolated diaphragm defects. Furthermore, our findings in the *Chtop* knockout mouse model (presented in Chapter 2) supported this view.

Finally, Mayer et al. [72] recently postulated that the primordial diaphragm can only develop properly if there is extensive, good contact with its underlying organs. On the left side these include the stomach and smaller left lobe of the liver, while on the right the main portion of the liver is the “leading” structure. According to this “mechanical view on CDH pathophysiology”, defective development of the primordial diaphragm (in their paper called PHMP) occurred more readily on the left side because this side has an intrinsic smaller contact area with the underlying organs.

4) Putative role for the liver?

The fourth unanswered question is an old one: is there a role for the liver? In 1996, Kluth et al. [73] suggested that an early ingrowth of the liver into the thorax – transient in 50% of the human cases – could be of major importance for the formation of the defect. This group recently elaborated on this theory using findings of electron microscope images of rodent diaphragm development [72]. A similar mechanical obstruction function for the liver was implicated through our results on the loss of function of the Chromatin target of Prmt1 (*Chtop*) gene [74] (Chapter 2.2). Mice lacking *Chtop* have numerous developmental abnormalities, including the dorsolateral ‘Bochdalek’ type of CDH in 40% of their offspring. Aberrant expression of genes involved in mesoderm and vasculature development as well as of a delay in the G2/M-phase of the cell cycle were found. Subsequent analysis of the cell cycle defect across different tissue types demonstrated that erythroid progenitors were less affected by *Chtop* loss of function than other cell types, such as mouse embryonic fibroblasts. Hence, *Chtop* mice display massive proliferation of erythroid cells and a fetal liver that expands rapidly during diaphragm development. In contrast, because diaphragm genesis is slowed down, the fetal liver may grow beyond the PPF before the primordial diaphragm has completely formed, and thus contribute to the defect. Interestingly, these mechanical effects are similar to the secondary mechanical effects hypothesized for lung development in CDH and may in turn also explain the reduced penetrance or extreme variability in diaphragm defect sizes (categorized in the Boston classification [75]) seen in mouse models and human syndromes.

A few other studies hinted at a role for the liver due to its close proximity to the diaphragm. In *Slit3*-null mice, the central tendon region of the diaphragm fails to separate from the liver tissue because morphogenesis is disturbed [76]. This is similar to our observations in nitrofen-exposed rodents (chapter 3) at embryonic stages E15 and E17 in which liver tissue is almost inseparable from the diaphragm. A few reports in humans describe a diaphragmatic defect combined with a hernia sac attached to the liver [77, 78]. Although rarely observed during corrective surgery, these findings might point to an early (transient) developmental role for the liver in diaphragm development in general. Or more importantly, these cases might help to explain the putative deteriorating role of a liver positioned intra-thoracically, which in turn is associated with a poorer prognosis [79].

5) Genetic pathways involved in diaphragm development: “Old candidates and new ideas”. Is there a role for alternative non-canonical RA signalling?

A few strong candidate genes regulating diaphragm development have been characterized, including *NR2F2*, *ZFPM2*, *GATA4*, *WT1*, *LRP2* and members of the Retinoic Acid (RA) signalling pathway (e.g. *RALDH2*, *STRA6*, *RARa*). Their candidacy is based on highly penetrant structural DNA changes in material of human CDH patients identified by aCGH/SNP approaches and mutation analyses. In addition, knockout mice models featuring a certain type of diaphragm defect have been characterized for these genes as well. Most of these candidates are transcriptional regulators with pleiotropic functions that only partially overlap. However, the common (dorsolateral) hernia suggests that they interact directly or genetically in the developing diaphragm. Since others have already extensively reviewed all these genes [29, 75, 80, 81], we only present a brief summary and figure (Figure 2) and updated the information below. This candidate list is expected to steadily grow with the increasing use and lower costs of high-throughput, high-resolution molecular techniques. Gene prioritization- and pathway analysis- programs are important for these identification processes as was recently demonstrated by the Boston group. Russell et al. demonstrated [82] that the “diaphragm-signalling network” not only encompasses transcription, growth/cell-cell signalling factors and molecules of extracellular matrix biosynthesis, but also epigenetically involved factors such as chromatin structure regulators.

NR2F2 – (nuclear receptor 2 type F2) *alias Coup-tfII (Chicken-ovalbumin upstream promoter-transcription factor II)* – was singled out as one of the most promising CDH candidate genes by gene-ontology analysis. It is positioned in the smallest overlapping region of patients with a distal 15q26 monosomy. Patients carrying this autosomal dominant microdeletion feature a characteristic lethal phenotype that affects several organ systems and a diaphragm defect in 85-90% of the cases. Supporting this premise, mouse null mutants showed a Bochdalek type of defect after tissue specific ablation of *Nr2f2*. In addition, NR2F2 was identified as a retinoic acid (RA) activated receptor and is able to sequester RXR in a functionally inactive complex, providing a link to the well-known “Retinoids pathway disruption hypothesis” of CDH. Clugston et al. showed evidence for both *NR2F2* mRNA and NR2F2 protein expression in the rodent PPF at embryonic stage E13.5 [83]. Remarkably, no specific CDH causing mutations have been identified in isolated CDH patients, suggesting no direct causal overlap between diaphragm defects in the complex 15q26 monosomy cohort and the isolated one. This could suggest that additional – possibly epigenetic – mechanisms affect the normal expression of 15q26 CDH-genes in this specific complex cohort. Future discrimination of its putative long-range, tissue-specific upstream regulators can lead to identification of alternative NR2F2 affecting mutations.

Finally, cumulative evidence shows an important general role for *NR2F2* at several stages of mammalian organ development, including an early role in embryonic stem cell state and differentiation [84-85].

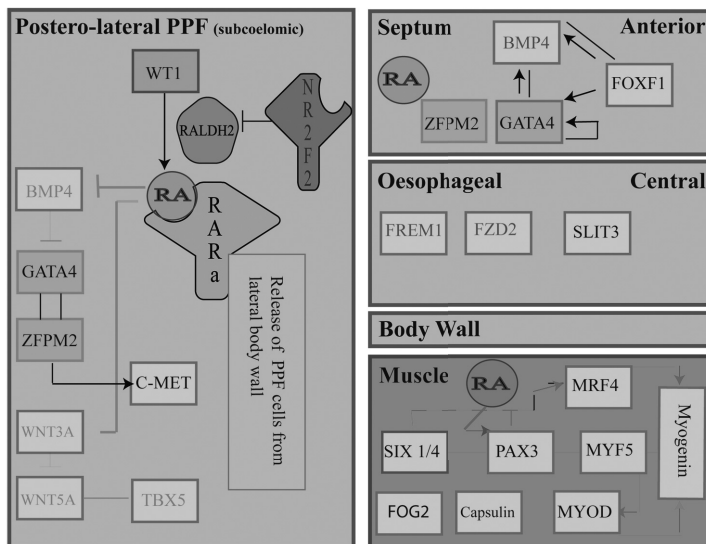


Figure 2 | Diaphragm signalling cascade

Depicted are the strong CDH candidate genes from literature [29, 75, 80, 81] (dark blue squares for *FOG2*, *WT1* and *GATA4*, green/grey/purple symbols for RA signalling members and *NR2F2*; dark brown) and their putative interactions at the specific location of the primordial diaphragm in which they have been demonstrated. According to the revised view on diaphragm embryogenesis, diaphragm tissue derives from four different mesenchymal components (depicted in the 4 grey boxes) i.e. the postero-lateral pleuro-peritoneal folds, the anterior septum transversum, the central esophageal mesentery and the lateral body wall mesenchyme. When completely fused, these structures form a supportive layer on which the “true” diaphragm muscle cells (that are derived from the hypaxial part of the somite) can migrate (represented as the light red box). Recently, several developmental studies [131] have shown that skeletal muscles of the body, limb and head have a distinct embryonic and cellular origin, while the genetic regulation at work in these domains are starting to be identified as shown for hypaxial muscle. Evidence for the genes and interactions depicted in the yellow boxes is based on our own preliminary data (chapter 2: *FZD2*, *FREM1*, *TBX5*) or from literature (*BMP4*, *FOXF1*, *WNT3A/5A*) [76, 132, 133] (see page 256 for color figure).

Apart from *NR2F2*, Clugston et al. [83] investigated the expression of *ZFP2*, *GATA4* and *WT1* and demonstrated that their co-expression is confined to the mesenchymal component of the E13.5 rodent PPF.

ZFP2 – (Zinc Finger Protein, Multitype 2) alias *FOG2* (*Friend of gata2*) – is considered a strong, yet not fully penetrant candidate responsible for the development of Bochdalek hernias in infants harboring 8q21-22 microdeletions [30]. These mutations have an autosomal dominant inheritance pattern. A few isolated CDH patients with unique *ZFP2* sequence variations have been described in literature as well [86, 87]. Furthermore, in an analysis of day E18.5 embryos derived from mice treated with N-ethyl-N-nitrosourea, Ackermann et al. identified a *zfp2* mutation causing both pulmonary hypoplasia and abnormal diaphragmatic development [87]. Finally, *ZFP2* and *NR2F2* physically interact during cardiac development [88] suggesting they

also could be parts of the same regulatory network in diaphragm development. In this respect, we should also mention **GATA4**; a zinc-finger transcription factor expressed in mesenchymal cells of the developing diaphragm, lung and heart. GATA4 protein often forms a complex with ZFPM2 (Figure 2) during development, modulating the expression of GATA4 target genes depending on the cell type and embryonic context [89-92]. GATA4's expression and activity are influenced by retinoids and GATA4 in turn influences RA signalling through activation of *LRAT* transcription in certain cell lines [93]. Heterozygous mutations of *Gata4* in C57B1/6 mice lead to diaphragmatic defects in the midline associated with dilated airways, thickened pulmonary mesenchyme and cardiac malformations [94]. Yet, penetrance of these defects is dependent on strain-specific modifier genes and diaphragm defects are not detected on mixed genetic backgrounds. So far, no human CDH patients have been described with point mutations in this gene. Several human cases with microdeletions on 8p23.1 exhibited both diaphragm and cardiac defects. Nevertheless, recent studies suggest – similar to the mouse model – that haploinsufficiency of additional genes on 8p may be involved in these 8p23-associated birth defects [95]. In a collaborative effort with the Houston research group, we [96] recently provided evidence that SOX7 might be one of these 8p23.1 candidates.

WT1 – (Wilms Tumor 1) – was initially identified as a tumor suppressor gene involved in the etiology of Wilms' tumor in humans. It is one of the genes expressed in the developing mouse mesothelium and subcoelomic mesenchyme of the lateral body wall from E10.5-E12.5. Analysis in knock out mice revealed its essential roles in the formation of numerous organ systems [97, 98] including the kidneys, coronary vessels and the diaphragm (septum transversum part). Norden et al. [66] recently identified an additional function of *WT1* in pleuro-pericardial fold formation: *WT1* indirectly induced apoptosis of mesenchymal cells at the distal attachment point of the pleuro-pericardial fold hereby mediating its release from the body wall. Via co-localization experiments and a reporter-gene construct, these authors proved that RA signalling via the enzyme RALDH2 acted downstream of *WT1*. This is interesting since RA signalling has long been suggested to be causal in the pathophysiology of CDH. In addition, in a similar study by IJpenberg et al. [65] co-expression of RA and *WT1* in the coelomic lining was already manifested at the level of liver morphogenesis and additionally in PPF development. In analogy with defects of the pleuro-pericardial folds, we suggest that *WT1* expression acts upstream of *RALDH2-RAR α* signalling in the cells of the lateral body wall which are going to contribute to the subcoelomic mesenchyme forming the PPF (Figure 2). In turn, through RA these cells delaminate (supposedly as part of an Epithelial Mesenchymal Transition process) from the epithelial part of the body wall and thereby contribute to the PPF mesenchyme. Clugston showed that particularly *RAR α* expression was devoid in the most rostral part of the PPF in nitrofen offspring, supports this theory [99].

RAR α pathways in CDH

As briefly mentioned in the introduction chapter, abnormal retinoid signalling is thought to contribute to the etiology of CDH [80, 99]. Only few complex human CDH cases – who display

major congenital anomalies besides their diaphragm defect – have been directly ascribed to genetic defects in crucial RA genes. No such key RA-mutations are demonstrated in isolated CDH cases so far. Consequently, only subtle disruptions of RA signalling – which might be secondary to yet unidentified factors – can explain the deviations in low retinol or retinol-binding protein levels established in isolated CDH cases [100-103].

RA functions as a repressor or co-activator through interactions with other pathways. It induces a distinct set of regulatory molecules depending on the structure or tissue in which it is produced and thereby putatively leads to organogenesis-specific programs. Both knockout and overexpression mice models showed that tight regulation of RA concentration is important during development [104, 105]. Its local tissue concentration is probably controlled by a complex interplay between degradation and synthesis, which is reflected in the dynamic expression patterns of *Rar*, *Rxr*, *Raldh*, *Crabpl1*, *Crabpl* and *Cyp* genes [106]. In relation to CDH, studies so far have solely focused on disruption of the classical canonical RA signalling arm and the function of RA-receptors as gene transcription regulators (Figure 3, Canonical RA pathway). However, cancer research has revealed two additional downstream RA-pathways that might bear upon RAR's role in balancing proliferation and apoptosis or the EMT of mesenchymal cells in the PPF and the lungs [107]. Besides the well-established nuclear location of RARs, these receptors were found in the cytosol and/or membranes of cells and rapidly activated mitogen-activated protein-kinases (Figure 3 Alternative RA pathway) [108]. In turn, these activated kinases induced a coordinated phosphorylation cascade that targeted RARa itself, its coregulators and histones. Interestingly, RAR phosphorylation also occurred in the absence of ligand, yet at residues different from those that are normally targeted and then resulted in down-regulation of RARa activity [107]. This new evidence implies the (partial) uncoupling of RARa activity and functioning from the synthesizing arm of the RA pathway. Consequently, it can be hypothesized that in CDH patients, RARa is inactivated in the PPF through retinoic acid-independent phosphorylation. Such putative abnormalities must be studied on a post-transcriptional level and could explain why RA disrupting mutations have not been found in CDH patients so far. This alternative RA-pathway also opens up the possibility of very local RARa disruption, induced by exogenous signals such as growth factors or cytokines. Finally, the second non-canonical role of RARa is its ability to associate with a subset of mRNAs (so far only shown in neuronal dendrites) and thereby directly repress the translation of these mRNAs [109].

The extended view on the classic and alternative RA signalling pathways is presented in Figure 3.

6) Lung and diaphragm: chicken or egg? Patho-morphology of the trachea and lungs in CDH, link to diaphragm defects?

Bronchial branching and pulmonary artery branching are considered the most affected processes in the maldevelopment of the lungs in CDH leading to fewer branch points for both these structures. Consequently, this results in fewer airway alveolar structures and fewer small lung vessels than in normal lungs. In addition, the morphology of the pulmonary vasculature is abnormal; the peripheral arteries are hypermuscular, with thick medial muscle layers that extend

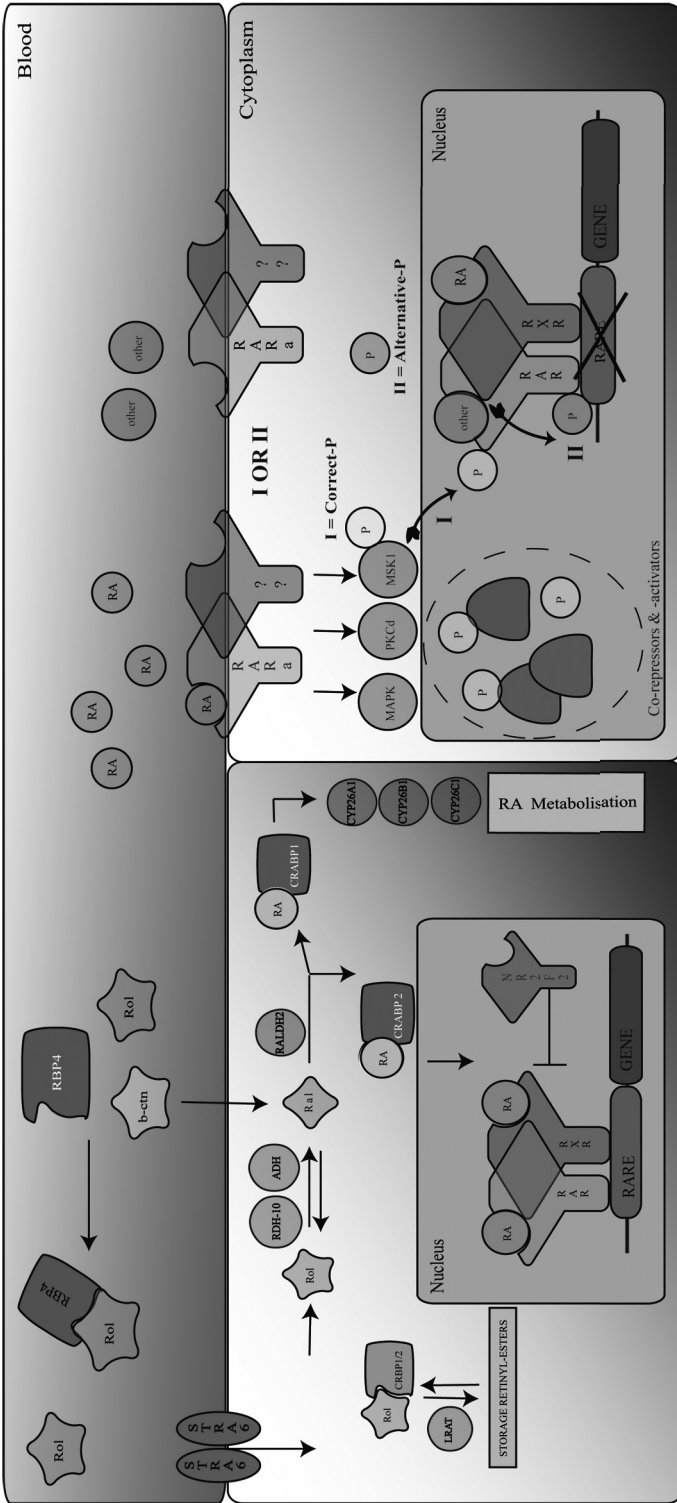


Figure 3 | Canonical and alternative RAR-alpha signalling pathway

Depicted are the classic canonical (left) and unconventional non-genomic (right) downstream pathways of RA signalling. When circulating retinol is taken up by RBP4, it can be transferred intracellularly by STRA6 and pass through the “basic” RA signalling cascade that ultimately results in the binding of nuclear RARs to specific response elements, thereby controlling the expression of a specific subset of genes. In addition, new non-genomic effects of RARs have emerged recently (as reviewed in [107]). In response to RA, which binds to RARs in the cytosol or at the cellular membrane, PKCδ, MAPK and MSK1 are activated through rapid non-genomic effects. MSK1, in turn phosphorylates RARα itself at a specific subunit. In the absence of RA, this phosphorylation event can also occur, yet at a different subunit leading to inactivation of (nuclear) RARα activity, instead of activation. RαI, retinol; RBP, retinol binding protein; STRA6, stimulated by retinoic acid 6; CRBP, cellular retinol binding protein; RAR, retinoic acid receptor; RXR, retinoid X receptor; RARE, retinoic acid response element. b-ctn, beta-ctn; RALDH, retinaldehyde dehydrogenase; CYP26, cytochrome P450 26 enzymes; ADH, alcohol dehydrogenase; RALDI, retinaldehyde; LRAT, Lecithin retinol acyl-transferase, NR2F2; Nuclear receptor 2, subfamily 2, member 2; CRABP1/2, Cellular Retinol-Binding Protein 1/2; MSK1, Mitogen Activated Kinase 1; PKCδ, Protein Kinase C, delta; MAPK, Mitogen Activated Protein Kinase, PKCδ; Mitogen Activated Protein Kinase C, MSK1: Mitogen and Stress Activated Kinase, P: Phosphorylation (see page 279 for color figure).

more distally on the arterioles than in healthy persons [110, 111]. Debate continues on whether these lung defects are caused separately from the diaphragm defect or by a common effector. Lung development is not a requirement for proper diaphragm development, since *fgf10* null mice have no lungs, but do have a diaphragm [112]. Unilateral lung hypoplasia without diaphragmatic defects has been described in humans as well [113]. Vice versa, *shh/gli3* double null mice do form somewhat hypoplastic lungs but have no diaphragm [114]. Consequently, the diaphragm develops independently from the lungs. However, this notion does not exclude the possibility that the same genetic- and environmental disturbances target similar precursor-cell types and processes in both the lungs and the diaphragm of CDH patients. These causative disturbances will probably encompass only one or a few large effect mutations in complex CDH-cases. On the other hand, in isolated CDH subjects there will be many smaller effect genes and modifiers. A causal correlation between maldevelopment of both embryonic structures is also likely, since both develop in close spatial proximity of each other and within the same time window. First evidence for this “one-effector-two organs” hypothesis comes from recent data of our group [61] showing that the mesenchymal layer is the primary target for lung defects in CDH-induced rodents. A disruption of cell cycle progression and subsequently an impaired proliferation of mesenchymal cells was characterized as the basic underlying cellular mechanism, which is in agreement with the earlier results in rodent diaphragm tissue [115]. Although these results are suggestive, this dual hit model needs to be proven in diaphragm and lung development in CDH patients. Finally, although key elements of lung signalling are starting to be identified using various knockout mice approaches (as reviewed in [116-118]), the framework of overlapping signalling molecules involved in diaphragm-development is still largely unknown and needs a more systemic biology approach using input from different research fields.

4.4 Future perspectives

As demonstrated in Chapter 2, molecular cytogenetic techniques have provided valuable insights into the genetic susceptibility of human CDH. Moreover, teratogenic, surgical, and genetic knockout models were instrumental to connect the identified human mutations to diaphragm maldevelopment [66, 68, 87, 94, 104, 119-122]. However, we believe that more is needed to unravel the developmental molecular network that contributes to CDH and to its phenotypic variability. Firstly, cumulative data from our own research group (Chapter 2) human CDH specific chromosomal hot spots, (Chapter 3) 15q26 monosomy transcriptome results) and from the group of Greer et al. [60] point to disruption of *early embryonic* genes and cellular differentiation processes. Obviously we cannot study these disruptions in human fetuses at a gestational age of 4-6 weeks. Secondly, genetically altered (rodent) *animal models* as a substitute for human material may display fundamental differences in *tissue-specific* expression patterns as compared to humans. Furthermore *timing* and *mechanism of gene regulation* may diverge from the human species. Together these remarks highlight the importance of developing a disease model

that reflects both the genetic background of the original patient and provides target-tissue in sufficient amounts and with crucial embryonic characteristics. Therefore I propose application of the innovative, induced pluripotent stem cell (iPSC) technique. This technique can generate CDH patient-specific stem cells from terminally differentiated skin cells using a combination of genetic- and expression-modulating factors (Oct3/4, Sox2, c-Myc, and Klf4) [123]. Successful application of the iPSC technique in cells exhibiting a specific genetic aberration have already been demonstrated for Prader-Willi [127] and Rett syndrome [123, 124] in re-differentiated neurons, and for Timothy syndrome [125, 126] in the cardiac lineage.

Generating iPSC cells from CDH-patients and healthy controls and evaluating the differences in cellular characteristics, might be useful to resolve a few of the issues raised in the third of paragraph of this discussion:

Firstly, it might enable identification of the cell marker(s) that characterise the PPF. Successful re-differentiation towards early mesenchyme (using factors such as Brachyury, NODAI and LEFTY) has already been described. The same holds true for hypaxial muscle re-differentiation (Pax3, Myf5, Mrf4 and Myogenin)[128-130]. A more challenging “trial-and-error” approach will be needed to establish the factors required later on in the PPF differentiation process. If technically feasible, it creates the opportunity to investigate the difference between mesenchymal precursors of the diaphragm and its “true” muscle progenitors, and thereby allows for a molecular identification of the differences between CDH and an eventration.

Secondly, the main power of this approach will be the ability to study known CDH causing (genetic) aberrations within their naturally occurring gene regulatory environment. We propose to start with skin fibroblasts of patients harboring a chromosome 15q26 deletion, as this to date is the strongest CDH-associated chromosomal hot spot in humans. In addition, these patients have been phenotypically characterized in detail and their genetic anomalies have been studied extensively by our group (Chapter 3). Interestingly, a recent paper reported on the role of the strong 15q26 candidate *NR2F2* in regulating early human embryonic stem cell state and cell fate [85]. We hypothesise that haploinsufficiency of *NR2F2* in patient 15q26 monosomy cell lines offers a unique opportunity to test the functional role of this gene in the proposed feed-back loop of human ESC pluripotency: subsequently we could expect patient cell lines to be reprogrammed more easily because of reduced *NR2F2* capacity.

Thirdly, iPSC will allow investigations to resolve whether Epithelial to Mesenchymal Transition (EMT) is indeed the primary disrupted process in the PPF of CDH patients or that an increased apoptosis or defects in proliferation are crucial. In addition a detailed analysis of differences in timing and expression of known CDH-candidates such as WT1 and NR2F2 as well as genes involved in EMT signalling (such as SNAI1, SNAI2 and CDH1-and CDH2) will be possible.

Finally, an interesting challenge for the above-mentioned cell model is; how to translate these fundamental research results into patient benefits rapidly and efficiently? Better insights into the basic disease-mechanisms of CDH may provide clinical geneticists and paediatricians with better tools on how and when to allocate treatment options. Furthermore, iPSC tissue specific-cell models allow for the testing of therapeutic interventions. For example, the iPSC

protocol may be used to create CDH-lung vascular specific cells and by that permits testing of antihypertensive drugs in inexhaustible, scalable and physiologically native material. iPSCs may also serve as a diaphragm tissue replacement therapy. By granting mainly research initiatives that have a translational component, many national and international funding organisations are already pushing the scientific field into this translational research strategy. Large international collaborations of researchers from different scientific backgrounds will be essential to accomplish this.

References

1. Reiss, I., et al., *Standardized postnatal management of infants with congenital diaphragmatic hernia in Europe: the CDH EURO Consortium consensus*. Neonatology, 2010. **98**(4): p. 354-64.
2. Tsao, K. and K.P. Lally, *The Congenital Diaphragmatic Hernia Study Group: a voluntary international registry*. Seminars in pediatric surgery, 2008. **17**(2): p. 90-7.
3. Lee, C., A.J. Iafrate, and A.R. Brothman, *Copy number variations and clinical cytogenetic diagnosis of constitutional disorders*. Nat Genet, 2007. **39**(7 Suppl): p. S48-54.
4. Itsara, A., et al., *De novo rates and selection of large copy number variation*. Genome Res, 2010. **20**(11): p. 1469-81.
5. Fu, W., et al., *Identification of copy number variation hotspots in human populations*. American journal of human genetics, 2010. **87**(4): p. 494-504.
6. Pinto, D., et al., *Functional impact of global rare copy number variation in autism spectrum disorders*. Nature, 2010. **466**(7304): p. 368-72.
7. Cooper, G.M., et al., *A copy number variation morbidity map of developmental delay*. Nat Genet, 2011. **43**(9): p. 838-46.
8. Shao, L., et al., *Identification of chromosome abnormalities in subtelomeric regions by microarray analysis: a study of 5,380 cases*. American journal of medical genetics. Part A, 2008. **146A**(17): p. 2242-51.
9. Boone, P.M., et al., *Detection of clinically relevant exonic copy-number changes by array CGH*. Human mutation, 2010. **31**(12): p. 1326-42.
10. Stranger, B.E., et al., *Relative impact of nucleotide and copy number variation on gene expression phenotypes*. Science, 2007. **315**(5813): p. 848-53.
11. Kleinjan, D.A. and V. van Heyningen, *Long-range control of gene expression: emerging mechanisms and disruption in disease*. American journal of human genetics, 2005. **76**(1): p. 8-32.
12. Kleinjan, D.J. and P. Coutinho, *Cis-ruption mechanisms: disruption of cis-regulatory control as a cause of human genetic disease*. Briefings in functional genomics & proteomics, 2009. **8**(4): p. 317-32.
13. Lupski, J.R. and P. Stankiewicz, *Genomic disorders: molecular mechanisms for rearrangements and conveyed phenotypes*. PLoS genetics, 2005. **1**(6): p. e49.
14. Reymond, A., et al., *Side effects of genome structural changes*. Curr Opin Genet Dev, 2007. **17**(5): p. 381-6.
15. Ricard, G., et al., *Phenotypic consequences of copy number variation: insights from Smith-Magenis and Potocki-Lupski syndrome mouse models*. PLoS Biol, 2010. **8**(11): p. e1000543.
16. Henrichsen, C.N., E. Chaignat, and A. Reymond, *Copy number variants, diseases and gene expression*. Human molecular genetics, 2009. **18**(R1): p. R1-8.
17. Chaignat, E., et al., *Copy number variation modifies expression time courses*. Genome Res, 2011. **21**(1): p. 106-13.
18. Lee, C. and S.W. Scherer, *The clinical context of copy number variation in the human genome*. Expert reviews in molecular medicine, 2010. **12**: p. e8.
19. Girirajan, S., et al., *A recurrent 16p12.1 microdeletion supports a two-hit model for severe developmental delay*. Nat Genet. **42**(3): p. 203-9.
20. Veltman, J.A. and H.G. Brunner, *Understanding variable expressivity in microdeletion syndromes*. Nat Genet. **42**(3): p. 192-3.
21. Alkalay, A.A., et al., *Genetic dosage compensation in a family with velo-cardio-facial/DiGeorge/22q11.2 deletion syndrome*. American journal of medical genetics. Part A, 2011.
22. Hammond, P., et al., *Discriminating power of localized three-dimensional facial morphology*. American journal of human genetics, 2005. **77**(6): p. 999-1010.
23. Hammond, P., *The use of 3D face shape modelling in dysmorphology*. Archives of disease in childhood, 2007. **92**(12): p. 1120-6.
24. Peetsold, M.G., et al., *The long-term follow-up of patients with a congenital diaphragmatic hernia: a broad spectrum of morbidity*. Pediatr Surg Int, 2009. **25**(1): p. 1-17.

25. Susman, M.R., D.J. Amor, and J.L. Halliday, *Non-invasive prenatal diagnosis--toward a new horizon*. The Medical journal of Australia, 2009. **191**(7): p. 414.
26. Sekizawa, A., et al., *Recent advances in non-invasive prenatal DNA diagnosis through analysis of maternal blood*. The journal of obstetrics and gynaecology research, 2007. **33**(6): p. 747-64.
27. Ohashi, Y., et al., *Quantitation of fetal DNA in maternal serum in normal and aneuploid pregnancies*. Hum Genet, 2001. **108**(2): p. 123-7.
28. Hall, A., A. Bostanci, and C.F. Wright, *Non-invasive prenatal diagnosis using cell-free fetal DNA technology: applications and implications*. Public health genomics, 2010. **13**(4): p. 246-55.
29. Holder, A.M., et al., *Genetic factors in congenital diaphragmatic hernia*. Am J Hum Genet, 2007. **80**(5): p. 825-45.
30. Wat, M.J., Veenma, D.C.M, *Genomic alterations that contribute to the development of isolated and non-isolated congenital diaphragmatic hernia*. J med Genet, 2011.
31. Machado, I.N., et al., *Copy number imbalances detected with a BAC-based array comparative genomic hybridization platform in congenital diaphragmatic hernia fetuses*. Genetics and molecular research : GMR, 2011. **10**(1): p. 261-7.
32. Teshiba, R., et al., *Identification of TCTE3 as a gene responsible for congenital diaphragmatic hernia using a high-resolution single-nucleotide polymorphism array*. Pediatric surgery international, 2011. **27**(2): p. 193-8.
33. Srisupundit, K., et al., *Targeted array comparative genomic hybridisation (array CGH) identifies genomic imbalances associated with isolated congenital diaphragmatic hernia (CDH)*. Prenat Diagn, 2010. **30**(12-13): p. 1198-206.
34. Fraser, P. and W. Bickmore, *Nuclear organization of the genome and the potential for gene regulation*. Nature, 2007. **447**(7143): p. 413-7.
35. Schoenfelder, S., I. Clay, and P. Fraser, *The transcriptional interactome: gene expression in 3D*. Curr Opin Genet Dev, 2010. **20**(2): p. 127-33.
36. Noordermeer, D., et al., *Variiegated gene expression caused by cell-specific long-range DNA interactions*. Nature cell biology, 2011. **13**(8): p. 944-51.
37. Schoenfelder, S., et al., *Preferential associations between co-regulated genes reveal a transcriptional interactome in erythroid cells*. Nat Genet, 2010. **42**(1): p. 53-61.
38. Bartkuhn, M. and R. Renkawitz, *Long range chromatin interactions involved in gene regulation*. Biochim Biophys Acta, 2008. **1783**(11): p. 2161-6.
39. Cope, N.F., P. Fraser, and C.H. Eskiw, *The yin and yang of chromatin spatial organization*. Genome biology, 2010. **11**(3): p. 204.
40. Dekker, J., *Gene regulation in the third dimension*. Science, 2008. **319**(5871): p. 1793-4.
41. Fedorova, E. and D. Zink, *Nuclear architecture and gene regulation*. Biochim Biophys Acta, 2008. **1783**(11): p. 2174-84.
42. Gondor, A. and R. Ohlsson, *Chromosome crosstalk in three dimensions*. Nature, 2009. **461**(7261): p. 212-7.
43. Hakim, O., M.H. Sung, and G.L. Hager, *3D shortcuts to gene regulation*. Curr Opin Cell Biol, 2010. **22**(3): p. 305-13.
44. Lawrence, J.B. and C.M. Clemson, *Gene associations: true romance or chance meeting in a nuclear neighborhood?* J Cell Biol, 2008. **182**(6): p. 1035-8.
45. Misteli, T., *Beyond the sequence: cellular organization of genome function*. Cell, 2007. **128**(4): p. 787-800.
46. Osborne, C.S. and C.H. Eskiw, *Where shall we meet? A role for genome organisation and nuclear sub-compartments in mediating interchromosomal interactions*. J Cell Biochem, 2008.
47. Papantonis, A. and P.R. Cook, *Genome architecture and the role of transcription*. Curr Opin Cell Biol, 2010. **22**(3): p. 271-6.
48. Sexton, T., F. Bantignies, and G. Cavalli, *Genomic interactions: chromatin loops and gene meeting points in transcriptional regulation*. Semin Cell Dev Biol, 2009. **20**(7): p. 849-55.
49. Williams, A., C.G. Spilianakis, and R.A. Flavell, *Interchromosomal association and gene regulation in trans*. Trends Genet, 2010. **26**(4): p. 188-97.

50. Dillon, N., *The impact of gene location in the nucleus on transcriptional regulation*. Dev Cell, 2008. **15**(2): p. 182-6.
51. Ferrai, C., et al., *Gene positioning*. Cold Spring Harb Perspect Biol, 2010. **2**(6): p. a000588.
52. Amano, T., et al., *Chromosomal dynamics at the Shh locus: limb bud-specific differential regulation of competence and active transcription*. Dev Cell, 2009. **16**(1): p. 47-57.
53. Bacher, C.P., et al., *Transient colocalization of X-inactivation centres accompanies the initiation of X inactivation*. Nat Cell Biol, 2006. **8**(3): p. 293-9.
54. Brown, J.M., et al., *Coregulated human globin genes are frequently in spatial proximity when active*. J Cell Biol, 2006. **172**(2): p. 177-87.
55. Kim, S.H., et al., *Spatial genome organization during T-cell differentiation*. Cytogenet Genome Res, 2004. **105**(2-4): p. 292-301.
56. Spilianakis, C.G., et al., *Interchromosomal associations between alternatively expressed loci*. Nature, 2005. **435**(7042): p. 637-45.
57. Williams, R.R., et al., *Neural induction promotes large-scale chromatin reorganisation of the Mash1 locus*. J Cell Sci, 2006. **119**(Pt 1): p. 132-40.
58. de Laat, W. and F. Grosveld, *Inter-chromosomal gene regulation in the mammalian cell nucleus*. Curr Opin Genet Dev, 2007. **17**(5): p. 456-64.
59. Noordermeer, D., et al., *Variiegated gene expression caused by cell-specific long-range DNA interactions*. Nat Cell Biol, 2011.
60. Clugston, R.D., W. Zhang, and J.J. Greer, *Early development of the primordial mammalian diaphragm and cellular mechanisms of nitrofen-induced congenital diaphragmatic hernia*. Birth defects research. Part A, Clinical and molecular teratology, 2010. **88**(1): p. 15-24.
61. van Loenhout RB, T.I., Fox EK, Huang Z, and P.M. Tibboel D, Keijzer R, *The pulmonary mesenchymal tissue layer is defective in an in vitro recombinant model of nitrofen-induced lung hypoplasia*. Am J Pathol, 2011(Accepted Sept 6th 2011).
63. Yu, J., et al., *Neural crest-derived defects in experimental congenital diaphragmatic hernia*. Pediatric surgery international, 2001. **17**(4): p. 294-8.
64. McCredie, J. and I.S. Reid, *Congenital diaphragmatic hernia associated with homolateral upper limb malformation: a study of possible pathogenesis in four cases*. The Journal of pediatrics, 1978. **92**(5): p. 762-5.
65. Klaassens, M., A. de Klein, and D. Tibboel, *The etiology of congenital diaphragmatic hernia: still largely unknown?* Eur J Med Genet, 2009. **52**(5): p. 281-6.
66. Ijpenberg, A., et al., *Wt1 and retinoic acid signalling are essential for stellate cell development and liver morphogenesis*. Developmental biology, 2007. **312**(1): p. 157-70.
67. Norden, J., et al., *Wt1 and retinoic acid signalling in the subcoelomic mesenchyme control the development of the pleuropericardial membranes and the sinus horns*. Circulation research, 2010. **106**(7): p. 1212-20.
68. Clugston, R.D., et al., *Understanding abnormal retinoid signalling as a causative mechanism in congenital diaphragmatic hernia*. American journal of respiratory cell and molecular biology, 2010. **42**(3): p. 276-85.
69. You, L.R., et al., *Mouse lacking COUP-TFII as an animal model of Bochdalek-type congenital diaphragmatic hernia*. Proc Natl Acad Sci U S A, 2005. **102**(45): p. 16351-6.
70. Vilhais-Neto, G.C., et al., *Rere controls retinoic acid signalling and somite bilateral symmetry*. Nature, 2010. **463**(7283): p. 953-7.
71. Vandenberg, L.N. and M. Levin, *Far from solved: a perspective on what we know about early mechanisms of left-right asymmetry*. Developmental dynamics : an official publication of the American Association of Anatomists, 2010. **239**(12): p. 3131-46.
72. Fakhro, K.A., et al., *Rare copy number variations in congenital heart disease patients identify unique genes in left-right patterning*. Proc Natl Acad Sci U S A, 2011. **108**(7): p. 2915-20.
73. Mayer, S., R. Metzger, and D. Kluth, *The embryology of the diaphragm*. Seminars in pediatric surgery, 2011. **20**(3): p. 161-9.

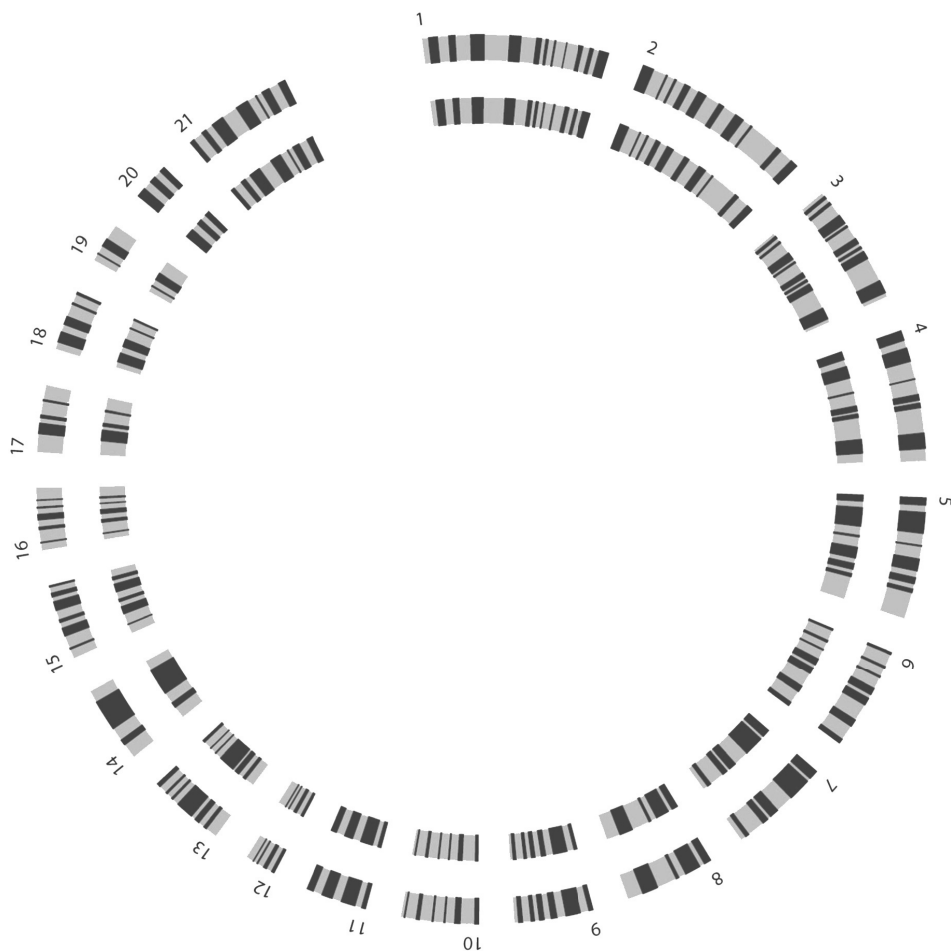
74. Kluth, D., et al., *Embryology of congenital diaphragmatic hernia*. Seminars in pediatric surgery, 1996. **5**(4): p. 224-33.
75. Gillemans, N., Szumska, D, Veenma, D, Esteghamat, F, Hou, J, van Ijcken, W, de Klein, A, Bhattacharya, S, Tibboel, D, Grosveld, F, Philipsen, S, van Dijk, T *Complex congenital diaphragmatic hernia in mice lacking Chromatin target of PRMT1*. PLoS genetics, 2011. Submitted.
76. Ackerman, K.G. and J.J. Greer, *Development of the diaphragm and genetic mouse models of diaphragmatic defects*. Am J Med Genet C Semin Med Genet, 2007. **145**(2): p. 109-16.
77. Liu, J., et al., *Congenital diaphragmatic hernia, kidney agenesis and cardiac defects associated with Slit3-deficiency in mice*. Mechanisms of development, 2003. **120**(9): p. 1059-70.
78. Sharma, S., et al., *A case of congenital diaphragmatic hernia with a hernia sac attached to the liver: hints for an early embryological insult*. Journal of pediatric surgery, 2007. **42**(10): p. 1761-3.
79. Arafah, M., D.T. Boqari, and K.O. Alsaad, *Left-sided congenital diaphragmatic hernia with multiple congenital cardiac anomalies, hernia sac, and microscopic hepatic heterotopia: a case report*. Pathology research international, 2011. **2011**: p. 967107.
80. Deprest, J., et al., *Fetal intervention for congenital diaphragmatic hernia: the European experience*. Seminars in perinatology, 2005. **29**(2): p. 94-103.
81. Goumy, C., et al., *Retinoid Pathway and Congenital Diaphragmatic Hernia: Hypothesis from the Analysis of Chromosomal Abnormalities*. Fetal Diagn Ther, 2010.
82. Bielinska, M., et al., *Molecular genetics of congenital diaphragmatic defects*. Ann Med, 2007. **39**(4): p. 261-74.
83. Russell, M.K., Longoni, M., Wells, J. et al., *Congenital diaphragmatic hernia candidate genes derived from embryonic transcriptomes*. Proc Natl Acad Sci U S A. 2012. **109**(8):2978-83.
84. Clugston, R.D., W. Zhang, and J.J. Greer, *Gene expression in the developing diaphragm: significance for congenital diaphragmatic hernia*. American journal of physiology. Lung cellular and molecular physiology, 2008. **294**(4): p. L665-75.
85. Lin, F.J., et al., *Coup d'Etat: an orphan takes control*. Endocrine reviews, 2011. **32**(3): p. 404-21.
86. Rosa, A. and A.H. Brivanlou, *A regulatory circuitry comprised of miR-302 and the transcription factors OCT4 and NR2F2 regulates human embryonic stem cell differentiation*. The EMBO journal, 2011. **30**(2): p. 237-48.
87. Bleyl, S.B., et al., *Candidate genes for congenital diaphragmatic hernia from animal models: sequencing of FOG2 and PDGFRalpha reveals rare variants in diaphragmatic hernia patients*. European journal of human genetics : EJHG, 2007. **15**(9): p. 950-8.
88. Ackerman, K.G., et al., *Fog2 is required for normal diaphragm and lung development in mice and humans*. PLoS Genet, 2005. **1**(1): p. 58-65.
89. Huggins, G.S., et al., *Friend of GATA 2 physically interacts with chicken ovalbumin upstream promoter-TF2 (COUP-TF2) and COUP-TF3 and represses COUP-TF2-dependent activation of the atrial natriuretic factor promoter*. The Journal of biological chemistry, 2001. **276**(30): p. 28029-36.
90. Manuylov, N.L. and S.G. Tevosian, *Cardiac expression of Tnnt1 requires the GATA4-FOG2 transcription complex*. TheScientificWorldJournal, 2009. **9**: p. 575-87.
91. Zhou, B., et al., *Fog2 is critical for cardiac function and maintenance of coronary vasculature in the adult mouse heart*. The Journal of clinical investigation, 2009. **119**(6): p. 1462-76.
92. Smagulova, F.O., et al., *GATA4/FOG2 transcriptional complex regulates Lhx9 gene expression in murine heart development*. BMC developmental biology, 2008. **8**: p. 67.
93. Crispino, J.D., et al., *Proper coronary vascular development and heart morphogenesis depend on interaction of GATA-4 with FOG cofactors*. Genes Dev, 2001. **15**(7): p. 839-44.
94. Cai, K. and L.J. Gudas, *Retinoic acid receptors and GATA transcription factors activate the transcription of the human lecithin:retinol acyltransferase gene*. The international journal of biochemistry & cell biology, 2009. **41**(3): p. 546-53.
95. Jay, P.Y., et al., *Impaired mesenchymal cell function in Gata4 mutant mice leads to diaphragmatic hernias and primary lung defects*. Developmental biology, 2007. **301**(2): p. 602-14.
96. Wat, M.J., et al., *Chromosome 8p23.1 deletions as a cause of complex congenital heart defects and diaphragmatic hernia*. American journal of medical genetics. Part A, 2009. **149A**(8): p. 1661-77.

97. Wat, M., Yu, Z, Veenma, D, Garcia, M, Hernandez, A, Holder, AM, Wat, JJ, Chen, Y, Dickinson, M, Tibboel, D, de Klein, A, Lee, B, Scott, DA, *Mouse model reveals the role of SOX7 in the development of congenital diaphragmatic hernia associated with recurrent deletions of 8p23.1*. Human Molecular genetics 2011. **ReSubmitted March 2012**.
98. Lee, S.B. and D.A. Haber, *Wilms tumor and the WT1 gene*. Exp Cell Res, 2001. **264**(1): p. 74-99.
99. Moore, A.W., et al., *YAC transgenic analysis reveals Wilms' tumour 1 gene activity in the proliferating coelomic epithelium, developing diaphragm and limb*. Mechanisms of development, 1998. **79**(1-2): p. 169-84.
100. Clugston, R.D., et al., *Understanding abnormal retinoid signalling as a causative mechanism in congenital diaphragmatic hernia*. Am J Respir Cell Mol Biol, 2010. **42**(3): p. 276-85.
101. Chassaing, N., et al., *Phenotypic spectrum of STRA6 mutations: from Matthew-Wood syndrome to non-lethal anophthalmia*. Human mutation, 2009. **30**(5): p. E673-81.
102. Kantarci, S., et al., *Mutations in LRP2, which encodes the multiligand receptor megalin, cause Donnai-Barrow and facio-oculo-acoustico-renal syndromes*. Nat Genet, 2007. **39**(8): p. 957-9.
103. Pasutto, F., et al., *Mutations in STRA6 cause a broad spectrum of malformations including anophthalmia, congenital heart defects, diaphragmatic hernia, alveolar capillary dysplasia, lung hypoplasia, and mental retardation*. American journal of human genetics, 2007. **80**(3): p. 550-60.
104. Beurskens, L.W., et al., *Retinol status of newborn infants is associated with congenital diaphragmatic hernia*. Pediatrics, 2010. **126**(4): p. 712-20.
105. Mark, M., N.B. Ghyselinck, and P. Chambon, *Function of retinoic acid receptors during embryonic development*. Nucl Recept Signal, 2009. **7**: p. e002.
106. Mark, M., et al., *A genetic dissection of the retinoid signalling pathway in the mouse*. Proc Nutr Soc, 1999. **58**(3): p. 609-13.
107. Niederreither, K. and P. Dolle, *Retinoic acid in development: towards an integrated view*. Nat Rev Genet, 2008. **9**(7): p. 541-53.
108. Rochette-Egly, C. and P. Germain, *Dynamic and combinatorial control of gene expression by nuclear retinoic acid receptors (RARs)*. Nucl Recept Signal, 2009. **7**: p. e005.
109. Masia, S., et al., *Rapid, nongenomic actions of retinoic acid on phosphatidylinositol-3-kinase signalling pathway mediated by the retinoic acid receptor*. Molecular endocrinology, 2007. **21**(10): p. 2391-402.
110. Maghsoodi, B., et al., *Retinoic acid regulates RARalpha-mediated control of translation in dendritic RNA granules during homeostatic synaptic plasticity*. Proc Natl Acad Sci U S A, 2008. **105**(41): p. 16015-20.
111. Mohseni-Bod, H. and D. Bohn, *Pulmonary hypertension in congenital diaphragmatic hernia*. Seminars in pediatric surgery, 2007. **16**(2): p. 126-33.
112. Sluiter, I., et al., *Vascular abnormalities in human newborns with pulmonary hypertension*. Expert review of respiratory medicine, 2011. **5**(2): p. 245-56.
113. Arkovitz, M.S., B.A. Hyatt, and J.M. Shannon, *Lung development is not necessary for diaphragm development in mice*. Journal of pediatric surgery, 2005. **40**(9): p. 1390-4.
114. Chou, A.K., et al., *Unilateral lung agenesis--detrimental roles of surrounding vessels*. Pediatric pulmonology, 2007. **42**(3): p. 242-8.
115. Li, Y., et al., *Sonic hedgehog signalling regulates Gli3 processing, mesenchymal proliferation, and differentiation during mouse lung organogenesis*. Developmental biology, 2004. **270**(1): p. 214-31.
116. Clugston, R.D., W. Zhang, and J.J. Greer, *Early development of the primordial mammalian diaphragm and cellular mechanisms of nitrofen-induced congenital diaphragmatic hernia*. Birth Defects Res A Clin Mol Teratol. 2010. **88**(1): p. 15-24.
117. Cardoso, W.V. and D.N. Kotton, *Specification and patterning of the respiratory system*, in *StemBook2008*: Cambridge (MA).
118. Cardoso, W.V. and J. Lu, *Regulation of early lung morphogenesis: questions, facts and controversies*. Development, 2006. **133**(9): p. 1611-24.
119. Warburton, D., et al., *Lung organogenesis*. Current topics in developmental biology, 2010. **90**: p. 73-158.

120. Kluth, D., et al., *Nitrofen-induced diaphragmatic hernias in rats: an animal model*. Journal of pediatric surgery, 1990. **25**(8): p. 850-4.
121. Mendelsohn, C., et al., *Function of the retinoic acid receptors (RARs) during development (II). Multiple abnormalities at various stages of organogenesis in RAR double mutants*. Development, 1994. **120**(10): p. 2749-71.
122. Yuan, W., et al., *A genetic model for a central (septum transversum) congenital diaphragmatic hernia in mice lacking Slit3*. Proc Natl Acad Sci U S A, 2003. **100**(9): p. 5217-22.
123. Suri, M., et al., *WT1 mutations in Meacham syndrome suggest a coelomic mesothelial origin of the cardiac and diaphragmatic malformations*. Am J Med Genet A, 2007. **143A**(19): p. 2312-20.
124. Takahasi K, Tanabe K, Ohnuki M, Narita M, Ichisaka T, Tomoda K, Yamanaka S. 200. Induction of pluripotent stem cells from adult human fibroblasts by defined factors. Cell, 131, 861-72.
125. Chamberlain, S.J., et al., *Induced pluripotent stem cell models of the genomic imprinting disorders Angelman and Prader-Willi syndromes*. Proceedings of the National Academy of Sciences of the United States of America, 2010. **107**(41): p. 17668-73.
126. Yang, J., et al., *Induced pluripotent stem cells can be used to model the genomic imprinting disorder Prader-Willi syndrome*. The Journal of biological chemistry, 2010. **285**(51): p. 40303-11.
127. Yazawa, M., et al., *Using induced pluripotent stem cells to investigate cardiac phenotypes in Timothy syndrome*. Nature, 2011. **471**(7337): p. 230-4.
128. Yoshida, Y. and S. Yamanaka, *iPS cells: a source of cardiac regeneration*. Journal of molecular and cellular cardiology, 2011. **50**(2): p. 327-32.
129. Walsh, R.M. and K. Hochedlinger, *Modeling Rett syndrome with stem cells*. Cell, 2010. **143**(4): p. 499-500.
130. Doss, M.X., et al., *Specific Gene Signatures and Pathways in Mesodermal Cells and Their Derivatives Derived from Embryonic Stem Cells*. Stem cell reviews, 2011.
131. Era, T., *Mesoderm cell development from ES cells*. Methods in molecular biology, 2010. **636**: p. 87-103.
132. Evseenko, D., et al., *Mapping the first stages of mesoderm commitment during differentiation of human embryonic stem cells*. Proc Natl Acad Sci U S A, 2010. **107**(31): p. 13742-7.
133. Bismuth, K. and F. Relaix, *Genetic regulation of skeletal muscle development*. Exp Cell Res, 2010. **316**(18): p. 3081-6.
134. Rojas, A., et al., *Gata4 expression in lateral mesoderm is downstream of BMP4 and is activated directly by Forkhead and GATA transcription factors through a distal enhancer element*. Development, 2005. **132**(15): p. 3405-17.
135. Sweetman, D., et al., *The migration of paraxial and lateral plate mesoderm cells emerging from the late primitive streak is controlled by different Wnt signals*. BMC developmental biology, 2008. **8**: p. 63.

Chapter 5

Appendices



5.1 Summary

Congenital diaphragmatic hernia (CDH) is a severe birth defect characterized by a hole in the postero-lateral part of the diaphragm muscle – a critical organ for proper respiration – and affects approximately 1 in 3000 live births. This defect can be surgically repaired usually within 2-5 days after birth. However, ventilatory support and pharmaceutical treatment of the co-occurring lung hypoplasia and pulmonary hypertension are insufficient in respectively 20% of isolated cases and 60% of complex ones leading to early perinatal death.

A clear understanding of the early embryonic processes and factors that lead to CDH is still missing. Their identification is hampered by the multifactorial and heterogenic nature of CDH. The same holds true for prognostic factors predicting treatment refraction. Albeit, valuable insights into the genetic susceptibility of CDH has recently been provided by the application of new molecular cytogenetic techniques to patients' DNA. Chromosomal aberrations are now detected in 20-30% of human cases and some of these recurrent, structural anomalies point to CDH associated loci and genes involved in the Retinoic Acid (RA) signalling pathway. The studies described in this thesis provide and evaluate new genetic and epigenetic perceptions on CDH' aetiology.

In chapter 2 we focused on different aspects of Copy Number Variations (CNVs) in CDH. Two large cohorts – including both isolated as well as complex cases – were screened for germline CNVs using high-resolution arrays. Results gave a valuable indication of the proportion of underlying *de novo* and inherited structural events, in which the latter could function as a disease-specific susceptible background. Besides overlap with various previously identified CDH associated hot spots, new CDH-candidate genes on chromosome 5p15.31, 17q12.2, 9p22.3 and 12q24 were proposed. These findings underscore the importance of screening all individuals with diaphragmatic defects by high-resolution techniques. The possibility of somatic mutations restricted to the affected diaphragm tissue was excluded by screening for CNVs in DNA isolated from diaphragm biopsies of a small subcohort of isolated CDH patients.

Targeted approaches searching for detrimental changes in ZFPM2 (n=52), SOX7 (n=77) and CHTOP (n= 43) were executed in studies from chapter 2 as well, yielding respectively three, zero and one changes which had not been previously described in the dbSNP database. Yet, allocation of any functional implication to these changes was hampered by the fact that over half were inherited or parents were unavailable. Importantly, the Chtop mutation- a main target of the protein arginine methyltransferase Prmt1- stresses on the possibility that DNA errors in chromatin-associated proteins might confer epigenetic susceptibility to CDH.

Article 2.4 continued on the search for CNVs, in this case structural aberrations that differed between twins discordant for esophageal atresia (n=7) or CDH (n=4). Results showed an identical copy number profile in each twin pair. Mosaic events – with a detection threshold of twenty per

cent – could not be detected either. Therefore, other factors (i.e. environmental or epigenetic) are involved in the MZ phenotypic differences in these investigated congenital anomaly cohorts. In the final article of chapter 2 we discussed whether and how a genetic aberration present at low-mosaic frequencies has the potential to mediate tissue-specific dysfunction in an affected complex CDH individual. Hypothetically, a higher incidence of the aberration in affected organs such as lung and diaphragm as compared to healthy ones could explain the patients' phenotype. High-resolution whole genome SNP array confirmed a low-level (20%) mosaic unbalanced translocation (5;12) in uncultured amniotic fluid cells. Subsequently, targeted Fluorescence In-Situ Hybridization (FISH) was used to analyse mosaic frequencies in several postmortem collected tissues. These results demonstrated that in contrast to our hypothesis, the mosaic frequency was independent of the affected status of the tissue. Differences in default gene-expression requirements between tissues could account for this phenotypic “organ” discrepancy.

In chapter 3 we focused on putative epigenetic mechanisms underlying diaphragm defects both in a human complex CDH model (3.1) as well as in a teratogen CDH-induced rodent model (3.3). Coordinated expression and interaction of functionally related genes at a certain transcription factory have been suggested in literature and may provide the cell with a mechanism by which it could coordinate the expression of genes of a common pathway. In turn, changes in these spatial patterns during development or as a consequence of cell-differentiation might serve as markers to identify diseased states. Following this, we hypothesized the three-dimensional clustering of 3 crucial “diaphragm” genes (NR2F2, GATA4 and ZFPM2) as a prerequisite for proper co-expression and normal diaphragm development and a perturbation of this process in patients with a diaphragm defect. We used dermal fibroblasts derived from a patient with a 15q monosomy as a model system, since this is the most common and strongest CDH associated chromosomal hot spot to date and results in only 1 functional NR2F2 allele. Results showed that the coordinated expression of these CDH candidates was independent of nuclear co-association. Since juxtapositioning of genes could be dependent on a certain stimulus, gene clustering was studied after retinoic acid (RA) induction also, giving similar results.

After ruling out spatial epigenetic effects in 15q monosomy fibroblasts, their transcriptome profiles were analysed in default and after a 48-hour exposure to four different RA-concentrations (3.2). We speculated that genes in the 15q26 region are both important for diaphragm development as well as for RA-signalling and suggested that overstimulation with RA would unmask a relative RA-deficiency in these patients. Indeed, results demonstrated that key components of RA homeostasis were profoundly up-regulated after RA stimulation in patient cell lines only. In addition, new light was shed on existing ideas of 15q26-candidate genes. Results further pointed out several new early mesenchymal and lung vascular candidate factors, underlining a concomitant effect on lung- as well as mesenchyme diaphragm development.

In the final article of chapter 3, we applied chromosome conformation capture technology (4C). 4C allows for screening the genome in an unbiased manner for DNA regions that are in close contact in the three-dimensional nuclear space to a region of interest, in our study the promoter

region of NR2F2. DNA spatial patterns identified at a certain developmental stage are thought to represent a blueprint of the genome's functional output at that specific time-window. Therefore, identification of the subnuclear environment of the NR2F2 gene in embryonic tissues of healthy rodent offspring as well as upon chemical interference with RA signalling will provide novel (epi) genetic insights into the role of NR2F2 in diaphragm- and lung organogenesis. Interactions of NR2F2 in heart-and liver served as non-CDH specific controls. Subtle differences for specific interactions were demonstrated upon nitrofen-treatment, pointing to new CDH candidate genes. Moreover, increased knowledge of the most abundant interaction partners of NR2F2 across all 4C samples, identified 1 specific domain on chromosome 14 and the Oct1 protein as the common regulatory source of the NR2F2 interactome.

Despite these remarkable results, careful interpretation is mandatory for several reasons. Firstly, literature recently suggested that the initial perturbation event of diaphragm development occurs at a much earlier stage (i.e. rodent day E13.5) than previously expected. Secondly, genetically altered (rodent) animal models as a substitute for human material may display fundamental differences in tissue-specific expression patterns as compared to humans. Finally timing and mechanism of gene regulation may diverge from the human species. Together these remarks stress on the importance of developing a disease model that reflects both the genetic background of the original patient and provides target-tissue in sufficient amounts and with crucial embryonic characteristics mimicking early developmental processes. The innovative induced Pluripotent Stem Cell (iPSC) technique fulfils these criteria and is suggested for future CDH research in the general discussion of Chapter IV. Furthermore, this discussion elaborates on the strengths and weaknesses of the studies in this thesis and provides new insights on diaphragm embryology.

5.2 Samenvatting

Congenitale Hernia Diafragmatica (CHD) is een ernstige aangeboren aandoening van het middenrif en wordt gekenmerkt door een gat in het postero-laterale gedeelte van deze essentiële ademhalingsspier. CHD komt voor bij één op de 3000 levendgeborenen. Chirurgische reparatie van het defect is meestal mogelijk binnen twee tot vijf dagen na de geboorte. Een vroege perinatale sterfte treedt echter op in 20% van de geïsoleerde, en 60% van de complexe CHD gevallen. Dit wordt veroorzaakt doordat ademhalingsondersteuning en medicamenteuze behandeling van de bijkomende longhypoplasie en pulmonaire hypertensie niet afdoende is.

Het multifactoriële en heterogene karakter van CHD bemoeilijkt een goed inzicht in welke vroeg embryologische processen en factoren deze aandoening veroorzaken. Dit geldt ook voor de prognostische factoren die het falen van therapie kunnen voorspellen. Wel zijn er in de laatste 5 jaar belangrijke inzichten verkregen door analyse van het DNA van patiënten met behulp van nieuwe molecuair cytogenetische technieken. Deze aanpak heeft er onder andere toe geleid dat men in 20 tot 30% van de patiënten een structurele chromosomale afwijking kan detecteren. Enkele van deze structurele afwijkingen komen veelvuldig voor en richten de aandacht op loci en genen die geassocieerd zijn met zowel CHD als ook met de vitamine-A signaalcascade. In de studies beschreven in dit proefschrift werden nieuwe genetische en epigenetische inzichten in de etiologie van CHD geïdentificeerd en geanalyseerd.

In hoofdstuk twee van dit proefschrift richten we onze aandacht op Copy-Nummer Variaties (CNVs) in CHD. Door gebruik te maken van arrays met een hoge resolutie werden twee grote cohorten met zowel geïsoleerde als complexe patiënten gescreend op het voorkomen van CNV's in de kiembaan. Hierdoor werd een goede indicatie verkregen van het aantal de novo en overgeërfd structurele afwijkingen dat aan CHD ten grondslag ligt of kan bijdragen. Naast een aantal chromosomale "hot spots" die al eerder met CHD waren geassocieerd, werden nieuwe kandidaat genen op respectievelijk chromosoom 5p15.31, 17q12.2, 9p22.3 en 12q24 geïdentificeerd. Al deze bevindingen benadrukken het belang om alle individuen met een diafragmadefect te screenen met molecuair genetische technieken van een hoge resolutie. Somatische mutaties, dus afwijkingen enkel en alleen in het aangedane diafragmaweefsel, werden uitgesloten door van een kleine subgroep van geïsoleerde CHD patiënten DNA te isoleren uit diafragmaweefsel. Meer gerichte strategieën, met als doel de identificatie van schadelijke mutaties in ZFPM2 (n=52), SOX7 (n=77) en CHTOP (n= 43) werden ook uitgevoerd. Dit resulteerde in respectievelijk drie, nul en één verandering van een enkele base (SNP), die niet voorkwamen in de "dbSNP" databank. Of dergelijke mutaties bijdragen aan CHD is niet altijd helder want vaak worden de mutaties overgeërfd van een normale ouder of is niet van beide ouders DNA aanwezig. Echter identificatie van de overgeërfd CHTOP mutatie – een DNA fout in een chromatine-geassocieerd eiwit en bovendien een cruciaal aangrijpingspunt van het arginine-methyltransferase eiwit PRMT – suggereert dat deze zou kunnen bijdragen aan een epigenetische vatbaarheid voor CHD.

In artikel 2.4 hebben we gezocht naar structurele afwijkingen die verschillend waren tussen eeneiige tweelingen die discordant waren voor slokdarm atresiën (n=7) of CHD (n=4). In alle tweelingenparen werd een identiek copy-nummer profiel gevonden. Tevens konden, met een detectie grens van 20%, geen afwijkingen in mozaïekvorm worden aangetoond. Andere factoren, zoals omgevings- en epigenetische factoren of zeldzame SNPs, zijn daarom verantwoordelijk voor de fenotypische verschillen in de eeneiige tweelingen van deze aangeboren afwijkings cohorten.

In het laatste artikel van hoofdstuk twee, bediscussiëren we, of en hoe, genetische afwijkingen met een laag-mozaïeke frequentie de potentie hebben om weefsel-specifieke disfunctie te genereren in aangedane complexe CHD individuen. Een hogere incidentie van de afwijking in de aangedane organen, zoals diafragma en longen, ten opzichte van de gezonde, kan hypothetisch gezien het variabele fenotype van de patiënt verklaren. Met behulp van een genoom-brede en -hoge resolutie SNP array konden we een laag- mozaïek (20%) ongebalanceerde translocatie bevestigen in het vruchtwater van de patiënt. Vervolgens werd een gericht FISH - Fluorescerend In-Situ-Hybridisatie -protocol toegepast om de mozaïek frequenties te bepalen in verschillende postmortem verkregen weefsels. In tegenstelling tot de algehele hypothese, was de mozaïekfrequentie niet afhankelijk van de aangedane status van het weefsel. Deze fenotypische discrepantie op orgaan niveau kan veroorzaakt worden door een verschillende behoefte in de default genexpressie spiegels.

In het tweede gedeelte van dit proefschrift richtten we onze aandacht op de mogelijk epigenetische mechanismen die ten grondslag kunnen liggen aan diafragma defecten bij de mens (hoofdstuk 3.1) of bij ratten in een teratogeen geïnduceerd CHD-model (hoofdstuk 3.3). In de literatuur wordt een gecoördineerde expressie en interactie van functioneel gelijke genen in transcriptiefabrieken gesuggereerd en dit geeft de cel de mogelijkheid om de expressie van genen uit één en dezelfde signaalcascade te reguleren. Veranderingen in de ruimtelijke oriëntatie gedurende een bepaalde ontwikkelingsfase of als gevolg van differentiatie kunnen dan dienen als ziekte markers. In navolging van dit idee, veronderstelden wij dat de driedimensionale clustering van drie kandidaat diafragma genen (*NR2F2*, *ZFPM2* en *GATA4*) noodzakelijk is voor co-expressie en gezonde diafragma ontwikkeling. Een ontregeling van dit proces werd gesuggereerd bij CHD patiënten. Als model systeem werden de huidfibroblasten van een 15q monosomie patiënt met slechts één functioneel *NR2F2* allel gebruikt, omdat dit tot nu toe de meest voorkomende en sterkst CHD geassocieerde chromosomale “hot spot” is. De gecoördineerde expressie van de onderzochte CHD genen bleek echter onafhankelijk te zijn van hun nucleaire co-associatie. Met behulp van RA stimulatie werd tevens onderzocht of het tegenover elkaar liggen misschien afhankelijk was van een stimulus. Dit bleek niet het geval.

Nadat ruimtelijke epigenetische effecten in 15q monosomie fibroblasten waren uitgesloten, analyseerden we ook hun genoom brede transcriptieprofielen, zowel in een normale kweek als na stimulatie met vier verschillende concentraties RA gedurende 48 uur. We veronderstelden dat de genen in de 15q26 regio zeer belangrijk zijn voor zowel de diafragma ontwikkeling als voor de RA-signaalcascade. Overstimulatie met RA zou daarom een relatieve RA deficiëntie in deze

patiënten kunnen onthullen. In overeenstemming met deze zienswijze, lieten de resultaten zien dat cruciale elementen in RA metabolisatie alleen verhoogd waren in de patiëntengroep. Tevens werden nieuwe inzichten verkregen in bestaande ideeën van 15q26 kandidaat genen. Daarnaast benadrukten de resultaten het belang van enkele vroege mesenchymale- en longvasculaire-factoren. Dit laatste onderstreept een samenvallend effect op zowel de long-als de mesenchymale diafragma ontwikkeling in CHD.

In het laatste artikel van hoofdstuk drie passen we de “chromosoom conformatie capture” techniek (4C) toe. Met behulp van 4C kan op een onbevooroordeelde manier het genoom gescreend worden op DNA regio's die dicht in de buurt liggen (in de 3-dimensionale nucleus) van een locus waarin men geïnteresseerd is. In ons geval was dat de promotor regio van het *NR2F2* gen. De ruimtelijke DNA patronen in een bepaald ontwikkelingsstadium worden namelijk verondersteld representatief te zijn voor de functionele “output” van het genoom in die specifieke tijdsperiode. Er werd gezocht naar nieuwe epigenetische inzichten in de rol van *NR2F2* tijdens de diafragma- en long-ontwikkeling, door de nucleaire micro-omgeving van het *NR2F2* gen te bepalen in embryonaal weefsel van gezonde ratembryo's en deze te vergelijken met de patronen van ratembryo's met een chemisch verstoorde Vitamine-A signaaltransductie. De interacties van *NR2F2* gen in hart- en leverweefsel werden gebruikt als niet CHD-specifieke controles. Subtiele verschillen in specifieke interacties werden inderdaad gevonden in de met Nitrofen-behandelde weefsels en deze richten op hun beurt de aandacht op enkele nieuwe CHD kandidaatgenen. Tevens werd gekeken naar de overlap tussen de weefsels van de meest voorkomende interacties van *NR2F2*. Op deze wijze werd een domein op chromosoom 14 geïdentificeerd als mede het eiwit Oct1 als de gemeenschappelijke regulator van het “*NR2F2* interactoom”. Ondanks deze opmerkelijke resultaten is voorzichtigheid geboden met interpretatie hiervan. Ten eerste heeft data uit de recente literatuur bewezen dat de allereerste verstoring in de diafragma ontwikkeling een stuk eerder plaatsvindt dan altijd werd gedacht. Ten tweede blijken de genetisch gemanipuleerde (ratten) diermodellen in vergelijking met de mens fundamentele verschillen te vertonen in de weefsel-specifieke gen expressie. Tenslotte blijkt ook het tijdstip zelf en de genregulatie mechanismen af te wijken van de humane soort. Dit alles benadrukt het belang van ontwikkeling van een CHD-model dat representatief is voor de genetische achtergrond van de patiënt. En bovendien een model dat in staat is om voldoende weefselspecifiek materiaal te genereren die de cruciale embryonale karakteristieken van de vroege ontwikkeling reflecteert. Het recent ontwikkelde en innovatieve iPSC (geïnduceerde Pluripotente Stam Cel) model voldoet aan deze criteria. In de algemene discussie van hoofdstuk vier wordt de toepassing van deze techniek dan ook gesuggereerd voor toekomstig CHD onderzoek. In de generale discussie worden tot slot de details uitgewerkt van de positieve en negatieve kanten van de studies in dit proefschrift en worden ook de nieuwste inzichten in diafragma ontwikkeling behandeld.

5.2 Dankwoord

Het mooie van een promotietraject is dat het met zijn vele ups en downs veel overeenkomsten vertoont met de life-events van het “echte” leven, gebeurtenissen waarvan ik er in een kort tijdsbestek een aantal zelf heb mogen ervaren: specialisatie-plek, aankoop eerste huis en eerste kind.

Vanuit een wat naïeve gedachte ging ik dit traject in met het idee en de hoop belangrijke ontdekkingen te doen, die mogelijk zelfs het handelen van dokters in de kliniek zou kunnen beïnvloeden. Alhoewel – net zoals in het echte leven – het soms niet helemaal gaat zoals je gepland had, is het een super leerzame, leuke en ook soms minder leuke periode geweest. Ik denk met name met enorm veel plezier terug aan alle mooie en warme contacten die ik heb mogen opdoen. Hieronder dan ook een dankwoord aan allen die hebben bijgedragen aan dit “promotie”-leven.

Het kan niet vaak genoeg benadrukt worden maar zonder de inzet en bereidwilligheid van alle ouders (en hun kinderen) is dit type erfelijkheidsonderzoek niet mogelijk. Ik heb enorm veel bewondering voor hun veerkracht in deze moeilijke en vaak onzekere periode van hun leven. Dank voor jullie deelname!

Mijn promotor, Prof. dr. D. Tibboel, beste Dick. Het duurde even voor ik het zogenaamde “u”-stadium voorbij was, wat zeker veroorzaakt werd door het respect dat je bij iedereen afdwingt met je enorme kennis en drive in je werk. Je probeert altijd het allerbeste en onderste uit de kan te halen bij iedereen die voor je werkt. Ik heb je echter ook leren kennen als een betrokken baas, die klaarstaat als het op privé vlak niet zo lekker loopt. Dank daarvoor en hopelijk is dit niet het einde van onze werkrelatie.

Mijn co-promoter, dr. A. de Klein, lieve Annelies. Ik kan me nog goed het moment herinneren waarop we mijn eerste potentiële CDH mutatie bespraken. Achteraf bleek dit een fout positief resultaat te zijn, maar je zei: “Daan geniet van dit moment van spanning, adrenaline en de mogelijkheid van een ontdekking, ook al blijkt het later niet te kloppen. Want uit dit soort momenten haal je de energie en het doorzettingsvermogen om je onderzoek te blijven doen”. En dat was de spijker op zijn kop! Annelies, je bent in de afgelopen 4½ jaar een beetje mijn tweede moeder geworden, streng (doch rechtvaardig) en met een heel groot hart. Dank!

De leden van de kleine promotiecommissie: prof. dr. B. Oostra, prof. dr. I. Reiss en prof. dr. E. Dzierzak. Beste Ben, je bent gedeeltelijk met emeritaat, maar al volledig afscheid nemen van je lange en bijzonder succesvolle onderzoek-carrière kon je nog niet; ik heb met heel veel plezier op de 9de verdieping gewerkt. Veel dank voor de snelle beoordeling van het manuscript zo vlak voor je grote reis. Beste Irwin, dank voor de vele telefoontjes waarin je meldde dat er weer een

nieuwe CDH patiënt was! Ik ben enorm blij dat we na alle mogelijke plannen in het buitenland, toch collega's in het Erasmus MC blijven. Ik kijk er enorm naar uit, om ook te leren van je klinische vaardigheden op het gebied van de neonatologie. Dear prof. Dzierzak, thank you for thoroughly analyzing my manuscript and for providing valuable comments, it really improved its quality!

De overige leden van de grote promotiecommissie: prof. dr. R. Wijnen en prof. dr. R Hofstra, hartelijk dank voor uw bereidheid zitting te nemen in de grote commissie. Beste René, met je "down-to-earth" en zeer benaderbare houding weet je het algemene beeld van de chirurgische professor een aardig positieve draai te geven. Met veel plezier kijk ik terug naar de biertjes en wijntjes op de mooie terrassen in Rome. Beste Prof. Hofstra, ik wens u heel veel succes met het invulling geven aan uw nieuwe baan in Rotterdam: het leiden van de genetica afdeling.

Alle verpleegkundigen, arts-assistenten en fellows van de kinder-IC, dank voor jullie hulp bij het afnemen van de vele buizen bloed!

Het gehele kinder-chirurgische team en met name Kees & Conny, heel veel dank voor het steeds weer bellen vlak voor een operatie en dank voor jullie hulp bij het verzamelen van de vele diafragma biopten. Tevens ben ik dank verschuldigd aan de gynaecologen en artsen van de prenatale afdeling voor het aanmelden en consent vragen van nieuwe hernia patiënten. En niet te vergeten het invalwerk van Liesbeth, Marie-Chantal, Sanne & Erwin: fijn dat ik de pieper af en toe kon overdragen om van een vrij weekend te kunnen genieten!

Alle analisten en secretaresses van de prenatale-, postnatale- & DNA diagnostiek: dank voor de vele karyogrammen, sedimenten, cellijnen en DNA isolaties! Alle cytogenetici, en met name Dian, Gosia, Lars, Laura & Cokkie: dank jullie wel voor het meedenken en opstellen van een vervolgplan voor de vele individuele CDH-casussen waar "iets" mee moest gebeuren. Alle genetici en in het bijzonder Yolanda van Bever, Alice Brooks en Lutgarde Govaerts wil ik bedanken voor hun expertise bij het maken van syndroom-diagnoses. Tenslotte: lieve Marjan, dankjewel voor je hulp en het eerste wegwijs maken met de MLPA experimenten, waarna ik ook nog vele malen een beroep op je praktische vaardigheden heb gedaan. Ik wens je enorm veel nieuwe knuffelmomenten toe met de veranderingen die er in je privéleven gaan plaatsvinden!

Alle co-autheurs wil ik bedanken voor hun bijdrage en de vele goede suggesties ter verbetering van het manuscript. Speciaal wil ik hier ook Ko Hagoort noemen: door jouw wijzigingen en aanvullingen werden de stukken naar een hoger niveau Engels getild, dank je wel!

Voor het 3D confocal-stuk wil ik in het bijzonder Gert van Capellen & Mariette van de Corput noemen: jullie kennis en kunde van de confocal-microscoop, het 3D FISH protocol en het programma Huygens was onontbeerlijk bij het uitvoeren van het eerste deel van mijn project. Ook dank aan student en later analist, Linda: dankjewel voor al je labelling en 3D FISHes! Ik hoop dat je inmiddels een plekje hebt gevonden in een leuk lab. Bert, uiteraard ook jij bedankt

voor je goede adviezen in deze reeks van experimenten. Ik heb bewondering voor de manier waarop je mensen uit verschillende vakgebieden (IT wereld, celbiologie en genetica) bij elkaar weet te brengen. Raak nooit die schijnbaar onuitputtelijke bron van energie kwijt, alhoewel het soms lastig kan zijn om je bij te houden (.....) met al je verschillende ideeën!

Voor het 4C stuk ben ik grote dank verschuldigd aan 4 echte vakmensen: Robert-Jan Palstra, Marcel Vermeij, Elzo de Wit & Rutger Brouwer.

Beste Robert-Jan, dank dat je me onder je hoede hebt genomen met het uitvoeren van de 4C experimenten. Het plezier en de kunde waarmee je PhD studenten en analisten begeleidt is een voorbeeld voor velen in het vak. Dank ook voor de persoonlijke gesprekken, het is echt leuk en inspirerend om met jou samen te werken! Beste Marcel, zonder jouw chirurgische vaardigheden was het nooit gelukt om alle verschillende weefsels te isoleren uit die kleine ratten-embryo's. Ook met jou heb ik genoten van onze gesprekken over uiteenlopende onderwerpen; ik hoop dat je geniet van de extra vrije tijd die je hebt nu je (gedeeltelijk) met pensioen bent. Beste Elzo, we hebben uitsluitend via de mail gecommuniceerd, dus ik weet niet eens hoe je eruit ziet, maar dank voor de vele R-scripten die het analyseren van de 4C data mogelijk hebben gemaakt, zonder dat was het ons nooit gelukt! Daarmee kom ik ook bij Rutger; ook jij hebt met je uitgebreide kennis van programmeren veel bijgedragen aan dit stuk, met name ook door de begeleiding van onze super-student Tom Brands. Beste Tom, ik heb vaak het idee dat je nog niet goed beseft hoe waardevol jouw talenten zijn in de genetica wereld van nu. Ik weet zeker dat er vele afdelingen zijn binnen het Erasmus die te springen staan om iemand met jouw kennis; ik hoop dan ook dat je na je studie een mooi plekje weet te vinden! Tenslotte nog dank aan Ilona Sluiter & Robert-Rottier voor het beschikbaar stellen van het restmateriaal van hun ratten-embryo's en daarnaast voor de vele coupes die ik heb mogen gebruiken voor de bevestiging van mijn expressie resultaten.

Voor de expressie & SNP array-stukken heb ik veel hulp gehad van analisten en PhD studenten uit de groep van prof. Uiterlinden: met name van Mila Jhamai & Marjolein Peters en van de Erasmus-Biomic Centre o.l.v. Wilfred van IJcken: Christel Kockx. Voor de statische analyses zijn onontbeerlijk geweest zowel Mario Pescatori als Andreas Kremer. Tenslotte wil ik nog speciaal Guido Breeveldt bedanken voor het aanleren van de Q-PCR techniek en de analisten Daphne Huigh, Hannie Douben & student Alice van Buidegom voor het uitvoeren van de vele Q-PCRs en FISHer. Hannie, je bent een rots in de branding in het lab van Annelies en daarnaast een van de aardigste personen die er rondlopen in het Erasmus.

Beste Prof.Hokken, beste Anita. Onze samenwerking is niet geheel gelopen zoals we beiden in het begin gepland hadden, echter ik ben er super trots op dat we het IGF1R-stuk samen nog in zo'n mooi tijdschrift hebben kunnen publiceren. Ik wens je veel succes toe met het onderzoek binnen de Stichting Kind en Groei!

Een belangrijk onderdeel van mijn promotietraject was de samenwerking met verschillende groepen in binnen- en buitenland:

Dear dr. Schaible & dear Juliana (Universitätsklinikum Mannheim). Thank you for all your efforts in sending me genetic material from your German CDH patients; as a result we were able to write a couple of papers together: I sincerely hope that this fruitful collaboration will continue in the future! I also really enjoyed our personal contact at the international CDH meetings.

From Houston, Texas: I specially want to thank Margaret Wat & Daryl Scott, who continue to contribute many interesting results to the CDH-research field.

From the Universitätsklinikum Hamburg-Eppendorf, prof. dr. Kutsche; I hope our story of the HCCS mutation will come to a succesfull end!

Tenslotte, en een stuk dichterbij huis, dank aan de long-groep van Prof. Dekhuijzen uit het UMCN, met name Jeroen van Hees, Theo Hafmans en dr. L. Heunks voor het beschikbaar stellen van de "controle" diafragma biopten. Het werk is nog niet af, maar ik heb er alle vertrouwen in dat er een mooi stuk uit zal voortvloeien!

Beste studenten Linda, Rianne, Chantal & Tom, dank voor jullie tomeloze inzet; het is en blijft enorm leerzaam om studenten te mogen begeleiden en geeft ook een beter inzicht in je eigen werkwijze (en of die nu wel zo handig is....).

Dank aan alle collegae op de 9de verdieping: alhoewel ik mezelf soms een "welcome gast" voelde op al die verschillende etages van het Ee-gebouw, heb ik me thuis gevoeld op de klinische genetica afdeling. Specifiek wil ik nog noemen Jeanette Lokker, beste Jeanette, dank voor alle administratieve dingen die geregeld moesten worden en nog belangrijker dank voor je luisterend oor.... Rachel, Marian, Guido, Erik, Renate & Yolanda ik kon altijd bij jullie terecht voor een praktische oplossing.

Beste computer technici Ton, Leo, Pim, Sjozef & Mario, ik hoop niet dat jullie al te vaak aan de telefoon gezocht hebben om mijn wat basale computer-vragen: Het was enorm plezierig om de "43210-weet raad" lijn te kunnen bellen.

Lieve Tom (de Vries Lentsch). Heel veel dank voor al die mooie adobe illustrator figuren. Ik weet dat je af en toe gek wordt van al die onmogelijk vragen die onderzoekers je stellen (en met name dan de tijdslimiet die ervoor staat). Dank ook voor je supermooie voorkant, daar kunnen niet genoeg rode flessen wijn tegenop.....

Kamergenoten van het eerste uur Najaf, Liesbeth & Maaike: Girls, I really enjoyed the (somewhat feminin) and grazy atmosphere in our room. Dear Najaf, I think all the pressure is on you now to get us to Oslo, now that the rest of us went back to clinic..... I wish you all the best for your personal plans as well. Beste Maaike, ik heb enorm veel bewondering voor de manier waarop je altijd super rustig bleef onder alle deadlines die je moest halen om je manuscript af te ronden en tegelijkertijd je huis te verbouwen. Ik hoop dat de neuro je bevalt. Lieve Lies, het gelukspoppetje wat je me ooit cadeau hebt gedaan heeft al heel veel goed werk verricht, ik ben meer dan bereid

om hem in te zetten voor alle dingen die jij nog wil bereiken in het leven. Het contact met jou is me heel waardevol.

Na een 100%-vrouwen periode werd onze kamer versterkt met Lennart en later Erwin. Beste Lennart, ik weet niet of je erg heb moeten wennen bij ons, maar met jouw komst werd nogmaals duidelijk dat vrouwen inderdaad van een andere planeet komen dan mannen en heel belangrijk dat daar niks mis mee is. Lieve Erwin, dank voor al het werk dat je hebt verricht aan het 15q-expressie stuk, het was een eitje om je te begeleiden als masterstudent. Ik heb enorm genoten van je wat droge (en cynische) humor. Ik wens je het allerbeste toe met jouw promotietraject!

Daarnaast waren er ook altijd voor wat gezelligheid tijdens de lunch (van de oogmelanomen groep) Anna, Thomas & Yolanda (en van het IVF-lab) Ilse, Cindy & Hikke (en tijdens de Pannekoek-meetings) Belinda, Cathryn, Laura, Josien & Rachel

Andere (oud) onderzoekers:

Beste Rhiannon, dank voor je “zen”-houding zo vlak voor mijn sollicitatie, ik heb ook enorm genoten van alle kopjes koffie bij Doppio. Lieve Ilse, dank voor je gezelschap op Texel; ik beloof je, ik zal je niet meer blootstellen aan al mijn obsessief-compulsieve neigingen (althoewel je zelf natuurlijk ook wat afwijkingen hebt....)

Dear Marialuisa & Francesca, you are proof that we need more foreign people in the Netherlands: thank you for all the nice Italian food (especially desserts)..and Francesca: please come back! Lieve Sanne, onze vriendschap is pas van korte duur, maar daarom niet minder waardevol; het was super leuk om met jou op de verschillende congressen te zijn. Ik ben nog steeds aan het duimen voor al je andere grootste plannen.....

Mijn paranimfen – “two tall, strong and golden ladies on each side of me”- wat kan ik me nog meer wensen? Lieve Laura/chickie, ik heb enorm veel bewondering voor je altijd positieve, energieke en “het-glas-is-hartstikke-vol-mentaliteit”. Dank voor alle mooie gesprekken met jou en Erno en voor de opvang van een hormonale Daan.....

Lieve Mir, met je keuze om je verdere leven met mijn broer te delen, ben je ook mijn zussie geworden. Je droge humor en vlijmscherpe analyses is wat de Veenma familie goed kan gebruiken en ik in het bijzonder. Dank, dat je met Roger, altijd aan mijn zijde staat. Tot snel (en vaak) in Barcelona.

Kirsten, met je getrappel in mijn buik, heb je vele overpeinzingen tijdens het schrijven van dit manuscript onderbroken. Ik kan me een leven zonder jou niet meer voorstellen.....blijf vooral veel glimlachen!

Joost, mijn lieve “macho” man. Alle diepte en hoogtepunten van de afgelopen 4 jaren, hebben weer eens bewezen waarom je zo goed bij mij past. Op naar het volgende life-event?

5.3 Curriculum Vitae

The author of this thesis was born on December 17th 1977 in Geleen, the Netherlands. In 1996 she completed high school education on Atheneum level on the “Sint Michiel scholengemeenschap”, Geleen, and started her study Medical Biology at the University of Amsterdam (UVA), the Netherlands. Within 4 years she received her Master in Science degree and continued studying at the medical department of the UVA. During her clinical rotation she worked for 2 months at the paediatric infectious disease department of the Kansas University Medical Centre” in Kansas, Missouri, USA. She received her medical degree, cum laude, in July 2005.

After working for 10 months as a paediatric resident in the Meander Medical Centre, Amersfoort, the Netherlands, she started as a resident on the Intensive Care Unit of the Erasmus-MC Sophia’s Children’s Hospital, Rotterdam in June 2006. During her work here she became even more aware of the importance of evidence-based medicine and in February 2007 she started working as a research-physician in the department of paediatric endocrinology of Erasmus MC (Prof.dr. A. Hokken-Koelega). She was responsible for the daily management of a clinical study about the safety and long term effects of growth hormone treatment in children born small for gestational age (SGA). In February 2008, she started her PhD degree under supervision of Prof. dr. D. Tibboel and dr. A. de Klein. She worked within the departments of paediatric surgery and clinical genetics on a SSWO subsidised project entitled: “Gene-environmental relationships in Congenital Diaphragmatic Hernia”. Aside from new CDH patient inclusions, this work included the implementation of two new innovative techniques (3D multi-colour FISH and Chromosome Conformation Capture sequencing technology) in the field of epigenetics. Moreover, new genetic factors were analysed in DNA from children with this birth defect using the most recent molecular-cytogenetic techniques available. From January 2011 until now she combined her research with a selected course of the Dutch Paediatric Society; entitled “Training Upcoming Leaders in Paediatric Science” (TULIPS). As from April 2012 she will start her residency Paediatrics in Rotterdam at the Erasmus-MC (head; dr. M. de Hoog).



5.4 PhD Portfolio

| | | | |
|--|-------------|---|--|
| Name PhD student: D.C.M.Veenma Erasmus MC Department: Paediatric Surgery Research School: MGC & Molecular Medicine | | PhD period: February 2008-December 2012 Promotor: Prof.dr.D.Tibboel Supervisor/co-promoter: dr. A. de Klein | |
| 1. PhD training | | | |
| | Year | Workload (Hours/ECTS) | |
| General academic skills | | | |
| – Biomedical English Writing and Communication | 2008 | 03 ECTS | |
| Research skills | | | |
| – Statistics, CCO2, Classical Methods for Data-analysis | 2009 | 5.6 ECTS | |
| – NVK, TULIPS: PhD curriculum 2011+2012 | 2011 | 54 Hours | |
| – NVK, TULIPS: Grant writing course, 8-9 th April | 2011 | 24 Hours | |
| In-depth courses | | | |
| – SNP's and Human Diseases | 2007 | 40 Hours | |
| – Browsing Genes and Genomes with Ensemble | 2007 | 32 Hours | |
| – International Course European school of Genetic medicine: Cardiogenesis and congenital cardiopathies: from developmental model to clinical applications | 2008 | 32 Hours | |
| Molecular Diagnostics III | 2008 | 16 Hours | |
| – Veilig werken in laboratoria | 2008 | 16 Hours | |
| – In vivo-Imaging from molecule to Organism | 2008 | 40 Hours | |
| – MGC Postgraduate school: Molecular and Cell Biology | 2009 | 06 ECTS | |
| – Analysis of microarray gene expression | 2009 | 16 Hours | |
| – Nexus Course | 2009 | 16 Hours | |
| – Nexus Course-Advanced | 2010 | 16 Hours | |
| – Biological interpretation of gene expression data with Explain | 2010 | 08 Hours | |
| – Basic Analysis on Gene-expression Data (BAGE) | 2010 | 16 Hours | |
| – Photoshop and Illustrator | 2010 | 16 Hours | |
| – Next generation sequencing | 2010 | 24 Hours | |
| – Research management for PhD students | 2011 | 16 Hours | |
| Presentations | | | |
| – Presentation Refereeravond kindergeneeskunde, cluster MMC Veldhoven en CZE Eindhoven: subject Neonatology | 2008 | | |
| – Presentation Symposium CDH Euro-consortium, Mannheim, 29-30 th Oct | 2009 | | |
| – Poster Voorjaarssymposium NVHG, Eindhoven, 23-24 th April | 2010 | | |
| – Poster MC-Gard Conference, Edinbrough, 1-5 th April | 2010 | | |
| – Poster Keystone Conference, Steamboat Springs, 8-13 th Jan | 2011 | | |
| – Poster Conference "Congenital Diaphragmatic Hernia: more questions than answers", Rome, 2-3 th Febr | 2011 | | |
| – Poster "ESHG Conference", Amsterdam, 28-31 th May | 2011 | | |

| | | |
|---|------|----------|
| International conferences | | |
| – KNAW Conference: the Role of DNA polymorphisms in complex traits and diseases, Amsterdam, The Netherlands | 2008 | 40 Hours |
| – MC-Card Conference: Higher order genome architecture, Edinbrough, Scotland, 1-5 th April | 2009 | 40 Hours |
| – NVHG: 60-jarig voorjaarssymposium, Eindhoven, 23-24 th April | 2009 | 16 Hours |
| – CDH Euro-consortium: Advances in Congenital Diaphragmatic Hernia, Mannheim, Germany, 29-30 th October | 2009 | 16 Hours |
| – WTCC conference: Signalling and Chromatin, Cambridge, UK, 7-10 th October | 2010 | 24 Hours |
| – Keystone: Functional consequences of Structural variation, Steamboat Springs, Colorado, USA, 8-13 th January | 2011 | 40 Hours |
| – Congenital Diaphragmatic Hernia: more questions than answers, Rome, Italy 2-3 th February | 2011 | 16 Hours |
| – European Human genetics Conference, Amsterdam, The Netherlands, 28-31 th May | 2011 | 32 Hours |
| Seminars and workshops | | |
| Minisymposium: Epigenetics and Disease | 2009 | 08 Hours |
| Workshop European Biology Organization: Retinoids | 2011 | 24 Hours |
| Didactic skills | | |
| - | | |
| Other | | |
| 2. Teaching activities | | |
| – Mentor 4 th year Technical Analyst-student | 2009 | |
| – Mentor 4 th year Master student “Environment and Physical science” | 2010 | |
| – Presentation Nexus Course | 2010 | |
| – Mentor 4 th year Technical Analyst-student | 2010 | |
| – Presentation Course Biomedical Research techniques | 2011 | |
| Mentor 3 rd year Technical Analyst-student | 2011 | |

5.5 List of publications

Mouse model reveals the role of SOX7 in the development of congenital diaphragmatic hernia associated with recurrent deletions of 8p23.1

Margaret J. Wat, Zhiyin Yu, **Danielle Veenma**, Monica Garcia, Andres Hernandez, Ashley M. Holder, Jeanette J. Wat, Yuqing Chen, Mary Dickinson, Dick Tibboel, Annelies de Klein, Brendan Lee, Daryl A. Scott

Re-submitted Human Molecular Genetics

Complex congenital diaphragmatic hernia in mice lacking Chromatin target of Prmt1

Nynke Gillemans, Dorota Szumska, **Danielle Veenma**, Fatemehsadat Esteghamat, Jun Hou¹, Wilfred van IJcken, Annelies de Klein, Shoumo Bhattacharya, Dick Tibboel, Frank Grosveld, Sjaak Philipsen, and Thamar B. van Dijk

Submitted Circulation

Developmental and Genetic aspects of Congenital Diaphragmatic Hernia

D. Veenma, A. de Klein and D. Tibboel,

Pediatric Pulmonology 2012 in press

Somatic CNV detection in MZ-twins discordant for Esophageal Atresia (EA) and Congenital Diaphragmatic Hernia (CDH) and in affected tissues

D. Veenma, E. de Jong, C. van de Ven, C. Meeuwissen, H. Eussen, H. Douben, M. Boter, D. Tibboel and A. de Klein.

Eur J Hum Genet. 2012 Mar;20(3):298-304

Genomic Alterations that Contribute to the Development of Isolated and Non-Isolated Congenital Diaphragmatic Hernia

M. Wat, **D. Veenma**, J. Hogue, A. Holder, Z. Yu, J. Wat, N. Hanchard, O. Shchelochkov, C. Fernandes, A. Johnson, K. Lally, A. Slavotinek, O. Danhaive, T. Schaible, S-W. Cheung, K. Rauen, V. Tonk, J. Belmont, D. Tibboel, A. de Klein, B. Lee, D. Scott.

J Med Genet (2011 May;48(5):299-307)

Comparable low-level mosaicism in affected and non-affected tissue of a complex Congenital Diaphragmatic Hernia (CDH) patient

D. Veenma, N. Beurskens, J. Douben, B. Eussen, L. Govaerts, M.H. Lequin, R. de Krijger, D. Tibboel, A. de Klein and D.van Opstal.

PLOS One (2010 Dec 21; 5(12): e15348)

Congenital Diaphragmatic Hernia and a complex heart defect in association with Wolf-Hirschhorn Syndrome

D. Veenma*, J. Tautz*, H. Eussen, L. Joosen, P. Poddighe, D. Tibboel, A. de Klein and T. Schaible.

*both authors contributed equally to this manuscript

American Journal of Medical Genetics (2010,152(A)(11): 2891-4)

The Retinol Status in Newborn Infants is Associated with Congenital Diaphragmatic Hernia

L. Beurskens, D. Tibboel, J. Lindemans, J. Duvekot, TE. Cohen-Overbeek, **D.Veenma**, A.de Klein, J.Greer, R. Steegers-Theunissen.

Pediatrics (2010, 126(4): 712-20)

Phenotype-genotype correlation in a familial IGF1R microdeletion case

D. Veenma, H. Eussen, L. Govaerts, S. de Kort, R. Odink, C. Wouters, A. Hokken-Koelega, A. de Klein.

J Med Genet (2010 Jul; 47(7): 492-8. Epub 2009 Dec 2)

PROP1, HESX1, POU1F1, LHX3 and LHX4 mutation and deletion screening and GH1 P89L and IVS3+1/+2 mutation screening in a Dutch nationwide cohort of patients with combined pituitary hormone deficiency.

L.de Graaff, J. Argente, **D. Veenma**, M. Drent, A. Uitterlinden, A. Hokken-Koelega.

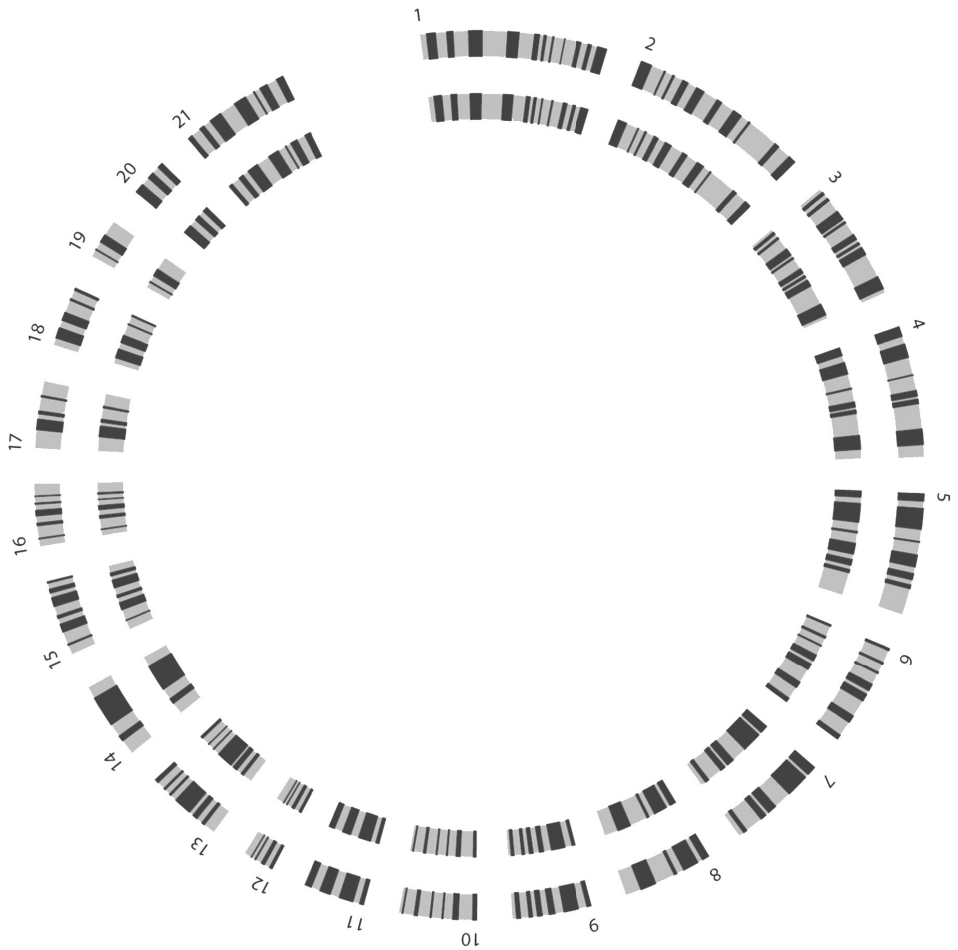
Horm Res Paediatr (2010; 73(5): 363-71. Epub 2010 Apr 14)

Genetic screening of a Dutch population with isolated GH deficiency (IGHD)

L. de Graaff, J. Argente, **D. Veenma**, M. Herrebout, E. Friesema, A. Uitterlinden, M. Drent, A. Campos-Barros, A. Hokken-Koelega.

Clin Endocrinol. (2009 May; 70(5): 742-50. Epub 2008 Sep 10)

Color figures



Chapter 1

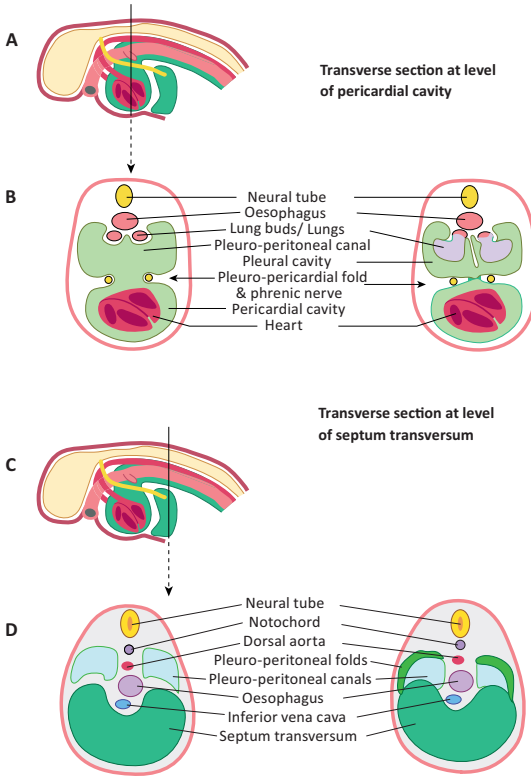


Figure 1 | Embryological overview of the development of the Pleuro-Pericardio-Peritoneal Folds (PPFs)

A: depicts the level of cross-sections in the embryo: PPFs at the level of the pericardial cavity. **B (left):** shows the development of the mesodermal pleuro-pericardial folds (PPFs) from the dorsolateral body wall. As these PPFs grow toward the midline (**B (right)**), they separate the heart from the expanding lungs resulting in a division of the thoracic cavity into one pericardial cavity and two pleural cavities. The phrenic nerves are positioned within these PPFs as they descend to innervate the diaphragm. **C:** PPFs at the level of the septum transversum. **D (left):** the pleuro-peritoneal folds arise from the posterior body wall as well and lie in a plane that is parallel to the septum transversum and perpendicular to the pleuro-pericardial folds. As they grow (**D (right)**) these folds will separate the pleural from the peritoneal cavities and attach to the other three diaphragm-building structures: the lateral body wall mesoderm, the septum transversum, and the dorsal mesentery of the esophagus (see page 12).

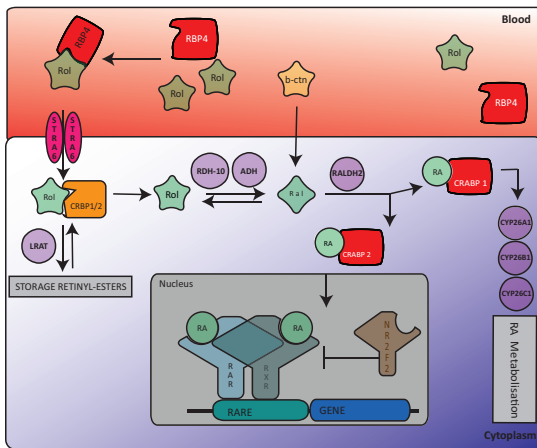
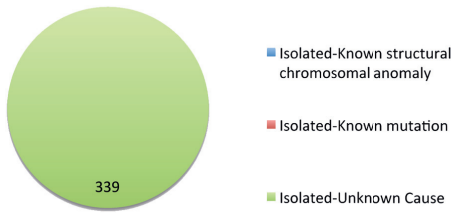


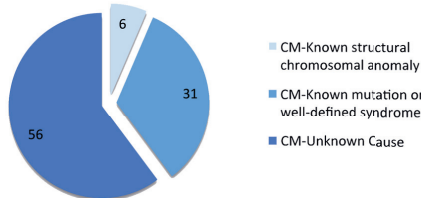
Figure 2 | Overview of ATRA metabolism and nuclear canonical RA-signalling

Circulating retinol is taken up by RBP4 and transferred intracellularly by STRA6. Transformation into retinaldehyde occurs mainly by RDH10, after which RALDH2 can generate RA. RA in turn can either bind to CRABP1 and be transported to CYP26 enzymes and metabolized into polar metabolites or bind to CRABP2 and be transported to the nucleus. In the nucleus RA will bind to a RAR/RXR heterodimer, which in turn can bind to RAREs located in the promoter area of specific genes and activate/inhibit transcription. Rol, retinol; RBP, retinol binding protein; STRA6, stimulated by retinoic acid 6; CRBP, cellular retinol binding protein; Ral, retinaldehyde; ADH, alcohol dehydrogenase; RALDH, retinaldehyde dehydrogenase; CYP26, cytochrome P450 26 enzymes; RAR, retinoic acid receptor; RXR, retinoid X receptor; RARE retinoic acid response element; B-ctn, beta-carotene; LRAT, Lecithin retinol acyltransferase; NR2F2; Nuclear receptor 2, subfamily F2 (see page 15).

Isolated



Complex-Multiple Major



Complex-Simple

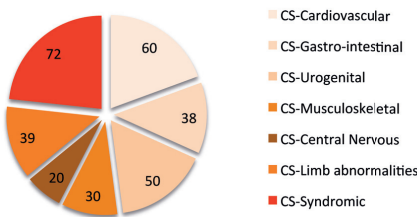


Figure 3 | Classification of patients Rotterdam CDH cohort

CDH patients can either present with an isolated defect only (Isolated) or as part of a complex phenotype (Complex), meaning that in the latter group the defect is accompanied by other congenital anomalies. Usually these additional birth defects only affect 1 other organ system or consist of minor abnormalities (Complex-Simple). The term Complex-Major describes those CDH subjects that are more severely affected, defined by the co-occurrence of *at least two other major* congenital anomalies. In turn, these three subgroups can be further subdivided based on the type of causative genetic aberration present (Isolated and Complex-Major) or based on the type of additional affected organ system (complex-Simple). CM, Complex-Major; CS, Complex-Simple (see page 22).

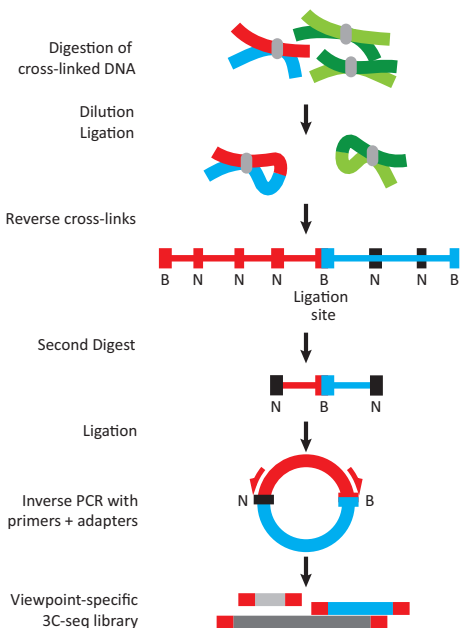
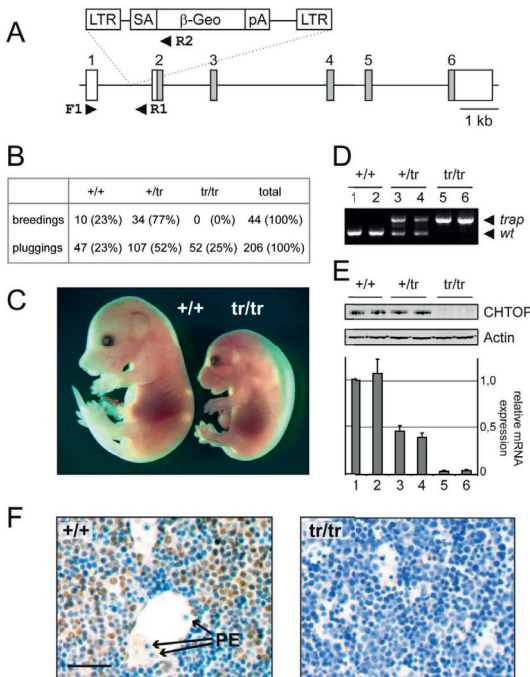


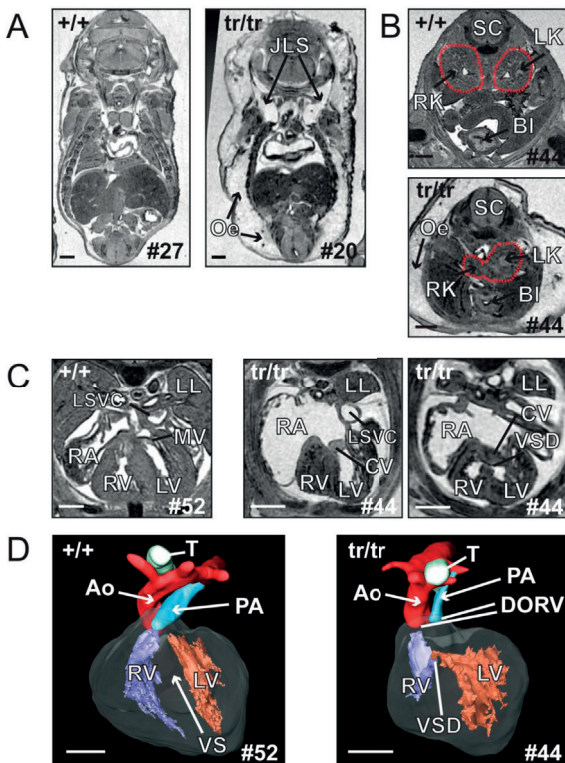
Figure 4 | Schematic overview of the 4C-seq method (4C-seq)

Sample preparation in *4C-seq* (4C-seq) is similar to the earlier published *4C-array* protocols [127] apart from some small adjustments (adding adapter-sequences) in the primer design stage. The *4C-seq* method has the advantage of improved signal to noise ratios over the *4C-array* approach. Briefly, nuclei are fixed with formaldehyde to cross-link co-localising chromatin (red and blue lines, light- and dark-green lines). DNA is digested with a restriction enzyme, for example Bgl-II. After dilution of the sample, cross-linked fragments are ligated (ideally only at one end), and subsequently cross-links are reversed. This way, the Bgl-II fragment of interest (red line) is ligated to fragments co-localised (blue line) within the studied cell-population. Next, ligation products are trimmed by digestion with a frequent cutting enzyme (NLA-III), because Bgl-II fragments are too big to be amplified by PCR. The trimmed products are circularised, such that an inverse PCR on the red fragment will amplify its interacting (blue) partners. Of note, the "contents" of the circles formed between cross-linked DNA fragments vary depending on the three-dimensional structure at the start of the protocol and whether ligation occurs to one or both ends of the cross-linked material (grey and black lines [127]). All these sequences can be analysed by next-generation sequencing (see page 27).

Chapter 2.2

**Figure 1 | Generation of *Chtop*^{tr/tr} mice**

A: Schematic representation of the *Chtop* genomic locus and the viral genetrapp vector. Exons are indicated, the coding region is shaded. F1, R1, and R2 represent oligonucleotides used for genotyping; LTR = long terminal repeat, SA = splice acceptor, b-Geo = combined selection and reporter gene, pA = poly-A tail. **B:** Genotype analysis of *Chtop*^{tr/tr} intercrosses at weaning (breedings) and embryonic (pluggings) stages. **C:** Wild-type (+/+) and mutant (tr/tr) embryos at E16.5 showing edema and growth retardation in the mutant. **D:** Genotype analysis on yolk sac cells by PCR. **E:** CHTOP protein levels (top panel) and mRNA levels (bottom panel) in embryonic fibroblasts. One of three independent experiments is shown. **F:** Detection of CHTOP protein by immunostaining of fetal liver (E13.5). Circulating primitive erythrocytes (PE) are negative for CHTOP staining. Bar, 100 μ m (see page 63).

**Figure 2 | MRI reveals developmental abnormalities in *Chtop*^{tr/tr} embryos**

A: Coronal sections demonstrating oedema (Oe) and cysts in the jugular lymph sacs (JLS). **B-C:** Transverse sections showing small and fused right kidney (RK) and multiple cardiac malformations. Two thoracic sections are shown from the same mutant. Structures indicated are spinal cord (SC), left kidney (LK), bladder (BI), left lung (LL), left superior vena cava (LSVC), right atrium (RA), right ventricle (RV), left ventricle (LV), mitral valve (MV), common valve (CV), and ventricular septal defect (VSD). **D:** 3D reconstruction of the wild-type and mutant hearts clearly demonstrates the VSD, narrowed pulmonary artery (PA), double outlet right valve (DORV), and right-sided aorta (Ao). T = trachea. Bars, 500 μ m (see page 66 for color figure).

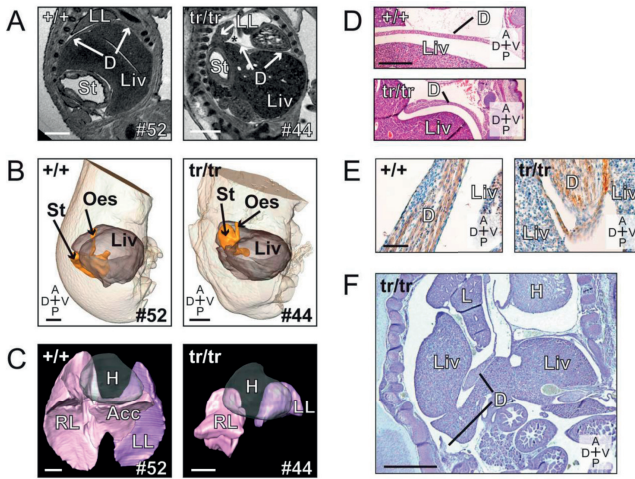


Figure 3 | Congenital Diaphragmatic Hernia in *Chtop*^{tr/tr} embryos

MRI pictures of sagittal sections from wild-type (+/+) and mutant (tr/tr) embryos (E15.5). **A:** The mutant displays a „Bochdalek“ type of CDH, with the hernia indicated with *. **B:** 3D reconstruction of the stomach and liver, demonstrating malrotation of the stomach and herniation of the stomach and liver into the thoracic cavity. Scale bar = 0.5 mm. **C:** 3D reconstruction of the lungs, demonstrating hypoplasticity in mutant lungs. **D:** Diaphragm thickening around the diaphragm defect (bottom panel) compared with the normal contralateral side of the diaphragm (top panel). **E:** Muscular cells are present in mutant diaphragms, as indicated by smooth muscle actin immunostaining. **F:** Sagittal section demonstrating dorsolateral CDH, resulting in massive expansion of the liver into the thoracic cavity. Structures indicated are: left lung (LL), right lung (RL), accessory lobe (Acc), diaphragm (D), liver (Liv), stomach (St), oesophagus (Oe), spleen (S), right crus (RC), and heart (H); axes: r – right; l – left; d – dorsal; v – ventral; a – anterior, p – posterior. Bars: 500 mm A-D, 100 mm E, 1 mm F (see page 67).

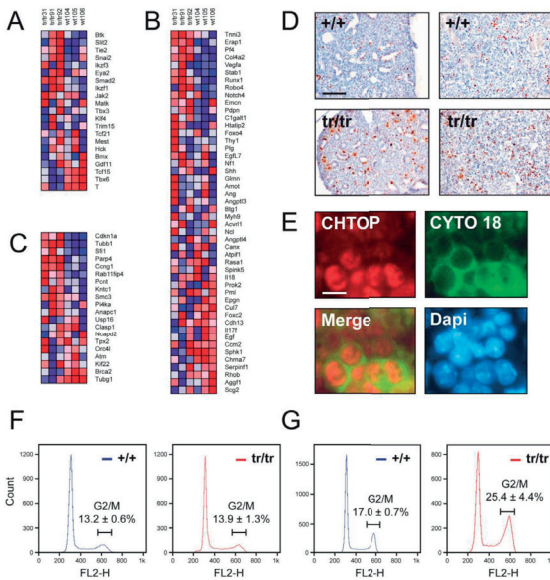


Figure 4 | Deregulated gene expression in *Chtop*^{tr/tr} embryos

Expression profiling was performed on E9.0 embryos (22-25 somite stage). Gene set analysis shows deregulation of: **A:** mesoderm development, **B:** vasculature development, and **C:** the G2/M-phase of the cell cycle. **D:** Immunostaining with an antibody against phosphorylated H3 demonstrates an increase of G2/M cells in mutant lung (left panels) and liver (right panels). One of three independent experiments is shown. **E:** Fetal liver cells (E13.5) with relative high levels of CHTOP (red channel) are hepatic precursors, as demonstrated by their coexpression of cytokeratin 18 (Cyto 18; green channel). DNA was visualized by Dapi staining (blue channel). **F:** FACS analysis shows that wild type and mutant fetal liver derived erythroblasts have similar DNA profiles. In contrast, propidium iodide staining reveals a delay of the G2/M-phase in mutant MEFs **G:** Data are from a single experiment that is representative of three independent experiments. Values represent the mean of 4 littermates ± SD. Bars: 200 nm **D**, 10 nm **E** (see page 68).

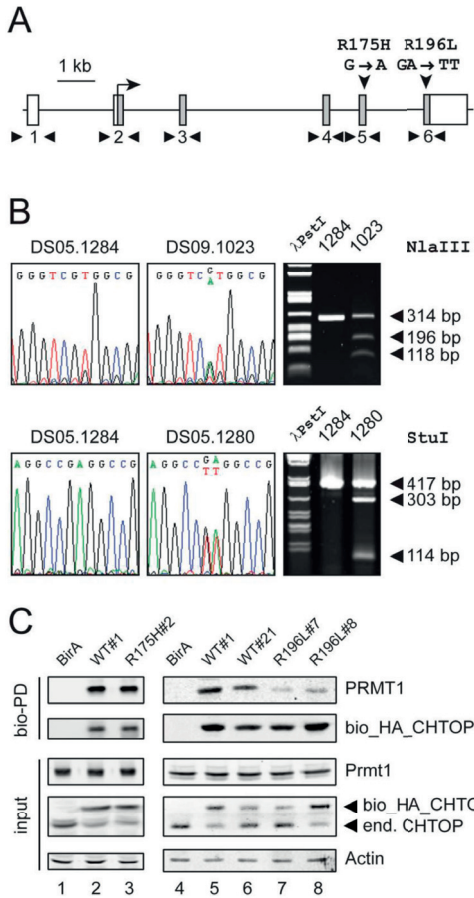


Figure 5 | Detection of CHTOP variations in CDH patients

A: Schematic representation of the human *Chtop* locus. Exons are indicated, the coding region is shaded. Vertical arrowheads indicate the positions of identified variations (R175H and R196L), horizontal arrowheads represent oligonucleotides used for amplification and sequencing. **B:** Identification of the G>A SNP and its validation by *Nla*III digestion (top panels); identification of the GA>TT mutation and its validation by *Stu*I digestion (bottom panels). DS05.1284 = control DNA; DS09.1023 and DS05.1280 = patient DNA. C: Bio_HA_CHTOP with SNP R175H (left panels) and mutation R196L (right panels) were introduced into MEL cells and tested for their interaction with PRMT1. In contrast to R175H, the R196L mutation greatly reduced the binding to PRMT1. Compare lanes 5 and 8 for relative high ectopic expression of CHTOP, and lanes 6 and 7 for relative low expression. Data are from a single experiment that is representative of three independent experiments (see page 71).

Chapter 2.3

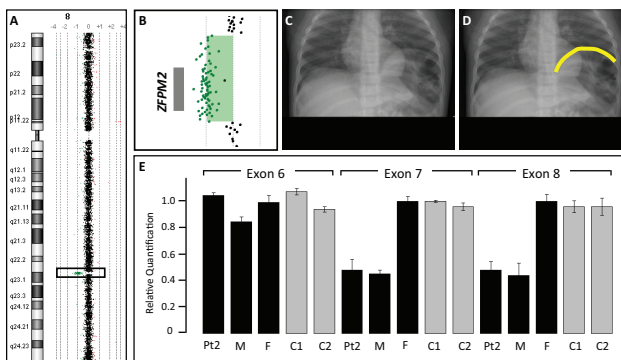


Figure 1 |

A: Array comparative genomic hybridization data from Patient 1 showing an 8q22.3q23.1 single gene deletion of ZFPM2. **B:** The relative location of the ZFPM2 gene in relation to aCGH data from the deletion region in Patient 1 is represented by a gray bar. **C:** A chest radiograph of Patient 1 demonstrating a severe diaphragmatic eventration containing loops of bowel. **D:** The same radiograph shown in panel C with the limits of the diaphragmatic eventration outlined in yellow. **E:** Quantitative PCR analysis demonstrates a normal copy number for ZFPM2 Exon 6 but a reduced copy number for Exons 7 and 8 in DNA from Patient 2 (Pt2) and his mother (M). Normal copy number values are seen in DNA from Patient 2's father (F) and DNA from two unrelated controls (C1, C2) (see page 87).

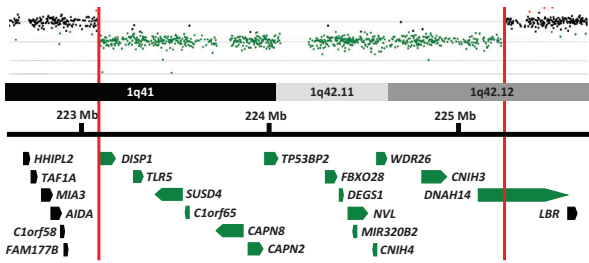


Figure 2 |

Array comparative genomic hybridization data from Patient 4 is shown above a schematic representation of a portion of the 1q41-1q42 region. Genes in this region are represented by block arrows. Red vertical bars mark the limits of the deletion in Patient 4 and delineate the minimal deleted region for congenital diaphragmatic hernia (CDH) in this region of the genome. Genes with all or a portion of their coding sequence inside the minimal deleted region are shown in green (see page 88).

Chapter 2.4

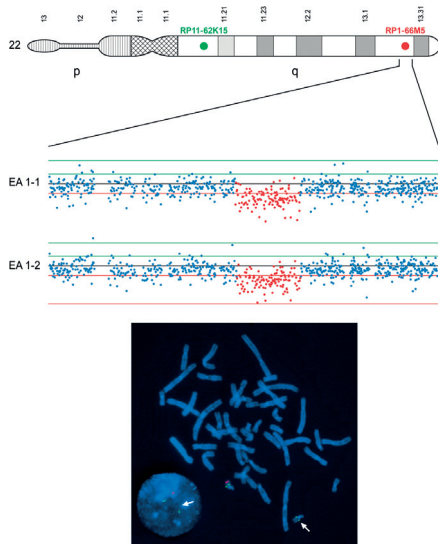


Figure 1 | SNP and Fluorescent In-Situ Hybridization results of inherited chromosome 22-CNV in EA pair-1

Nexus results (Top) of the 666 Kb deletion on chromosome 22q13.3 in both individuals of EA pair-1 showing a clear drop in log2 intensity signal validated by FISH (Bottom) on metaphase chromosomes of the affected EA twin-1. Probes: control: RP11-62K15 (green) and target: RP11-66M5 (red). Parental analysis (results not shown) demonstrated that this genomic event is inherited from the mother and therefore less likely pathogenic. In addition, no gene is allocated to this region neither are any miRNA transcripts hampering the identification of functional elements in this region as well (see page 109).

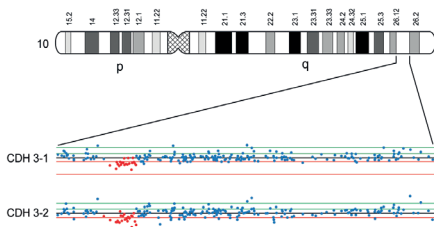
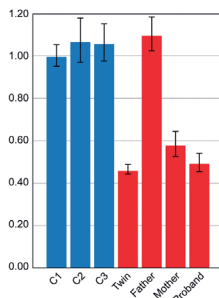


Figure 2 | SNP and relative Q-PCR results of inherited chromosome 10-CNV in CDH pair-3.

Nexus result (Top) of the chromosome 10q26 deletion event in CDH pair-3 showing a clear drop in log2 intensity signal, which was confirmed by relative q-PCR (bottom) in the affected proband, the unaffected twin and the mother (see page 110).



Chapter 2.5

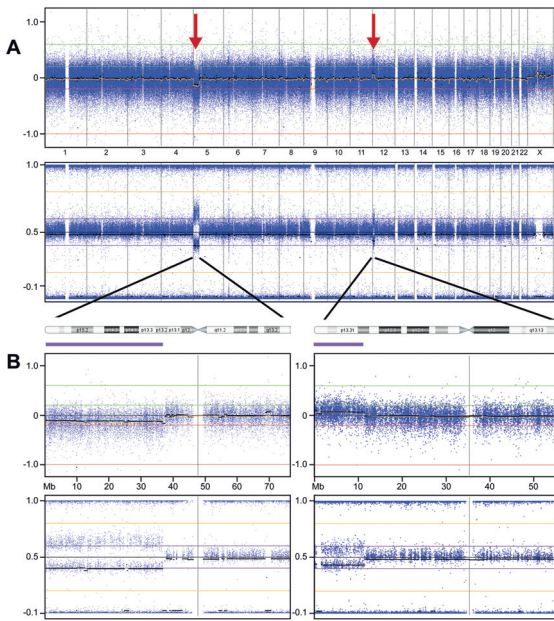


Figure 1 | Results High-resolution SNP array using uncultured umbilical cord blood material

A: Whole genome array: Log₂ intensity (Top) and B-Allele Frequencies BAF (Bottom). Top: Y-axis: Relative Copy Number State. X-axis: autosomes number 1-22 and the two sex chromosomes.

Displayed are the relative and normalized log₂ intensities of all available SNPs on the array across the patients' genome. At the beginning of chromosome 5 a slight drop of log₂ intensity is visible representing the deletion of part of the short arm of chromosome 5 in a low-mosaic state. Similarly, the mosaic 12p duplication is depicted as a small peak of log₂ intensity at the beginning of chromosome 12. Bottom: confirmation of aberrations by the more clearly visible changes in BAF. **B:** Enlarged views of the results of chromosome 5 (left) and 12 (right) showing both the log₂ intensity window as well as the BAF results (see page 124).

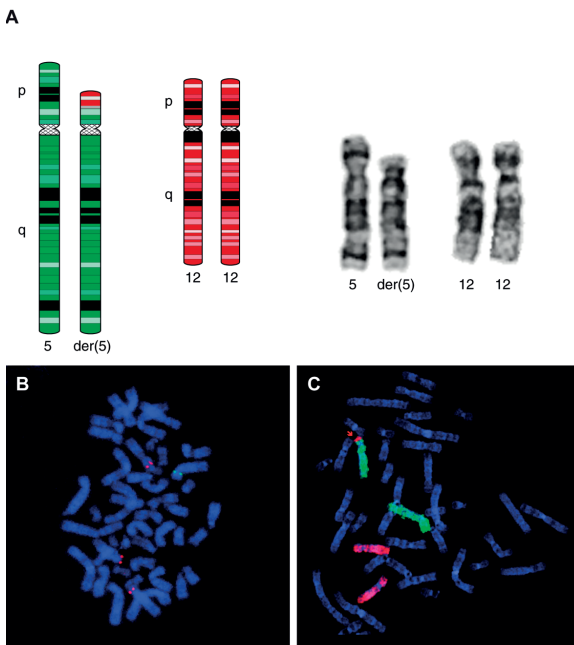


Figure 2 | Fluorescent In-Situ Hybridization results using cultured amniotic fluid and skin material

A: Left: Schematic representation of the unbalanced $der(5)t(5;12)(p13.2;p12.3)$ and its normal chromosome 12 counterpart. Right: Partial Karyotype of the patient showing both the normal and abnormal chromosome 5 and both normal chromosomes 12. **B:** Fluorescent In-Situ Hybridization (FISH) on a metaphase spread of 1 umbilical cord-fibroblast-cell presenting 1 copy of BAC clone RP11-7M4 (Green) on the normal chromosome 5 and 3 of clone RP11-62P15 (red) on both chromosomes 12 and the $der(5)$. **C:** Whole-Chromosome Paint FISH results of 1 AF-cell showing duplication of part of the short arm of chromosome 12 (WCP12: red) at the expense of part of 1 copy of chromosome 5 (WCP5:green) (see page 125).

Chapter 3

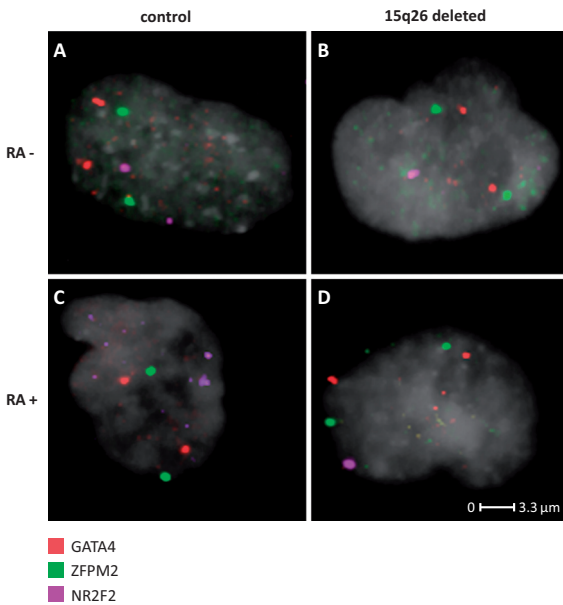


Figure 1 | Nuclear organization of CDH candidate genes in interphase fibroblast nuclei.

Representative 2D FISH images of distances between putative CDH genes *NR2F2*, *GATA4* and *ZFPM2* are shown and analyzed based on multicolor signals of BAC clones RP11-784A9, RP11-241B23 and RP11-1029P14 respectively. FISH spots of the three genes in Control (A and C) and 15q26-deleted CDH patient cells (B and D) and in an unstimulated (A and B) and RA-stimulated (C and D) condition. No co-localization of CDH-candidate genes was detected in both cell lines. Bar = 3.3 μm . (red = *GATA4*, green = *ZFPM2*, purple = *NR2F2*, gray = nuclear DAPI counter stain) (see page 141).

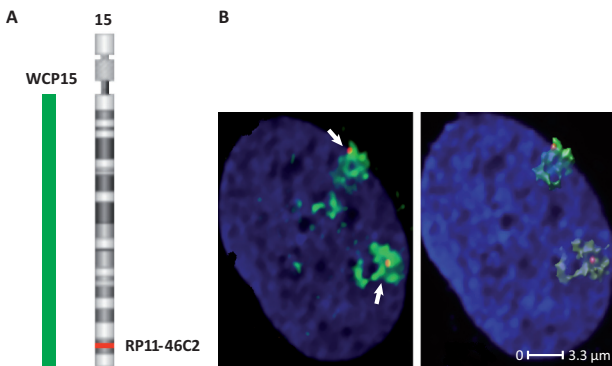


Figure 2 | *NR2F2* localization relative to its chromosome territory 15

A: Schematic diagram depicting the used FISH probes RP11-46C2 (red) and whole-chromosome territory 15 (CT15) paints (green). **B:** Representative FISH image of the nuclear position of chromosome territory 15 and the *NR2F2* alleles relative to each other in a control nucleus. (B, left) Visualization of an unprocessed xy-projection image. (B, right) Deconvolved and 3D volume rendered image showing a preferred territorial surface position of *NR2F2* for one allele, and a complete CT interior position of the other allele. Both alleles show an almost complete overlap with their respective CTs and show no signs of relocalisation. Nuclei are stained with DAPI (blue). Bar = 3.3 μm (see page 142).

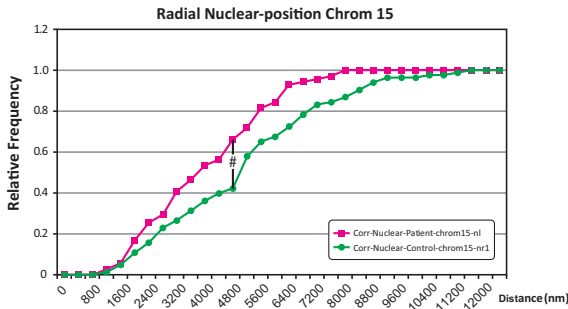


Figure 3 | Nuclear position of partial CT15q in control and CDH 15q26-deleted cell lines

This cumulative frequency graph shows the radial position of partial Chromosome Territory 15 (CT15) in control (dark green) and CDH-15q26 deleted (red) fibroblast nuclei. It only represents the position of the normal, un-translocated pCT15 in patient DFP1 and its normal pCT15 counterpart in control DFC1. Distances are corrected for nuclear volume. Distribution differences were calculated using the Wilcoxon-Mann-Whitney test (see # $p = 0,003$). In each experiment 150 nuclei were analyzed (see page 143).

Chapter 3.3

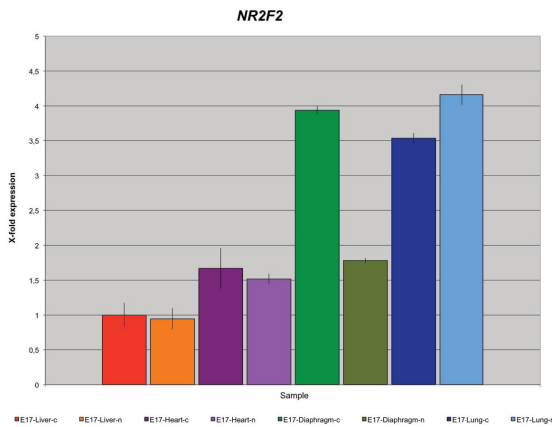


Figure 1 | Relative mRNA expression levels of NR2F2

Illustration of relative mRNA expression levels of *NR2F2* detected by real-time Q-PCR in four different tissues (liver, heart, diaphragm, lung) of a rodent-CDH model with (n; nitrofen) and without nitrofen (c;control). Tissues of five-six pups were harvested and pooled at embryonic day E17. Levels in control-liver (dark red) were used as an internal control. (see page 180)

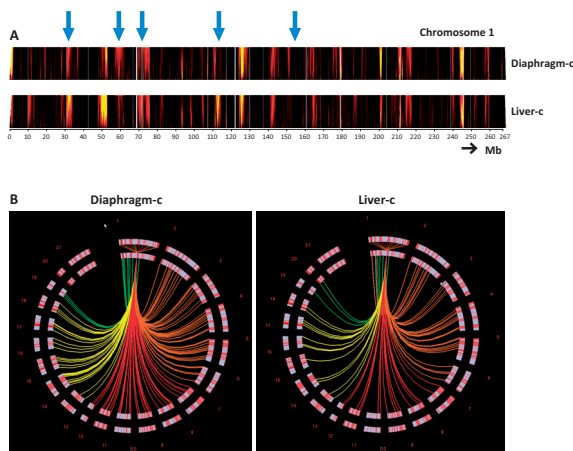


Figure 2 | Domainograms of NR2F2 in rodent E17-control tissues

A: in-cis interactions in control-diaphragm (Top) and control-liver tissue (Below) showing an overall similar genomic 3D environment, although minor differences (arrows) in the interaction efficiency of a subset of interaction partners may be suggested by these representations.

B: Circos plot depicting the interactions of *NR2F2* with other chromosomes in control-diaphragm (Left) and control-liver tissue (Right), again demonstrating grossly similar patterns. Each line represents a trans interaction. Chromosomes are plotted around the circle. Colours indicate the chromosomes that were contacted in each quadrant (see page 181).

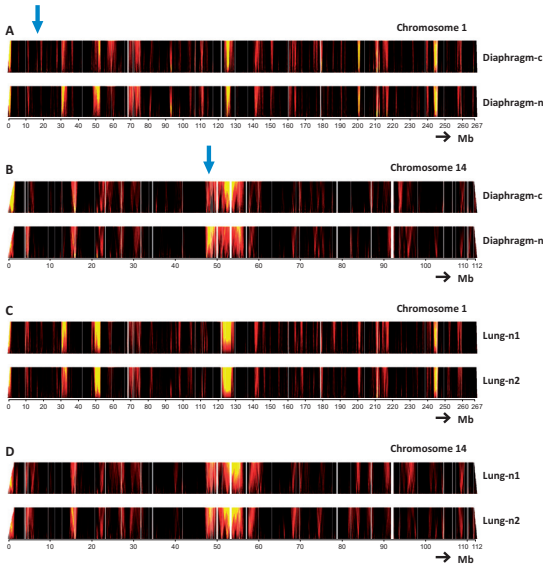


Figure 3 | Domainograms of rodent *NR2F2* upon nitrofen-induction at E17

Comparing the in-cis **A**: and in-trans (using chromosome 14) interactions **B**: in control-diaphragm (Top) and nitrofen-treated diaphragm (Below) tissue respectively showing an overall similar genomic 3D environment although, very subtle differences (arrow) in the interaction efficiency (i.e. frequency) occurred in these subsets also. **C/D**: Similar as in A/B for duplo experiments of nitrofen-lung-induced tissues; index 1 (Top) and index 2 (Below) (see page 182).

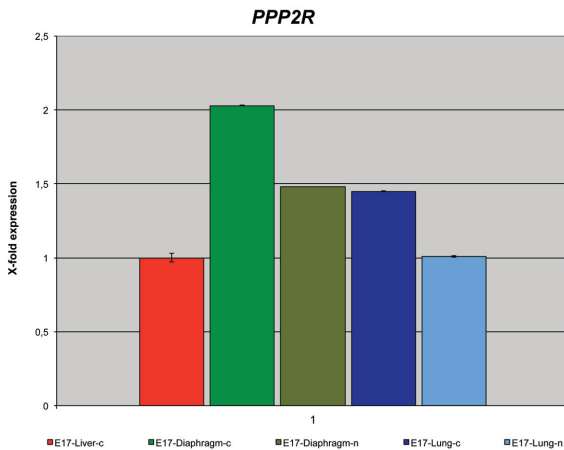
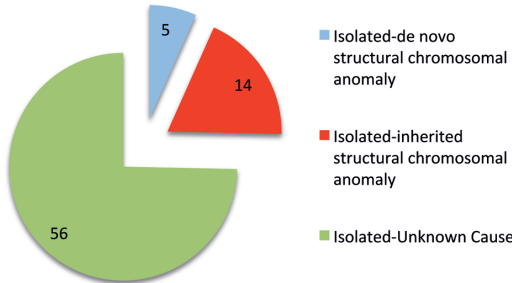


Figure 4 | Relative mRNA expression levels of *PPP2R*

Illustration of relative mRNA expression levels of *NR2F2* detected by real-time Q-PCR in CDH affected (diaphragm, lung) tissues of a rodent-CDH model with (n; nitrofen) and without nitrofen (c;control). Tissues of five-six pups were harvested and pooled at embryonic day E17. Levels in control-liver (dark red) were used as an internal control (see page 183).

Chapter 4

Isolated



Complex

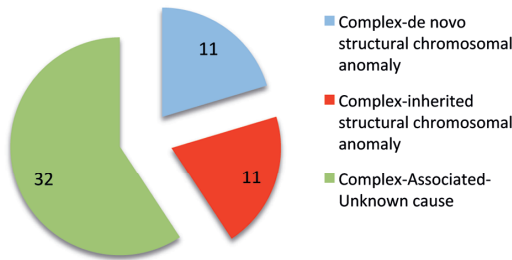


Figure 1 | Circular plots of genome-wide copy number screen results of 117 “Rotterdam” CDH subjects

Patients are classified depending on the absence (isolated CDH, n=67) or presence (complex, n=50) of additional birth defects. The blue colour represents the number of patients with a causative de novo structural chromosomal anomaly. Depicted in red is the proportion of patients identified with an inherited structural aberration, and green representing a remainder CDH subgroup with a yet unidentified (genetic) cause. Inherited CNVs could confer susceptibility to CDH after all, since they hardly occurred in two normal control populations. Remarkably, 5 out of 16 de novo CNVs were present in isolated CDH cases (see page 201).

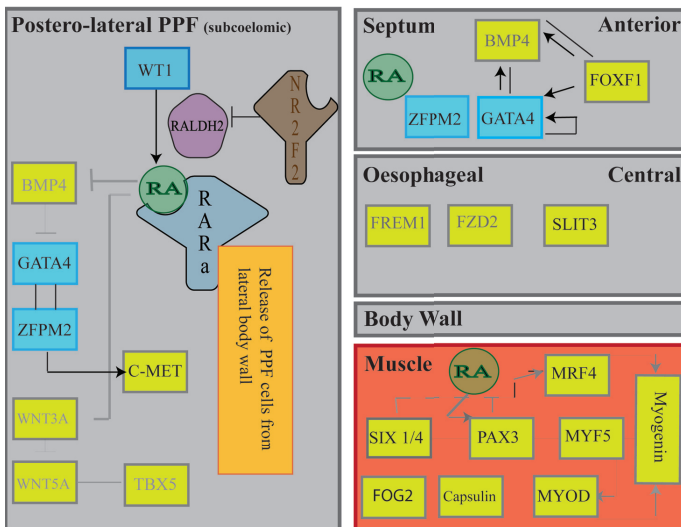


Figure 2 | Diaphragm signalling cascade

Depicted are the strong CDH candidate genes from literature [29, 75, 80, 81] (dark blue squares for *FOG2*, *WT1* and *GATA4*, green/grey/purple symbols for RA signalling members and *NR2F2*; dark brown) and their putative interactions at the specific location of the primordial diaphragm in which they have been demonstrated. According to the revised view on diaphragm embryogenesis, diaphragm tissue derives from four different mesenchymal components (depicted in the 4 grey boxes) i.e. the postero-

lateral pleuro-peritoneal folds, the anterior septum transversum, the central esophageal mesentery and the lateral body wall mesenchyme. When completely fused, these structures form a supportive layer on which the “true” diaphragm muscle cells (that are derived from the hypaxial part of the somite) can migrate (represented as the light red box). Recently, several developmental studies [131] have shown that skeletal muscles of the body, limb and head have a distinct embryonic and cellular origin, while the genetic regulation at work in these domains are starting to be identified as shown for hypaxial muscle. Evidence for the genes and interactions depicted in the yellow boxes is based on our own preliminary data (chapter 2: *FZD2*, *FREM1*, *TBX5*) or from literature (*BMP4*, *FOXF1*, *WNT3A/5A*) [76, 132, 133] (see page 207).

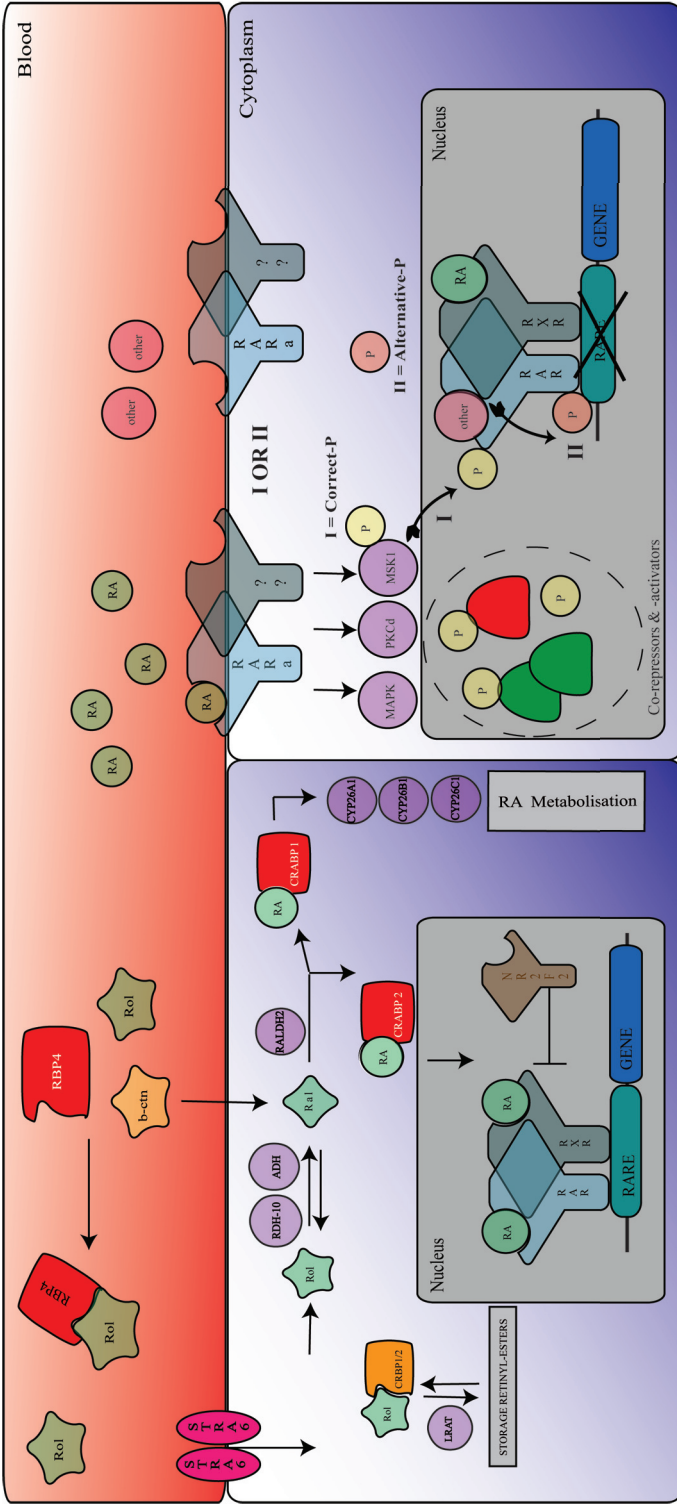


Figure 3 | Canonical and alternative RAR-alpha signalling pathway

Depicted are the classic canonical (left) and unconventional non-genomic (right) downstream pathways of RA signalling. When circulating retinol is taken up by RBP4, it can be transferred intracellularly by STRA6 and pass through the “basic” RA signalling cascade that ultimately results in the binding of nuclear RARs to specific response elements, thereby controlling the expression of a specific subset of genes. In addition, new non-genomic effects of RARs have emerged recently (as reviewed in [107]). In response to RA, which binds to RARa in the cytosol or at the cellular membrane, PKCδ, MAPK and MSK1 are activated through rapid non-genomic effects. MSK1, in turn phosphorylates RARa itself at a specific subunit. In the absence of RA, this phosphorylation event can also occur, yet at a different subunit leading to inactivation of (nuclear) RARa activity, instead of activation. Retinol; RBP, retinol binding protein; STRA6, stimulated by retinoic acid 6; CRBP, cellular retinol binding protein; Ral, retinaldehyde; ADH, alcohol dehydrogenase; RALDH, retinaldehyde dehydrogenase; CYP26, cytochrome P450 26 enzymes; RAR, retinoic acid receptor; RXR, retinoid X receptor; RARE retinoic acid response element. B-ctn, beta-carotene; LRAT, Lecithin retinol acyl-transferase, NR2F2; Nuclear receptor 2, subfamily F2. MAPK; Mitogen Activated Protein Kinase, PKCδ; Mitogen Activated and Stress Activated Kinase, P. Phosphorylation (see page 210).